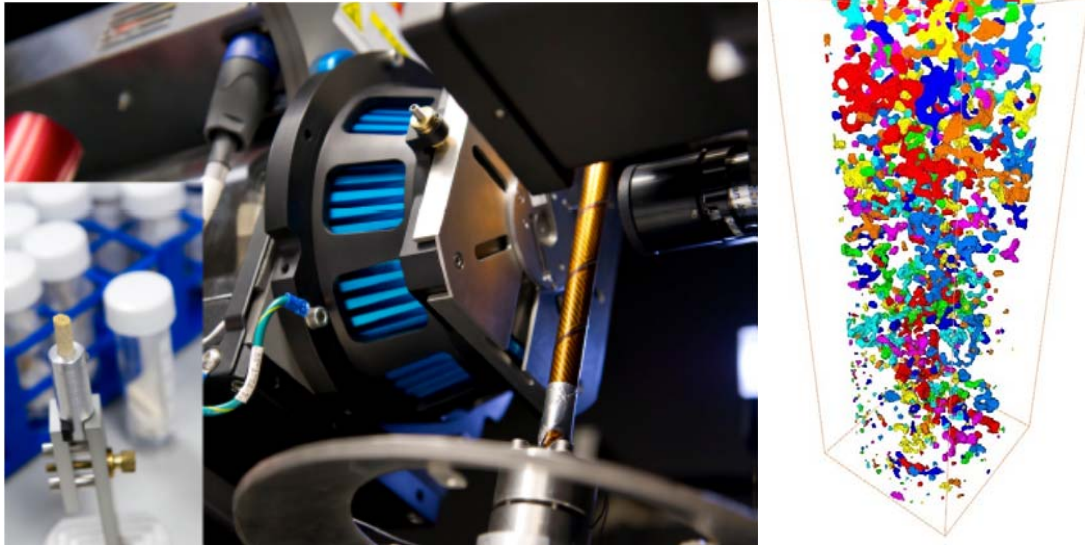


# Digital Core Analysis and its Application to Reservoir Engineering



Martin J. Blunt

Professor of Petroleum Engineering  
Visiting Professor, Politecnico di Milano  
Department of Earth Science and Engineering,  
Imperial College London  
[m.blunt@imperial.ac.uk](mailto:m.blunt@imperial.ac.uk)

## Course Notes

MAY 2014

## TABLE OF CONTENTS

<b>TABLE OF CONTENTS</b>	<b>2</b>
<b>1. COURSE OVERVIEW AND MOTIVATION</b>	<b>4</b>
RECOMMENDED BOOKS	4
<b>2. PHILOSOPHY</b>	<b>6</b>
<b>3. MULTIPLE PHASES IN EQUILIBRIUM</b>	<b>7</b>
3.1 YOUNG-LAPLACE EQUATION	7
3.2 EQUILIBRIUM AT A LINE OF CONTACT	8
3.3 SPREADING COEFFICIENT	10
3.4 TWO FLUIDS IN A CAPILLARY TUBE	10
3.5 WETTABILITY	12
<b>4. POROUS MEDIA</b>	<b>17</b>
4.1 X-RAY IMAGING	17
4.2 ELECTRON MICROSCOPY TO IMAGE MICRO-POROSITY	22
4.3 TOPOLOGICALLY REPRESENTATIVE NETWORKS	23
<b>5. PRIMARY DRAINAGE</b>	<b>25</b>
5.1 TYPICAL VALUES OF THE CAPILLARY PRESSURE	27
5.2 HOW IS CAPILLARY PRESSURE MEASURED?	28
<b>6. IMBIBITION</b>	<b>33</b>
6.1 PORE-SCALE DISPLACEMENT, TRAPPING OF THE NON-WETTING PHASE AND SNAP-OFF	33
6.2 PORE-SCALE IMAGES OF TRAPPED PHASES	37
6.3 TYPICAL CAPILLARY PRESSURE CURVES AND SECONDARY DRAINAGE	43
6.4 DIFFERENT DISPLACEMENT PATHS AND TRAPPING CURVES	44
<b>7. LEVERETT J FUNCTION</b>	<b>50</b>
7.1 CAPILLARY PRESSURE AND PORE SIZE DISTRIBUTION	53
<b>8. EFFECT OF WETTABILITY ON CAPILLARY PRESSURE</b>	<b>59</b>
8.1 TRAPPING CURVES IN MIXED-WET SYSTEMS	65
8.2 TRANSITION ZONES	67
8.3 AMOTT WETTABILITY INDICES	68
8.4 EXAMPLE EXERCISES	69
<b>9. FLUID FLOW AND DARCY'S LAW</b>	<b>71</b>
9.1 STOKES FLOW	71
9.2 REYNOLD'S NUMBER AND FLOW FIELDS	72
9.3 AVERAGED BEHAVIOUR AND DARCY'S LAW	77
9.4 OTHER WAYS TO WRITE DARCY'S LAW AND HYDRAULIC CONDUCTIVITY	80
9.5 UNITS OF PERMEABILITY AND THE DEFINITION OF THE DARCY	81
9.6 DEFINITION OF FLOW SPEED AND POROSITY	82
9.7 ESTIMATING PERMEABILITY	82
9.8 EXAMPLE PROBLEM INCALCULATING PERMEABILUTY	84

<b>10. MOLECULAR DIFFUSION AND CONCENTRATION</b>	<b>86</b>
<b>11. CONSERVATION EQUATION FOR SINGLE-PHASE FLOW</b>	<b>89</b>
11.1 ANALYTICAL SOLUTION OF THE ADVECTION-DIFFUSION EQUATION	94
11.2 DIFFUSION AND DISPERSION	96
<b>12. CAPILLARY AND BOND NUMBERS</b>	<b>102</b>
<b>13. RELATIVE PERMEABILITY</b>	<b>105</b>
13.1 RELATIVE PERMEABILITIES FOR SANDSTONES AND PREDICTIONS USING PORE-SCALE MODELLING	108
13.2 IMBIBITION AND OIL RECOVERY PROCESSES	113
13.3 ANALYSIS OF RELATIVE PERMEABILITY IN MIXED-WET CARBONATES	119
13.4 COMPARISON OF NETWORK MODEL RESULTS WITH EXPERIMENTAL DATA	136
13.5 IMPACT OF RELATIVE PERMEABILITY ON FIELD-SCALE RECOVERY	141
<b>14. THREE-PHASE FLOW</b>	<b>146</b>
14.1 SPREADING, WETTING AND OIL LAYERS	146
14.2 THREE-PHASE RELATIVE PERMEABILITY AND TRAPPED SATURATIONS	154
14.3 RELATIVE PERMEABILITY PREDICTIONS USING PORE-SCALE MODELLING	157
14.4 LAYER DRAINAGE AND WETTABILITY	159
14.5 WHY DUCKS DON'T GET WET	160
<b>15. CONSERVATION EQUATION FOR MULTIPHASE FLOW</b>	<b>163</b>
15.1 NOTE ABOUT NOMENCLATURE	166
15.2 RICHARDS EQUATION	166
<b>16. FRACTIONAL FLOW AND ANALYTIC SOLUTIONS</b>	<b>168</b>
16.1 BUCKLEY-LEVERETT SOLUTION	173
16.2 SHOCKS	179
16.3 WELGE CONSTRUCTION	180
16.4 WAVE, PARTICLE SPEEDS AND DEFINITIONS	183
16.5 EFFECT OF GRAVITY	184
16.6 AVERAGE SATURATION AND RECOVERY	186
16.7 OIL RECOVERY AND THE IMPACT OF WETTABILITY	192
<b>17. ANALYTIC SOLUTIONS FOR SPONTANEOUS IMBIBITION</b>	<b>196</b>
17.1 COUNTER-CURRENT IMBIBITION	196
17.2 EXTENSIONS TO ANALYTIC THEORY AND RESERVOIR SIMULATION	207
<b>18. BIBLIOGRAPHY AND FURTHER READING</b>	<b>208</b>
18.1 RELEVANT RESEARCH PAPERS	208
18.2 PAPERS FROM IMPERIAL COLLEGE	210
<b>19. HOMEWORK PROBLEMS</b>	<b>213</b>
<b>20. PREVIOUS EXAM PAPERS</b>	<b>218</b>

## 1. COURSE OVERVIEW AND MOTIVATION

---

Access to sustainable, affordable water, energy and food are some of the major technological challenges of the 21<sup>st</sup> century. How do we manage precious and scarce water resources, while preventing pollution? How do we extract the most of our remaining supplies of conventional oil and gas? How can we extract, safely, shale gas and oil? Can we collect and store carbon dioxide in the subsurface to prevent atmospheric emissions and help avoid dangerous climate change? Can we manage to provide sufficient energy for a growing world's population with an aspiration for improved prosperity? An understanding of these challenges involves multiphase flow in porous media – the flow of water, oil and gas with associated pollutants – underground in geological formations.

The subject of multiphase flow in porous media is undergoing a revolution, not just as a result of its many important applications, but because of developments in our quantitative understanding of how fluids are arranged and move, combined with the ability to image fluids at the micron-scale inside rocks.

This course will apply concepts of multiphase flow in porous media to understand and design recovery from oil and gas reservoirs, with an emphasis on the understanding of pore-scale phenomena. This is one of the major challenges referred to above – at present we recover only around one third of the oil from fields we have discovered. How can we improve this to the 50-60% now achievable with the best engineering methods, and beyond?

It is assumed that you already know about hydrocarbon phase behaviour, reservoir simulation and the principal reservoir drive mechanisms. You will also need to know Darcy's law and the meaning of relative permeability and fractional flow, although these are described again in these notes.

### RECOMMENDED BOOKS

---

1. *Fundamentals of Reservoir Engineering*, L. P. Dake, Elsevier, (1991), ISBN 0-444-41830-X.

This is the best book for the whole class and describes material balance, phase behaviour and Buckley-Leverett analysis.



2. *Petroleum Engineering Principles and Practice*, J. S. Archer and C. G. Wall, Graham and Trotman, (1986), ISBN 0-86010-665-9.

This book was co-authored by John Archer, a Professor of Reservoir Engineering at Imperial who later was Vice-Chancellor of Heriot-Watt University.

3. *Applied Petroleum Engineering*, B. C. Craft and M. F. Hawkins, Prentice Hall, (1991), ISBN 0-13-039884-5.

Excellent on material balance, but has a very practical focus with little explanation of the methods used.

4. *Waterflooding*, G. P. Willhite, Society of Petroleum Engineers, (1986), ISBN 1-55563-005-7.

Another good textbook, but does not cover all the material in this class.

5. *The Reservoir Engineering Aspects of Waterflooding*, F. F. Craig, Jr., Society of Petroleum Engineers, (1971), ISBN 0-89520-202-6.

6. *Enhanced Oil Recovery*, L. W. Lake, Prentice Hall, Englewood Cliffs, (1989) 500 pages.

This is a truly excellent and detailed book – one of the very best in petroleum engineering. It does cover much of the material in these notes, but – for improved oil recovery – at a level of detail which is much greater than we have time for in this course.

7. *Groundwater*, R. A. Freeze and J. A. Cherry, Prentice Hall, Inc, Englewood Cliffs, (1979).

This is a standard hydrology text, but does not cover multiphase flow, and does not have a focus on oil recovery.

8. *Porous Media: Fluid Transport and Pore Structure*, F. A. L. Dullien, Academic Press, San Diego, 2<sup>nd</sup> Edition, (1992).

This is a fabulous research reference book that covers much of the scientific material in these notes and contains a lot of experimentally-based physical insight into multiphase flow.

9. *Dynamics of Fluids in Porous Media*, J. Bear, Dover Publications, Inc, New York, (1972).

A classic in its field – indeed it help establish the subject of flow in porous media as a discipline. Very mathematical, but contains a lot of useful information.

10. *Capillary and Wetting Phenomena: Drops, Bubbles, Pearls, Waves*, P-G de Gennes, F. Brochard-Wyart and D. Quéré, Springer (2002).

The first author is the charismatic, and now sadly deceased, physics Nobel Prize winner, Pierre-Gilles de Gennes. A fascinating book, packed full of interesting analysis, but not directly relevant to flow in porous media. Acquire a French accent, light up a Gaulois, wave your hands and voilà – brilliant insights into physics!

## 2. PHILOSOPHY

---

These notes contain a synopsis of the class and cover most of the material necessary to understand the course. However, there are places where explanations and examples given in lectures are essential to understand the material fully, so be prepared to make some supplementary notes. I like to encourage discussion in lectures, so don't be shy about asking questions.

### 3. MULTIPLE PHASES IN EQUILIBRIUM

---

We start with a fundamental presentation of the equations that govern contacts between fluids and solids and the meniscus that separates fluid phases.

#### 3.1 YOUNG-LAPLACE EQUATION

---

If we have multiple phases present in a porous medium, then there is a pressure difference across the interfaces between these phases. The pressure difference is given by the Young-Laplace equation:

$$P_c = \sigma \left( \frac{1}{r_1} + \frac{1}{r_2} \right) \quad (3.1)$$

where  $r_1$  and  $r_2$  are the principal radii of curvature of the fluid interface (the radii of curvature measured perpendicular to each other).  $\sigma$  is the interfacial tension between the phases – it has the units of a force per unit length (N/m) or an energy per unit area (J/m<sup>2</sup>).

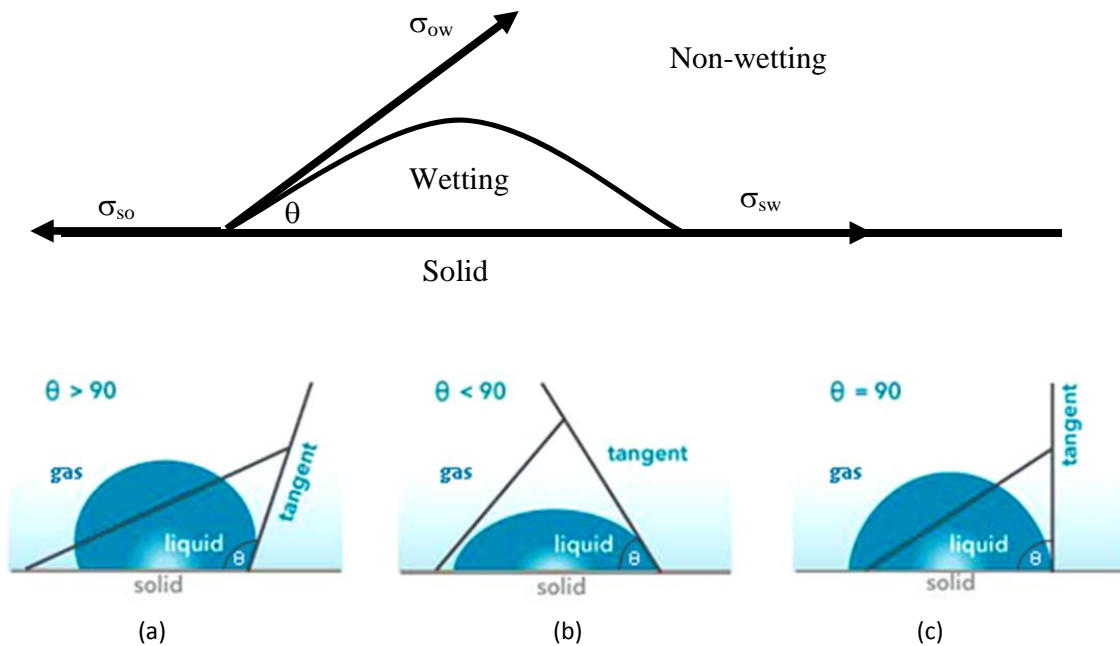
The non-wetting phase has the higher pressure.

It is possible to derive this equation using principles of force or energy balance (see Dullien or de Gennes – the books listed at the beginning of the notes), but is somewhat cumbersome, as it involves the three-dimensional geometry of curved surfaces. It is, however, relatively straightforward to derive specific cases – as below – from first principles. This we will do later when we consider the pressure difference between two phases in a circular cylindrical tube. For now, though, it is helpful to assert that the Young-Laplace equation is valid.

The second major concept we need to introduce is that of contact angle. While the Young-Laplace equation considers the pressure across an interface, it does not address how that interface interacts with a solid surface.

### 3.2 EQUILIBRIUM AT A LINE OF CONTACT

Consider a wetting fluid (say water) resting on a solid surface surrounded by a non-wetting phase (such as oil or gas).



**Contact angle,  $\theta$ , between two phases, measured through the denser phase. (a) non-wetting liquid. (b) wetting liquid. (c) intermediate-wet liquid.**

A horizontal force balance gives:

$$\sigma_{so} = \sigma_{sw} + \sigma_{ow} \cos \theta \quad (3.2)$$

This is the Young equation. The contact angle is given by:

$$\cos \theta = \frac{\sigma_{so} - \sigma_{sw}}{\sigma_{ow}} \quad (3.3)$$

What is the vertical force balance? Intermolecular forces in the solid counter-act the vertical tension as the solid is very slightly perturbed.

Thomas Young was an early 19<sup>th</sup> century English physicist and all-round genius who worked on everything from deciphering hieroglyphics to the wave theory of light. Young's modulus (in elasticity) and the Young double slit experiment recognise just two of his contributions to science.

Pierre-Simon (the Marquis de) Laplace was a brilliant French mathematician and physicist of the same age. His contributions include astronomy, statistics and the Laplace transform. The Laplace equation is generally considered to be  $\nabla^2\phi=0$ ; Eq. (3.1) is sometimes called the 'Laplace equation' which is confusing; and Eq. (3.2) the 'Young-Laplace equation,' which possibly under-states the relative contributions of Young and Laplace to this subject.



**Spot the difference. One is an insightful English physicist; the other a brilliant French mathematician, clinging to a post-revolutionary title.**

### 3.3 SPREADING COEFFICIENT

---

Define a spreading coefficient as:

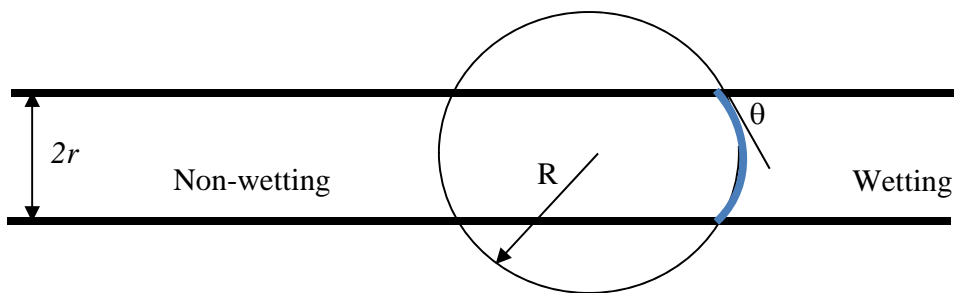
$$C_s = \sigma_{so} - \sigma_{sw} - \sigma_{ow} \quad (3.4)$$

If  $\sigma_{so} > \sigma_{sw} + \sigma_{ow}$  or  $C_s > 0$ , there is no solution for  $\theta$  in Eq. (3.4). The water spreads over the solid surface. This is complete wetting and  $\theta = 0$ .

### 3.4 TWO FLUIDS IN A CAPILLARY TUBE

---

Now consider two fluids in a capillary tube of radius  $r$ :



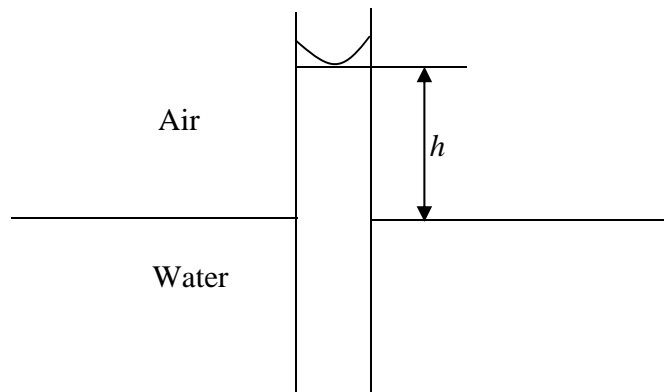
**Two fluids in equilibrium in a cylindrical tube. The blue arc is the interface between the wetting and non-wetting phases.**

The radius of curvature  $R = r/\cos\theta$  (we can derive this using simple trigonometry).

Thus we find:

$$P_c = P_{nw} - P_w = \frac{2\sigma}{r} \cos\theta \quad (3.5)$$

Imagine now water rising up in a capillary tube of radius  $r$ , as shown below.



**Capillary rise in a tube – here water is the wetting phase.**

$$\rho gh = \frac{2\sigma}{r} \cos\theta \quad (3.6)$$

What would happen for mercury/air? The interface would be lower than the free (flat) surface, as in this case mercury is the non-wetting phase.

Eq. (3.6) can be derived without the Young-Laplace equation, using an energy balance. Water rises up the tube, since this is energetically favourable: there is a lower energy for water to coat the solid (glass) surface than air. This though is balanced by potential energy, as the water rises against gravity. So, the water continues to rise until the change in potential energy is just balanced by the change in interfacial energy.

Imagine that the height of the interface changes by a small amount: if this lowers the energy, then the interface will move until it reaches a position of equilibrium. The equilibrium height is found when changes in potential and interfacial energy are equal for small fluctuations in this height: this is the stable configuration.

The gravitational potential energy of a mass  $m$  at a height  $h$  is  $mgh$ . From a height  $h$  to  $h+dh$ , the water in the tube has a mass  $A\rho dh$ , where  $A$  is the area ( $\pi r^2$ ). Then if we change the height from  $h$  to  $h+dh$ , the change in potential energy is:

$$\Delta E_p = \pi r^2 \rho g h dh \quad (3.7)$$

This must be equal to the energy gained when the water moves up the tube. Now consider that  $\sigma_{sa}$  is the energy per unit area (interfacial tension) of an interface between the solid and air, while  $\sigma_{sw}$  is the energy per unit area of interface between solid and water. Then the energy change for the water to move from  $h$  to  $h+dh$  is:

$$\Delta E_s = 2\pi r(\sigma_{sa} - \sigma_{sw})dh = 2\pi r\sigma\cos\theta dh \quad (3.8)$$

since  $2\pi r h$  is the area of wetted solid (glass) surface, and we have used the Young equation, (3.2). Conservation of energy asserts that the energies in Eqs. (3.7) and (3.8) are the same, leading to Eq. (3.6) directly:

$$\begin{aligned} \Delta E_s &= \Delta E_p \\ 2\pi r\sigma\cos\theta dh &= \pi r^2 \rho g h dh \\ 2\sigma\cos\theta &= r\rho g h \\ \frac{2\sigma\cos\theta}{r} &= \rho g h \end{aligned} \quad (3.9)$$

### 3.5 WETTABILITY

---

The contact angle is traditionally measured through the denser phase (water for oil/water and gas/water, and oil for gas/oil). If:

$\theta = 0$ , we have complete wetting.

$\theta < 90^\circ$ , the fluid is wetting (water-wet).

$\theta \approx 90^\circ$ , the fluid is of intermediate or neutral wettability.

$\theta > 90^\circ$ , the fluid is non-wetting (oil-wet).



Clean rocks are generally water-wet, since the polar surface of the solid – say quartz or calcite – interacts strongly with the water making its interfacial tension lower than the tension (energy per unit area) with oil or gas.

Why then are most reservoir rocks not completely water-wet? In contact with a solid surface, surface active components of the oil – high molecular weight molecules called asphaltenes – adhere to the solid surface rendering it less water-wet. Regions of the solid surface that are not directly contacted by oil remain water-wet. Thus many oil reservoirs are what is known as mixed-wet or fractionally wet – different regions of the pore space have different wettabilities. This important concept is developed later in these notes.

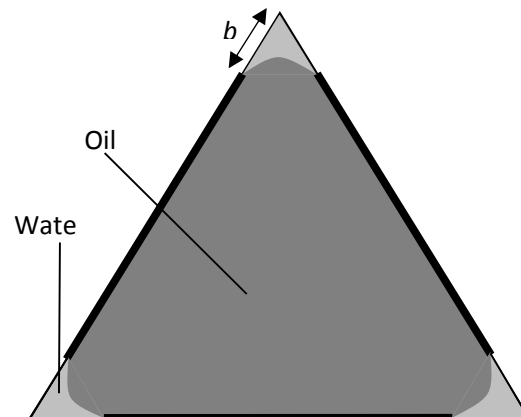
In other settings – aquifers and soils – it is the presence of organic material, particularly surfactants or other compounds that adhere to the solid surface – that alter the wettability. In general the contact angle is governed by a subtle balance of surface forces between the fluids and the rock.

The wettability change typically takes around 1,000 hours to complete, so since oil has been in a reservoir over geological times, there is plenty of time for the wettability alteration to occur. The wettability alteration also has sufficient time to take place in most polluted soils.

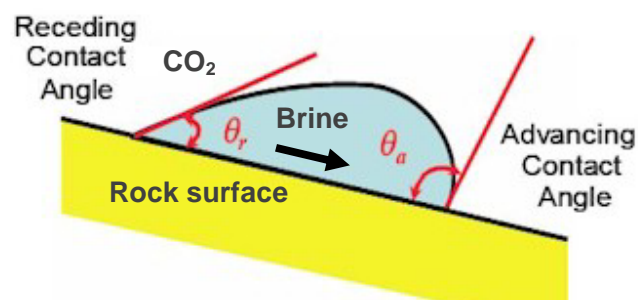
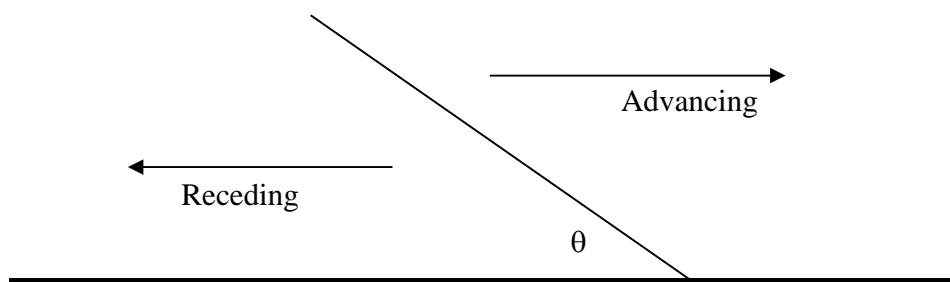
Overleaf is a schematic of what happens in a single pore with an idealized triangular cross-section: regions of the surface directly contacted by oil have an altered wettability (this is not necessarily oil-wet, but is not strongly water-wet either) while the corners remain water-wet.

The contact angle is also usually different depending on the flow direction. The static contact angle (no movement of the solid/wetting/non-wetting contact), the advancing contact angle (denser phase advancing) and the receding contact angle may all be different.

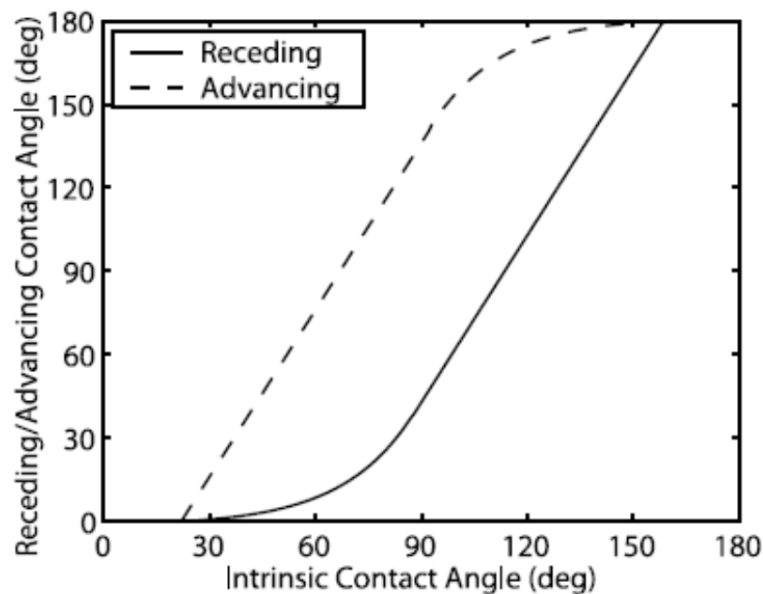
The reason for this is chemical inhomogeneities on the surface and small-scale surface roughness. The figure below shows how the advancing and receding contact values vary with the intrinsic contact angle (the angle measured at rest on a smooth surface).



Oil and water in a triangular pore after primary drainage (oil migration into the reservoir). The areas directly contacted by oil (shown by the bold line) have an altered wettability, while the corners that are water-filled remain water-wet.  $b$  is the length of the water-wet surface.

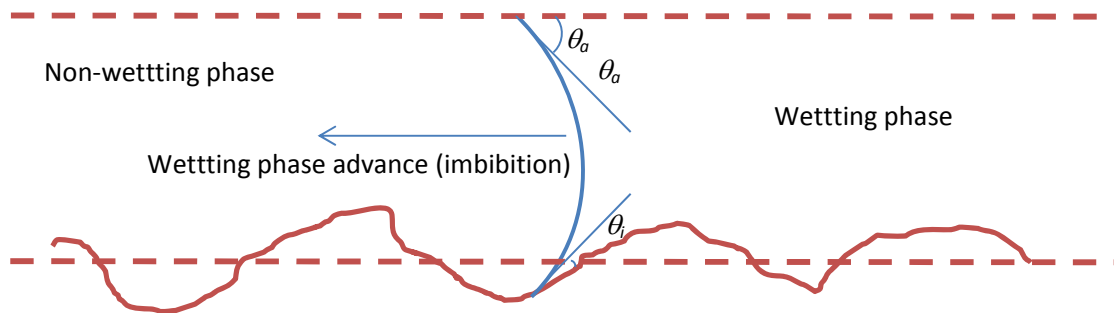


Advancing and receding contact angles (<http://www.adhesionbonding.com>).



**Relationship between intrinsic contact angle (the angle at rest on a smooth surface) and the advancing and receding contact angles, based on the measurements by Morrow (1975). The principal reason for this contact angle hysteresis is surface roughness – in a porous medium, the solid surfaces are not smooth.**

The main effect is small-scale surface roughness, shown schematically below. While the molecular-scale contact angle may indeed be the intrinsic value, the apparent angle viewed on the larger scale – and the angle which will control the capillary pressure (that is the interfacial curvature) for displacement is different. Displacement is impeded by the highest pressure in the displacing (advancing) phase necessary for the contact to move: hence the apparent angles are different in imbibition (wetting phase advancing) than drainage (non-wetting phase advancing). The interface is impeded at the points where the pressure in the advancing phase is largest – we need to capture this to calculate the correct capillary pressures for displacement.



A schematic of surface roughness (the solid surface is indicated by the irregular brown line) and its impact on contact angle.  $\theta_i$  is the intrinsic contact angle – the angle at the surface (regardless of orientation): in this example it is close to zero, indicating a strongly water-wet system. However, the effective dynamic contact angle for imbibition  $\theta_a$  is larger – this is the angle that gives the correct curvature in the Young-Laplace equation and is observed at a larger scale with an apparently smoother solid surface (shown by the dashed line). The roughness impedes imbibition: a higher wetting phase pressure is required for displacement than on a smooth surface. For drainage the displacement is limited by roughness oriented in the other direction and the apparent contact angle is smaller than  $\theta_i$ , impeding the advance of the non-wetting phase.

## 4. POROUS MEDIA

---

We now properly introduce multiple phases in a porous medium. Before proceeding with the description of macroscopic, averaged, properties, we will first use some illustrative examples in an attempt to provide some insight into displacement and fluid configurations at the pore scale. The emphasis in this section will be on understanding and appreciating the complexity of the pore space at the micron (pore) scale.

### 4.1 X-RAY IMAGING

---

In recent years there has been a revolution in our ability to see inside the pore space of rocks using X-rays. The development of modern imaging methods relies on the acquisition of three-dimensional reconstructions from a series of two-dimensional projections taken at different angles: the sample is rotated and the adsorption of the X-rays in different directions is recorded and used to produce a three-dimensional representation of the rock and fluids. In the 1980s these methods were first applied in laboratory-based systems to measure two and three-phase fluid saturations for soil science and petroleum applications with a resolution of around 1-3 mm. The first micro-CT (micron or pore-scale) images of rocks were obtained by Flannery and co-workers at Exxon Research using both laboratory and synchrotron sources. In a synchrotron a bright monochromatic beam of X-rays is shone through a small rock sample. Several rocks were studied with resolutions down to around 3  $\mu\text{m}$ . Dunsmuir *et al.* extended this work to characterize pore space topology and transport in sandstones.

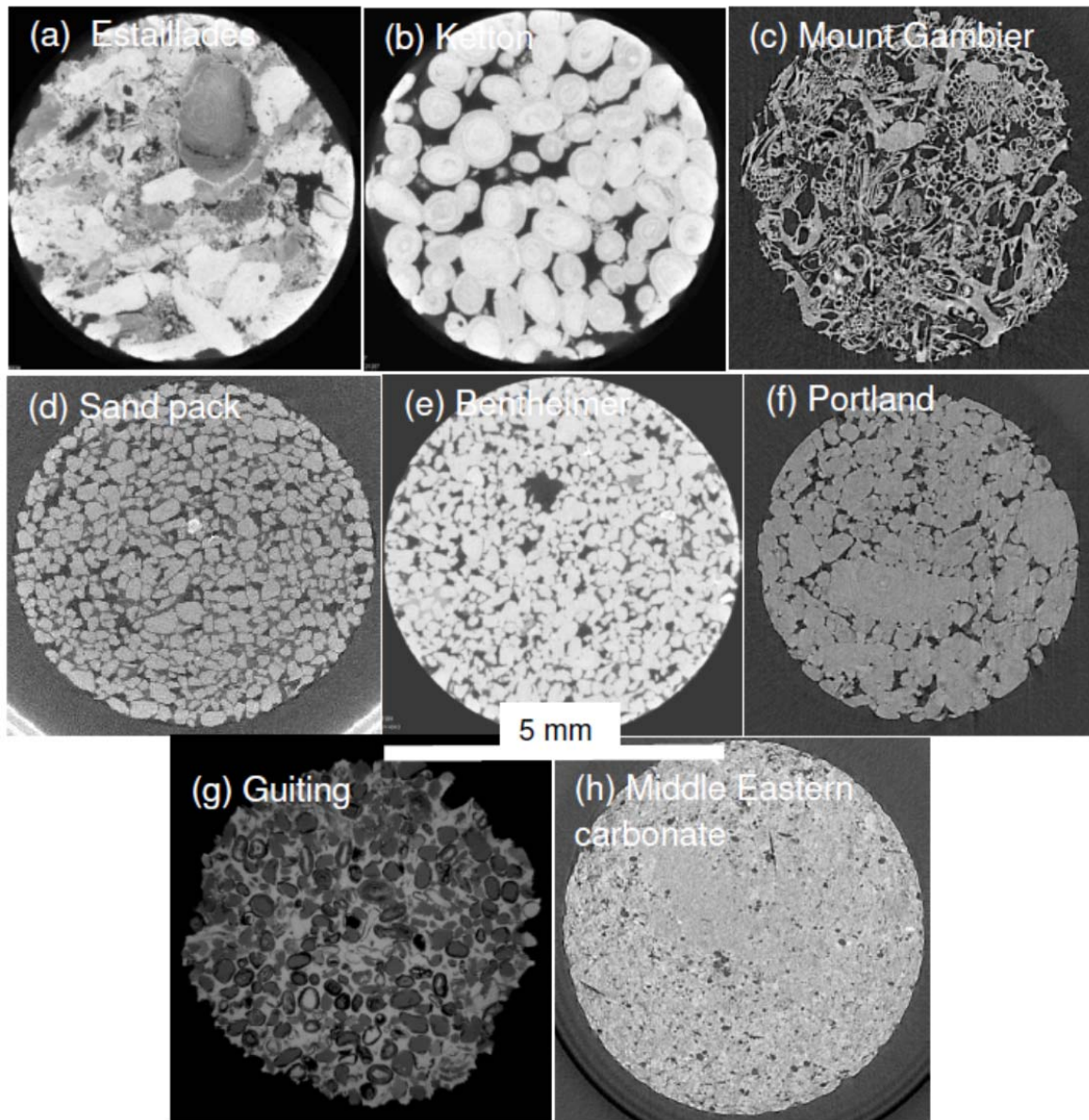
One of the pioneers of the continued development of this technology has been the team at the Australian National University in collaboration with colleagues at the University of New South Wales. They have built a bespoke laboratory facility to image a wide variety of rock samples and then predict flow properties. The base image is a three-dimensional map of X-ray adsorption; this is thresholded to elucidate different mineralogies, clays and, principally, to distinguish grain from pore space.

The now-standard approach to image the pore-space of rocks is to use a laboratory instrument, a micro-CT scanner, which houses its own source of X-rays. A picture of the inside of our instrument at Imperial College is shown on the front cover of these notes together with the core holder into which a small cylinder of rock is fitted.

Here the X-rays are polychromatic and the beam is not collimated – the image resolution is determined primarily by the proximity of the rock sample to the source. These machines offer the advantage that access to central synchrotron facilities or a custom-designed laboratory is not required, and there is no constraint on the time taken to acquire the image, allowing signal to noise to be improved. The disadvantage is that the intensity of the X-rays is poor compared to synchrotrons while the spreading of the beam and the range of wavelengths introduces imaging artefacts.

The figure on the next page shows two-dimensional cross-sections of three-dimensional grey scale images for eight representative rock samples: several carbonates, including a reservoir sample, a sandstone and a sand pack. The images were acquired either with a synchrotron beamline (SYRMEP beamline at the ELETTRA synchrotron in Trieste, Italy) or from a micro-CT instrument (Xradia Versa).

For the quarry carbonates shown in the figure (Estailades, Ketton, Portland, Guiting and Mount Gambier) a connected pore space is resolved, although the details of the structure are complex and at least two of the samples – Ketton and Guiting – are likely to contain significant microporosity that is not captured. Also included is a carbonate from a Middle Eastern aquifer. In this case, while some pores are shown with a voxel size of almost 8  $\mu\text{m}$ , it is likely that there is significant connectivity provided by pores that are below the resolution of the image.



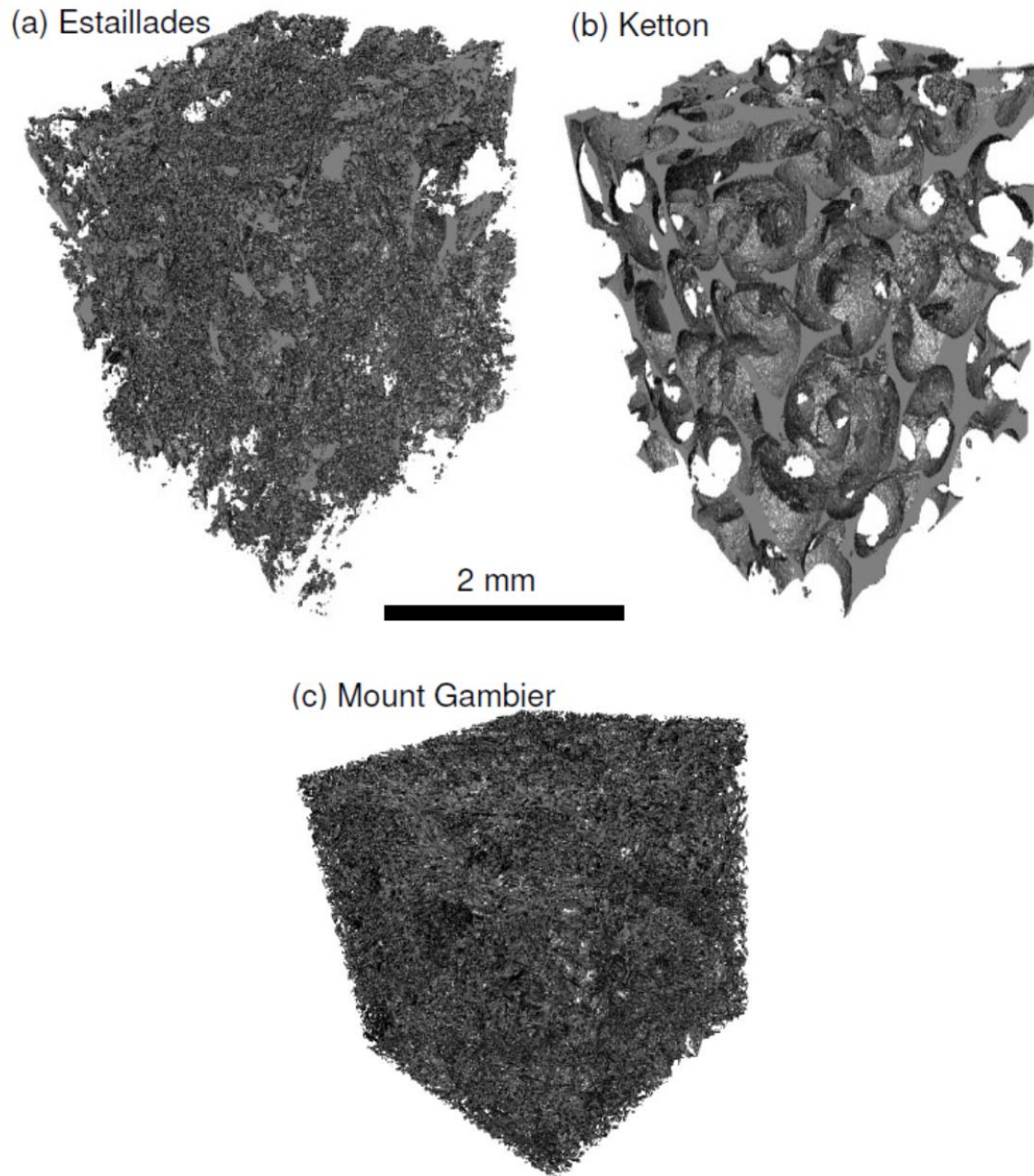
**(Previous page) Two-dimensional cross-sections of three-dimensional micro-CT images of different samples. These are grey scale images where the pore space is shown dark. (a) Estailades carbonate. The pore space is highly irregular with likely micro-porosity that cannot be resolved. (b) Ketton limestone, an oolitic quarry limestone of Jurassic age. The grains are smooth spheres with large pore spaces. The grains themselves contain micro-pores that are not resolved. (c) Mount Gambier limestone is of Oligocene age from Australia. This is a high-porosity, high-permeability sample with a well-connected pore space. (d) A sand pack of angular grains. (e) Bentheimer sandstone, a quarry stone used in buildings, including the pedestal of the Statue of Liberty in New York. (f) Portland limestone. This is another oolitic limestone of Jurassic age that is well-cemented with some shell fragments. Portland is another building material used, for instance, in the Royal of School of Mines at Imperial College. (g) Guiting carbonate is another Jurassic limestone, but the pore space contains many more shell fragments and evidence of dissolution and precipitation. (h) Carbonate from a deep highly-saline Middle Eastern aquifer. The final figure (bottom) is a three-dimensional view of the Estailades limestone.**

I now show, overleaf, example three-dimensional images of three carbonates where only the pore space is shown. Ketton is a classic oolitic limestone composed of almost spherical grains with large, well-connected pores between them. Estailades has a much more complex structure with some very fine features that may not be fully captured by the image. Mount Gambier has a very irregular pore space, but it is well connected and the porosity and permeability are very high. Overall, while a resolution of a few microns can resolve the pore space for some permeable sandstones and carbonates, many carbonates and unconventional sources, such as shales, contain voids that have typical sizes of much less than a micron.

Typical X-ray energies are in the range 30-160 keV for micro-CT machines – with corresponding wavelengths 0.04-0.01 nm – while synchrotrons have beams of different energies for which those with energies less than around 30 keV are ideal for imaging. Resolution is determined by the sample size, beam quality and the detector specifications; for cone-beam set-ups (in laboratory-based instruments) resolution is also controlled by the proximity of the sample to the beam, while detecting adsorption at a sufficiently fine resolution. Current micro-CT scanners will produce images of around  $1000^3$ - $2000^3$  voxels. To generate a representative image, the cores are normally a few mm across, constraining resolution to a few microns; sub-micron resolution is possible using specially designed instruments and smaller samples. Developments



in synchrotron imaging may allow much larger images to be acquired, but at present most images have an approximately 1000-fold range from resolution to sample size.

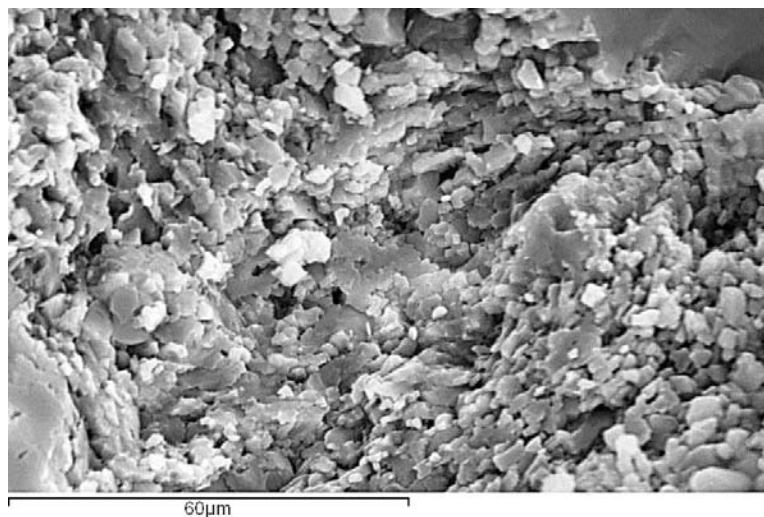
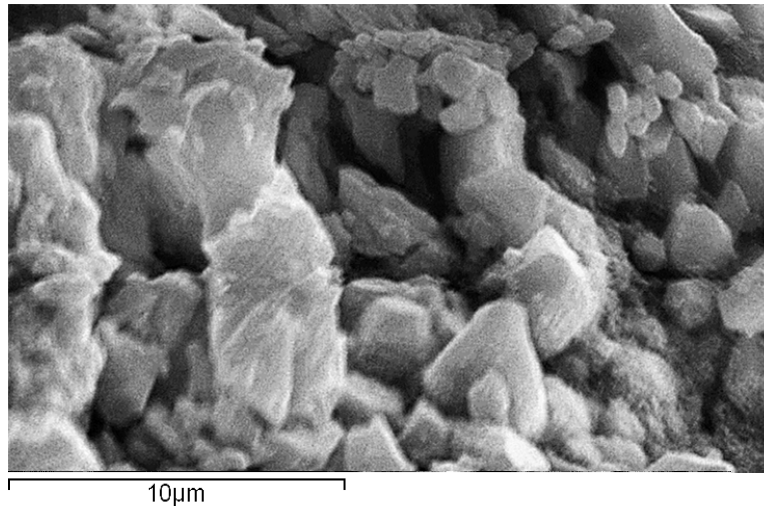


**Pore-space images of three quarry carbonates: (a) Estailades; (b) Ketton; (c) Mount Gambier. The images shown in cross-section in Figures 1(a), (b) and (c) have been binarized into pore and grain. A central  $1000^3$  (Estailades and Ketton) or  $350^3$  (Mount Gambier) section has been extracted. The images show only the pore space.**

## 4.2 ELECTRON MICROSCOPY TO IMAGE MICRO-POROSITY

---

Micro-porosity – small pores typically within larger grains – can be imaged using electron microscopy techniques. The figure below shows images of Ketton and Indiana showing small pore spaces, smaller than 1 micron ( $\mu\text{m}$ ), that are generally below the resolution of micro-CT scanners, but which may contribute significantly to the connectivity and porosity of the rock.



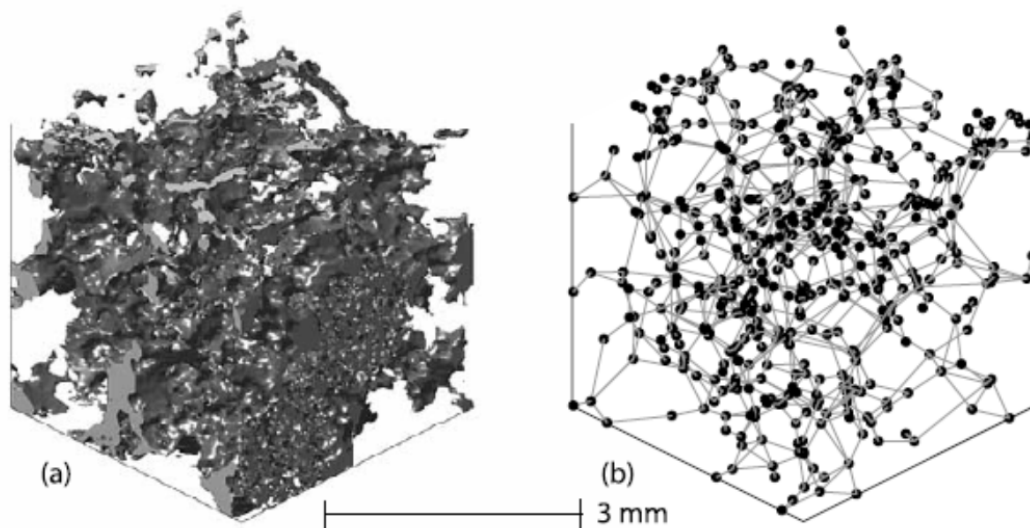
**Scanning electron microscope images for Ketton limestone (*top*) and Indiana limestone (*bottom*) at 2000x and 4000x magnification respectively, showing micro-porosity: small pores within larger grains.**

### 4.3 TOPOLOGICALLY REPRESENTATIVE NETWORKS

---

The final conceptual step is to describe the pore space of the rock in terms of a network. This is a topologically representative description of the pore space, where the larger voids between grains are called pores and these pores are connected together through narrower connections, called throats. Each pore and throat in reality has a complex shape in cross-section, but we will describe these – for simplicity – as triangles. This allows the wetting phase to reside in the corners of the pore space while the non-wetting phase occupies the centres. This way of viewing the rock allows us to understand multiphase flow and – in some cases – make quantitative predictions of flow and transport properties. I will not go through the details of how a network is extracted – there are several different methods to do this; I will simply show some illustrative examples.

The figure below shows the pore space and network for Berea sandstone, a benchmark used for many experiments and modelling studies.



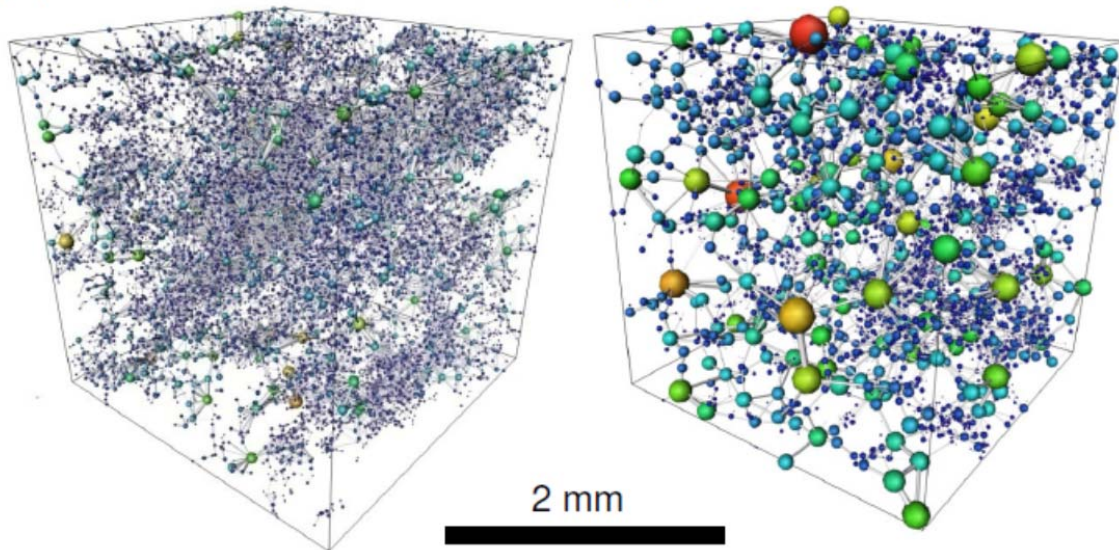
**Figure showing (a) the void space of a simple sandstone (Berea) and (b) the associated topologically representative network of pores and throats.**

The next figure shows the more complex networks for carbonates – based on the images shown previously.

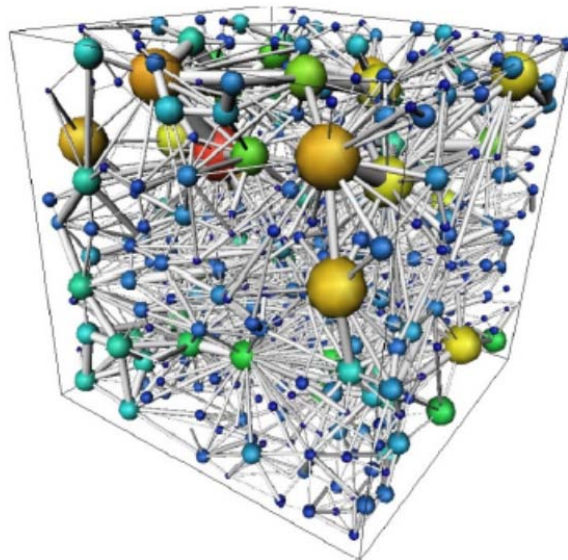


(a) Estailades

(b) Ketton



(c) Mount Gambier



Pore networks extracted from the images shown previously: (a) Estailades; (b) Ketton; (c) Mount Gambier. For illustrative purposes, only a section of the Mount Gambier network is shown. The pore space is represented as a lattice of wide pores (shown as spheres) connected by narrower throats (shown as cylinders). The size of the pore or throat indicates the inscribed radius. The pores and throats have angular cross-sections – normally a scalene triangle – with a ratio of area to perimeter squared derived from the pore-space image.

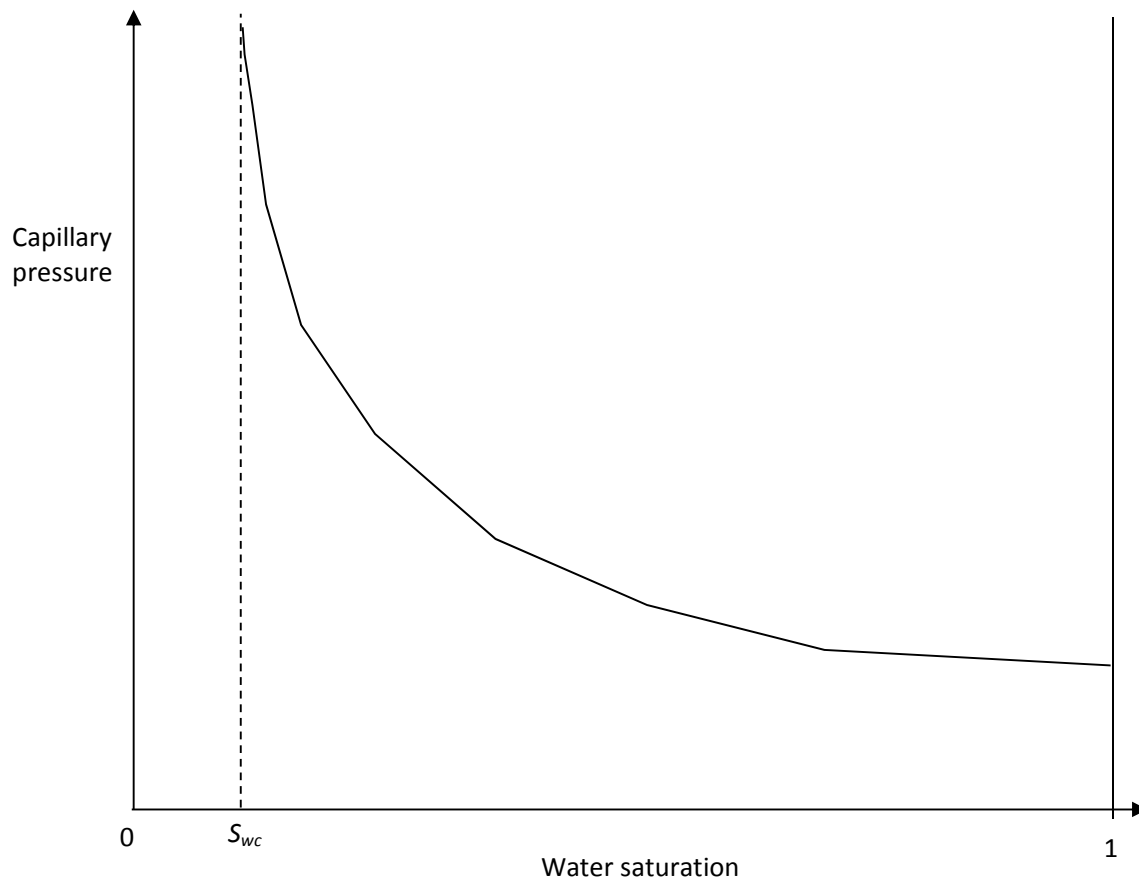
## 5. PRIMARY DRAINAGE

---

Now consider a porous medium that is initially fully saturated with water, and is water-wet. Then a non-wetting phase (oil) enters the porous medium. Imagine that this is done sufficiently slowly that the pressure drop across the oil (from Darcy's law, described later) is small in comparison with the capillary pressure. This process is called primary drainage and is the process by which oil migrates from source rock to fill a reservoir. It is also the process by which injected carbon dioxide displaces brine in a storage aquifer.

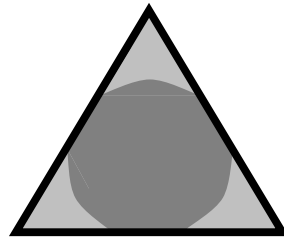
If we return to the Young-Laplace equation (6.1), the non-wetting phase will preferentially fill the larger pore spaces: for these the radius of curvature for the meniscus is larger, resulting in a lower capillary pressure. A lower capillary pressure means that – for a given wetting phase pressure – a lower non-wetting phase pressure for invasion. As the non-wetting phase pressure is increased, smaller regions of the pore space (lower radii of curvature) can be accessed. As a consequence, primary drainage proceeds as a sequence of filling events, accessing progressively smaller pores. In a network representation, filling pores is easy, since they are larger than the connecting throats. Hence, the invasion of the non-wetting phase is limited by the throat radius. The non-wetting phase will next fill the largest-radius throat that is connected to a pore already filled with non-wetting phase. This largest throat and the adjoining pore fill, and then again the largest-radius throat is filled. This is technically known as an invasion percolation process. There are subtleties associated with trapping the wetting phase (how does the water escape), but this is a good model of primary drainage and motivates why a network representation of the pore space is useful for the understanding of fluid displacement.

At a macroscopic – core – scale, if we average the behaviour over millions of individual pores and throats, we can plot the capillary pressure (the pressure difference between the phases) as a function of water saturation.



**Schematic of the primary drainage capillary pressure. Experimental examples will be shown later.  $S_{wc}$  is the connate or irreducible water saturation.**

The oil invades progressively smaller regions of the pore space. We find a connate or irreducible water saturation  $S_{wc}$  where further increases in capillary pressure result in little or no decrease in water saturation. At this point the water may either be trapped in wetting rings around rock grains, or (more likely) contained in roughness, grooves and corners of the pore space. While, in theory, this water could be displaced, it would require a huge amount of time and a very high capillary pressure to do so.



**Schematic of oil in the centre of the pore space and water in the corners at the end of primary drainage.**

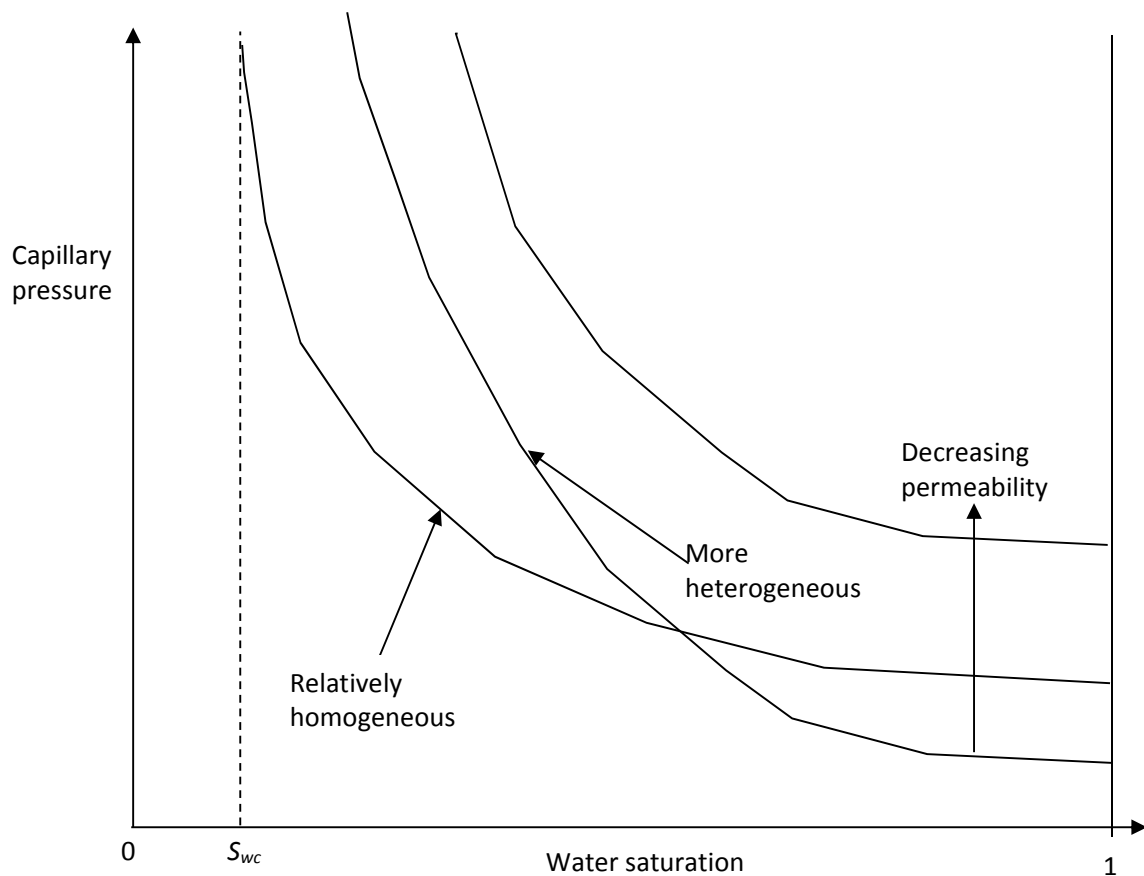
During and after primary drainage, regions of the pore space that come in direct contact with oil may alter their wettability as described before.

### 5.1 TYPICAL VALUES OF THE CAPILLARY PRESSURE

---

In most reservoir sandstones pore sizes  $R$  are in the range  $1 - 100 \mu\text{m}$  – see the previous pore-space images.  $P_c \approx 2\sigma/R$  (see section 6 – assuming a contact angle close to zero).  $\sigma_{ow} \approx 50 \text{ mN/m}$  for say alkane/water.  $P_c$  is around  $0.1/R$  or in the range  $10^3 - 10^5 \text{ Pa}$ . These values are higher for mercury/air, since  $\sigma$  is higher.

The figure below shows the effect of heterogeneity and permeability on the capillary pressure: lower permeability normally reflects smaller pore (throat) sizes and a higher capillary pressure, while a more heterogeneous structure leads to a wider range of capillary pressures as more of the pore space is invaded.

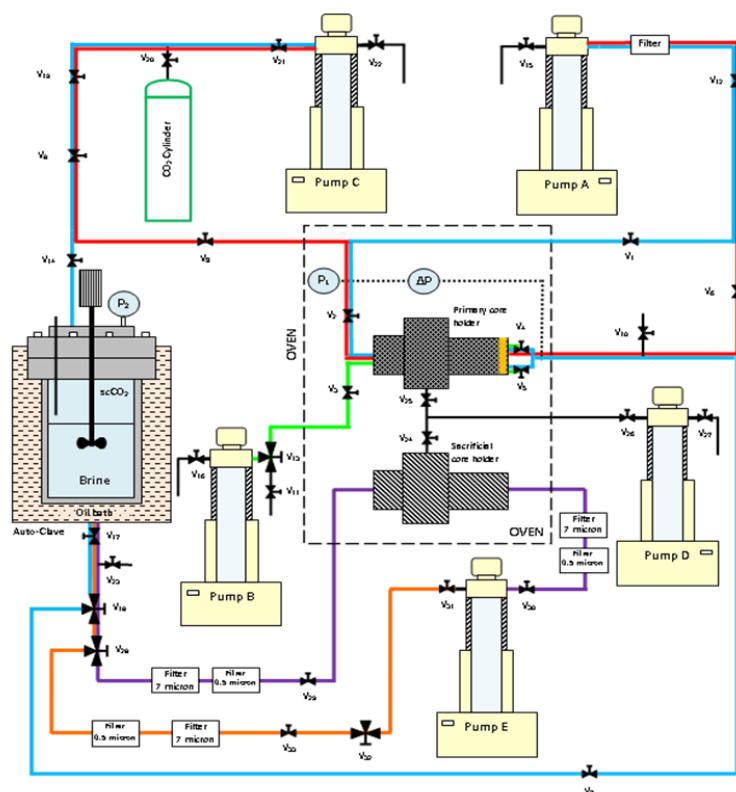


**Schematic of the primary drainage capillary pressure showing the effect of permeability and heterogeneity in the pore size distribution.**

## 5.2 HOW IS CAPILLARY PRESSURE MEASURED?

The standard method to measure primary drainage capillary pressure is through mercury injection. Here a small, dry rock sample – usually around 5 mm across – is placed under vacuum and then mercury is injected as the non-wetting phase. The volume of mercury that enters the rock sample is recorded as a function of the imposed pressure. Here we do not see any irreducible saturation, so the mercury can, in theory, invade the entire (connected) pore space.

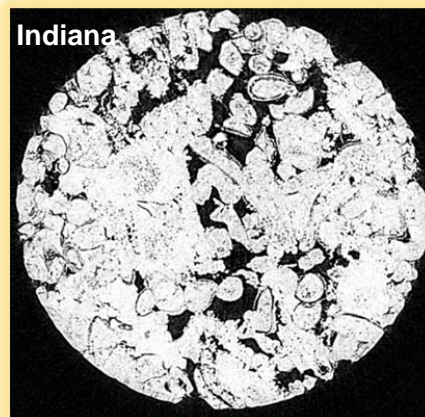
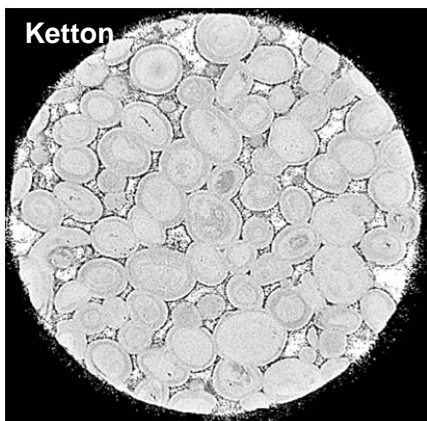
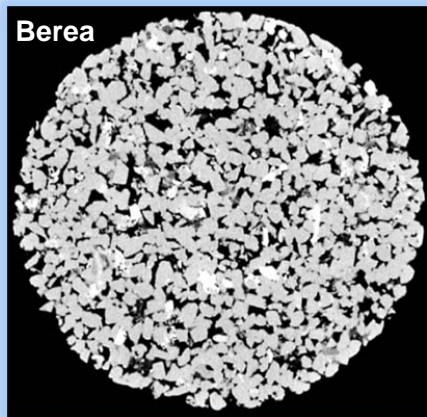




An apparatus to measure displacement and capillary pressure in a rock sample. This apparatus is designed specifically to study displacements involving carbon dioxide. The upper picture shows a picture of the apparatus at Imperial College, while the lower diagram shows the apparatus and flow loops. Note the complexity of the experiment: flow is controlled through pumps and each displacement cycle takes many days to complete, reproducing the slow flow conditions usually seen in reservoirs (from Rehab Al-Maghraby's PhD thesis, 2013).

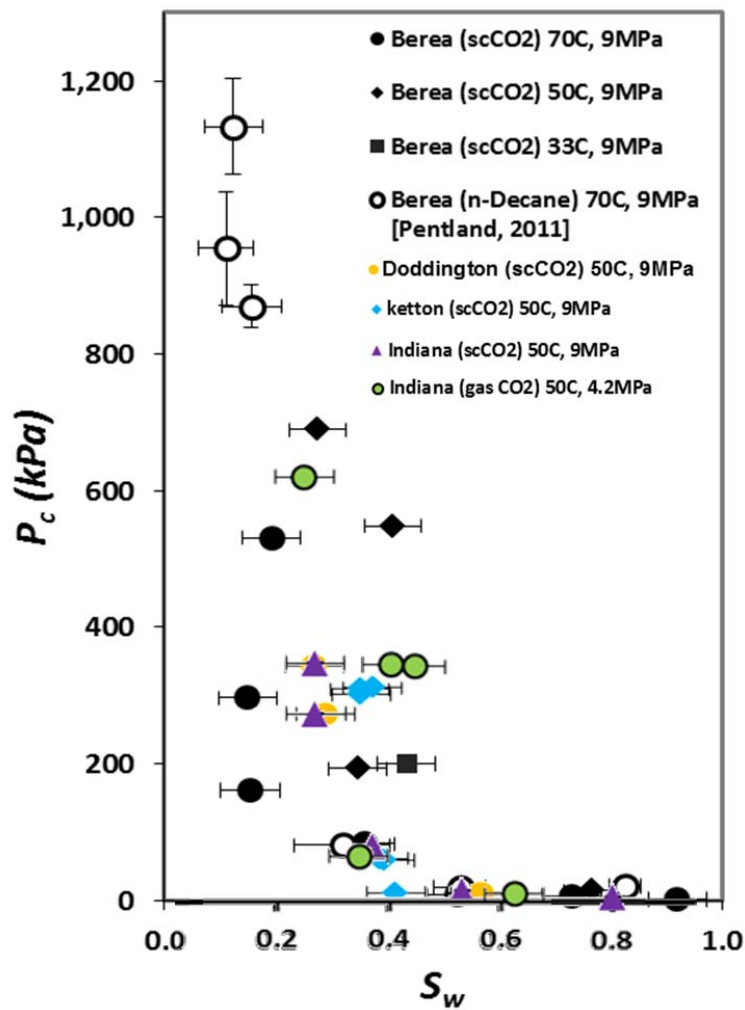
It is also possible to measure capillary pressure on experiments with two fluids – such as water and oil – although this is more difficult. Later I will show some mercury injection capillary pressure curves measured on different rock samples. I will also present capillary pressures measured when a core is initially fully saturated with brine and then oil (or carbon dioxide) is injected at some known pressure and the volume that is injected is recorded. There is a porous plate at one end – essentially a ceramic disc with a very high capillary pressure – that prevents any injected non-wetting phase leaving the system.

To help illustrate the results, overleaf I show pictures of the rock samples studied taken with X-rays at a resolution of around 7 microns, where the pore space is clearly visible. We have seen some of these samples previously. Then the measured capillary pressures for primary drainage are shown: the apparatus was shown above. Note how there is a region of relatively low pressure when the non-wetting phase invades the larger pores followed by a steep rise where smaller and smaller pores and throats are invaded. The magnitude and shape of the curve is an indicator of pore size and structure.



	Length (mm)	Width (mm)	Porosity, $\phi$	$K_{brine} \text{ (m}^2\text{)}$	$K_{brine} \text{ (mD)}$
Berea	75.16	38.24	0.2188	$4.6 \times 10^{-13}$	460
Doddington	76.44	38.24	0.214	$1.565 \times 10^{-12}$	1565
Ketton	76.5	37.78	0.2337	$2.81 \times 10^{-12}$	2809
Indiana	76.49	37.84	0.1966	$2.4 \times 10^{-13}$	244

**Micro-CT images of four rock samples on which capillary pressure was measured. The table shows their properties. Note how the trend is permeability is evident from the grain sizes.**



Measured primary drainage capillary pressure: note how the magnitude of the pressure relates to the average pore size, evident in the micro-CT images.

## 6. IMBIBITION

---

Imbibition is the opposite process to drainage, where wetting fluid invades a porous medium containing non-wetting fluid. We normally only consider secondary imbibition, which is the invasion of wetting fluid into non-wetting fluid after primary drainage. That is, there is some wetting fluid initially present in the porous medium. This is the process that occurs when water is injected to displace oil in a reservoir, when the aquifer encroaches into a gas field during production, or when brine displaces stored carbon dioxide, as the carbon dioxide rises in the storage aquifer.

The capillary pressure for imbibition is always lower than for primary drainage. There are three reasons for this:

- trapping of non-wetting fluid;
- contact angle hysteresis;
- different displacement mechanisms at the pore scale.

In drainage, the non-wetting fluid advances through the porous medium by a connected piston-like advance. That is, regions can only be filled with non-wetting fluid if they are adjacent to a region that also contains non-wetting fluid. Both wetting and non-wetting phases remain connected.

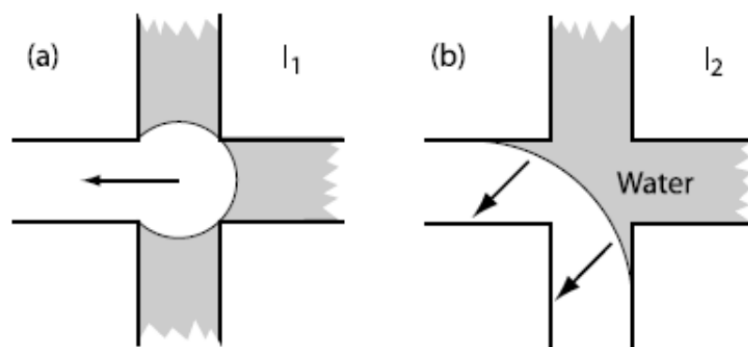
### 6.1 PORE-SCALE DISPLACEMENT, TRAPPING OF THE NON-WETTING PHASE AND SNAP-OFF

---

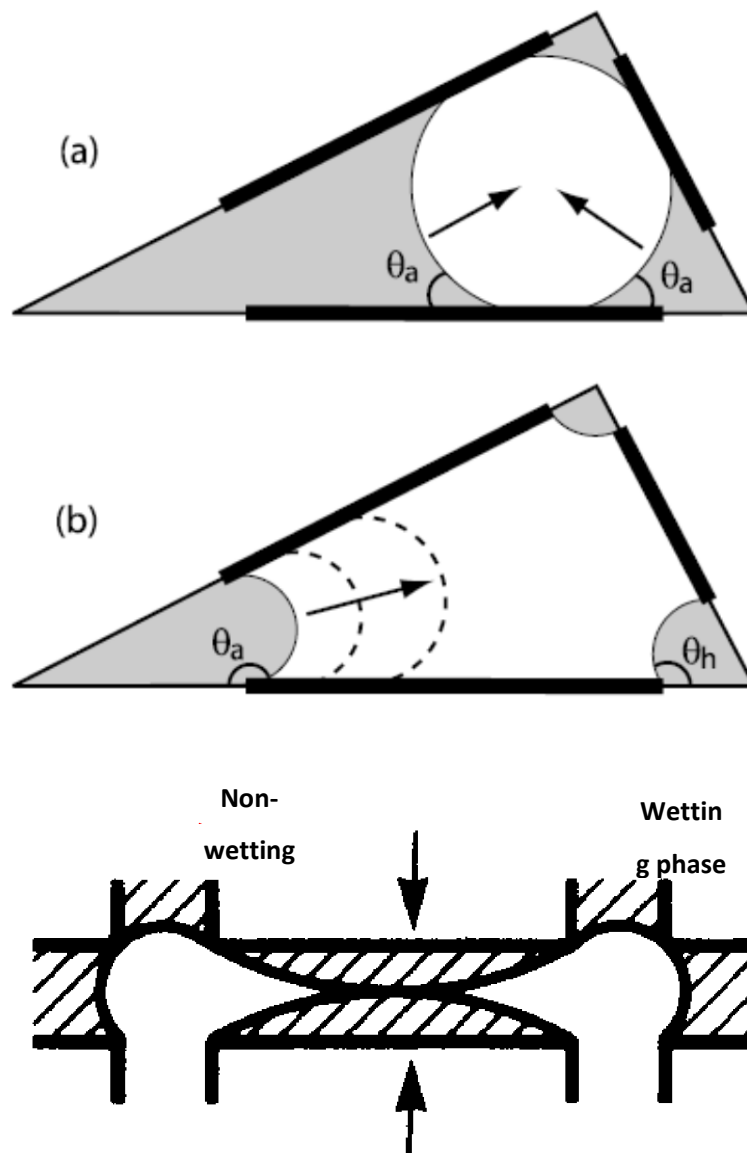
In imbibition, it is possible for the wetting phase to trap the non-wetting phase. This is through bypassing and snap-off. Bypassing is when invading fluid surrounds and strands a ganglion of non-wetting phase: this occurs due to local inhomogeneities in the pore structure (or local capillary pressure). However, the more important process is snap-off. Here water flows through wetting layers and fills narrow regions of the pore space in advance of the main wetting front. This is the principal mechanism by which non-wetting phase is surrounded and trapped.

For reference I show some schematic pictures of pore-scale displacement below. As the pressure in the wetting phase increases, wetting layers in the pore space thicken. There comes a point at which the meniscus between the wetting and non-wetting phases loses contact with the solid – it is no longer possible to place the interface in the pore space. At this point, the throat fills rapidly with wetting phase.

In imbibition, piston-like advance is favoured in the narrow throats, but impeded by the wide pores (the water wants to be in the narrow regions of the pore space). However, there is a subtlety: it is easier (that is the radius of curvature is smaller) for the wetting phase to fill a pore if more of the surrounding throats are also full of water. This is shown in the diagram below: in a series of classic papers Roland Lenormand (Lenormand *et al.*, 1984) described these imbibition processes as  $I_n$ , where the  $n$  refers to the number of connecting throats filled with non-wetting phase.  $I_1$  is more favoured than  $I_2$  which, in turn, is more favoured than  $I_3$ . The result of this, is that – at the pore scale – the wetting front tends to be flat, filling in any local channels filled with non-wetting phase. This tends to suppress trapping. Hence, without snap-off – described next – most of the non-wetting phase is recovered from the porous medium (which is good for oil and gas recovery, but bad for carbon dioxide storage).



**Pore filling processes in water (wetting phase) injection. (a)  $I_1$ , when all but one of the connected throats is full of water. This is the most favourable displacement.  $I_2$ , where two throats are initially filled with oil. This is less favoured as the threshold capillary pressure is lower – the radius of curvature of the interface as it invades is larger.**



The snap-off process. Here water flows along the corners of the pore space. An instability occurs when the wetting layer in the corner loses contact with the surface – any further increase in water pressure leads to the rapid filling of the centre of the throat. (a) Snap-off at a positive capillary pressure (oil pressure greater than the water pressure). (b) Forced snap-off, when the water layer is pinned in the corner: a negative capillary pressure (a higher pressure in the water than the oil) is necessary to force the water over the oil-wet surface. The bottom figure illustrates how the non-wetting phase is pinched-off when viewed along the length of the throat.

In the snap-off process, as the wetting phase pressure increases, the wetting layers in the corners of the pore space swell, as mentioned previously. It is possible that these layers swell to a sufficient thickness that they lose all contact with the solid. This always occurs in the narrowest portions of the pore space – the smallest throats. This creates an unstable configuration, and the wetting phase then rapidly fills the throat. This process only occurs for slow flow – there has to be sufficient time for the wetting phase to flow, slowly, along wetting layers, and for low contact angles. So, all the narrow regions of the pore space – anywhere in the rock – are filled. If we fill all the throats around a pore, then the non-wetting phase in the pore is trapped – it cannot escape. This is the origin of residual saturation, a very important concept in multiphase flow that will be discussed in detail.

As mentioned above, snap-off is favoured for low contact angles, while connected piston-like advance dominates as the contact angle becomes larger (but is still less than  $90^\circ$ , as we only consider water-wet systems here). Eq. (3.5) gave the capillary entry pressure for piston-like advance for invasion of a cylindrical throat of radius  $r$ . We now consider which process is favoured – snap-off or piston-like advance. For snap-off, we do have to have an angular pore. If the pore is square in cross-section, it is easy to calculate the critical radius of curvature at which the meniscus first loses contact with the solid. This gives a critical capillary pressure:

$$P_c = \frac{\sigma}{r} \cos\theta (1 - \tan\theta) \quad (6.1)$$

where  $r$  is now the inscribed radius of the pore (or throat). The ratio of the capillary pressure for snap-off to piston-like advance for the same throat is:

$$\frac{P_{c,snap-off}}{P_{c,piston}} = \frac{1}{2} (1 - \tan\theta) \quad (6.2)$$

This is always less than one. The process with the highest capillary pressure is favoured in imbibition and hence – if possible – piston-like advance will occur rather than snap-off. However, this requires that an adjoining pore is also full of wetting phase, which may not be the case. So, snap-off does occur, but only when pore-filling is suppressed because of the large pore size and different cooperative pore filling mechanisms. This means that porous media with a



large difference between pore and throat sizes will see a lot of snap-off and trapping, while porous media with similar sized pores and throats will see less trapping and a more connected wetting phase advance. Furthermore, Eq. (6.2) indicates that snap-off becomes less favourable as the contact angle increases. This is true even if we include different pore shapes and the effects of cooperative pore filling: as the contact angle increases there is less snap-off and a lower residual saturation.

During imbibition the water pressure *increases*, meaning that the capillary pressure *decreases*. Imbibition ends at a water saturation  $1 - S_{or}$ , where  $S_{or}$  is the residual oil saturation. This residual oil is very important, as it determines how much oil can be recovered from a reservoir. It is also significant in carbon dioxide storage, since this residual is trapped, cannot move and therefore cannot escape back to the surface.

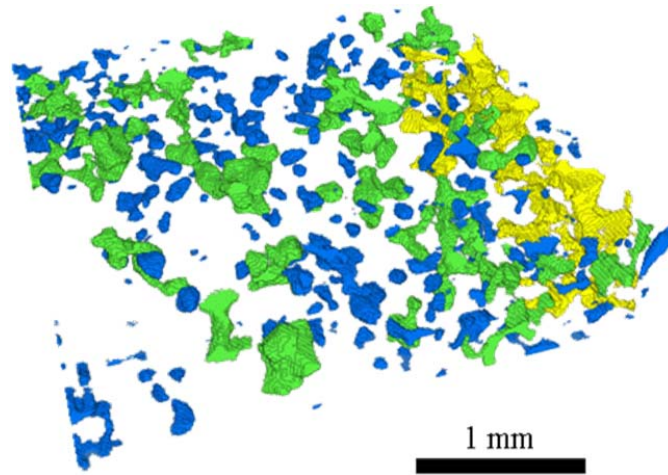
## 6.2 PORE-SCALE IMAGES OF TRAPPED PHASES

---

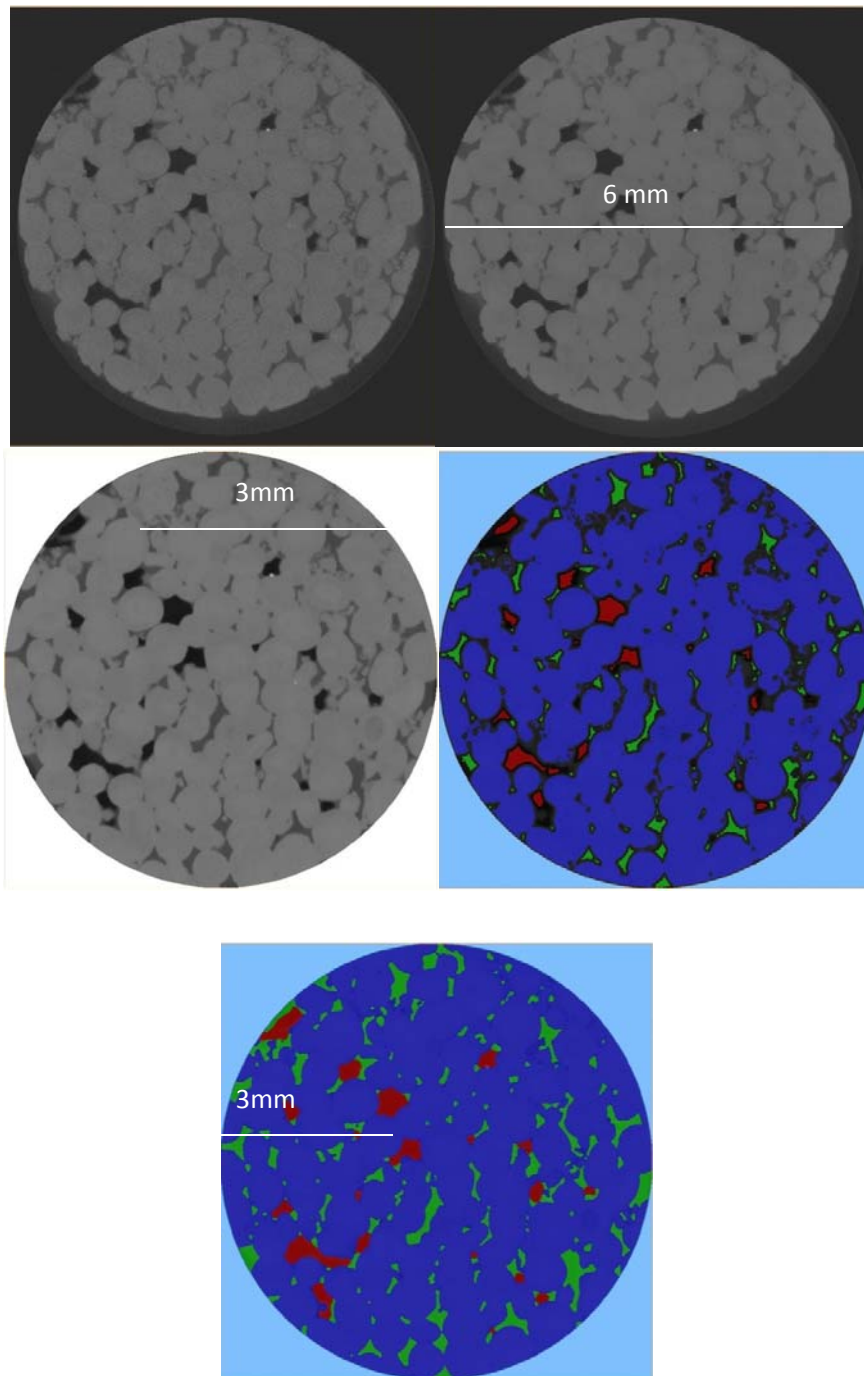
We can image residual saturations directly using micro-CT scanning: the figure overleaf shows these trapped clusters (the non-wetting phase is dense carbon dioxide at high pressures and temperatures) in Doddington sandstone. As mentioned above, the principal process governing the amount of trapping is snap-off.

We can also illustrate the saturation distributions of carbon dioxide after primary drainage and brine injection in a carbonate – Ketton, whose pore space has been shown previously. Last, we show images from different rock samples. In all cases approximately  $2/3^{\text{rds}}$  of the saturation initially present in the pore space is trapped.

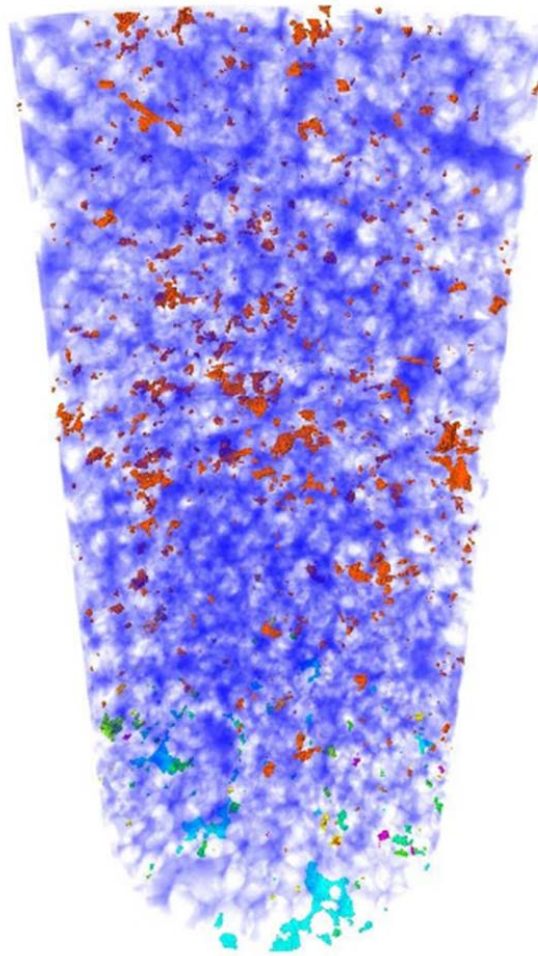
These figures show that ganglia of many sizes are trapped, from clusters filling a single pore to large clusters that almost span the system. Indeed we see an approximately power-law distribution of cluster sizes consistent with percolation theory (Andrew *et al.*, 2013; 2014).



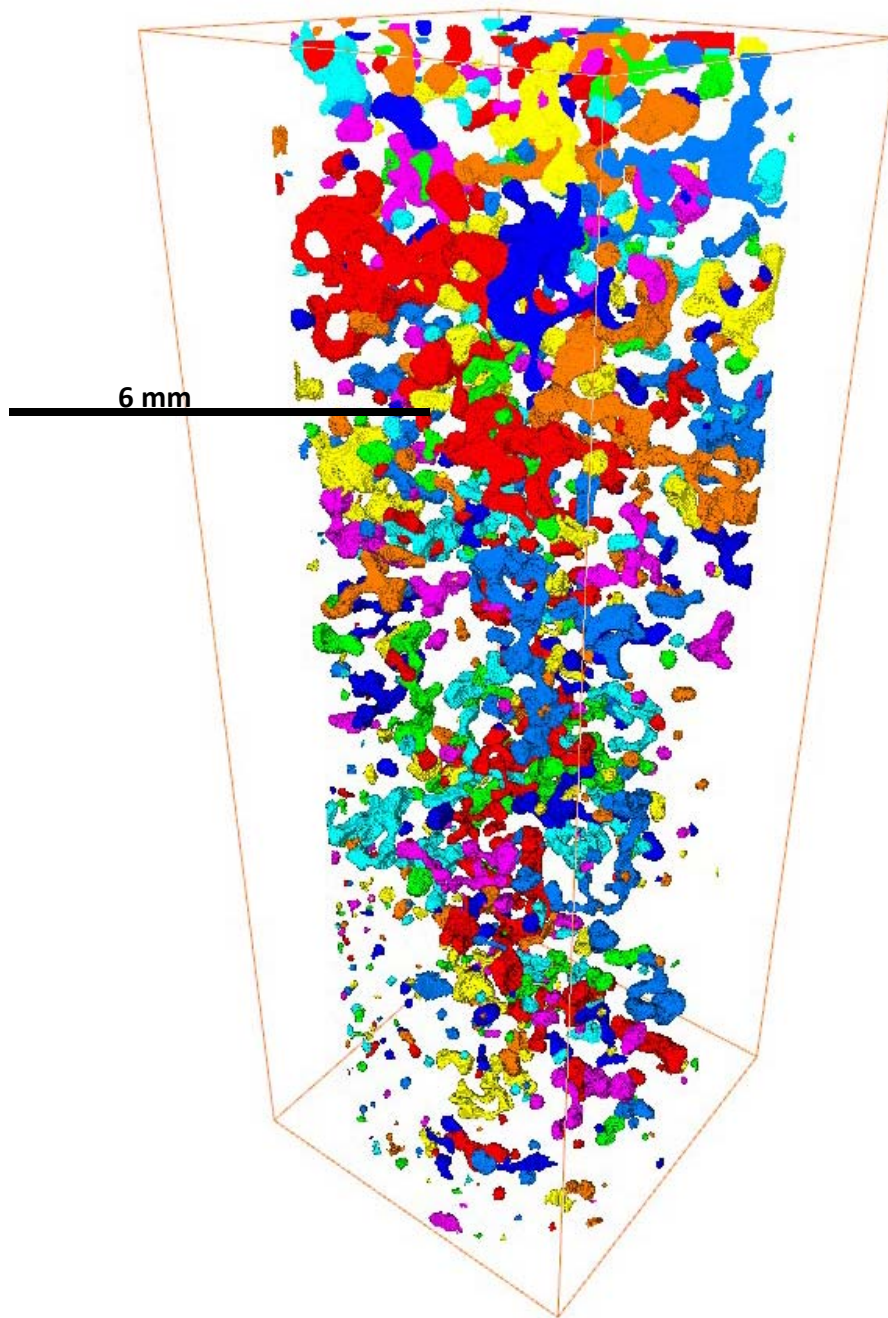
A micro-CT image of Doddington sandstone showing the residual CO<sub>2</sub>. The colours indicate the size of trapped cluster. The image has a resolution of approximately 10 microns and water and rock are not shown. The overall residual saturation is 25% (from Iglauer *et al.*, 2011).



**Image processing, consisting of 4 steps; filtering (A-B), cropping (B-C), watershed seed generation (C-D) and the application of the watershed algorithm (D-E). The raw image (A) shows scCO<sub>2</sub> (the darkest phase), brine (the intermediate phase) and the rock grains (the lightest phase). The rock grains are around 700 $\mu$ m across. (from Andrew *et al.*, 2013).**

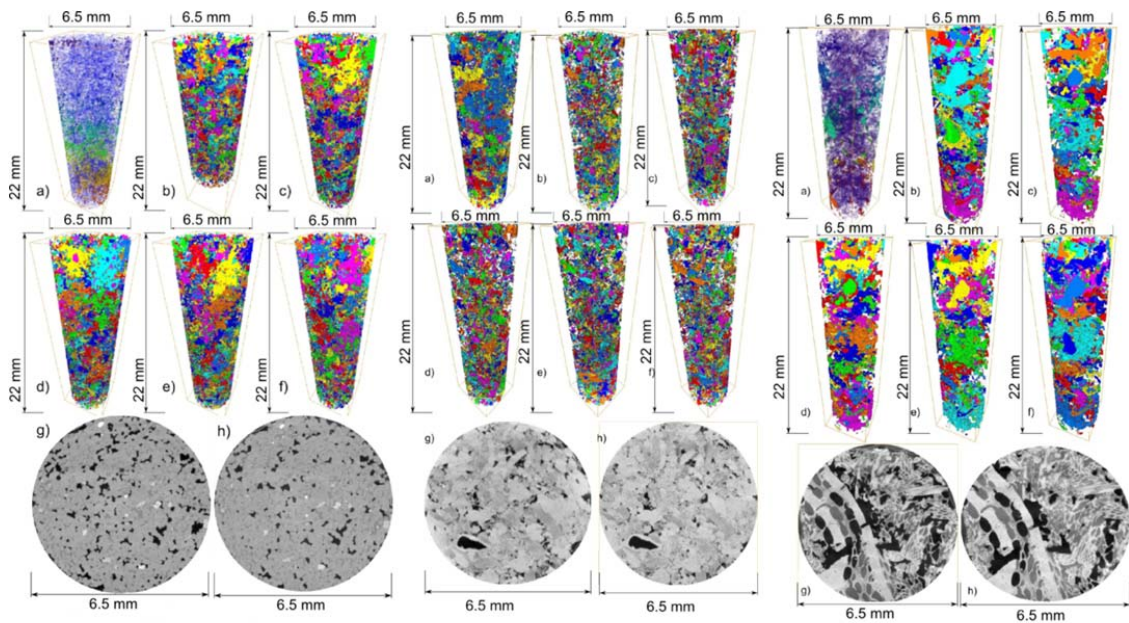


**Visualization of the fluids in the pore space of Ketton limestone at the end of primary drainage. The pale blue represents a connected cluster of non-wetting phase (carbon dioxide, CO<sub>2</sub>, as a dense, supercritical phase, at high pressure and temperatures, typical of conditions in a deep storage aquifer). The other colours represent smaller disconnected clusters of the carbon dioxide (Andrew *et al.*, 2013).**



**Three-dimensional rendering of CO<sub>2</sub> after brine injection. Each unique CO<sub>2</sub> ganglion is displayed as a different colour. Each ganglion is isolated, and so is trapped (Andrew *et al.*, 2013).**

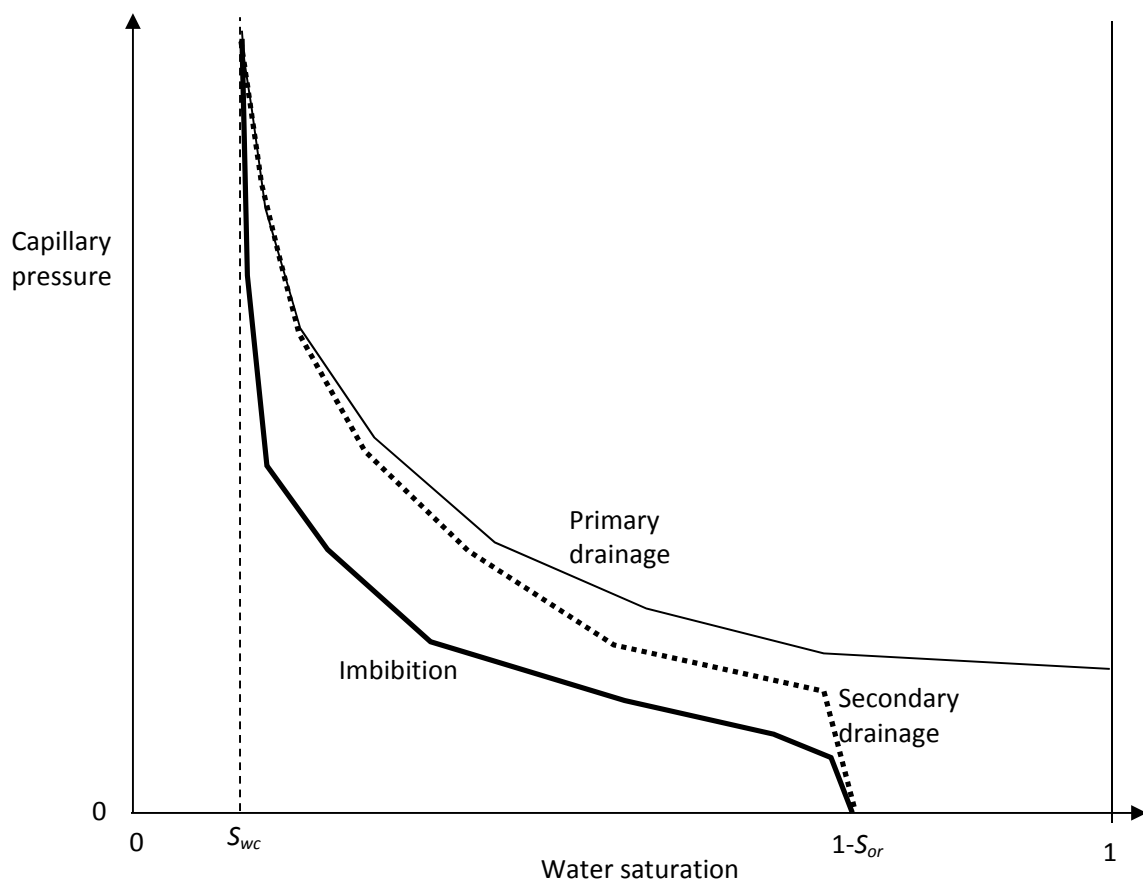




Three-dimensional rendering of CO<sub>2</sub> after brine injection. Each unique CO<sub>2</sub> ganglion is displayed as a different colour. Each ganglion is isolated, and so is trapped. Left Bentheimer sandstone, middle Estailades limestone, right Mount Gambier limestone. The results from five experiments from each rock type are shown: the top left image shows the fluid distribution after primary drainage, while the other five are shown after waterflooding. The bottom row shows two-dimensional slices of the raw images. From Andrew *et al.* (2014).

### 6.3 TYPICAL CAPILLARY PRESSURE CURVES AND SECONDARY DRAINAGE

The final sequence of saturation change is secondary drainage, where non-wetting fluid re-invades the porous medium after imbibition. Typical capillary pressure curves for the flooding sequence – primary drainage, waterflooding (imbibition in this case) and secondary drainage – are shown for a water-wet rock.



**Illustrative capillary pressure curve showing primary drainage, imbibition and secondary drainage.**

Why is the capillary pressure for secondary drainage lower than for primary drainage? This has to do with the trapped non-wetting phase that becomes reconnected during secondary drainage. Rather than think of the curve as being lower, consider the secondary drainage shifted along the saturation axis, to represent the trapped saturation.

The key features to note in the capillary pressure are the irreducible wetting phase saturation, the residual non-wetting phase saturation, the shapes of the curves and their relative magnitude.

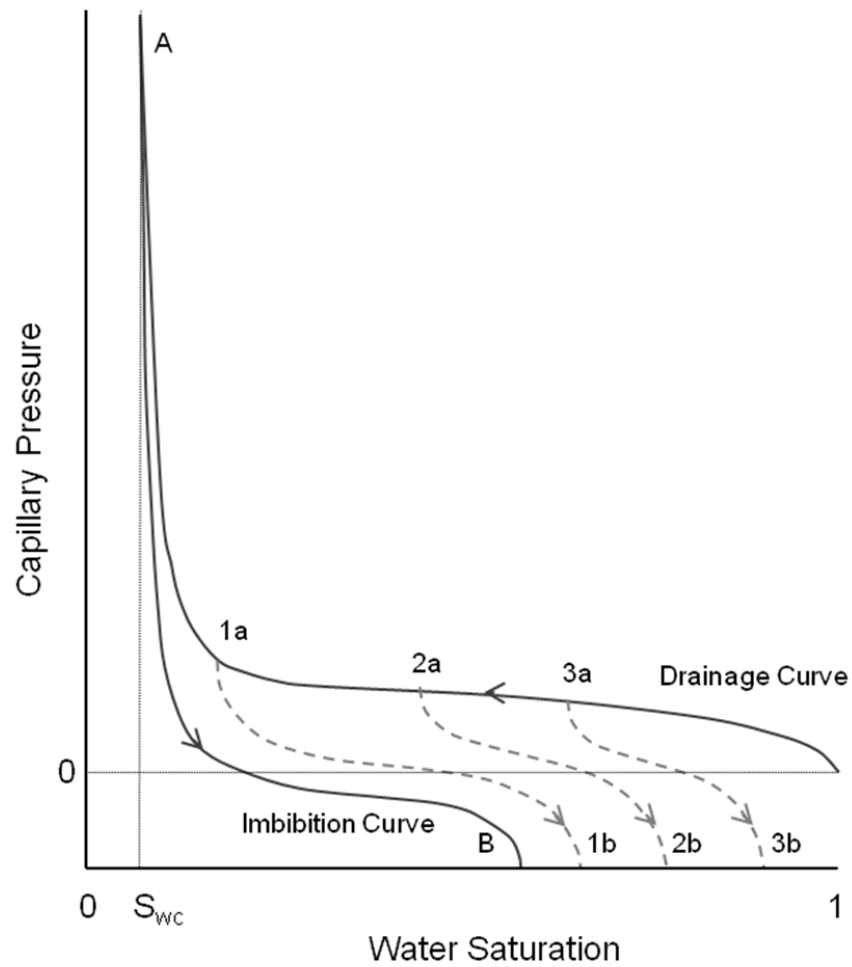
#### 6.4 DIFFERENT DISPLACEMENT PATHS AND TRAPPING CURVES

---

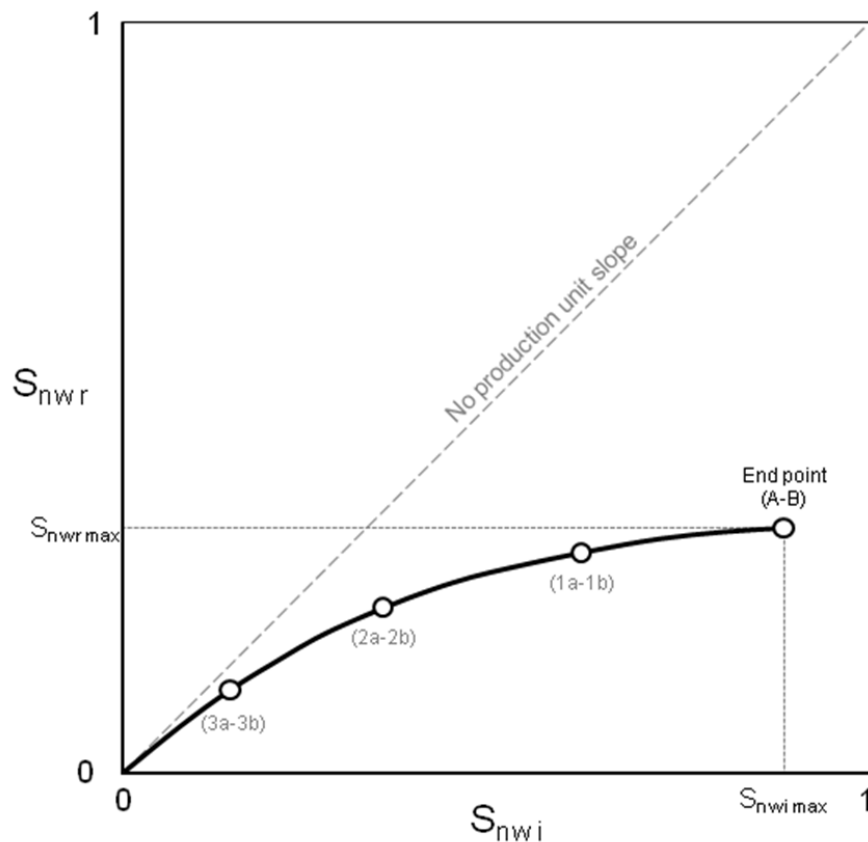
The figure below shows a schematic of different saturation paths, where the non-wetting phase is injected to an initial saturation and then wetting phase is injected. The amount of trapping depends on the initial saturation: as the non-wetting phase invades progressively more of the pore space, there are more places where it can be trapped. This phenomenon is observed in the transition zone of oil fields (discussed later) and during carbon dioxide (CO<sub>2</sub>) injection, where it is unlikely that the injected CO<sub>2</sub> will completely fill the pore space everywhere.

The physical picture is as follows. During primary drainage the non-wetting phase fills progressively smaller portions of the pore space. If primary drainage stops at some intermediate saturation, then only the larger pores have been filled. During water flooding (imbibition), trapping occurs preferentially in the larger pore spaces. Hence, the more of these pores that have been filled initially with non-wetting phase, the more that can be trapped. However, notice the characteristic curvature of the trapping curve (the relationship between initial and residual saturation shown in the subsequent figure): at low initial saturations, only the very largest pores are invaded and these are trapped, so the curve has a slope of almost one (which represents everything being trapped), but the slope decreases with initial saturation. When the initial saturation is high, only small pores are being filled and these contribute very little to the overall amount of trapping.



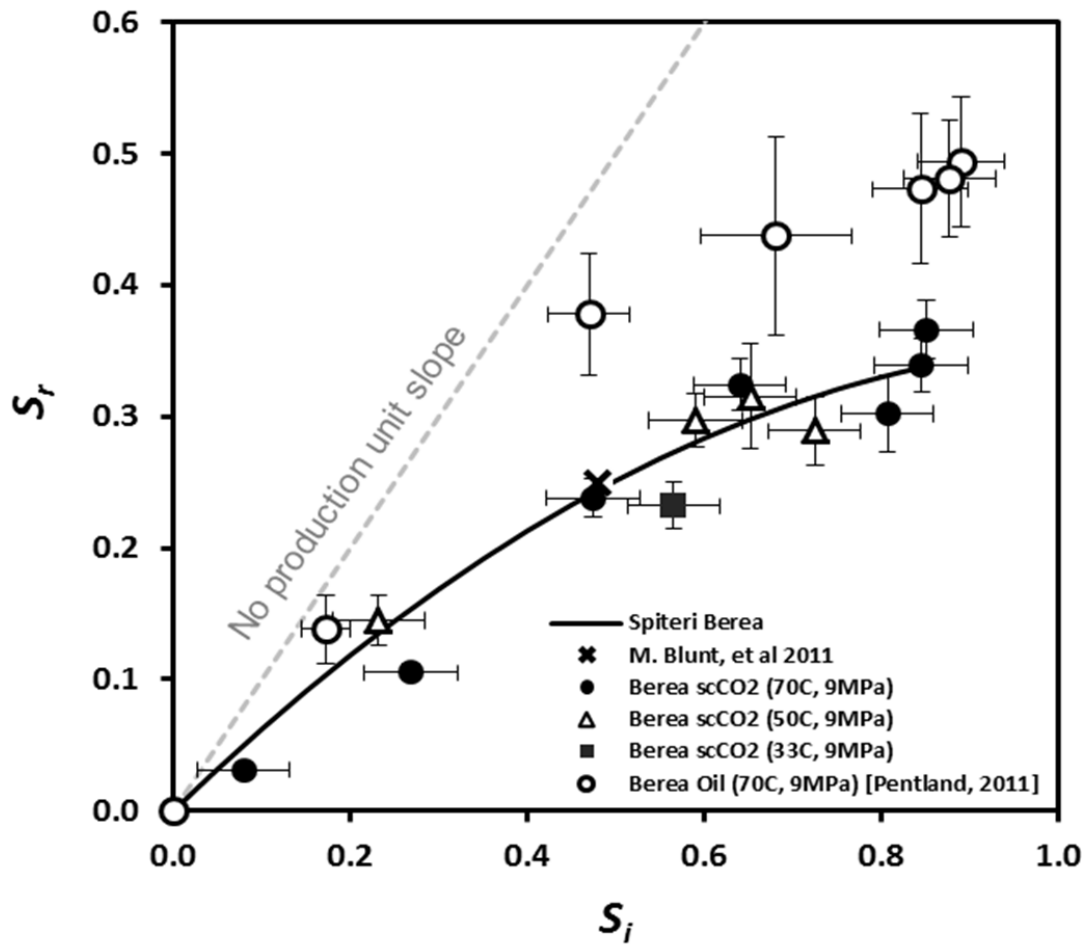


A schematic of primary drainage and imbibition capillary pressure curves where primary drainage ends at different initial saturations. This in turn determines the amount trapped during subsequent imbibition (water flooding).



**The trapping curve – the relationship between initial and residual non-wetting phase saturation – based on the capillary pressure curves shown previously.**

The next figure shows an experimentally-measured trapping curve for Berea sandstone from the Imperial PhD thesis of Rehab Al-Maghraby (see also Al-Maghraby and Blunt, 2012). The upper set of points are for an oil/water system which is assumed to be strongly water-wet with lots of trapping. Less trapping is observed when the non-wetting phase is super-critical (sc) carbon dioxide: here it is hypothesized that the contact angles are larger, representing a weakly water-wet system that has, consequently, less snap-off.



An experimentally-measured trapping curve for Berea sandstone, comparing the relationship for an oil/water system and one with supercritical (high pressure) CO<sub>2</sub> and brine. Less non-wetting phase is trapped for the CO<sub>2</sub> system implying higher contact angles in this case.

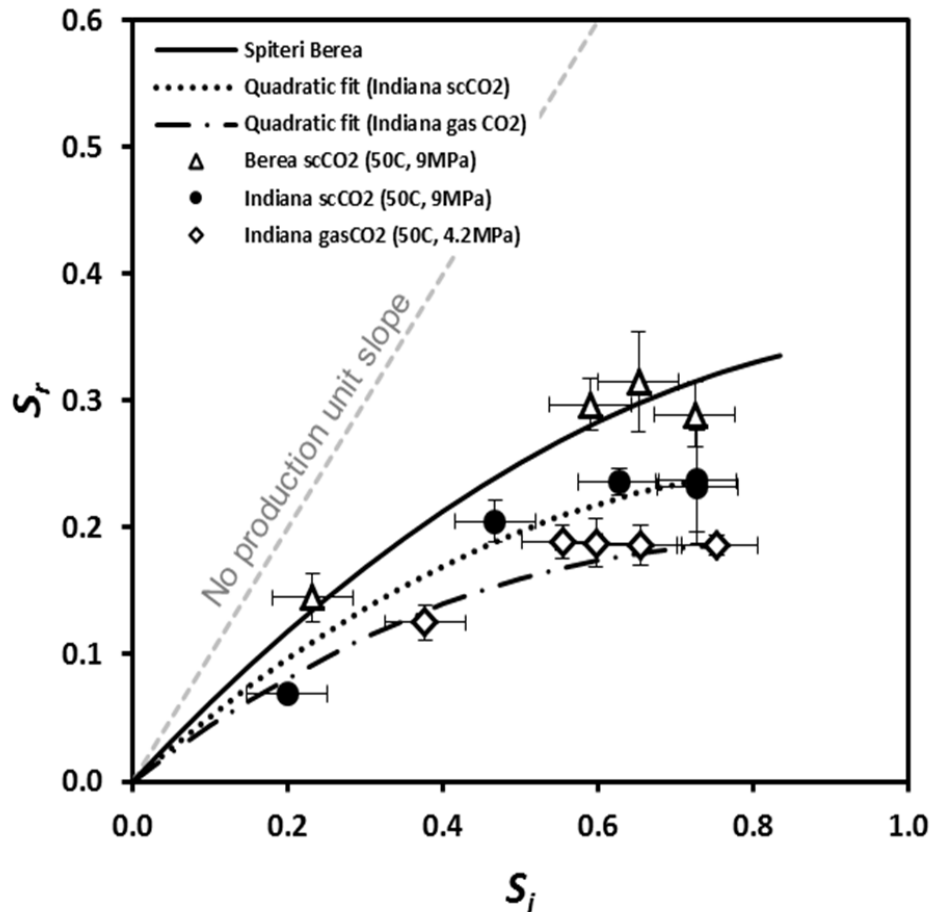
Trapping curves are normally fit by empirical curves: these have no physical significance, but are a convenient way to make sense of the data and provide convenient input into numerical reservoir simulators. The most used model is due to Land (1968) and was originally developed for the trapping of gas. The residual saturation is written:

$$S_r^* = \frac{S_i^*}{1 + CS_i^*} \quad (6.3)$$

where  $C$  is a constant fit to the data and  $S^*$  is a normalized saturation, defined by:

$$S^* = \frac{S}{1 - S_{wc}} \quad (6.4)$$

where  $S_{wc}$  is the connate or irreducible water saturation.



An Berea,  
with supercritical (high pressure) CO<sub>2</sub> as the non-wetting phase. Here – in contrast to Berea - more non-wetting phase is trapped for the CO<sub>2</sub> system (El-Maghraby and Blunt, 2012).

Another model by Spiteri *et al.* (2008) – used in the figures above to match the data – is to assume a quadratic (parabolic) match as follows:

$$S_r = \alpha S_i - \beta S_i^2 \quad (6.5)$$

where  $\alpha$  and  $\beta$  are parameters chosen to reproduce the data.

As discussed above, in general, less trapping implies less snap-off and hence a less strongly water-wet system (larger contact angles). When the system becomes oil-wet or mixed-wet, we see a different behaviour which is discussed later.

## 7. LEVERETT J FUNCTION

---

This is a way of expressing the capillary pressure in dimensionless form, which takes account for different average pore size and interfacial tensions. This is a very useful scaling for dealing with laboratory measurements that may be performed with fluid pairs and at conditions – in terms of average porosity and permeability – different from in the field.

The capillary pressure is written as follows:

$$P_c(S_w) = \sqrt{\frac{\phi}{K}} \sigma \cos \theta J(S_w) \quad (7.1)$$

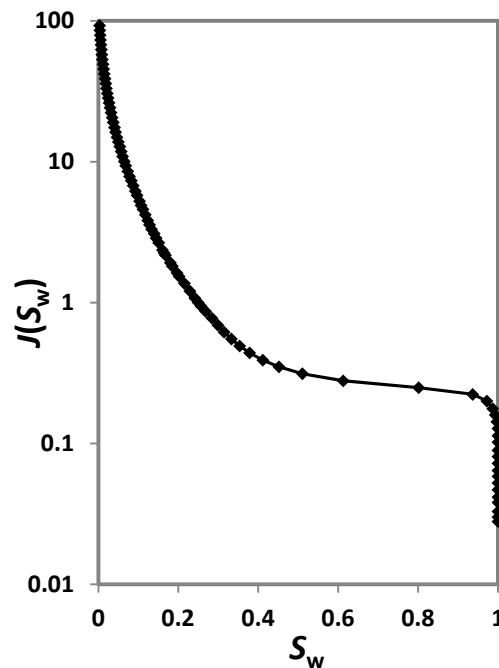
$J$  is the dimensionless J-function, which is a function of saturation (as is capillary pressure). The motivation behind this expression is the capillary pressure for a single tube, Eq. (3.5), where a typical pore radius is written as  $\sqrt{(K/\phi)}$ . This last expression can be derived from considering a bundle of capillary tubes of radius  $R$  a distance  $d$  apart.

The  $J$  function only includes information about the geometry of the porous medium.

Sometimes the  $\cos \theta$  term is ignored, and it is assumed that the system is strongly water-wet ( $\cos \theta = 1$ ) for primary drainage. For imbibition, the  $\cos \theta$  scaling is no longer appropriate, since other displacement mechanisms (snap-off and cooperative pore filling) control the behaviour and the contact angle term is always neglected.

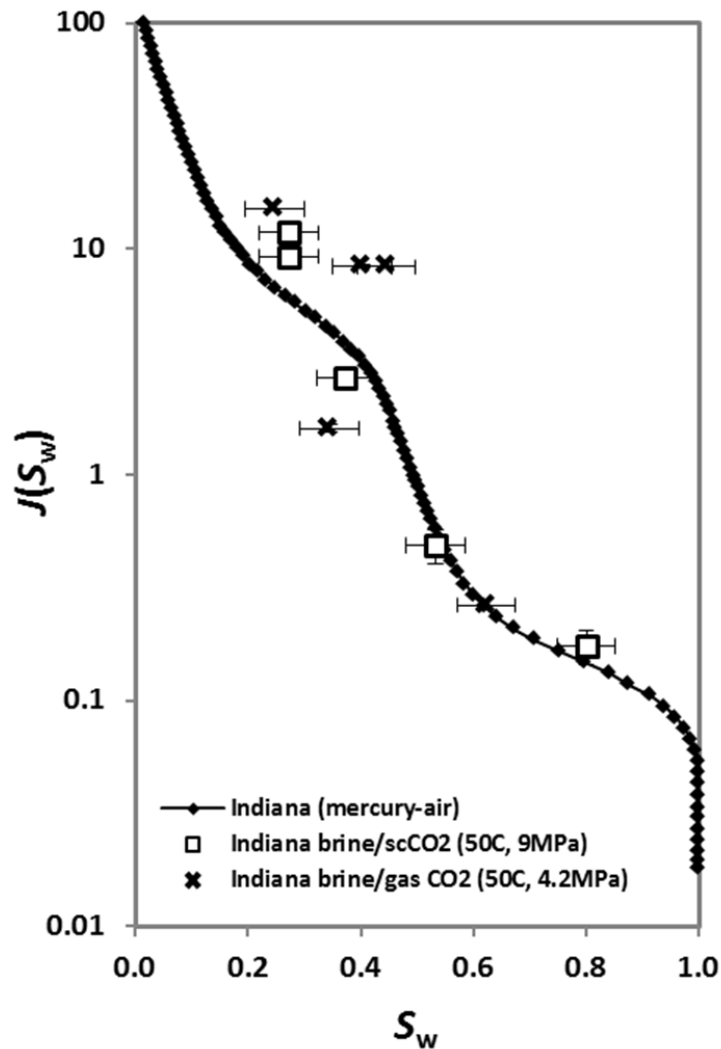
Below is a measured mercury injection capillary pressure rescaled as the J-function for Berea sandstone. Mercury is always the non-wetting phase, and so this represents a drainage displacement. Note that the minimum value of the  $J$  function – the dimensionless entry pressure – is typically less than 1 (around 0.2-0.3) in the example above. By a J-function value of 1, most of the pore space has been accessed by the non-wetting phase. Much larger values are possible, as the non-wetting phase forces its way into narrow corners and cracks of the pore space as well as the smallest pores themselves. However, often these high values are simply

experimental artefacts: a huge capillary pressure is imposed and insufficient time is given to achieve capillary equilibrium. In general, be cautious about using J-function values much above 1 in quantitative calculations, as they may not correspond to a true state of equilibrium.



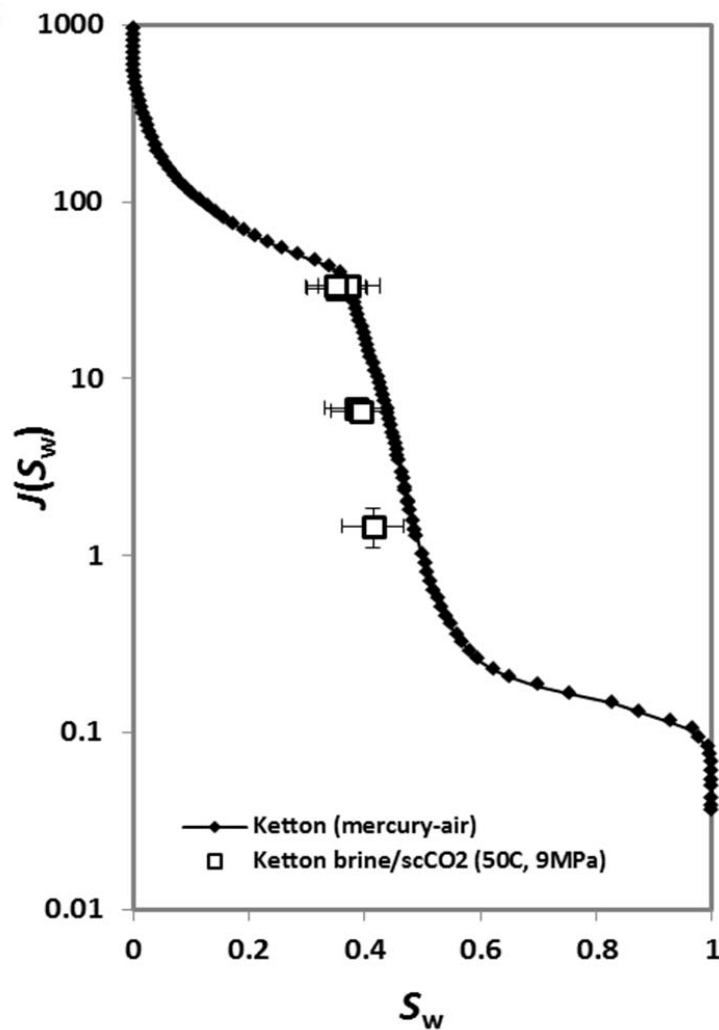
**An example Leverett J-function measured by mercury injection during primary drainage on Berea sandstone. Not that the majority of the displacement occurs for  $J < 1$ . Also, since mercury displaces a vacuum there is no irreducible or connate wetting phase saturation in this experiment.**

In carbonates, however, with micro-porosity, there may be significant displacement for  $J > 1$ , as the non-wetting phase enters these small pores, as shown in the figures below.



The Leverett J-function measured by mercury injection during primary drainage, and by displacement of brine by CO<sub>2</sub> on Indiana limestone. Notice that when different measurements with different fluids are represented as a J function they lie on the same curve to within experimental error. Also note that the curve shows regions where the saturation changes rapidly with pressure, indicating at low pressure the intergranular porosity and, at high pressure, the micro-porosity within grains.





The Leverett J-function measured by mercury injection during primary drainage, and by displacement of brine by CO<sub>2</sub> on Ketton limestone. As in Indiana, there is a clear signature of intergranular (macro) porosity and intragranular (micro) porosity.

### 7.1 CAPILLARY PRESSURE AND PORE SIZE DISTRIBUTION

It is possible to relate the capillary pressure to the pore size distribution: this is routinely performed on the results of mercury injection tests. First, Eq. (3.5) is used to convert the capillary pressure into a throat radius, assuming piston-like displacement into a circular tube. Hence, instead of  $P_c$  as a function of saturation (the wetting phase saturation, even though for mercury injection this is a vacuum), we define an effective radius as a function of saturation:

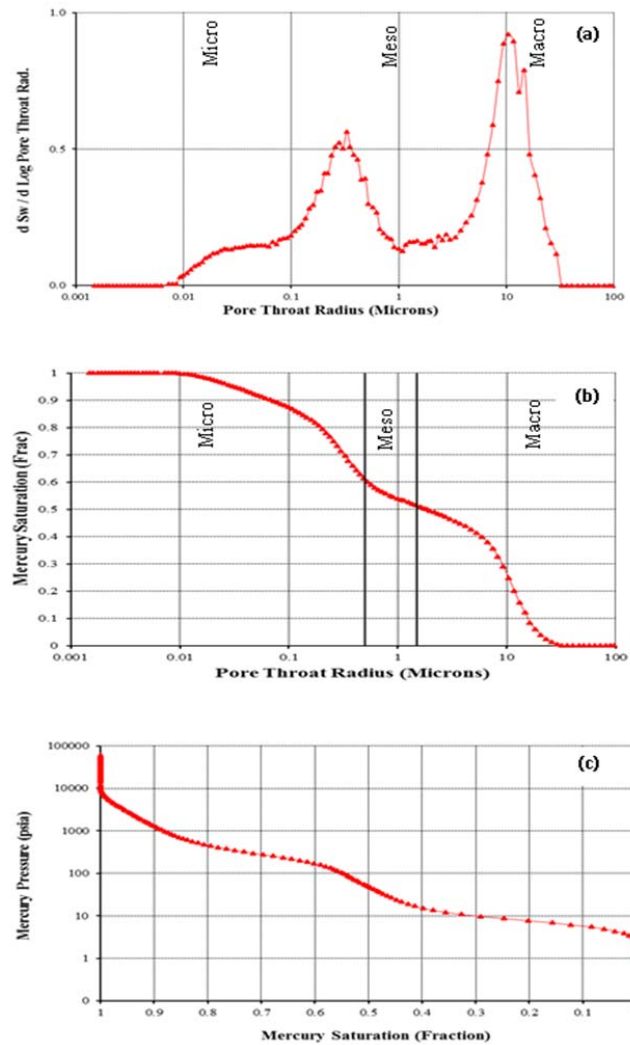
$$r(S) = \frac{2\sigma \cos\theta}{P_c(S)} \quad (7.2)$$

Then the radius distribution is computed. Usually this is done by defining:

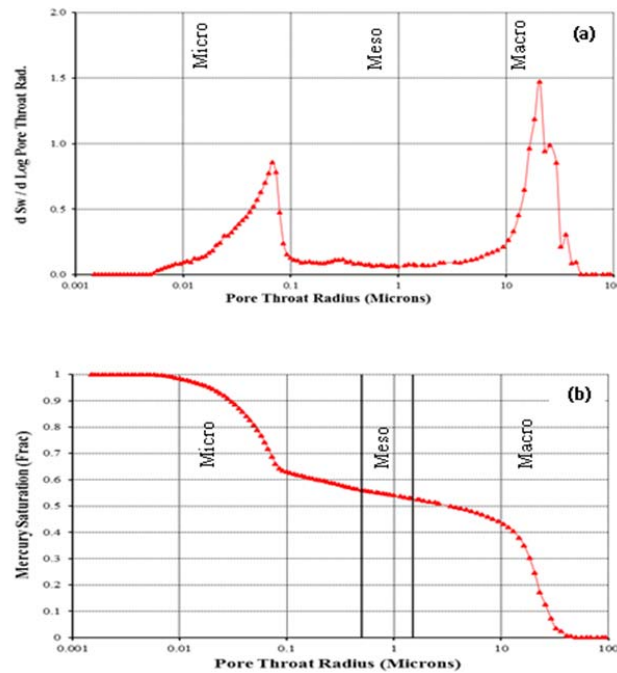
$$G(r) = \frac{dS}{d(\ln r)} = r \frac{dS}{dP_c} \frac{dP_c}{dr} = -P_c \frac{dS}{dP_c} = -\frac{dS}{d\ln P_c} \quad (7.3)$$

$G(r)$  is an indication of the number of throats of radius  $r$ . Logarithmic axes are used since there is typically a wide variation in capillary pressure and hence effective pore size. It is not strictly the throat size distribution, since the displacement process during primary drainage – technically similar to invasion percolation – allows the filling of regions with wide pores and throats which are only accessed through a smaller throat at a high pressure. However, it does give some indication of the range of pore sizes in the material.

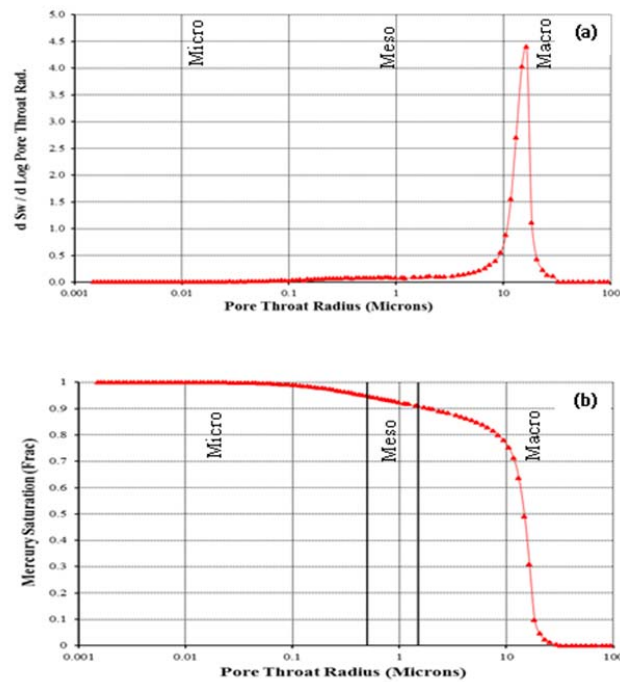
Below I show some example distributions on our example rock types: note that for the carbonates we see a bimodal distribution showing macro-pores and microporosity.



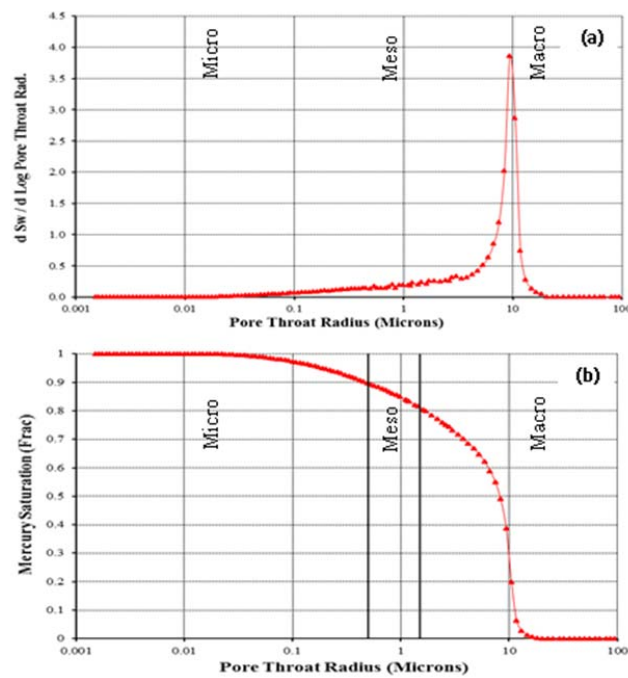
The mercury injection capillary pressure for Indiana limestone (bottom). This is converted into saturation as a fraction of effective throat radius (middle) from which a throat size distribution is computed (top) using Eqs. (10.2) and (10.3). Here we see a very wide range of throat size with a clear indication of macro and micro-porosity.



The relationship between apparent radius and saturation, together with the inferred throat size distribution for Ketton limestone. Here there is a clear distinction between the large, intergranular, pores and the much smaller intragranular micro-porosity.



The throat size distribution for Doddington sandstone. Here there is a relatively narrow distribution of large pore spaces – here there is no microporosity.



The throat size distribution for Berea sandstone. Here again there is a relatively narrow distribution of large pore spaces, but they are smaller on average, and have a larger range of size than for Doddington.

## 8. EFFECT OF WETTABILITY ON CAPILLARY PRESSURE

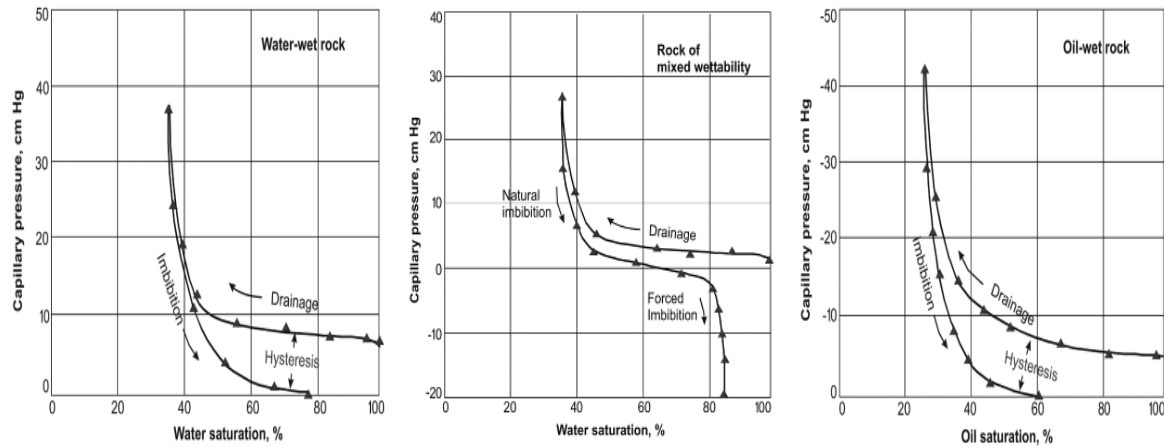
---

As we discussed before, most reservoir rocks contain both oil-wet and water-wet regions. This means that during water invasion a negative capillary pressure (a water pressure higher than the oil pressure) needs to be applied to force oil out of the oil-wet regions.

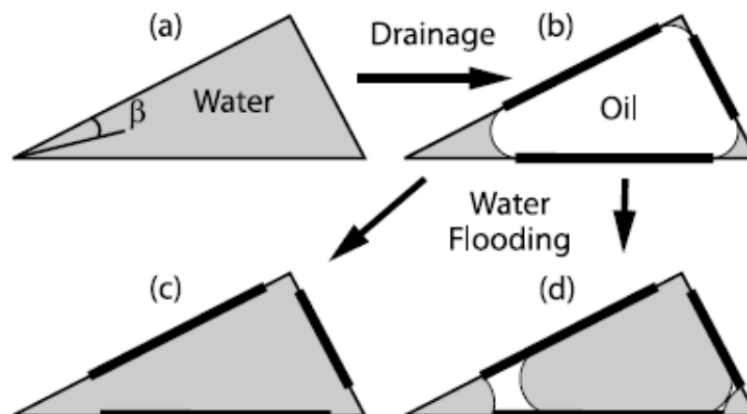
Below are some classic experiments (Killins *et al.*, 1953) illustrating the effect of wettability. The curves are good for illustrative purposes but do not show the correct residual for the oil-wet case, since this is difficult to measure with any accuracy experimentally. Then I will provide a physical explanation for the behaviour. The emphasis is how to relate the macroscopic behaviour to the pore-scale physics and the configuration of fluids at the micron scale.

The degree of trapping is dependent on the presence and connectivity of oil layers sandwiched between water in the corners and water in the centres of oil-wet pores. This is illustrated on the next page. If the surface is oil-wet, then water becomes the non-wetting phase. This means that it preferentially fills the centres of the largest pores. However, water is still retained in the corners after primary drainage. Hence, between water in the corners and water in the centre, there is an oil layer.

These oil layers maintain connectivity of the oil phase down to low saturation. As the water pressure increases, the oil layers become increasingly thin and will eventually become unstable, allowing trapping. However, the flow rate through these layers is very low and so – experimentally – you have to wait a very long time to see the oil drain down to its true residual saturation. This situation is similar to the irreducible water saturation in primary drainage: again we have layer flow and waiting longer can allow lower water saturations to be achieved.

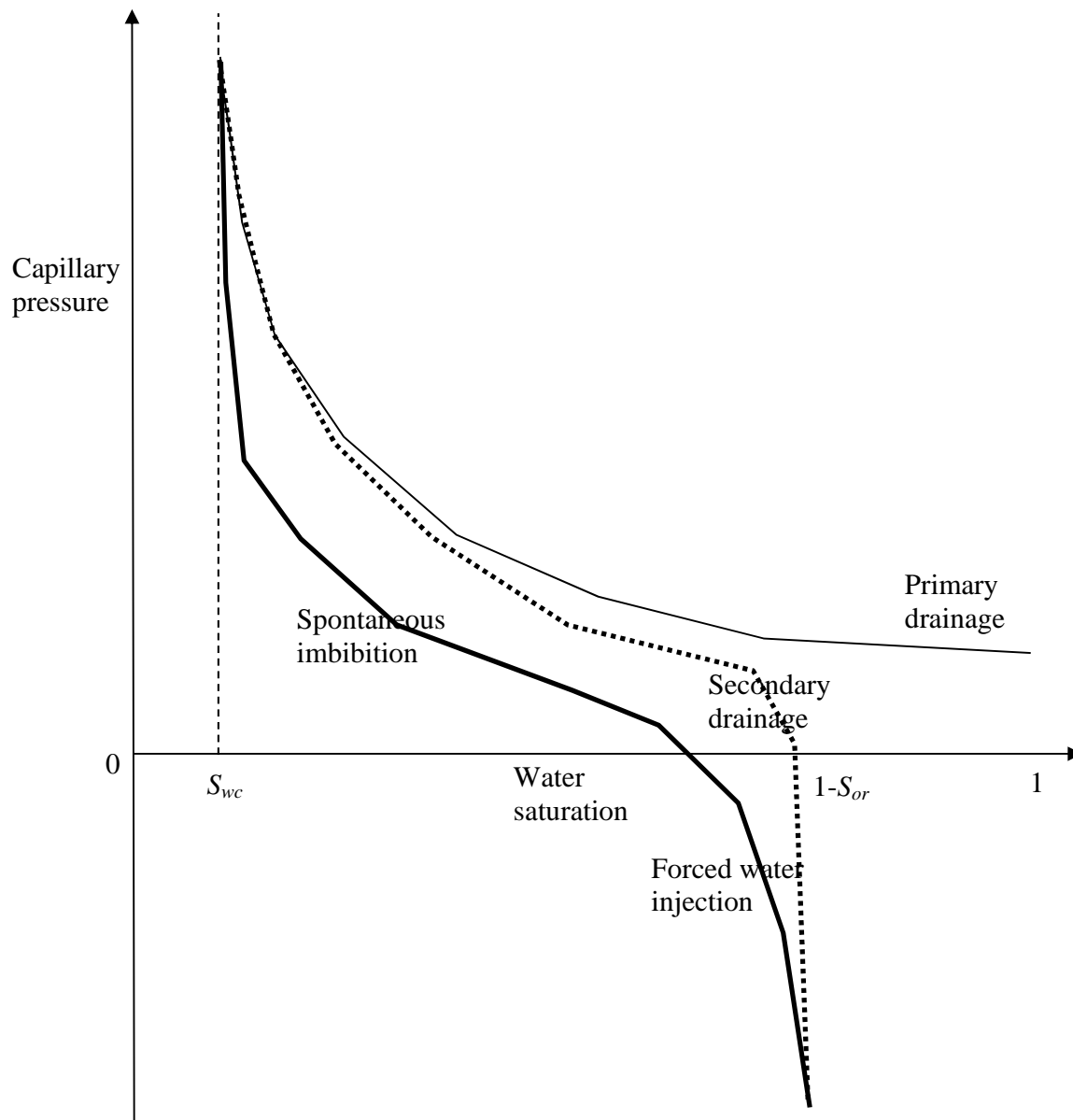


Capillary pressure ( $P_c$ ) curves, for water-wet, mixed-wet and oil-wet rock. Note that the capillary pressure becomes negative if the sample is not water-wet (Killins *et al.*, 1953). The term “imbibition” is here incorrectly used to describe forced displacement at a negative capillary pressure – in these notes we confine imbibition to refer only to a spontaneous process occurring at a positive capillary pressure.



Possible configurations of oil and water in the pore space of a single pore or throat. Initially the porous medium is completely saturated with water. After drainage, the non-wetting phase (oil) resides in the centres of the pore space, with water confined to the corner. The regions of the pore space directly contacted by oil may change their wettability. When water is injected, the water can fill the entire pore space, or – if the altered wettability surface is oil-wet – a layer of oil can form sandwiched between water in the corner and water in the centre. This oil layers allows the oil to remain connected and drain to very low saturation, albeit very slowly.



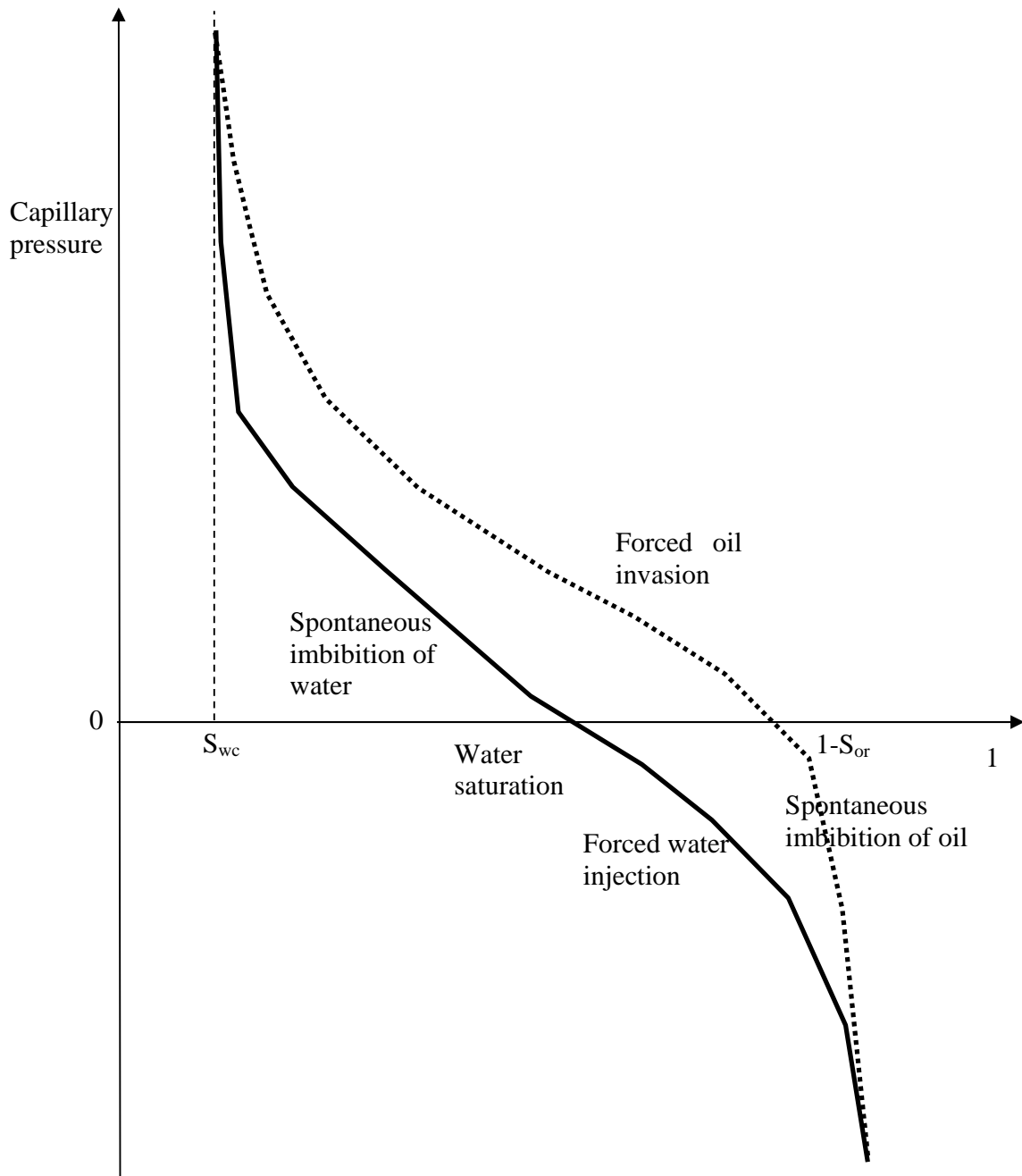


Typical capillary pressures for a weakly water-wet system. Note that there is some parts of the pore space that require forced water injection to access: it is unusual in natural samples to have a capillary pressure curve during waterflooding that is entirely positive. Only the waterflooding and secondary drainage curves are shown: generally primary drainage shows only water-wet characteristics (either mercury injection is used, or the displacement occurs before oil has altered the wettability of the system).

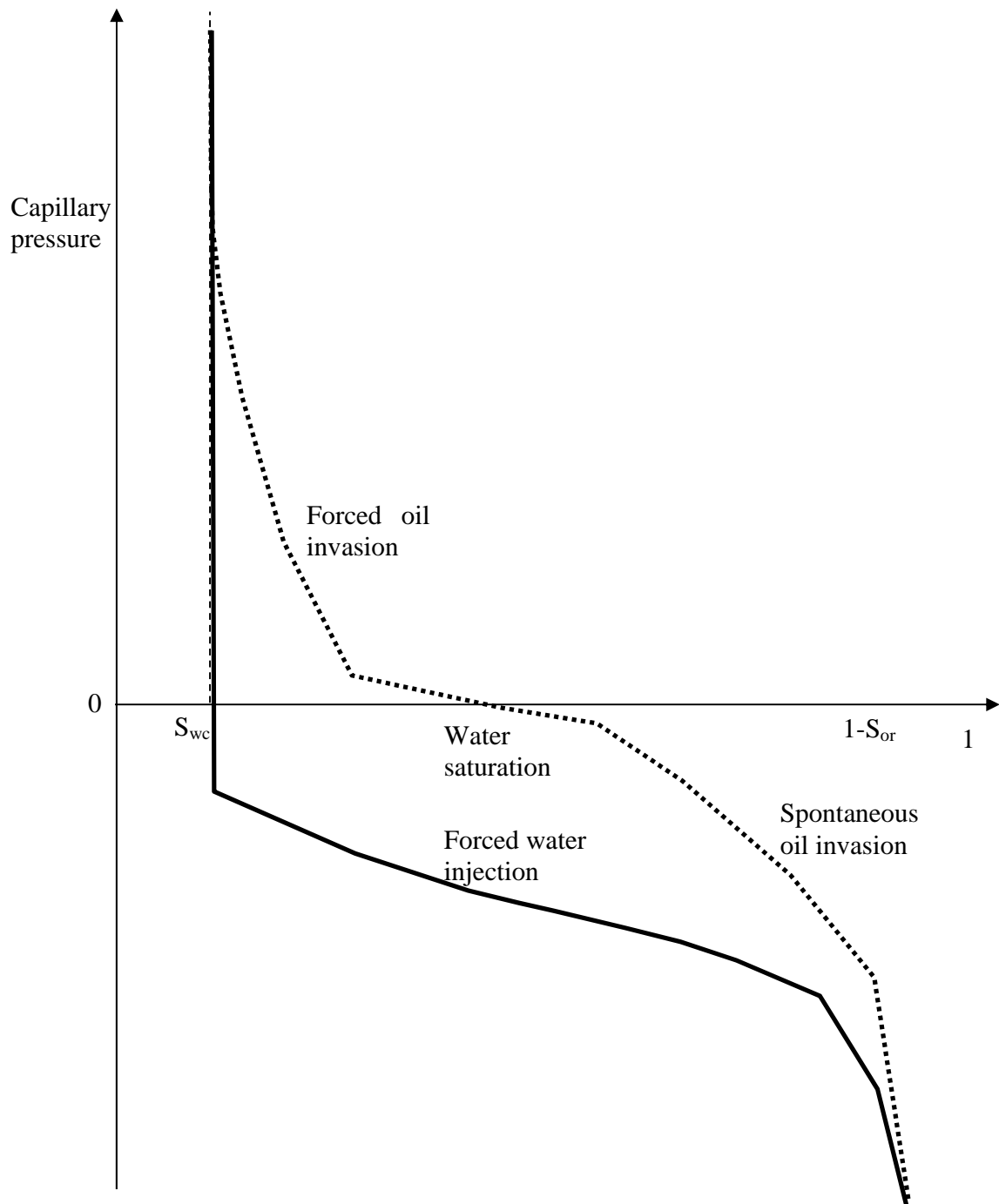
The figure shown above represents a weakly water-wet system. Here some water is displaced during forced water injection. However, the medium does not spontaneously imbibe any oil, indicating that there are no connected oil-wet pathways through the system.

The region of the water invasion curve where the capillary pressure is negative is called forced water injection. Where the capillary pressure is positive we have, as before spontaneous imbibition, or spontaneous water injection. To avoid confusion, imbibition and drainage is used only when the corresponding capillary pressure is positive.

The next figure represents a system that spontaneously displaces both oil and water – this is a characteristic feature of a mixed-wet system – there are continuous pathways of both water-wet and oil-wet patches in the pore space. The oil imbibes in the same way as water in a water-wet system, with snap-off of water accommodated through oil layer flow. This can lead to considerable trapping of water as a non-wetting phase. In contrast, there is less trapping of oil, again due to the connectivity of oil layers.



**Typical capillary pressures for a mixed-wet system. Here there are connected regions of both water-wet and oil-wet pores and we see imbibition (spontaneous uptake) of both oil and water.**



**Typical capillary pressures for an oil-wet system. We see no water imbibition, but a significant amount of spontaneous displacement (imbibition) of oil.**

The final figure above is a strongly oil-wet system that has no spontaneous imbibition of water. The residual oil saturation is lower than the water-wet medium; this is because the oil maintains connectivity down to low saturation thanks to the presence of oil layers.

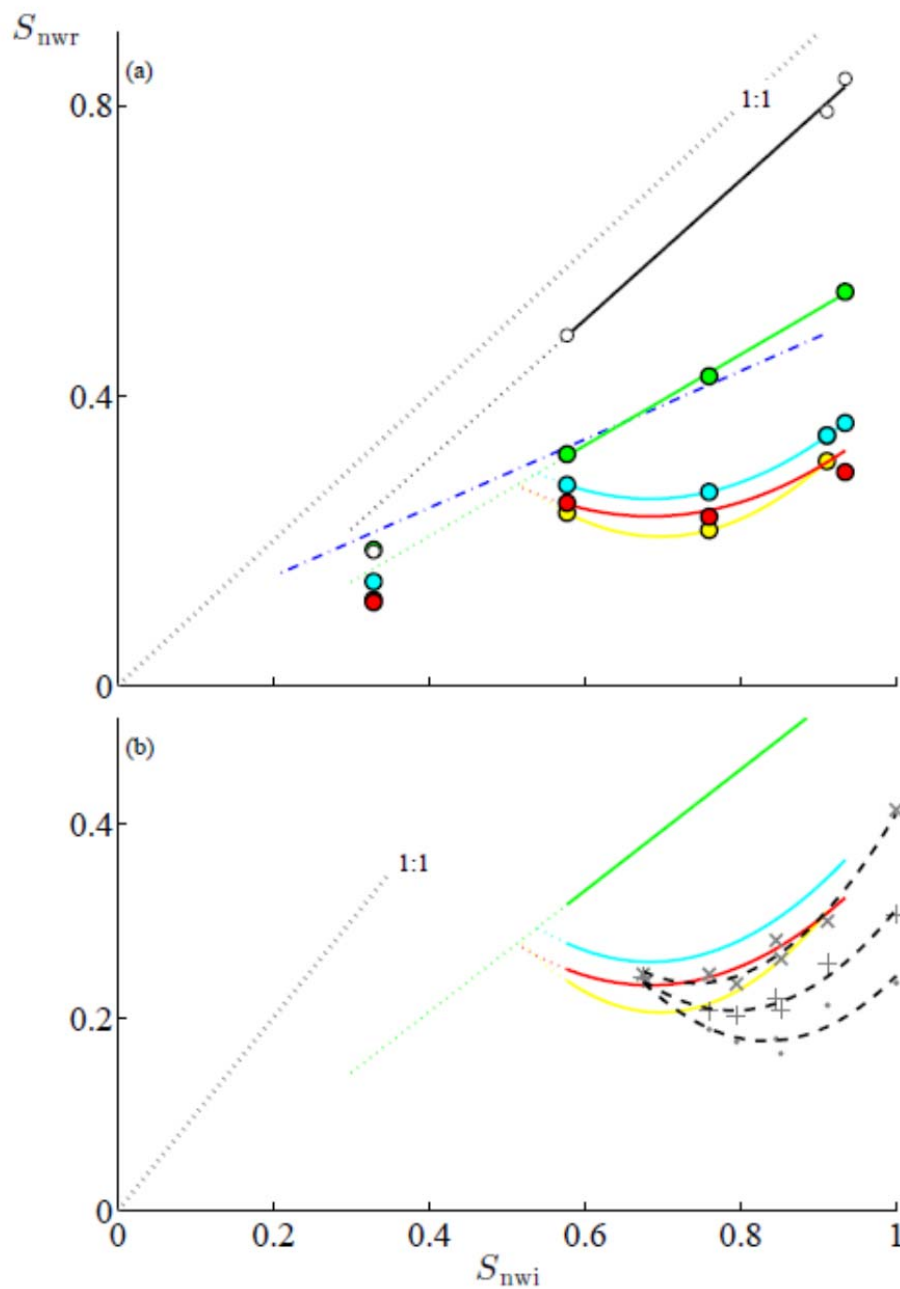
## 8.1 TRAPPING CURVES IN MIXED-WET SYSTEMS

---

In a mixed-wet system the relationship between initial and residual saturation becomes more complex. First, the remaining oil saturation is controlled by the extent to which oil is allowed to drain from the system through layers. Hence, as more water is injected, more oil is produced and the remaining oil saturation decreases. As mentioned before, it is very difficult to obtain a true residual, or minimum, saturation experimentally, as the oil continues to flow, very very slowly, until low saturations are reached.

Second, the relationship between initial and remaining oil saturation is non-monotonic. For low initial saturations, the remaining saturation increases with initial saturation for the obvious reason that the more oil initially present, the more oil that can be trapped. However, at higher initial saturations, the residual decreases. This surprising phenomenon is due to the presence and stability of oil layers. At higher initial oil saturation (and hence imposed capillary pressure in primary drainage), the water is pushed further into the corners of the pore space. This makes oil layers, formed during subsequent water flooding, thicker and more stable – meaning a more negative capillary pressure is required (higher water pressure) to collapse them. This extends the layer drainage regime, allowing more oil to be recovered. At the very highest initial saturations, the remaining oil saturation may increase again, as there is more oil present, and there is a subtle competition between displacement and connectivity in the oil-wet and water-wet regions of the pore space, and the layers do, eventually, lose connectivity.

This curious behaviour has been seen experimentally, and can be predicted using pore-scale modelling. Some experimental data is shown overleaf.



Experimental data showing the variation of remaining oil saturation as a function of initial oil saturation in mixed-wet Indiana carbonate. The top graph is data from Imperial College (Tanino and Blunt, 2013) while the bottom is from Salathiel (1973). The different curves represent different amounts of waterflooding from 1 to over 200 pore volumes injected.

## 8.2 TRANSITION ZONES

---

During primary oil migration (primary drainage) into a hydrocarbon reservoir, both the saturation and capillary pressure varies with height above the free water level – this is defined as the depth when the oil and water pressures are the same, so the capillary pressure is zero. Above the free water level, the capillary pressure increases with depth, as analysed earlier for a meniscus in a capillary tube, Eq. (3.6). For a reservoir with variable permeability and porosity, we invoke J-function scaling to determine the water saturation at a given height  $h$  above the free water level. It is the saturation such that:

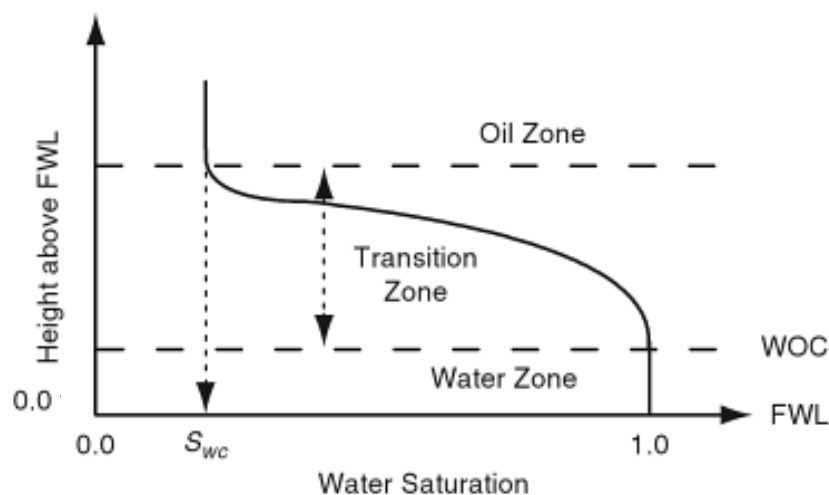
$$\Delta\rho gh = P_c(S_w) = \sqrt{\frac{\phi}{K}} \sigma \cos\theta J(S_w) \quad (8.1)$$

where  $\Delta\rho$  is the density difference between oil and water. This can be rewritten:

$$S_w(h) = J^{-1}\left(\frac{\Delta\rho gh}{\sigma \cos\theta} \sqrt{\frac{K}{\phi}}\right) \quad (8.2)$$

This initial distribution of saturation – normally established from a primary drainage capillary pressure curve is shown in the figure overleaf for a homogeneous medium. The initial saturation, in turn, affects the wettability for subsequent waterflooding once the oil has aged the surface: higher capillary pressure (low initial saturation) forces the oil into contact with more of the solid, favouring oil-wet conditions; intermediate saturations may lead to a mixed-wet rock, while a high initial water saturation means that there is little initial contact between the oil and solid and the medium remains largely water-wet. Later we will explore the implications for oil recovery by waterflooding, once we have discussed how multiple fluids flow in the pore space. For now it is sufficient to note that many oil reservoirs experience a transition from water-wet to oil-wet conditions with height above the oil-water contact: in low permeability rocks this transition zone may extend 10s m, as evident when representative numbers are put into Eq. (8.1).

Imagine, for instance, a permeability of around 10 mD ( $10^{-14} \text{ m}^2$ ), a porosity of 0.16, a density difference of  $200 \text{ kgm}^{-3}$  and  $\sigma \cos \theta = 0.025 \text{ Nm}^{-1}$ . Then, the water saturation will decline to close to its irreducible (connate) value for  $J=1$  (see the previous sections). This then gives a height of around 50 m – essentially there is a variation of saturation with height across the entire reservoir and it is wrong to assume that the initial saturation is the irreducible value.



A schematic of the transition zone, where the saturation varies as a function of height above the free water level (FWL), defined as where the capillary pressure is zero. The water-oil contact (WOL, or the oil-water contact, OWL) is found from down-hole log measurements of resistivity where there is first a noticeable presence of water (low resistivity) in the formation. This distribution of saturation also affects the wettability during waterflooding.

### 8.3 AMOTT WETTABILITY INDICES

This is a quantitative and useful measure of wettability measured on core samples and first described by Amott (1959): remember that it is difficult to measure contact angles *in situ* (although see Andrew *et al.*, 2014b), and in any event, this does not directly relate to capillary pressure. Start with a core at waterflood residual oil.

1. Perform spontaneous oil invasion ( $P_C < 0$ ).
2. Then perform forced injection of oil ( $P_C > 0$ ).
3. Then spontaneous imbibition of water ( $P_C > 0$ ).



4. Then last forced water injection ( $P_C < 0$ ).

The wettability indices for oil and water are defined by:

$A_O$  = Increase in oil saturation in step 1/Total increase from steps 1 and 2.

$A_W$  = Increase in water saturation in step 3/Total increase from steps 3 and 4.

Clean sand and rock will have  $A_O = 0$  and  $A_W = 1$ . We rarely see  $A_O = 1$ . Sometimes we have rocks where one value is low (around 0.1) and the other is 0 – little or no spontaneous displacement, implying contact angles everywhere close to  $90^\circ$ . However, the most common situation, for a reservoir sample, is mixed-wettability where both oil and water spontaneously imbibe and neither index is zero.

Many researchers, rather depressingly, are unable to cope with two numbers to represent wettability and so use instead the (completely useless!) Amott-Harvey index  $A_W - A_O$ . Please never do this – the concept was introduced when it was considered that there was one uniform contact angle in the rock, and so, by definition, one of the Amott indices had to be zero. However, this is extremely unhelpful for mixed-wet systems: there is a significant difference between a mixed-wet rock with an Amott-Harvey index of 0 (meaning that around half the pores are oil-wet and the other half water-wet) and an intermediate-wet rock with uniform contact angles close to  $90^\circ$  that also has an Amott-Harvey index of 0. Be sure to distinguish between these two cases.

## 8.4 EXAMPLE EXERCISES

---

1. Return to our discussion of the oil/water transition region in oil reservoirs. In many reservoirs – such as Prudhoe Bay off the North slope of Alaska – the reservoir is weakly water-wet near the oil/water contact and becomes more oil-wet with height away from the contact. Explain in your own words why we see this wettability trend.

2. Consider equilibrium at a line of contact for the following three situations: oil/water, gas/oil and gas/water. Derive a relationship between the oil/water, gas/oil and gas/water contact angles and interfacial tensions.
3. Consider a dome-shaped gas reservoir. The gas is trapped by a layer of shale that has a permeability 0.1 mD and porosity 0.2. The gas is in pressure communication with the surrounding aquifer. Estimate the height of gas in the reservoir. The gas density is  $200 \text{ kg/m}^3$  and the water density is  $1000 \text{ kg/m}^3$ . The gas/water interfacial tension is 60 mN/m. (Hint: Draw a cartoon of the reservoir. Gas can accumulate until there is a sufficient capillary pressure for gas to enter the shale layer. Use the Leverett J function and a dimensionless entry pressure of 0.3. The capillary pressure is the pressure difference due to density differences.)
4. Explain why a water-wet porous medium has a higher residual oil saturation than an oil-wet medium. Explain why a porous medium with oil/water contact angles close to  $90^\circ$  gives a lower residual oil saturation than a porous medium with a contact angle close to 0. Two porous media have an Amott-Harvey index of 0, indicating that they are neither oil-wet nor water-wet. One medium has  $A_W = A_O = 0$ , while the other has  $A_W = A_O = 0.4$ . Which system do you expect to have the lower residual oil saturation? Explain your answer carefully.

## 9. FLUID FLOW AND DARCY'S LAW

---

We now introduce flow into our analysis – in particular Darcy's law for flow in a porous medium and provide a pore-scale basis for the relationship between flow rate and pressure gradient. We start with a consideration of single-phase flow (one fluid – by default water – saturates the pore space completely, and we consider the water movement and that of solutes dissolved in the water) before extending the analysis to multiphase flow (where oil, water and gas may all be present).

### 9.1 STOKES FLOW

---

There are two fundamental concepts that we will use to describe fluid flow. This is not specifically flow in a porous medium, but the movement of any fluid. The first concept is conservation of mass, written as:

$$\nabla \cdot \rho \mathbf{v} = 0 \quad (9.1)$$

I will not derive this equation here – which is simple to do considering flow into an arbitrary volume and applying Green's theorem – but I will return to similar derivations for multiphase flow later in these notes.

The second concept is the conservation of momentum for a fluid. This is the Navier-Stokes equation that is used to describe the flow of everything from volcanic magma, to air and oceans. It can be written as:

$$\rho \left( \frac{\partial \mathbf{v}}{\partial t} + \mathbf{v} \cdot \nabla \mathbf{v} \right) = -\nabla P + \mu \nabla^2 \mathbf{v} \quad (9.2)$$

where  $\rho$  is density and  $\mathbf{v}=(u,v,w)$  is the vector of velocity,  $P$  is pressure, and  $\mu$  is the viscosity.

In our case we can make a number of simplifications. If we consider relatively incompressible fluids, such as oil or water, or, for gas, flow in a small domain (the pore scale) where changes in pressure – and hence density – are small compared to the overall pressure, then the density is constant, or is almost constant to a very good approximation. We can write instead of Eq. (9.1):

$$\nabla \cdot \mathbf{v} = 0 \quad (9.3)$$

Eq. (9.3) is an expression of conservation of volume and can be derived directly (assuming incompressible fluid) directly, in much the same way as the expression for conservation of mass.

We also consider flows where the flow field changes slowly over time, and so we can neglect any explicit time dependence in the Navier-Stokes equation. Furthermore, flow is very slow, compared to, say, air flows, and in this limit the term with the velocity multiplied by itself can be ignored (physically it means that viscous forces dominate over inertial forces – this is discussed further below – and means that we can dismiss some of the more complex effects, namely turbulence, which occur in other, more unconfined flows). Then we are left with the steady-state Stokes equation:

$$\mu \nabla^2 \mathbf{v} = \nabla P \quad (9.4)$$

With modern linear solvers and fast computers, it is possible to solve these last two equations numerically on the pore-space images we have introduced previously. We are now able to use standard desk-top computers to solve billion-cell problems.<sup>1</sup>

## 9.2 REYNOLD'S NUMBER AND FLOW FIELDS

---

The concept of slow flow can be quantified through the introduction of the Reynold's number  $R_e$  which is the ratio of inertial to viscous forces for fluid flow (Landau and Lifshitz, 1959):

$$R_e = \frac{\rho v L}{\mu} \quad (9.5)$$

where  $\rho$  (as before) is the fluid density,  $\mu$  its viscosity,  $v$  a characteristic flow speed and  $L$  a characteristic length. In a porous medium the fluid moves slowly through the labyrinthine interstices between rock grains, or through a complex fracture network. The characteristic

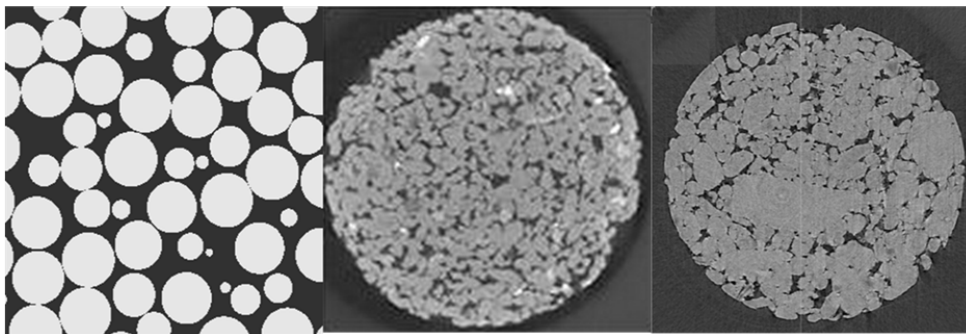
---

<sup>1</sup> We use the OpenFoam library to solve the Navier-Stokes equation: there are a number of excellent public domain solvers, readily downloaded from the internet that can be employed.

length is that of a pore throat, or a narrow restriction between larger pore spaces which impedes the flow.  $L$  is typically around  $10\text{--}100\ \mu\text{m}$  ( $10^{-5}\text{--}10^{-4}\ \text{m}$ ) for consolidated rock and of order  $10^{-3}\ \text{m}$  for sand and gravel. The flow speed typically  $10\ \text{m/day}$  (roughly  $10^{-4}\ \text{ms}^{-1}$ ) or less for groundwater movement (natural flow speeds in arid areas can be  $1\ \text{m}$  a year or smaller) and is one or two orders of magnitude lower in oil reservoirs. For water  $\rho = 10^3\ \text{kgm}^{-3}$  and  $\mu = 10^{-3}\ \text{kgm}^{-1}\text{s}^{-1}$ , giving  $Re \approx 10^{-1}\text{--}10^{-3}$ . Viscous forces dominate and we have laminar flow in porous media (turbulent flow generally occurs for  $Re \approx 1000$ ).

It is possible to average the Navier Stokes equation, which describes flow of a single fluid, for slow, laminar flow past many obstacles. The flow is averaged over a representative volume element containing several rock or sand grains. Since the Reynold's number is low, viscous forces predominate. A pressure gradient, or force, is required for flow at a constant velocity. It is possible to derive a linear relation between volumetric flow rate and pressure gradient, known as Darcy's law (Bear, 1972), which we will consider later.

First though, I will show some illustrative examples of the pore space, pressure distribution and flow fields. The flow is relatively uniform in the more homogeneous systems, such as a bead pack, but is confined to a few tortuous channels in the more heterogeneous media, such as many of the carbonates we study.

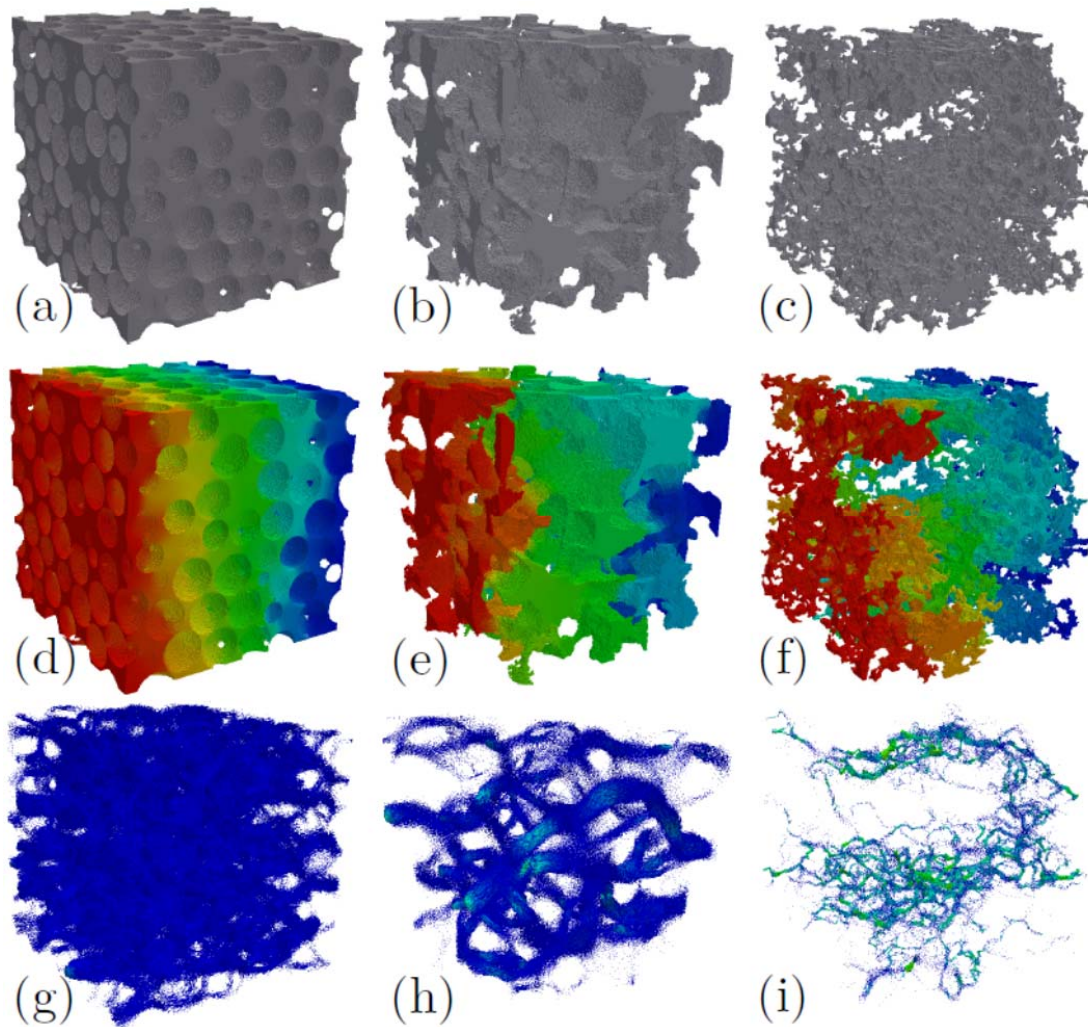


(a)

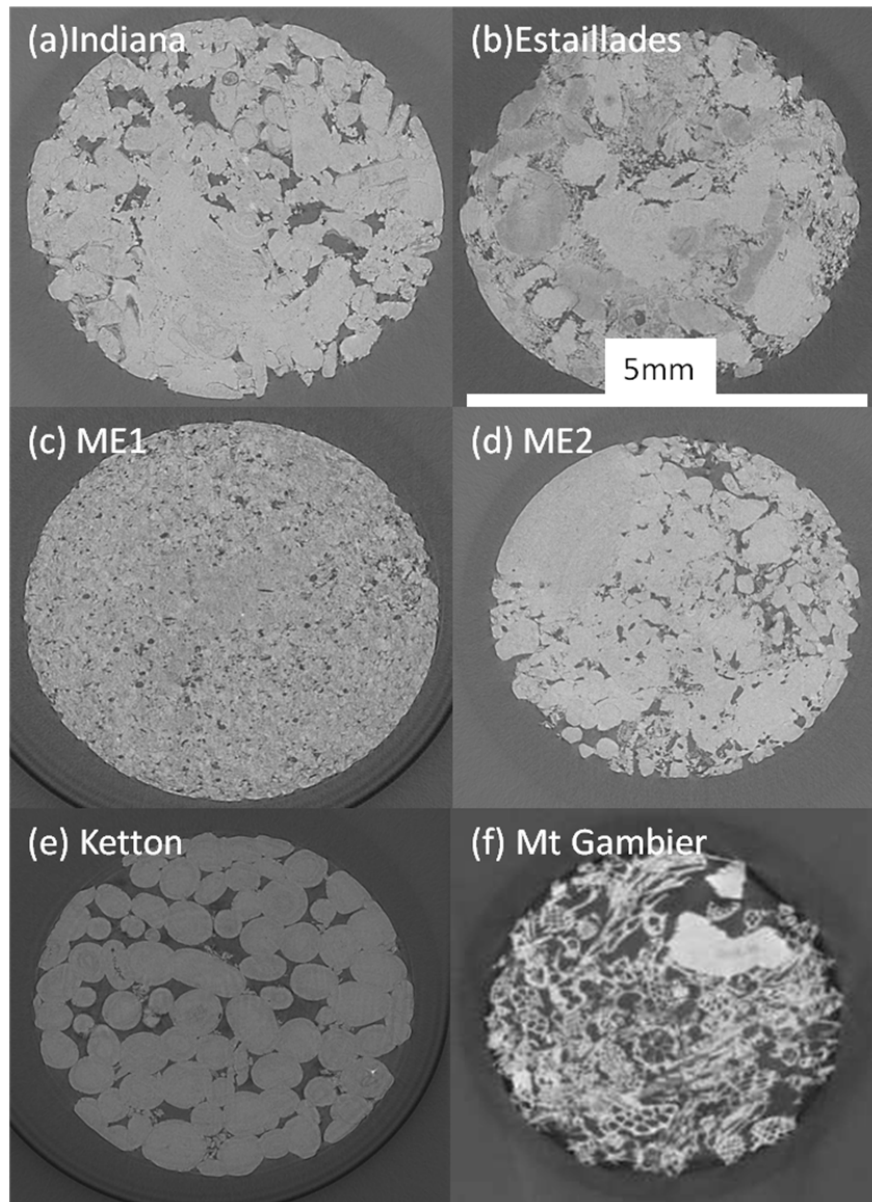
(b)

(c)

**Two-dimensional cross-sections of three-dimensional images of (a) a bead pack, (b) Bentheimer sandstone, and (c) Portland limestone.**

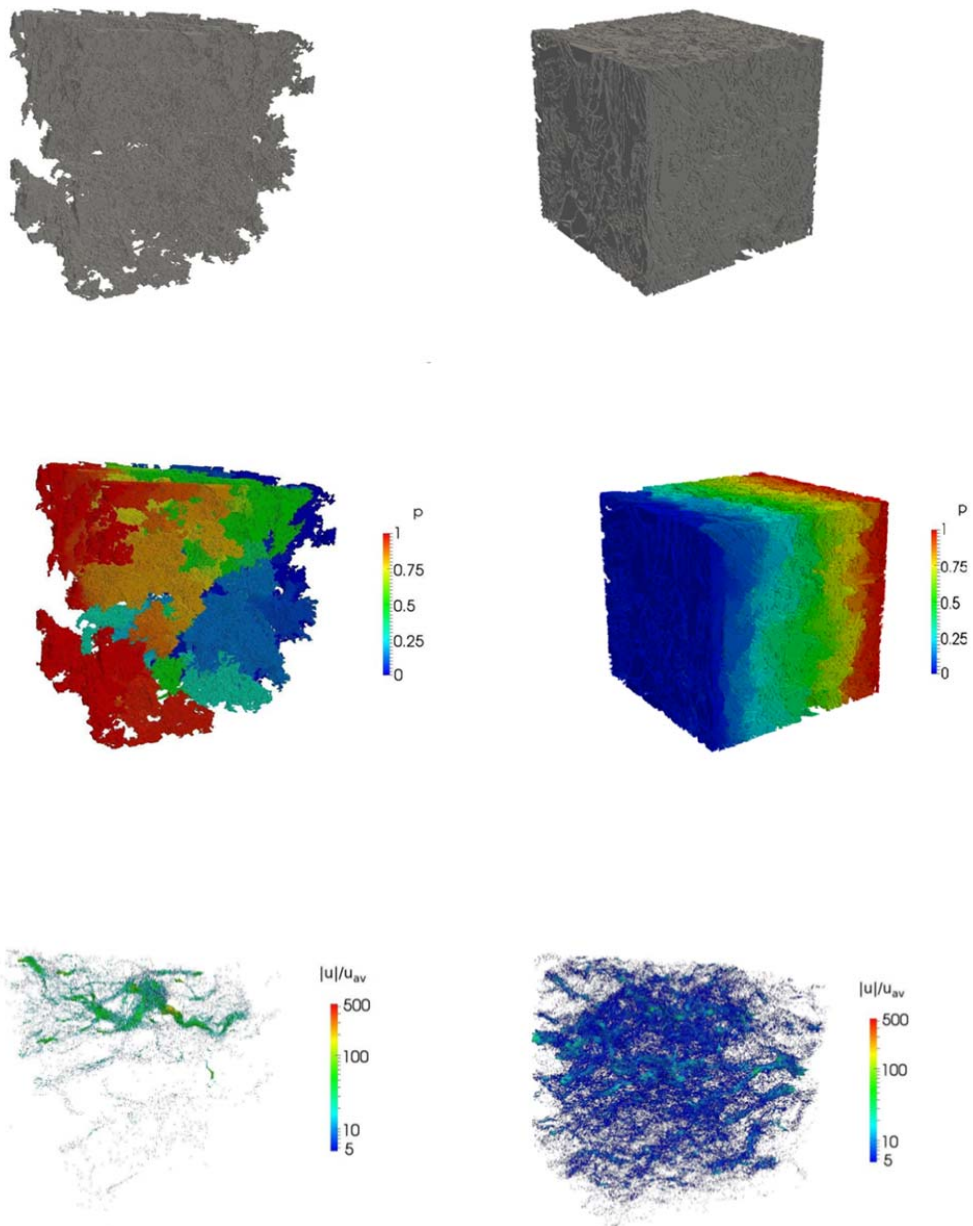


The pore space of the three porous media shown in the previous figure: (a) bead pack; (b) Bentheimer; (c) Portland. Then the pressure field for flow from left to right is shown, with red representing high values and blue low values: flow goes from high to low pressure. The final row illustrates the flow field, with the regions of highest flow indicated. While flow is relatively uniform through the pore space of a bead pack, in the carbonate it is confined to a few tortuous channels (from Bijeljic *et al.*, 2011).



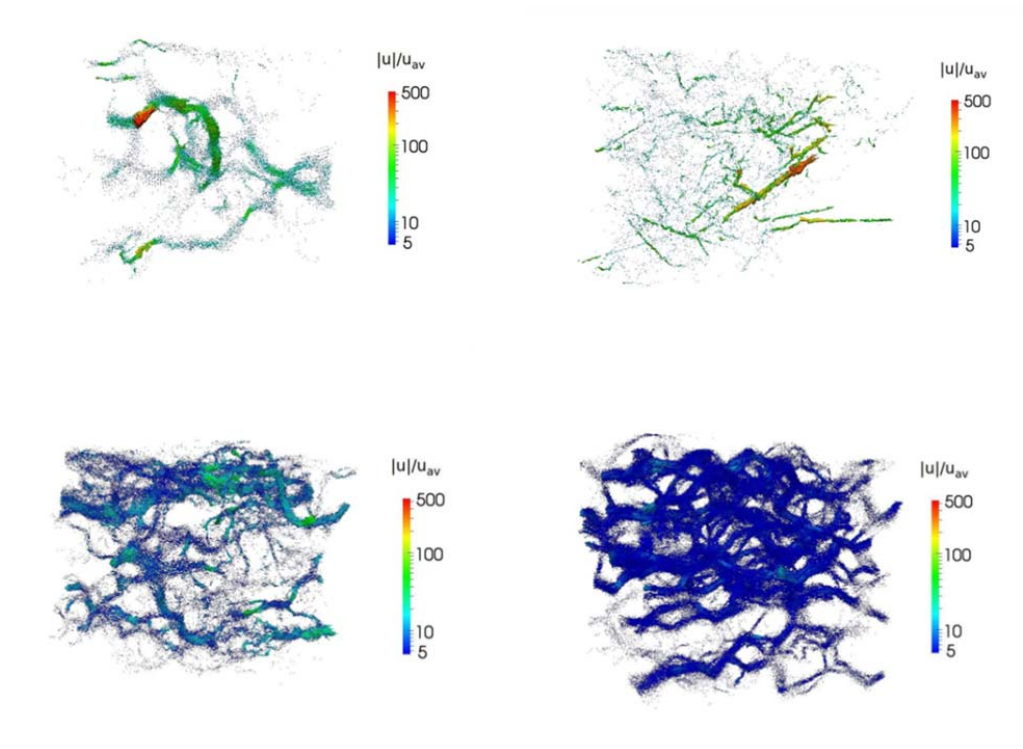
**Two-dimensional cross-sections of three-dimensional images of various carbonate samples, including two cases from a deep Middle Eastern aquifer ME1 and ME2).**





The pore space of the Estailades and Mount Gambier, with the corresponding computed pressure and flow fields. Estailades has very tortuous flow paths indicating a poorly-connected pore space, while Mount Gambier, despite its geologically complex structure, is well-connected and supports a relatively uniform flow (Bijeljic and Blunt, 2013).





**Normalized flow fields for: top left, Indiana limestone; top right, ME1; bottom left, ME2; and bottom right Ketton limestone.**

### 9.3 AVERAGED BEHAVIOUR AND DARCY'S LAW

The local velocity in the pore space is highly variable – indeed we see, typically, eight orders of magnitude variation in flow speed in the samples shown above. However, there is a way to simplify this if we are only interested in the average flow.

We find, empirically, that there is a linear relationship between flow rate and pressure gradient: this can be derived rigorously mathematically as well. This relationship is Darcy's law:

$$q = -\frac{K}{\mu}(\nabla P - \rho \mathbf{g}) \quad (9.6)$$

$q$  is not a local flow velocity, even though it has the units of a speed. It is the volume of fluid flowing per unit area (and this area includes both solid and pore) per unit time. It is, in essence, the sum of all the highly variable local speeds in the overall direction of flow multiplied by the porosity. The minus sign indicates the physically obvious fact that flow goes from high to low pressure – that is along a negative gradient in pressure. Notice that in Eq. (9.6) I have also included the effect of gravity:  $\mathbf{g}$  is the vector of gravitational acceleration.<sup>2</sup>

We can help motivate this, and aid the discussion of relative permeability, by quoting the Poiseuille law: this is an expression that relates flow rate to pressure gradient in a single circular cylindrical tube and can be derived directly from the Navier-Stokes equation:

$$Q = -\frac{\pi r^4}{8\mu}(\nabla P - \rho \mathbf{g}) \quad (9.7)$$

where  $Q$  is the volume of fluid flowing per unit time and  $r$  is the radius of the capillary. Note the fourth power: this means that conductance is very sensitive to the size of the channel through which the fluid flows.

This fourth power of radius – or area squared – is unlike that encountered for, say, electrical current. The current in a wire – with a fixed potential (voltage) drop – is simply proportional to the area of the wire. Why? There is a flux of electrons – double to area to flow and the current doubles too. So, why a different relationship when it is fluid flow, not electrical current. The key distinction here is that the electrons move at a speed determined by the potential gradient and the metal in the wire – it is independent of the cross-sectional area of the wire. For fluid flow, however, the situation is different, since we have a no-flow  $\mathbf{v}=0$  boundary condition on the

---

<sup>2</sup> Darcy's law is named after Henry Darcy, a French Civil Engineer, who, in 1856, published a now-famous book "Les fontaines publiques de la ville de Dijon." The book is available in a 2004 English translation. The main body of the work concerns the design of a network of pipes to bring spring water into the city. As an apparent aside, and written in an appendix, is the first statement of this famous law, based on a series of flow experiments in sand filters. Flowing water through sand is an extremely effective way to remove bacteria (and even viruses) from the water: the larger organisms are simply trapped in the pore space as they (or clumped groups of them) cannot pass through the narrower pores, or are absorbed on the huge surface area a porous medium presents. This explains how, for instance, mountain streams run clear drinkable water, while the nearby fields are full of cow pats and sheep droppings. And last, why is he Henry and not Henri if he was French? Well, he had an English wife, so anglicized his first name!

solid surface. This means that flow speed increases away from the solid – governed by the viscosity – and so the flow is faster in large pores than in small pores. The total flux,  $Q$ , is related to the average speed multiplied by the area to flow. In this case, both terms increase with pore size.

We will meet this behaviour later for multiphase flow: how well each phase flows is exceptionally sensitive to the size of the pores that it moves through.

Now consider that we have an array of parallel tubes a distance  $d$  apart. Then the porosity is  $\pi^2/d^2$  and the Darcy velocity  $q$  is  $Q/d^2$ . Then we can write Eq. (9.7) as:

$$q = -\frac{\phi r^2}{8\mu}(\nabla P - \rho g) \quad (9.8)$$

or, in equivalence to Darcy's law, Eq. (9.6):

$$K = \frac{\phi r^2}{8\mu} \quad (9.9)$$

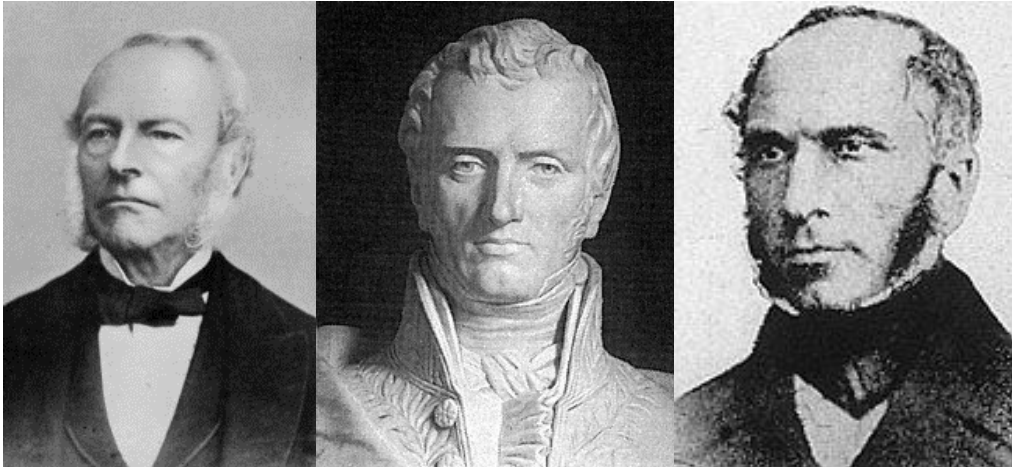
Note that the factor  $\phi/8$  is typically much less than one; if we account for tortuous flow through a less well connected pore space, the permeability is typically 1,000 times lower in magnitude than the area of a typical pore (radius squared). We will use this concept later when we discuss the effects of flow rate.

We can use Eq. (9.9) to estimate a typical pore size from the more easily measured macroscopic parameters  $K$  and  $\phi$ . We find:

$$r \sim \sqrt{\frac{K}{\phi}} \quad (9.10)$$

This relationship was used for the derivation of the Leverett J-function (see section 8) and explains the relationship between capillary pressure and its dimensionless form.

On a lighter note, below are pictures of some famous names in this subject. I have been unable to find a picture of the most famous person specifically for this course: M C Leverett (of J-function fame). It is interesting to note that both Darcy and Navier were born in Dijon.



**George Stokes, Claude-Louis Navier and Henry Darcy. Spot the odd one out – the scientist who was not born in Dijon.**

#### 9.4 OTHER WAYS TO WRITE DARCY'S LAW AND HYDRAULIC CONDUCTIVITY

---

We can write Darcy's law for flow in one direction as follows:

$$q = -\frac{K}{\mu} \left( \frac{\partial P}{\partial x} - \rho g_x \right) \quad (9.11)$$

Similar equations can be written for flow in the y and z directions.

Often you need to calculate the total flow  $Q$  (with dimensions volume per unit time) through a system of cross-sectional area  $A$ . Since  $q=Q/A$ , Darcy's law may be written:

$$Q = -\frac{KA}{\mu} \left( \frac{\partial P}{\partial x} - \rho g_x \right) \quad (9.12)$$

and for many linear flows the term  $\partial P / \partial x$  can be substituted by  $\Delta P / L$ , where  $\Delta P$  is a pressure drop over a distance  $L$ .

The hydrology literature is principally concerned with the flow of water and Darcy's law is often seen written in terms of a hydraulic conductivity,  $K_H$  defined as:

We can write Darcy's law for flow in one direction as follows:

$$K_H = \frac{K \rho g}{\mu} \quad (9.13)$$

where  $g$  is the acceleration due to gravity and the density and viscosity are those of water.  $K_H$  has the dimensions length/time.  $K_H$  is  $1 \text{ ms}^{-1}$  if the volumetric flow rate of water moving vertically under gravity is  $1 \text{ ms}^{-1}$ . Darcy's law can then be written:

$$q = -K_H \frac{\partial p}{\partial x} \quad (9.14)$$

where:

$$p = \frac{P}{\rho g} + z \quad (9.15)$$

is the sum of the pressure head  $P/\rho g$  and the elevation head,  $z$ , where  $z$  is the vertical coordinate (upwards). Since we will be concerned with the flow of air and oil, as well as water, in this course, we will use Darcy's equation in the form (9.11).

## 9.5 UNITS OF PERMEABILITY AND THE DEFINITION OF THE DARCY

---

The permeability  $K$  is a property of the geometry of the porous medium. Except for gas flows at very high speeds, the permeability is not a function of flow rate or the properties of the fluid, such as viscosity and density.  $K$  has the dimensions of a length squared. Conventionally permeability is measured in units of a Darcy (D): if there is a flow of  $1 \text{ cm}^3 \text{ s}^{-1}$  of a fluid of viscosity  $10^{-3} \text{ kg m}^{-1} \text{ s}^{-1}$  or  $10^{-3} \text{ Pa s}$  (water) through a cube of rock 1 cm in all directions, the

permeability is 1 Darcy if there is a pressure drop of 1 atmosphere across it ( $1 \text{ atm} \approx 10^5 \text{ Pa}$ ).  $1 \text{ D} \approx 10^{-12} \text{ m}^2$ . Although the Darcy is not an SI unit it is a convenient measure of permeability. For consolidated rock, the mD (milli-Darcy) unit is often used.  $1,000 \text{ mD} = 1 \text{ D}$ .

## 9.6 DEFINITION OF FLOW SPEED AND POROSITY

---

Although  $q$  has the units of velocity (and is often called the Darcy velocity) it is strictly speaking not a real flow speed. The actual flow velocity in a system with porosity  $\phi$  is  $q/\phi$ . Remember that  $q$  is defined as the volume of fluid passing through the soil or rock per unit area per unit time. Imagine that we have a slab of rock  $1 \text{ cm}^2$  in cross-section with a porosity  $\phi = 0.5$ . If  $q = 1 \text{ cm s}^{-1}$ , then each second  $1 \text{ cm}^3$  of fluid enters the rock. It fills the void space. If  $\phi = 0.5$  this  $1 \text{ cm}^3$  of fluid fills  $2 \text{ cm}^3$  of rock. Hence each second the fluid encroaches a further  $2 \text{ cm}$  into the slab. This corresponds to a flow speed of  $q/\phi$  or  $2 \text{ cm s}^{-1}$ . For unconsolidated sand or gravel  $\phi$  is approximately  $0.3$ – $0.35$ . For consolidated rock, deep underground, typical values are  $0.1$ – $0.2$ . For fractured rock  $\phi$  may be as low as  $0.0001$ – $0.02$ , while for some vuggy carbonates,  $\phi$  is as high as  $0.4$ . Soils generally have higher porosities. Loamy soil typically has  $\phi = 0.3$ , while clays have  $\phi$  in the range  $0.4$ – $0.85$ .

### Porosity of natural soils. [Terzaghi and Peck, 1948]

Description	Porosity %
Uniform sand, loose	46
Uniform sand, dense	34
Glacial till, very mixed-grain	20
Soft glacial clay	55
Stiff glacial clay	37
Soft very organic clay	75
Soft bentonite clay	84

## 9.7 ESTIMATING PERMEABILITY

---

It is easy to see that for most porous sedimentary rock  $K$  should be in the range of  $10$ – $10,000$  mD (millidarcies) from Eq. (9.9). A porous rock or soil is only approximately modelled by a bundle of parallel tubes, but to estimate  $K$  we may guess that  $r$  represents a typical throat size ( $10$ – $100 \text{ } \mu\text{m}$ ), while  $d$ , the distance between throats is the grain diameter ( $100$ – $1000 \text{ } \mu\text{m}$ ), giving

$K$  in the range 0.1–10 D. If we account for diagenesis or compaction, which shrinks and closes some of the pore throats, leading to a tortuous confined pathway for fluid flow, then  $K$  may be orders of magnitude lower (as seen in deep oil reservoirs), whereas for unconsolidated gravel, the pore and grain size is much larger and permeabilities of 1000s of Darcies are possible.

Permeability varies widely for different types of soil or rock. As can be seen in the tables below, typical permeability values vary by ten orders of magnitude from granite (where the fluid flows in small, poorly connected fractures) to clean gravel, with wide well-connected pore spaces. Aquifers, consisting of sand or silt, normally have permeabilities between 1 and 1,000 D. Bedrock and oil reservoirs may have permeabilities in the range from fractions of a mD to 1 D.

**Physicochemical properties of rocks and soil (Lyman et al., 1990).**

Rock/Soil Type	Porosity (%)	Particle Density (g/cm <sup>3</sup> )	Bulk Density (g/cm <sup>3</sup> )	Permeability (cm <sup>2</sup> )
<b>UNCONSOLIDATED</b>				
Gravel	25–40	2.65	1.59–1.99	10 <sup>-6</sup> –10 <sup>-1</sup>
Sand	25–50	2.65	1.33–1.99	10 <sup>-9</sup> –10 <sup>-5</sup>
Loam	42–50	2.65	1.33–1.54	10 <sup>-10</sup> –10 <sup>-6</sup>
Silt	35–50	2.65	1.33–1.72	10 <sup>-12</sup> –10 <sup>-8</sup>
Clay	40–70	2.25	0.68–1.35	10 <sup>-15</sup> –10 <sup>-12</sup>
<b>CONSOLIDATED</b>				
Sandstone	5–30	2.65	1.86–2.52	10 <sup>-13</sup> –10 <sup>-9</sup>
Shale	0–10	2.25	1.98–2.25	10 <sup>-16</sup> –10 <sup>-12</sup>
Granite	0–5	2.70	2.57–2.70	10 <sup>-16</sup> –10 <sup>-13</sup>
Granite (fractured)	0–10	2.70	2.43–2.70	10 <sup>-11</sup> –10 <sup>-7</sup>
Limestone	0–20	2.87	2.30–2.87	10 <sup>-12</sup> –10 <sup>-9</sup>
Limestone (Karstic)	5–50	2.71	1.36–2.57	10 <sup>-9</sup> –10 <sup>-5</sup>
Basalt (permeable)	5–50	2.96	1.48–2.81	10 <sup>-10</sup> –10 <sup>-5</sup>

**Typical permeability values (Bear, 1972).**

$\log_{10}K \text{ (m}^2\text{)}$	-7	-11	-16	-20
$K(D)$	100 000	10	0.0001	$10^{-8}$
Permeability	Pervious		Semipervious	Impervious
Aquifer	Good		Poor	None
Soils	Clean gravel	Clean sand or sand and gravel	Very fine sand, silt, loess, loam	
	Peat		Stratified clay	Unweathered clay
Rocks	Oil rocks		Sandstone	Good limestone dolomite
				Breccia, granite

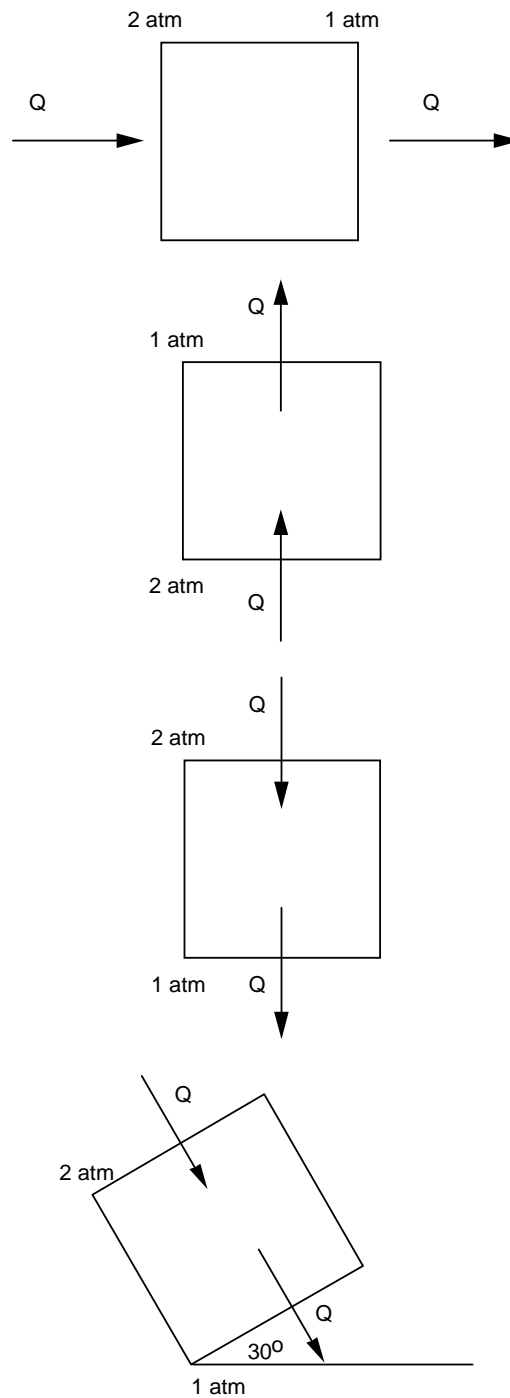
**Soil classification based on particle size (Bedient et al., 1994).**

Material	Particle size (mm)
Clay	<0.004
Silt	0.004 – 0.062
Very fine sand	0.062 – 0.125
Fine sand	0.125 – 0.25
Medium sand	0.25 – 0.5
Coarse sand	0.5 – 1.0
Very coarse sand	1.0 – 2.0
Very fine gravel	2.0 – 4.0
Fine gravel	4.0 – 8.0
Medium gravel	8.0 – 16.0
Coarse gravel	16.0 – 32.0
Very coarse gravel	32.0 – 64.0

**9.8 EXAMPLE PROBLEM INCALCULATING PERMEABILUTY**

In the four situations shown overleaf, the porous medium has a permeability of one Darcy, a cross-sectional area of  $1 \text{ cm}^2$ , and a length of  $1 \text{ cm}$ . The saturating fluid has a viscosity of  $1 \text{ cp}$  ( $1 \text{ cp} = 10^{-3} \text{ Pa s}$ ) and a density  $10^3 \text{ kgm}^{-3}$ . For the inlet and outlet pressures shown, determine  $\Delta\Phi$  and the total flow rate  $Q$  in  $\text{cm}^3\text{s}^{-1}$ .  $g$ , the acceleration due to gravity =  $9.81 \text{ ms}^{-2}$ . You may take  $1 \text{ atm} = 10^5 \text{ Pa}$  and  $1D = 10^{-12} \text{ m}^2$ .



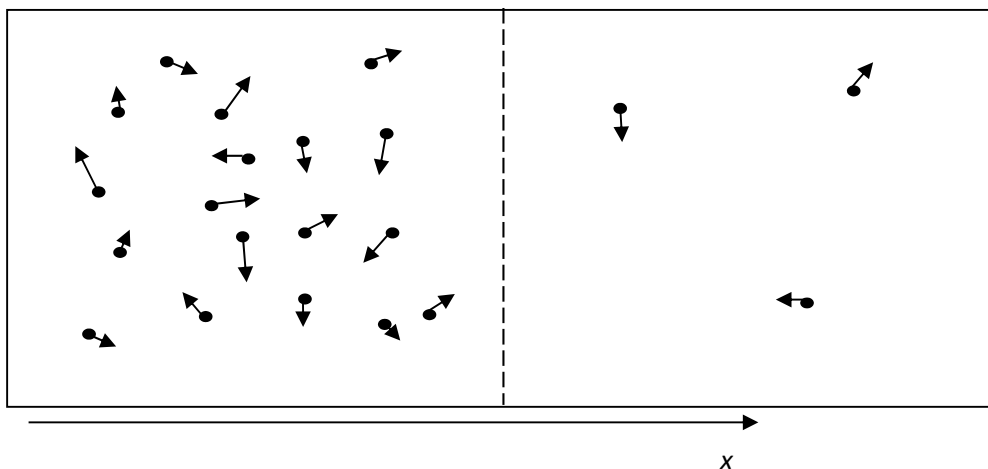


## 10. MOLECULAR DIFFUSION AND CONCENTRATION

Darcy's law describes the flow of a single species in a porous medium — typically water or oil. Later we will return to study flow with multiple phases. However, before broaching this difficult subject, we will first discuss transport of species dissolved in a single phase.

Imagine that some pollutant is dissolved in the water, or consider a chemical constituent present in the oil. The pollutant (solute) not only follows the flow of the water, but intermingles slowly with clean water because of molecular diffusion. In this section we write down an expression for the diffusive flux.

Imagine — as in the figure below — that we have a porous medium saturated with water which is not moving (in fact, we could do the same analysis if we considered a container just holding water). Initially on the left-hand-side the water is salty and on the right it is not very salty.

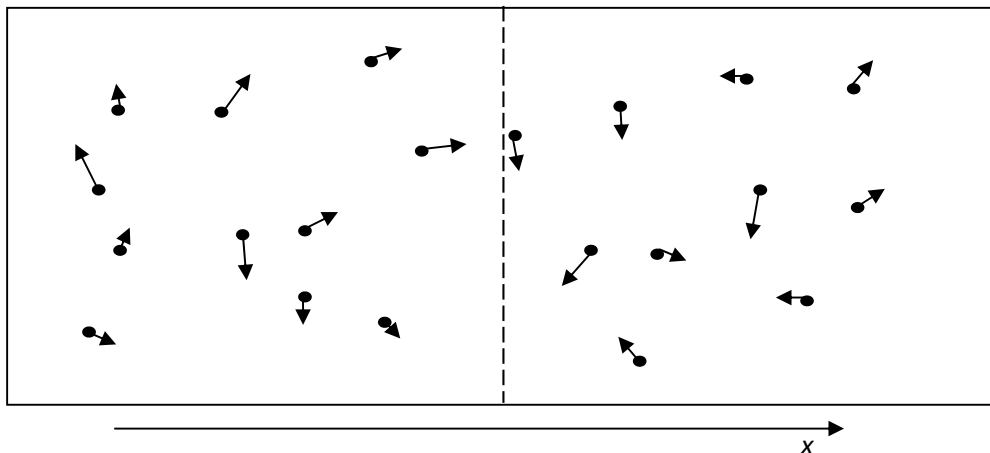


**Diffusion in a porous medium. On the left – initially – there are more particles of a solute than on the right. The arrows represent the random velocities of the particles due to thermal motion. The dashed line is there for illustrative purposes.**

The salt (solute) particles have a random motion – this is due to thermal fluctuations which cause the particles to move constantly in random directions. After a long time this means that the particles will be evenly distributed in the system. While the particle motion is random, on average particles will move from left to right simply because there are more particles on the left to begin with. An individual particle is just as likely to move to the right or the left.

This random motion of the solute is called molecular diffusion. It tends to smear out concentration gradients.

There is a flux of particles (solute) from high concentration to low concentration.



**Diffusion in a porous medium. Eventually, the average concentration will be the same across the sample.**

What is the flux? We will define a flux as the mass of solute moving per unit area per unit time – it has units of  $\text{kgm}^{-2}\text{s}^{-1}$ .

Fick's law of diffusion (in a porous medium) states:

$$J^\alpha = -\phi D^\alpha \nabla C^\alpha \quad (10.1)$$

$J$  is the flux and  $D$  is the diffusion coefficient in a porous medium.  $C$  is the concentration measured in mass per unit volume of water. The subscript  $\alpha$  refers to the solute – different solutes have different diffusion coefficients. Note the minus sign – the flux is in the opposite direction to the concentration gradient. This is like Darcy's law, where the flow is in the opposite direction to the pressure gradient.

Why is there the factor of  $\phi$  – the porosity? This is simply a convention. Diffusion coefficients in porous media are lower than for bulk fluids. So the porosity factor corrects for this. In fact, the

diffusion coefficient in Eq. (10.1) is still lower than in bulk – by a factor of 2 or 3 typically, because of the tortuosity of the pore space.

What are the units of the diffusion coefficient? It has units length<sup>2</sup>/time or m<sup>2</sup>s<sup>-1</sup> in SI units. The value is often very small – many low molecular weight solutes have diffusion coefficients at room temperature in the range 10<sup>-9</sup> to 10<sup>-10</sup> m<sup>2</sup>s<sup>-1</sup>.

If we assume that the concentration gradient is in one direction – the x direction in the two figures above, Eq. (10.1) simplifies to:

$$J^\alpha = -\phi D^\alpha \frac{\partial C^\alpha}{\partial x} \quad (10.2)$$

The last issue to discuss is how to relate this flux to situations when the water is also moving. If the water is moving, molecular diffusion still takes place. In this case the average motion of the water in the flow field is added to the random thermal motion of the molecules. The Darcy velocity  $q$  is the volume of fluid per unit area per unit time. If we multiply this by the concentration  $C^\alpha q$  is the mass per unit area per unit time, or a flux. This is the flux of solute ignoring diffusion. If we consider both diffusion and advection (flow) the total flux is:

$$J^\alpha = qC^\alpha - \phi D^\alpha \frac{\partial C^\alpha}{\partial x} \quad (10.3)$$

where  $q$  is given by Darcy's law, Eq. (6.6). In three dimensions we can write:

$$J^\alpha = qC^\alpha - \phi D^\alpha \nabla C^\alpha \quad (10.4)$$

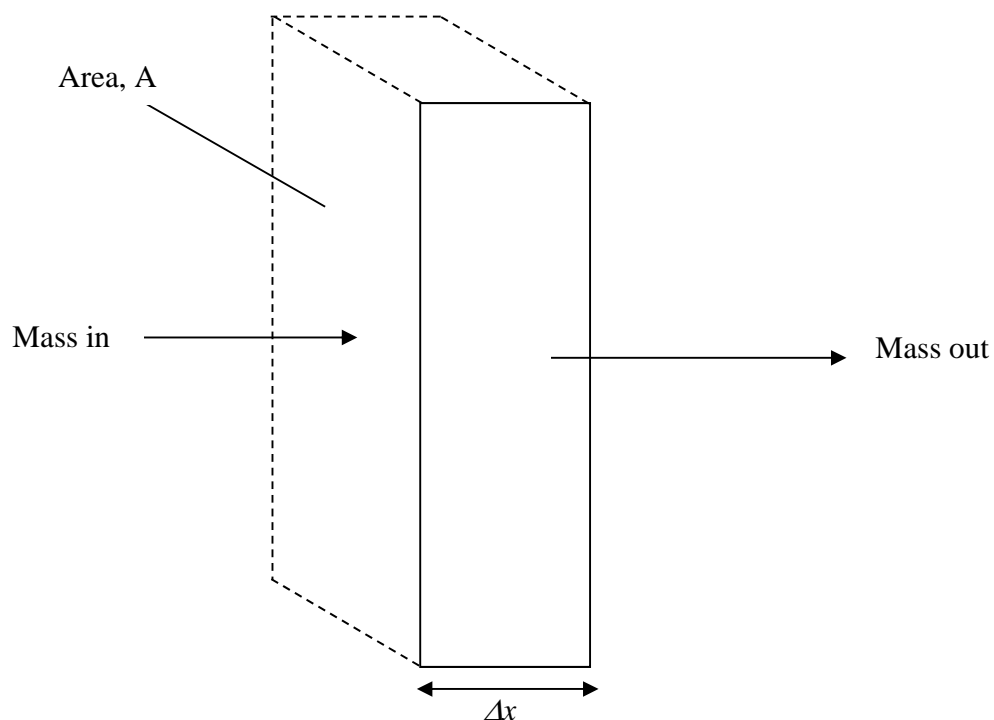
Variations in permeability cause different portions of contaminant plume to follow different pathways through a porous medium. Molecular diffusion causes the contaminant to mix with clean water, causing a dilution of the plume. These two effects combined result in the formation of diluted, dispersed plumes that pollute large bodies of water, a concept that will be discussed in more detail later.

## 11. CONSERVATION EQUATION FOR SINGLE-PHASE FLOW

---

Now we will derive an equation for the conservation of mass of a component  $\alpha$  in a porous medium. This component is considered to be dissolved in water where  $C^\alpha$  is the density of species  $\alpha$  per unit pore volume. The porosity is  $\phi$ . Then  $\phi C^\alpha$  is the mass of  $\alpha$  per unit volume of the soil or rock. We start by considering flow in one direction (the  $x$  direction) through a small volume of length  $\Delta x$  along  $x$  with cross-sectional area  $A$ .

This is an important exercise, and I will expect you to be able to go through the steps yourself. As the class develops we will derive conservation equations for different situations of interest and then solve these equations. I will also expect you to be able to derive – and solve – new equations describing new physical phenomena that you might not have met hitherto.



**A schematic of transport in one dimension used to derive a conservation equation.**

Referring to the figure above, the mass entering the volume per unit time =  $AJ^\alpha(x)$ , while the mass leaving the volume per unit time =  $AJ^\alpha(x+\Delta x)$

Expand the mass leaving as a Taylor series ( $A$  is a constant):

$$\text{Mass leaving} = A J^\alpha(x) + A \Delta x \frac{\partial J^\alpha}{\partial x} + O(\Delta x^2) \quad (11.1)$$

Hence the difference in the mass in minus out is  $-A \Delta x \frac{\partial J^\alpha}{\partial x}$ . Now consider conservation of mass: Mass in per unit time – mass out per unit time = rate of change of mass in the volume  $A \Delta x$ :

$$-A \Delta x \frac{\partial J^\alpha}{\partial x} = A \Delta x \frac{\partial \phi C^\alpha}{\partial t} \quad (11.2)$$

Hence we can write – assuming that  $\phi$  is constant in time:

$$\phi \frac{\partial C^\alpha}{\partial t} + \frac{\partial J^\alpha}{\partial x} = 0 \quad (11.3)$$

We can repeat this analysis for flow along the  $y$  and  $z$  axes. If  $q_x$ ,  $q_y$  and  $q_z$  represent the flows in the  $x$ ,  $y$  and  $z$  directions respectively, the three dimensional version of Eq. (11.3) is:

$$\phi \frac{\partial C^\alpha}{\partial t} + \frac{\partial J_x^\alpha}{\partial x} + \frac{\partial J_y^\alpha}{\partial y} + \frac{\partial J_z^\alpha}{\partial z} = 0 \quad (11.4)$$

The three-dimensional conservation equation can also be more elegantly and simply derived using vector calculus and Green's theorem. Consider an arbitrary volume  $V$  of the porous medium bounded by a surface  $S$  with a flux  $J^\alpha$  through it. Then the equation of mass conservation is:

$$\phi \int \frac{\partial C^\alpha}{\partial t} dV + \int J^\alpha \cdot d\mathbf{S} = 0 \quad (11.5)$$

We use Green's theorem to convert the surface integral into a volume integral:

$$\phi \int \frac{\partial C^\alpha}{\partial t} dV + \int \nabla \cdot \mathbf{J}^\alpha dV = 0 \quad (11.6)$$

and if this is true for an arbitrary volume the integrands must be related by:

$$\phi \frac{\partial C^\alpha}{\partial t} + \nabla \cdot \mathbf{J}^\alpha = 0 \quad (11.7)$$

which is the same as Eq. (11.4).

We can instead perform an overall volume balance. If we assume that the fluid is incompressible – that is the water density  $\rho_w$  is a constant – then the volume flowing into any arbitrary volume is the same as the volume flowing out. From the definition of the Darcy velocity, this leads to:

$$\nabla \cdot \mathbf{q} = 0 \quad (11.8)$$

We can then substitute Fick's law of diffusion and Darcy's law to find  $\mathbf{J}^\alpha$ , Eq. (10.4). If we assume that the diffusion constant is constant then Eq. (11.7) becomes:

$$\phi \frac{\partial C}{\partial t} + \mathbf{q} \cdot \nabla C = \phi D \nabla^2 C \quad (11.9)$$

where I have now dropped the superscript  $\alpha$  for convenience. In one dimension:

$$\phi \frac{\partial C}{\partial t} + q \frac{\partial C}{\partial x} = \phi D \frac{\partial^2 C}{\partial x^2} \quad (11.10)$$

Eqs. (11.9) or (11.10) are called the advection-diffusion equation. The dissolved contaminant follows the overall flow of the fluid (water) by Darcy's law (convection or advection) as well as diffusing through the system by Fick's law. Later on we will extend this equation to multiphase flow.

In essence this conservation equation may be written in words as:

$$\frac{\partial}{\partial t}(\text{Mass per unit volume}) + \frac{\partial}{\partial x}(\text{Mass flux}) = \text{Diffusion} \quad (11.11)$$

It is possible to estimate the magnitude of the terms in Eq. (11.10) and so see whether diffusion or convection dominate. Imagine that the contaminant has spread over some distance  $x = X$  in a time  $t = T$ . We're not going to attempt to solve any of these equations exactly – this comes later – but as a crude estimate we may estimate that the three terms in Eq. (11.10) have magnitude:

$$\begin{aligned} \phi \frac{\partial C}{\partial t} + q \frac{\partial C}{\partial x} &= \phi D \frac{\partial^2 C}{\partial x^2} \\ \frac{\phi C}{T} + \frac{\phi C}{X} &\sim \frac{\phi D C}{X^2} \end{aligned} \quad (11.12)$$

This is a common way of analyzing complex equations. We are going to compute the relative magnitude of each of the three quantities in Eq. (11.12). If advection dominates, we equate the first two terms to find:

$$\frac{X}{T} \sim \frac{q}{\phi} \quad (11.13)$$

which we know already:  $X/T$ , or the typical flow speed is  $q/\phi$ .

If diffusion dominates, we equate the first and third terms of Eq. (11.12) to obtain:

$$X \sim \sqrt{DT} \quad (11.14)$$

Thus for convective flow the pollutant spreads linearly with time, whereas if diffusion dominates, the spread is proportional to the square root of time. The ratio of the diffusive to convective terms is:

$$\frac{\text{Diffusion}}{\text{Convection}} \sim \frac{\phi D}{qX} = \text{Pe} \quad (11.15)$$



This defines a dimensionless Peclet number,  $Pe$ . The length scale  $X$  is generally considered to be a representative scale in the porous medium, which is a mean grain (or pore) size: say around  $100\text{ }\mu\text{m}$  ( $0.1\text{ mm}$ ). Typical flow speeds  $q/\phi$  are of the order  $1\text{ m/day}$  or around  $10^{-5}\text{ ms}^{-1}$  and lower. The diffusion coefficient in water for most petroleum components (typical pollutants in groundwater) is around  $10^{-9}\text{ m}^2\text{s}^{-1}$ . This gives a Peclet number of around 1 – diffusion and advection are typically similar in magnitude at the pore scale.

Molecular diffusion is more significant over lengths,  $X$  less than approximately  $0.1\text{ mm}$  (corresponding to a time of around  $10\text{ s}$ ), but that for large flows over hundreds of metres taking place over months and years, convection is by far the more important process.

We have derived differential equations that describe the flow of a dissolved contaminant in an incompressible fluid. These equations can either be solved analytically for simple cases, or numerically. Except for small scale phenomena, convection, or flow computed using Darcy's law, is much more significant than molecular diffusion.

Also – rather interestingly – the same conservation equation pertains within a pore, if we ignore the porosity in the equations: we simply invoke conservation of mass in a volume of flowing fluid. We can also apply Fick's law (again without the porosity term, but the flow field is governed not by Darcy's law, but from a solution of the Navier Stokes equation, presented in section 12. Primitively, the movement of a dissolved solute within the pore space is governed by the equation:

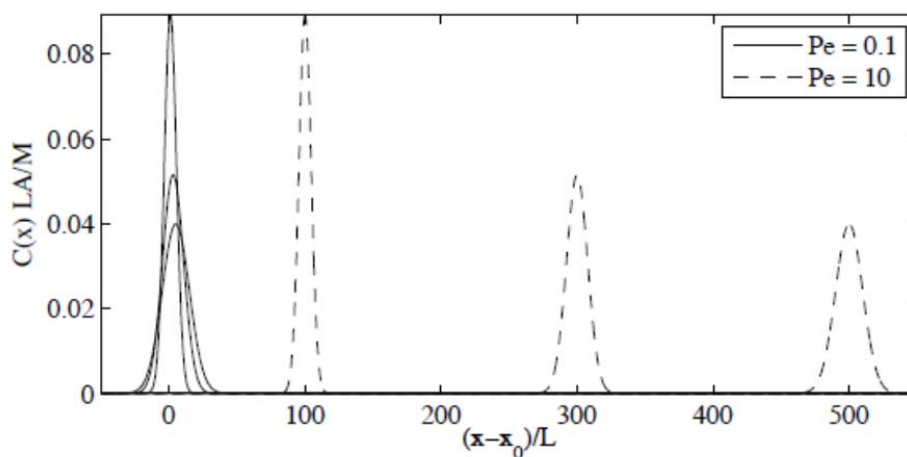
$$\frac{\partial C}{\partial t} + \mathbf{v} \cdot \nabla C = D \nabla^2 C \quad (11.16)$$

where  $\mathbf{v}$  is the local flow velocity and  $D$  is, strictly, the molecular diffusion coefficient.  $\mathbf{v}$  is given by the solution of the Navier-Stokes equation; it is this equation that can be used to describe transport at the pore scale.

Strictly speaking, Eqs. (11.9) and (11.10) are upscaled versions of Eq. (11.16) where now the Darcy velocity,  $q$ , is given by Darcy's law. The problem – as we discuss later – is the diffusive flux. This contains contributions not only from diffusion, but from the random motion of the particles in a spatially heterogeneous flow field, which we have – so far – ignored.

## 11.1 ANALYTICAL SOLUTION OF THE ADVECTION-DIFFUSION EQUATION

We will now present some solutions to Eq. (11.10). These solutions also apply to heat transport and can be found in the classic work by Carslaw and Jaeger (1946). In the end, there is no one correct way to arrive at a solution. Instead, we can use physical inference to find a functional form that is likely to work. Below I show the solution to the equation for solute that is originally injected as a point source. Physically, we expect the plume to move with some average velocity  $v=q/\phi$  and then spread out dependent on the degree of diffusion. This is what we see. We will use this insight to develop a possible mathematical form of the solution.



**A schematic of the solution of the advection-diffusion equation for an initial point source of solute at  $x=0$ . The different Peclet numbers correspond to different average velocities.**

We can transform the governing partial differential equation into an ordinary differential equation using the following variable:

$$z = \frac{x - vt}{\sqrt{t}} \quad (11.17)$$

where  $v=q/\phi$  and we assume that the solution  $C$  can then be written as follows:

$$C = \frac{g(z)}{\sqrt{t}} \quad (11.18)$$

and we solve for the (unknown) function  $g(z)$ . There is – in principle – no reason why this has to be the case. All I need to demonstrate is that the solution obeys the governing partial differential equation and the boundary conditions. Near the end of this course, I will present another solution for a non-linear diffusion problem that uses a different set of variables, because the boundary conditions are different.

Then we define the following derivatives:

$$\frac{\partial g}{\partial t} = \left( -\frac{v}{\sqrt{t}} - \frac{z}{2t} \right) \frac{dg}{dz} \quad (11.19)$$

$$\frac{\partial g}{\partial x} = \frac{1}{\sqrt{t}} \frac{dg}{dz} \quad (11.20)$$

$$\frac{\partial^2 g}{\partial x^2} = \frac{1}{t} \frac{d^2 g}{dz^2} \quad (11.21)$$

and Eq. (11.10) becomes:

$$g + z \frac{dg}{dz} + 2D \frac{d^2 g}{dz^2} = 0 \quad (11.22)$$

This can be written:

$$\frac{d}{dz} \left( 2D \frac{dg}{dz} + gz \right) = 0 \quad (11.23)$$

Hence, for an arbitrary constant  $C$ :

$$2D \frac{dg}{dz} + gz = C \quad (11.24)$$

We also know that – from our schematic solution – that the concentration will be zero at large distances from the origin (large  $z$ ): hence both  $g$  and  $dg/dz$  tend to zero for infinite  $z$ . This means that  $C$  in Eq. (11.24) is zero and we can readily integrate:

$$4D \ln g = -z^2 + C' \quad (11.25)$$

for another constant  $C'$ . Then we can write:

$$C(x, t) = \frac{M}{\sqrt{4Dt}} e^{-(x-vt)^2/4Dt} \quad (11.26)$$

where  $M$  is the initial mass (per unit area) of concentration. These are the solutions shown in the figure shown previously.

This relationship makes use of the identity:

$$\int_{-\infty}^{\infty} C(x, t) dx = M \quad (11.27)$$

since:

$$\int_{-\infty}^{\infty} e^{-z^2} dz = \sqrt{\pi} \quad (11.28)$$

Note that Eq. (11.26) shows a mean (maximum) concentration that moves a distance  $x=vt$ , with a typical spread  $x-vt = 2\sqrt{Dt}$ , similar to our simple scaling analysis.

## 11.2 DIFFUSION AND DISPERSION

---

The governing partial differential equation and its solution are classical in the literature, as mentioned previously. However, they are a very poor approximation of what really happens in a porous medium, particularly the heterogeneous pore spaces we have shown earlier. The

limitation in the derivation is that we assume a uniform flow field where the only flux associated with changes in concentration is due to molecular diffusion.

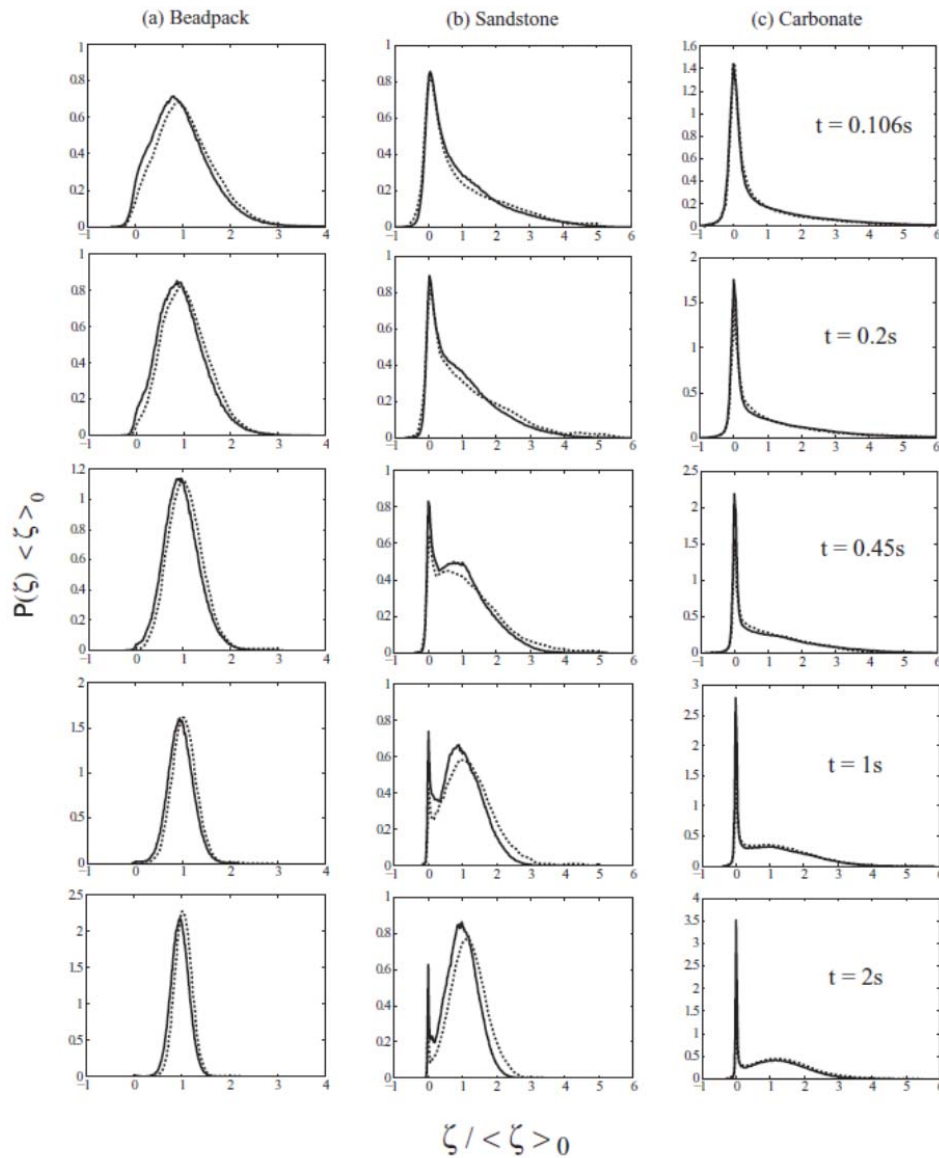
In reality – in porous media with tortuous pore spaces – the spreading and mixing of a solute is controlled by two factors: molecular diffusion that leads to a local – pore-scale – mixing of concentration; and variations in flow speed that allow the solute to follow different flow paths through the porous medium. It is this second effect that normally dominates, with huge spreading of a dissolved plume of solute caused not so much by local-scale mixing, but governed by the variations in the flow field.

This is evident from an examination of the flow paths shown when we introduced Darcy's law. In particular, refer back to the images and flow fields shown in section 9. To have an idea of what transport really looks like in heterogeneous porous media, the figure below shows simulated concentration profiles – for an effective point source injection as described above – compared to measurements of water movement at the scale of a few mm to cm made using NMR techniques. For simplicity, the curves are shown in a dimensionless form. The  $y$  axis represents concentration times average distance moved, while the  $x$  axis is the distance divided by average speed times a dimensionless distance. A system with no diffusion (or dispersion) would then travel at unit speed on the graph. With simple diffusion – obeying Eq. (11.26) – we would see a Gaussian-type profile centred on 1. This is seen for the bead pack. Here the flow field is uniform and there is Fickian-type smearing controlled by molecular diffusion and small-scale heterogeneity in the flow field.

For the more heterogeneous porous media – the sandstone and carbonate – the behaviour is different: most of the solute resides in locally stagnant regions of the pore space and hardly move, with a very long dispersed plume of solute in the faster flowing regions. There is no obvious concept of a typical speed with smearing about this average.

A full understanding of this phenomenon and how, properly, to describe dispersive transport, is a rich topic of current research. An exploration of the ideas and how to describe transport mathematically in these cases is beyond the scope of this course: needless to say an approach based on fluctuations in velocity and/or travel times is necessary, which does not fit neatly into an effective partial differential equation – it is evident from the figures, that we cannot match

the experiments simply by tweaking the effective diffusion (or dispersion) coefficient while leaving the functional form of the behaviour the same.



**Predicted (solid lines) and measured (dotted lines) dimensionless concentration profiles for a bead pack, sandstone and carbonate. Note that with the exception of the beadpack, the behaviour does not resemble a solution to the governing advection-diffusion equation. From Bijeljic *et al.* (2011).**

If – and in reality this is rarely, if ever, the case – we can indeed describe transport as the solution to an advection-diffusion-type equation, then traditionally we can write the following identical in functional form to Eq. (11.9):

$$\phi \frac{\partial C}{\partial t} + q \frac{\partial C}{\partial x} = \phi D \frac{\partial^2 C}{\partial x^2} \quad (11.29)$$

but where now  $D$  is the effective dispersion coefficient that accounts for both molecular diffusion and the random nature of the flow field. This equation is called the advection-dispersion equation. This coefficient  $D$  can be written as follows:

$$D = D_{dis} + D_m = \alpha v + D_m \quad (11.30)$$

where now  $D_m$  is the molecular diffusion coefficient in the porous medium, and  $\alpha$  is the dispersivity – it has the dimensions of a length and represents, physically, the typical scale of heterogeneity in the porous medium. However, natural geological media have structure over all length scales, and so the apparent dispersivity – and hence the spreading of a contaminant plume – appears to become more significant with scale, as more heterogeneity is encountered. The table below illustrates this phenomenon, where the dispersivity is, approximately, around one tenth of the scale of the system.

Eq. (11.30) can be derived assuming that the solute experiences a series of random perturbations every time it moves a distance  $\alpha$  – the velocity  $v$  in the dispersion coefficient represents the fact that the number of perturbations encountered in a given time is proportional to the flow speed.

In the plane of the aquifer (a nearly horizontal plane) the plume is therefore highly dispersed due to variations in permeability that cause huge fluctuations in the local flow rate. The permeability  $K$  will typically vary by several orders of magnitude or more over lengths of a few metres in heterogeneous formations. A contaminant plume does not flow at a constant rate and direction, but forms a ragged front due to variations in permeability. This causes the plume to spread. Small amounts of molecular diffusion mix the contaminant with clean water. The combined effects of permeability variation and diffusion dilute the plume and disperse the

contamination over a wide region of the aquifer. In virtually all circumstances the precise location of the contaminant cannot be predicted with any certainty unless the distribution of permeability in the subsurface is known: at every scale from the pore-scale onwards, the distribution of contaminant is rarely, if ever, accurately predicted by an average displacement and some Gaussian-type variation about this mean.

Overall, the characterization of dispersion as a diffusive process is flawed, since this does not – at any scale – the pore scale or the field scale – characterize transport in even a qualitative sense. The community does not – at present – have a good way to describe transport on all scales, although much of the mathematical and physical insight has been developed.

In some sense, multiphase flow, which we will now return to, is easier and we will revisit diffusive processes in this context – specifically capillary-controlled displacement – later.



**Standard deviation and correlation scale of the natural logarithm of hydraulic conductivity or transmissivity (Gelhar, 1993).**

Medium	Type*	$\sigma_f$	Correlation scale (m)		Overall scale (m)	
			Horizontal	Vertical	Horizontal	Vertical
alluvial-basin aquifer	T	1.22	4,000		30,000	
sandstone aquifer	A	1.5–2.2		0.3–1.0		100
alluvial-basin aquifer	T	1.0	800		20,000	
fluvial sand	A	0.9	> 3	0.1	14	5
limestone aquifer	T	2.3	6,300		30,000	
sandstone aquifer	T	1.4	17,000		50,000	
alluvial aquifer	T	0.6	150		5,000	
alluvial aquifer	T	0.4	1,800		25,000	
limestone aquifer	T	2.3	3,500		40,000	
Chalk	T	1.7	7,500		80,000	
alluvial aquifer	T	0.8	820		5,000	
fluvial soil	S	1.0	7.6		760	
Eolian sandstone outcrop	A	0.4	8	3	30	60
glacial outwash sand	A	0.5	5	0.26	20	5
sandstone aquifer	T	0.6	$4.5 \times 10^4$		$5 \times 10^5$	
sand and gravel aquifer	A	1.9	20	0.5	100	20
prairie soil	S	0.6	8		100	
weathered shale subsoil	S	0.8	< 2		14	
fluvial sand and gravel aquifer	A	2.1	13	1.5	90	7
Homra red Mediterranean soil	S	0.4–1.1	14–39		100	
gravely loamy sand soil	S	0.7	500		1,600	
alluvial silty-clay loam soil	S	0.6	.1		6	
glacial outwash sand and gravel outcrop	A	0.8	5	0.4	30	30
glacial lacustrine sand aquifer	A	0.6	3	0.12	20	2
alluvial soil (Yolo)	S	0.9	15		100	

\*Types of data: T, transmissivity; S, soils; A, three-dimensional aquifer.

## 12. CAPILLARY AND BOND NUMBERS

---

Now we will return to multiphase flow in porous media and the concept of capillary pressure. In this course, I presume that the fluid configurations are controlled by the Young-Laplace equation and contact angles. Fluid flow is slow and – as we show later – we presume that each phase flows independently.<sup>3</sup>

However, do capillary forces really dominate at the pore scale and what are the effects of buoyancy forces and flow rate?

If a representative pore radius is  $R$ , then a typical capillary pressure is of order  $\sigma/R$ . The viscous pressure drop over a length  $L$  is given from Darcy's law (where  $\Delta P$  is a pressure drop – hence the removal of the minus sign):

$$q = \frac{K \Delta P}{\mu L}; \Delta P = \frac{q \mu L}{K} \quad (12.1)$$

The ratio of a typical pressure drop to a capillary pressure is then:

$$\text{Ratio} = \frac{q \mu L R}{\sigma K} \quad (12.2)$$

$LR/K$  is a dimensionless ratio (consider the units – permeability has the units of length squared). In porous media this ratio is typically around 1,000 if  $L$  is a pore length. Typically  $L/R$  is around 2-10.

Why isn't this ratio  $LR/K$  closer to 1? Recall the discussion in section 9, which showed that permeability typically has a numerical value that is much lower than the square of a typical pore radius.

The capillary number is defined by:

---

<sup>3</sup> This approximation can be relaxed and dynamic models of multiphase flow show that there is viscous coupling between the phases. However, for this course, we will ignore these effects.

$$N_{cap} = \frac{q\mu}{\sigma} \quad (12.3)$$

Representative values for the capillary number for field-scale displacement are typically  $10^{-8}$  to  $10^{-6}$  or lower. If  $N_{cap}$  is around 0.001, then viscous and capillary forces are approximately equivalent at the pore scale – see Eq. (12.2).

In most natural flows in aquifers and oil reservoirs, capillary forces dominate at the pore scale:  $q$  is generally around  $10^{-8}$  to  $10^{-5}$ ,  $\mu$  is around  $10^{-3}$  Pa.s (for water), while  $\sigma$  for oil/water systems is typically 0.05 N/m at ambient conditions and around half that number at oilfield temperatures. This leads to values of capillary number in the range  $10^{-6}$  and lower. Viscous forces, however, dominate at the large (inter-well) scale: this can be seen by substituting  $L=100-1,000$  m (the inter-well scale) in Eq. (12.2).

We can perform a similar analysis for buoyancy. The pressure drop over a vertical distance  $L$  is  $\Delta\rho gL$ , where  $\Delta\rho$  is the density difference between the phases. The ratio of buoyancy to capillary forces is given by:

$$\text{Ratio} = \frac{\Delta\rho gLR}{\sigma} \quad (12.4)$$

Sometimes a Bond number is defined by:

$$B = \frac{\Delta\rho gL^2}{\sigma} \quad (12.5)$$

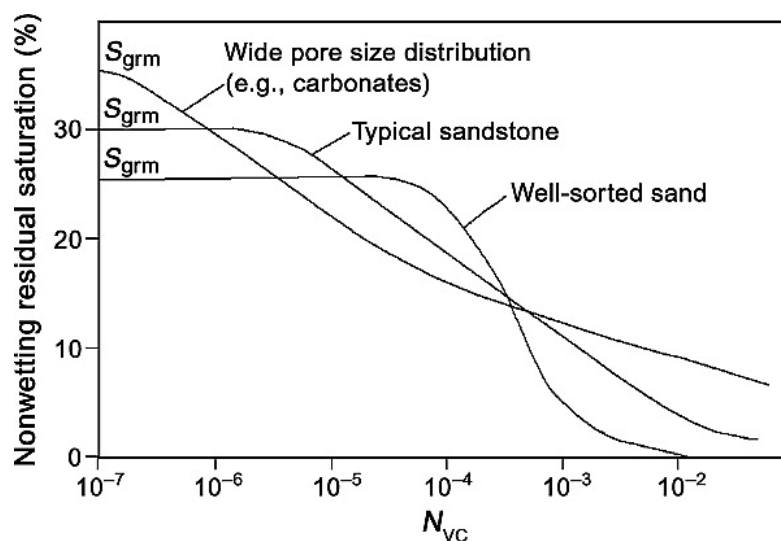
Once again using representative numbers – say a density difference of  $200 \text{ kg.m}^{-3}$  and a pore length of  $10^{-4}$  m – the Bond number is of order  $10^{-3}$ . Buoyancy forces are small in comparison with capillary forces at the pore scale.

The reason why this is important, is that *if* viscous or buoyancy forces were to dominate at the pore scale then two things happen:

1. The non-wetting phase (oil) is rarely trapped, since the invasion of water occurs through a flat connected front with essentially no snap-off and little bypassing.
2. Even if some ganglia of oil are stranded, viscous forces can push these blobs out of the pore space.

The result is that if the capillary number is around 0.001 or larger, the residual oil saturation can be very low. Therefore, if we could increase the capillary number in this range – by increasing the flow rate  $q$ , or reducing the interfacial tension  $\sigma$ , we would have a very efficient oil recovery process. This is physics behind surfactant flooding. Here surfactants are added to the injected water, lowering the oil/water interfacial tension to 0.1 mN/m or smaller. If the capillary number increases to the range of 0.001 or above, then very high oil recoveries are observed.

The decrease in residual saturation as a function of capillary number is shown in the graph below (taken from Lake, 1989).



A schematic of residual saturation as a function of capillary number (here denoted  $N_{vc}$ ). At capillary numbers higher than around  $10^{-3}$  – meaning that viscous forces begin to dominate over capillary forces at the pore scale – the residual saturation can fall to very low values. This is the basis for surfactant flooding if the interfacial tension is reduced to a sufficiently low value, the capillary number is high enough to allow low residual saturations to be achieved, giving good oil recovery (Lake, 1989).

### 13. RELATIVE PERMEABILITY

---

We will now extend Darcy's law to cases when multiple fluid phases are flowing. We assume that each phase flows in its own sub-network of the pore space without affecting the flow of the other phases. This is applicable for flow at low capillary and Bond numbers, where capillary forces dominate at the pore scale.

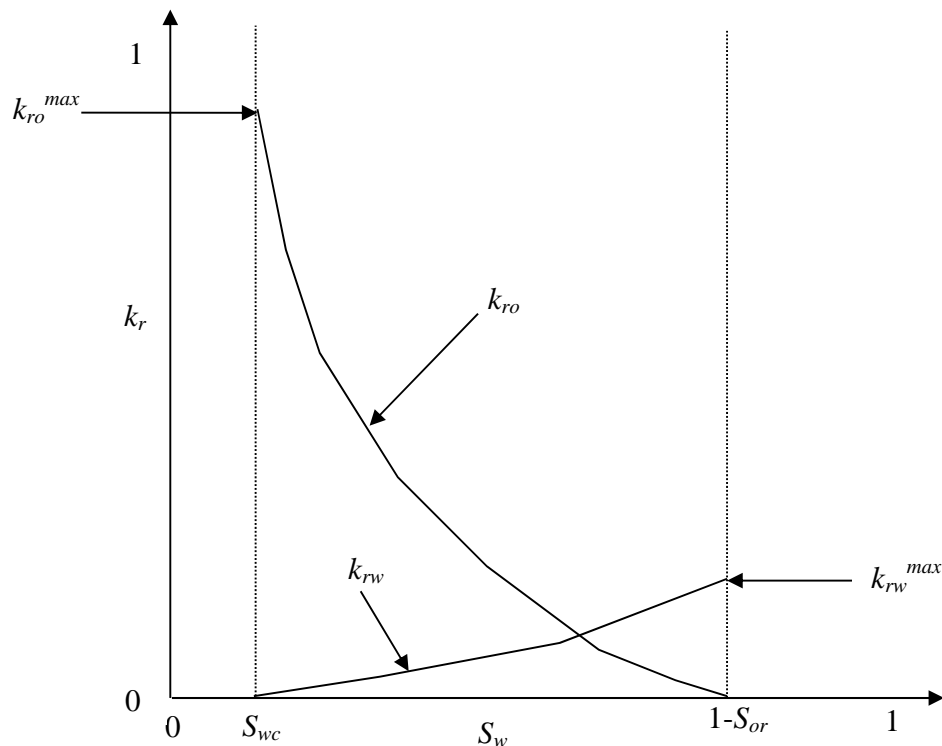
For single-phase flow in one dimension, we have Eq. (9.11). Then the extension to multiphase flow of fluid  $p$  is (Muskat and Meres, 1933):

$$q_p = -\frac{Kk_{rp}}{\mu} \left( \frac{\partial P_p}{\partial x} - \rho_p g_x \right) \quad (13.1)$$

$k_{rp}$  is the relative permeability of phase  $p$ . It represents the mobility of the phase as a fraction of what it would be for single-phase flow. It is traditionally plotted as a function of saturation.

In this course, we will accept this characterization of multiphase flow. For slow flow, dominated by capillary forces, this is a reasonable approximation. However, the relative permeabilities are not simply unique functions of saturation. As we found for capillary pressure, the relative permeabilities will also depend on wettability (and this can change during the course of a displacement, or series of displacements) and saturation history. Moreover, at higher flow rates, the relative permeabilities will also be functions of this flow rate, as well as viscosity ratio. Last, the flow of one phase can also affect the flow of the other, through viscous coupling at the fluid interfaces. All of these effects may be significant, particularly when capillary forces are no longer dominant at the pore scale. However, in this treatment we will only consider the impact of pore structure, wettability and saturation path: this alone reveals a rich and important behaviour which is sufficient to explain and explore most displacement processes seen in oilfields and aquifers.

Below are typical relative permeability curves for a water-wet medium. The curves are shown for waterflooding from the connate or irreducible water saturation.



**Typical relative permeability curves for waterflooding a water-wet medium.** The points to note are the steep decrease in oil relative permeability with water saturation, the low water relative permeability (including its final value) and the high value of residual oil saturation  $S_{or}$ .

The key features, evident for a water-wet medium are as follows.

1. **Typical values of the maximum oil and water relative permeability.** At the beginning of water injection – marking the end of primary drainage – the oil fills most of the pore space. Since wettability is altered after oil invasion, the oil will reside in the larger regions of the pore space. As a consequence, the oil relative permeability at the beginning of waterflooding – the maximum value – is close to 1: typically 0.8 or greater. In contrast, the water – for a water-wet system – fills the narrower regions of the pore space, trapping oil in the larger pores. This means that the water always has poor connectivity and the relative permeability remains low: typically at the end of waterflooding the water relative permeability is only around 0.1 or lower. This is different – as described below – if the system is not strongly water-wet.

2. **Why the maximum oil relative permeability is higher than the maximum water relative permeability.** This is covered by the discussion for the previous point. Remember, in a water-wet system, water remains in the small pores, while oil is in the large pores (where it is trapped during waterflooding).
3. **Why the sum of the relative permeabilities is less than 1 for all saturations, and why the sum is much less than when the curves cross.** Any interface between oil and water, across a pore space, prevents flow. Hence, the more interfaces between the phases, the more flow is restricted. This is particularly true when water invades by snap-off, cutting off oil flow through the largest pores, while remaining poorly connected itself. Hence, two phases in combination have a much lower conductance than for single-phase flow (one or more of the relative permeabilities is typically always very low). When the relative permeabilities cross is when there is most phase interference and both values are likely to be small.

In the following, we will amplify these points through experimental and modelling results. Relative permeability is very difficult to measure accurately; sophisticated apparatus is used to measure this important quantity – a discussion of experimental techniques if, however, beyond the scope of this course. By default the data refers to water injection, since commonly this is the most important process involving multiphase flow in oil reservoirs. The picture below shows some of our apparatus used to measure relative permeability at Imperial College. There is an adapted medical X-ray scanner (with a resolution of around 1 mm) that can monitor fluid movement within rock cores several cm across and up to 1 m long.



**A photograph of the apparatus at Imperial College used to measure relative permeability.**

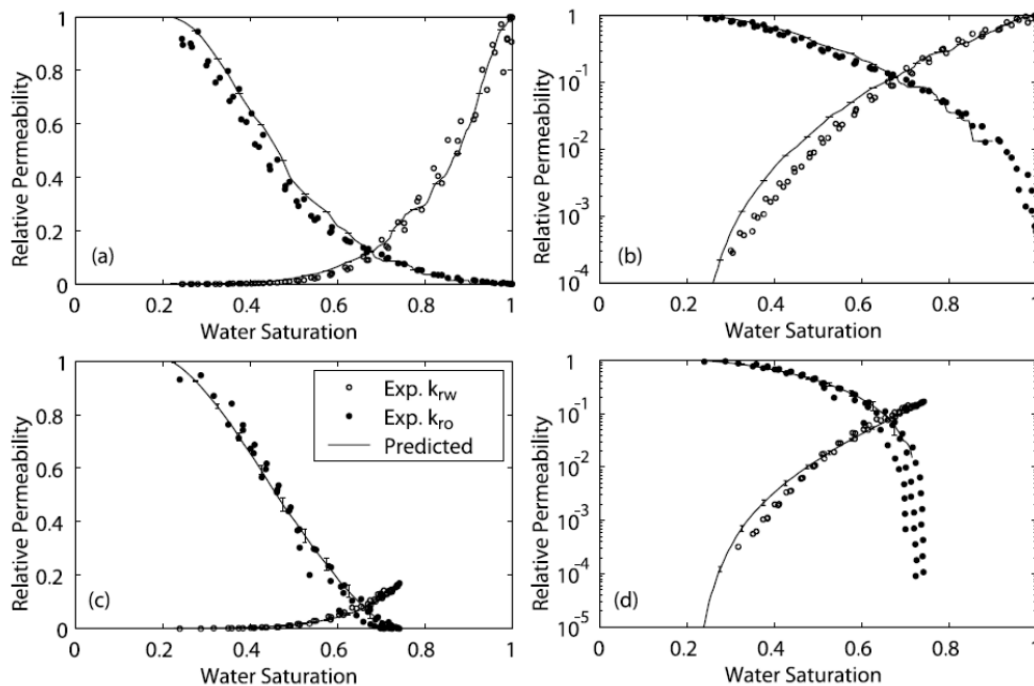
The key controls on relative permeability are wettability and the connectivity of the pore structure,,, again discussed in more detail later in this section.

### 13.1 RELATIVE PERMEABILITIES FOR SANDSTONES AND PREDICTIONS USING PORE-SCALE MODELLING

---

The points above can be illustrated in the relative permeability curves shown below. The experimental results are part of a classic series of measurements made on Berea sandstone for both two and three-phase (oil, water and gas flowing – discussed later) by Oak (1990). These measurements have served as a benchmark for analysis in the literature, because Berea is a standard quarry sandstone used by many researchers and the raw data is available in spreadsheet form. The results of three sets of experiments are shown.





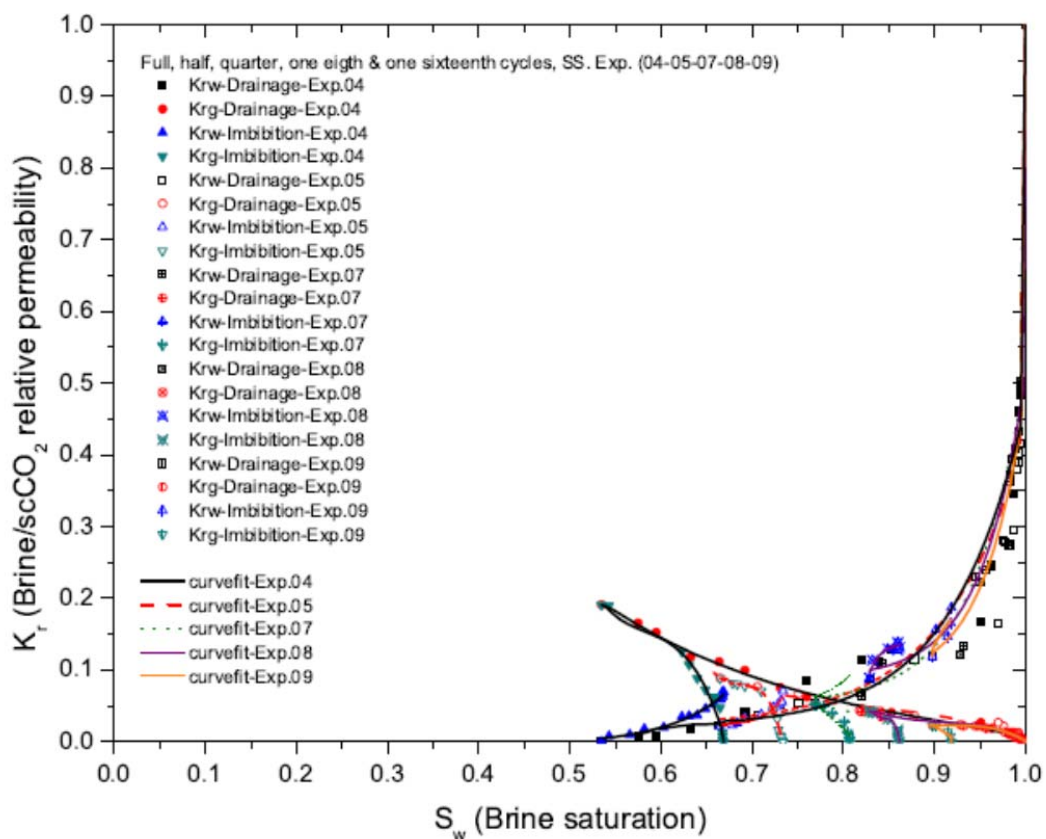
**Measured (points) and predicted (lines) relative permeability curves in a water-wet Berea sandstone. The curves are shown on both linear and logarithmic axes. The primary drainage curves are shown at the top, and the waterflooding curves at the bottom. Network modelling – capturing the connectivity of the pore space using a random lattice of pores and throats, combined with an accurate assessment of pore-scale displacement processes – can predict the behaviour accurately.**

Also shown are network modelling predictions performed by Valvatne and Blunt (2004). These predictions use the network for Berea presented earlier in these notes and employ the pore-scale displacement processes we have described. Primary drainage is an invasion percolation process: it is assumed that the wetting phase (water) is strongly wetting and the contact angle is zero. We make good predictions of the measured data. For waterflooding, there is an uncertainty. As discussed in section 6, the (advancing) contact angle is larger in this case, mainly due to the roughness of the solid surface. In network modelling we assign an effective contact angle that accounts for roughness and the converging/diverging nature of the pores: this angle is around  $60^\circ$ . With this larger contact angle – which tends to suppress snap-off in some pores – we predict the relative permeability curves accurately.

The measured data and the predictions show the features mentioned above. Note that the residual saturation is around 0.3 and the maximum water saturation is only about 0.1. Blocking

the flow in the largest 30% of the pore space reduces the water conductivity by a factor of 10. This is an important observation: small changes in fluid configuration that prevent flow through a few large channels has a big impact on relative permeability.

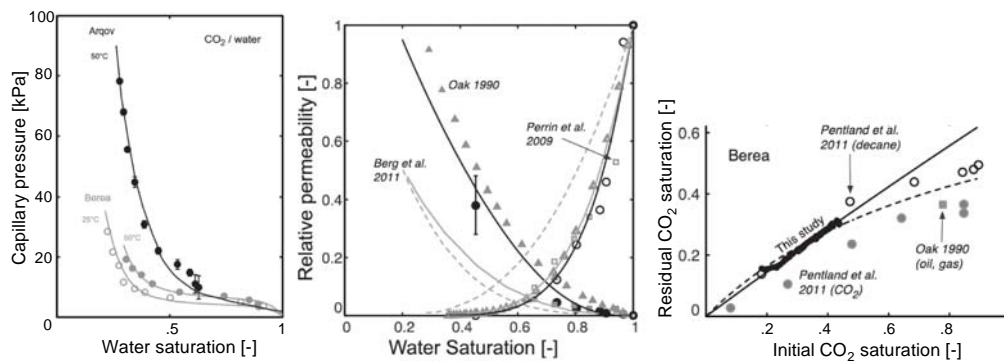
We can also study the effect of different displacement paths on the relative permeability. The data in the curves below are taken from Akbarabadi and Piri (2013). Here carbon dioxide is the non-wetting phase and is injected into a Berea core to different initial saturations. Then brine is injected to displace the carbon dioxide, resulting in different curves (relative permeability hysteresis) and different amounts of trapped non-wetting phase, as discussed previously.



**Measured relative permeability on Berea sandstone.** Here carbon dioxide is the non-wetting phase and is injected to different initial saturations before brine injection. Here we see the relative permeability hysteresis: notice the different residual saturations, dependent on the initial saturation, as discussed previously.

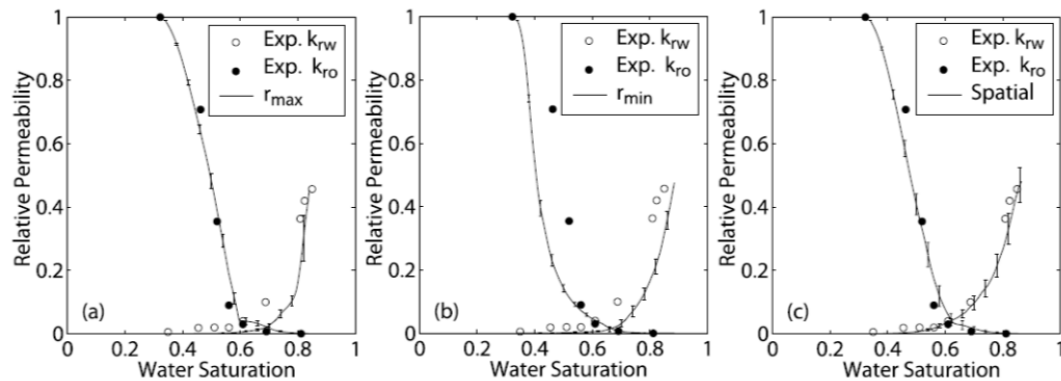
We can continue our study of relative permeability with more results where carbon dioxide is the non-wetting phase (the application here is carbon dioxide storage in aquifers). The graphs

below show primary drainage capillary pressure (section 8), relative permeability and trapping curves (section 9) on Berea sandstone, comparing the results of Perrin *et al.* (2012) with those of other researchers. This is the combination of multiphase properties that control fluid movement and recovery in the subsurface.



**Measured primary drainage capillary pressure, relative permeability and trapping curves for carbon dioxide injection in Berea sandstone. This is taken from the work of Perrin, Krevor *et al.* (2012).**

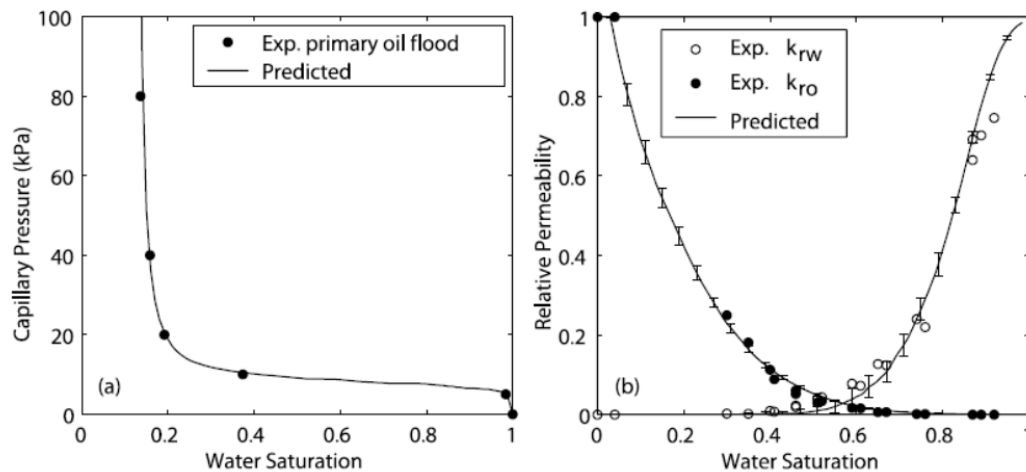
We can also consider the effects of wettability on the relative permeability curves. This will be presented in more detail later in the context of carbonate rocks. In general carbonates tend to experience a stronger wettability alteration in contact with crude oil than sandstones. So, while we see the whole range of behaviour from water-wet to strongly oil-wet in sandstones, more typically in carbonates we see mixed-wet to oil-wet properties. The figure below shows predicted waterflood relative permeabilities for a mixed-wet reservoir sandstone compared to the data. The predictions use different models to assign wettability: there is some discussion in the literature over whether large or small pores are more likely to undergo a significant wettability change. The results are also taken from Valvatne and Blunt (2004).



**Predicted and measured relative permeability for a mixed-wet reservoir sandstone. The predictions (lines) use different assumptions as to which pores become oil-wet after primary drainage: the results are relatively insensitive to this assignment.**

In a mixed-wet system the key features are a low residual oil saturation (noted previously for capillary pressure, section 10), and low oil and water relative permeabilities. The low residual is due to the connectivity and slow drainage of oil layers. The low oil relative permeability is also easy to explain: where the system is oil-wet, the oil resides in the smallest pore spaces and in layers that, while interconnected, have a very low conductance. The water relative permeability is also low: this is a significant feature that has a major impact on waterflood oil recovery at the field scale and is discussed further later. When water is first injected, it fills, preferentially, the water-wet regions – the smallest water-wet pores and throats. The water saturation increases, but the connectivity of the water is poor and so the relative permeability remains low. Then water fills the oil-wet regions – and the largest oil-wet pores first. Again, to begin with, the connectivity remains low; it is only at the highest water saturations that water becomes well connected through the larger regions of the pore space and the relative permeability rises rapidly. Its maximum value is higher than for water-wet systems, since the residual oil saturation is lower (there is more water in the rock) and the water occupies, preferentially, the larger oil-wet pores.

The final set of sandstone curves are for an oil-wet reservoir rock. Again good predictions can be made. In the figure below, the layer drainage regime is evident; this is where the oil relative permeability is low, but allows flow down to a very low residual saturation. The water relative permeability can reach high values, once water is well connected through the pore space in the larger pores.



**Predicted and measured primary drainage capillary pressure and waterflood relative permeability for an oil-wet reservoir sandstone. Good predictions are made. Note the low oil relative permeability at higher water saturations – this is the oil layer drainage regime, where oil can be displaced to a very low residual saturation (less than 10%). Once the water becomes well connected through the pore space occupying the larger pores, its relative permeability rises quickly.**

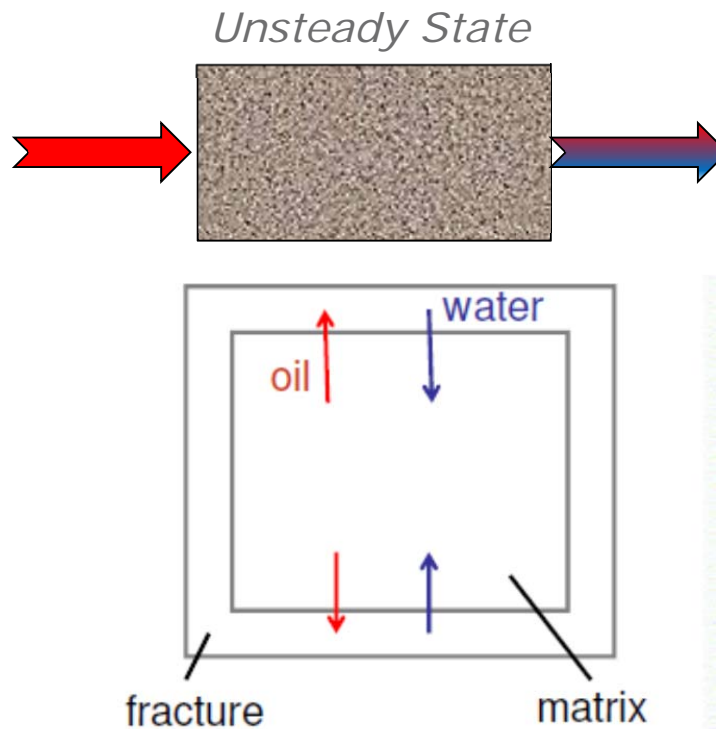
### 13.2 IMBIBITION AND OIL RECOVERY PROCESSES

There are two distinct recovery processes in oilfields when water is injected to displace brine. The first is direct displacement, shown in the diagram on the next page: water is injected and essentially pushes out oil. At the pore scale, we know that capillary forces dominate and the recovery is controlled by the residual saturation. How fast this recovery occurs is controlled by the relative permeabilities: the ideal is a low water relative permeability that holds water back and a high oil relative permeability, allowing oil to flow rapidly and be displaced ahead of the water. This is discussed later, but qualitatively, a low residual saturation says how much oil can be recovered in theory (a low residual indicates high recovery) while the relative permeability gives the rate at which recovery occurs.

The second process is imbibition. This is simple to imagine – it is the same as placing a piece of rock in water: the water spontaneously enters the rock under the influence of capillary pressure. This is the dominant recovery process in fractured reservoirs – typically seen for brittle rocks, such as carbonates. Here the injected water, rather than forcing out the oil, flows rapidly along

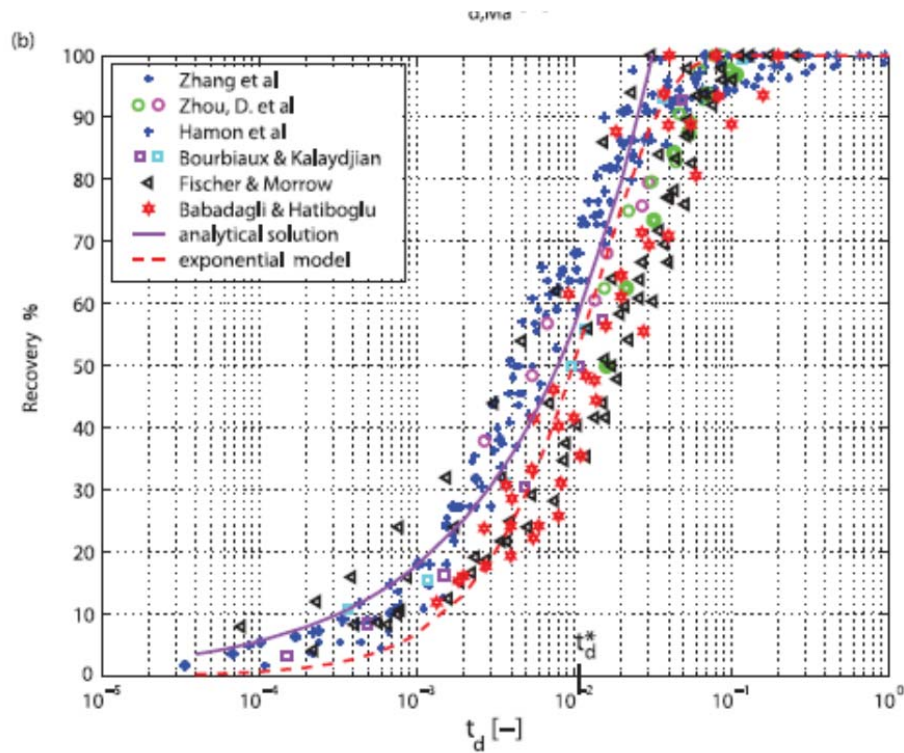
the high permeability fractures. Then water enters the matrix (normal unfractured rock) by imbibition. This is a process controlled by capillary forces, with some help due to the density difference between water and oil that helps push the water into the bottom of a matrix block. Again this process is shown schematically below. In this case the recovery is controlled by how much oil remains after spontaneous imbibition: from our discussion of capillary pressure, this saturation (when the capillary pressure is zero) is much lower than the residual saturation for mixed-wet systems. The rate of recovery is controlled by the water relative permeability, typically at low saturation, since this is the saturation range of interest and limits how fast the oil can be displaced.

Both of these problems can be analysed through analytical solutions (in one dimension) to the governing flow equations; these are presented later in the course. Here we explain the results physically in terms of the relative permeabilities and capillary pressures.



**A schematic of the two types of recovery process in reservoirs. The top picture shows displacement, where water is injected to displace oil. This occurs in most unfractured reservoirs. However, where there is extensive fracturing, and these fractures provide high permeability paths for flow, the behaviour is different: shown in the bottom picture. Here recovery occurs by imbibition of water into the matrix (normal unfractured rock).**

In imbibition, the recovery as a function of time has a characteristic behaviour that has been studied by many authors. Shown below is a compilation of 48 datasets in the literature, compiled by Schmid and Geiger (2012) in a classic paper that also presents a closed-form analytic solution to the flow equations for this problem (which is presented later in these notes).



**Recovery – as a percentage of the final recovery – as a function of dimensionless time for spontaneous imbibition for 48 experiments in the literature compiled by Schmid and Geiger (2012). The exponential model uses Eq. (13.6) with  $\alpha = 0.05$ .**

In the figure above, the recovery is plotted as a function of dimensionless time. A full discussion giving an analytical solution is provided near the end of this class; however, we can use physical principles to estimate likely time-scales. We will show that this is a diffusive problem mathematically, so we can readily examine the likely scaling of the displacement.

The driving force is capillary pressure, which is the interfacial tension divided by a typical pore radius. As before (section 7) we can relate this to the square root of the permeability divided by the porosity. Imagine that the wetting phase has invaded a distance  $x$  into the porous medium. Hence the pressure gradient driving flow can be written:

$$\frac{\partial P}{\partial x} = \frac{\sigma}{x} \sqrt{\frac{\phi}{K}} \quad (13.2)$$



Then from the multiphase Darcy law, Eq. (13.1), assuming that flow is limited by the water relative permeability, we can find the flow rate, which determines how fast the distance  $x$  changes with time:

$$q = \phi \frac{dx}{dt} \sim \frac{\sigma K k_{rw}}{\mu_w} \sqrt{\frac{\phi}{K} \frac{1}{x}} \quad (13.3)$$

The porosity term for  $dx/dt$  converts a Darcy velocity into a speed. Eq. (13.3) has the solution:

$$x(t) = \sqrt{At} \quad (13.4)$$

where:

$$A = \frac{\sigma k_{rw}}{2\mu_w} \sqrt{\frac{K}{\phi}} \quad (13.5)$$

Note that the distance travelled (and hence recovery) scales – at early time, before the imbibing front reaches the ends or boundaries of the system – as the square root of time. This mathematically and physically is a diffusive process, as opposed to recovery by direct displacement where recovery and front movement increases linearly with time.

Eventually, the wetting front reaches the end of the system (say a distance  $x=L$ ); from then on recovery is much slower. Empirically – simply a match to the compilation of recovery results shown previously – we find that the recovery can be written as:

$$R = R_{\infty}(1 - e^{-\alpha t_D}) \quad (13.6)$$

where  $R$  is the oil recovery,  $R_{\infty}$  is the ultimate recovery.  $\alpha$  is a constant used to match the data and  $t_D$  is a dimensionless time. This is the analytical match shown on the previous graph. In our analysis, it would be given by:

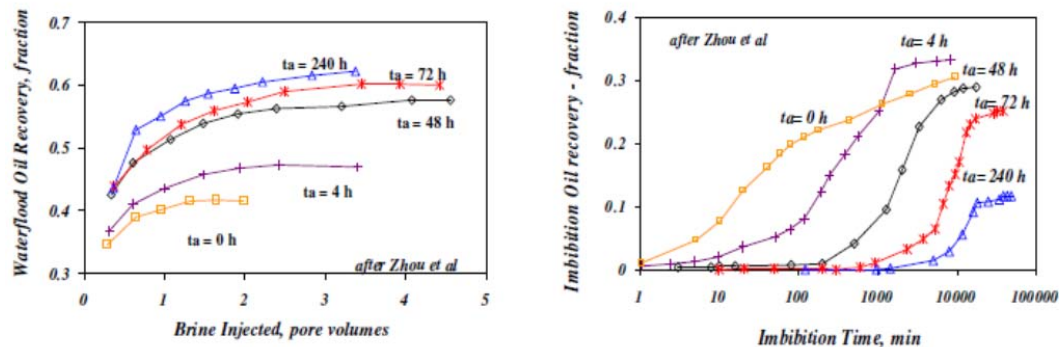
$$t_D = t \frac{\sigma k_{rw}}{\mu_w L^2} \sqrt{\frac{K}{\phi}} \quad (13.7)$$

However, this is not necessarily accurate, as this was a simplistic analysis; a more complex but analytically correct expression is found in Schmid and Geiger (2012) that accounts for the flow of both water and oil: this is presented later in the course.

We can use Eq. (13.7) though to estimate timescales for imbibition recovery. What is a typical imbibition time for a water-wet rock of size 1 cm? This is the real time necessary for have  $t_D$  around 1 in Eq. (13.7). Using  $\sigma = 0.04$  N/m,  $\mu_w = 10^{-3}$  Pa.s,  $K = 10^{-14}$  m<sup>2</sup> (10 mD) and  $\phi = 0.2$ , we find, for a typical end-point relative permeability value of 0.1 (a water-wet rock), times around 100s: imbibition is typically quite quick for small systems. What about a matrix block 10 m across? Notice that the time-scale increases as length squared, and so in this case imbibition takes a million times longer, or around 3 years.

A further complexity arises when we consider mixed-wet systems. Shown below is a comparison of waterflood and imbibition recoveries as a sandstone core becomes more mixed-wet in character. Imbibition becomes less favourable as more of the pore space becomes oil-wet, since there is no recovery from these regions. Furthermore, recovery is much slower, since the water relative permeability is very low, as discussed above: recall that if there is little imbibition, then the water flow is governed by displacement at low water saturations. This makes an enormous difference to recovery rates and may make recovery uneconomic in a field setting: if we consider our previous example, but with, say, a 1 m block size and a representative but low matrix block permeability (say 1 mD) and relative permeability (say  $10^{-4}$ ) in Eq. (13.7), we find an imbibition time of 100 years, which is uneconomic for field-scale recovery.

In contrast, the waterflood recovery improves as the system becomes more mixed-wet. This is a consequence of the lowered residual oil saturation. Also, as discussed in more detail later, the low water relative permeability holds back the injected water, allowing oil to escape and providing – in this case – a favourable displacement efficiency.

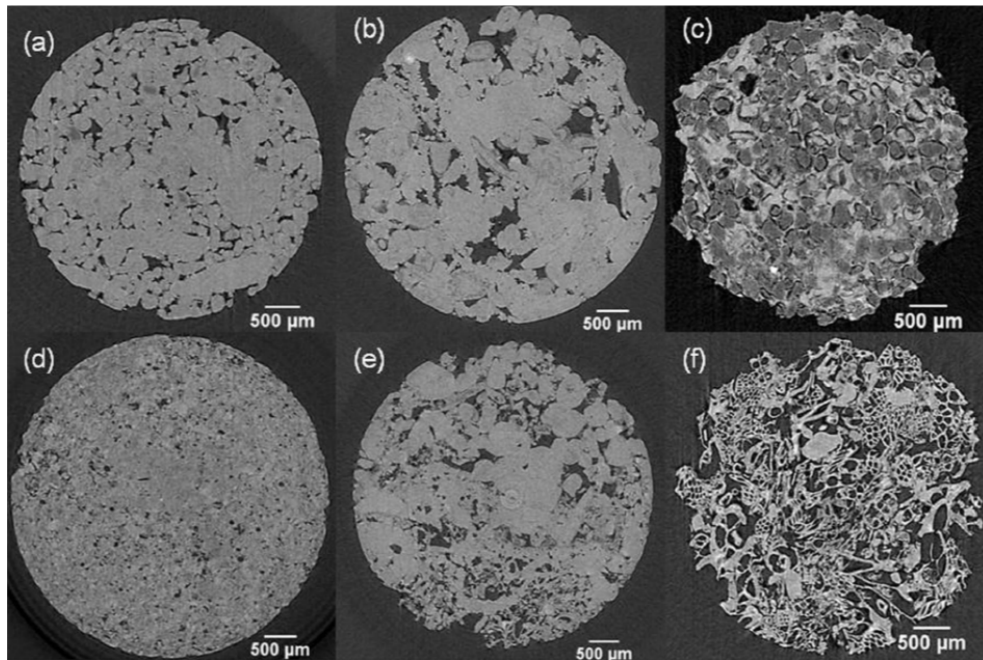


**Waterflood recovery (left) and imbibition recovery (right) for sandstone cores aged for the length of time (in hours) indicated on the graphs. The more the core is aged in crude oil (essentially soaked in crude for different amounts of time), the more mixed-wet in character it becomes. No ageing is least favourable for waterflooding, because of the high residual oil saturation in this water-wet case, but is favourable and fastest if recovery is controlled by imbibition (from Behbahani *et al.*, 2005).**

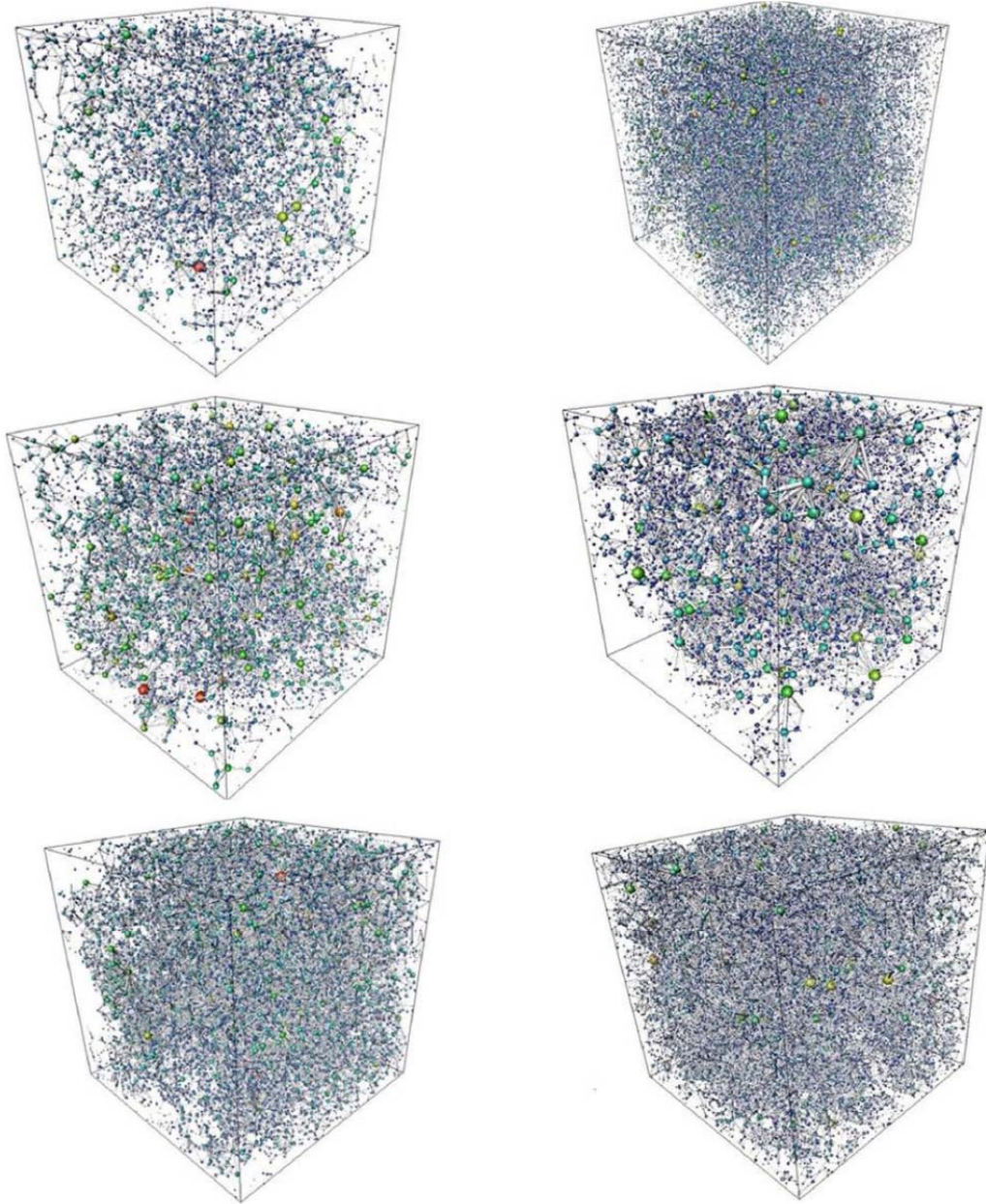
### 13.3 ANALYSIS OF RELATIVE PERMEABILITY IN MIXED-WET CARBONATES

In this section we will go through a network analysis of relative permeability, to show how we predict multiphase flow properties, their behaviour and how this relates to field-scale recovery. We will also compare the results against experimental data in the literature. The emphasis in this section will be on mixed-wet systems, which comprise the vast majority of carbonate rocks, which in turn contain most of the world's remaining reserves of conventional oil, mainly in the Middle East. Most of the analysis is taken from Gharbi and Blunt (2012).

We start by showing images of the carbonates that we will study and the networks extracted from these images. This forms the basis of the modelling.



**Two-dimensional cross sections of three-dimensional micro-CT images of different carbonate samples. (a) Portland limestone. (b) Indiana limestone. (c) Guiting carbonate. (d) Middle Eastern Carbonate 1, a carbonate sample from a deep highly-saline Middle Eastern aquifer. (e) Middle Eastern Carbonate 2, a second sample from a deep highly-saline Middle Eastern aquifer. (f) Mount Gambier limestone.**



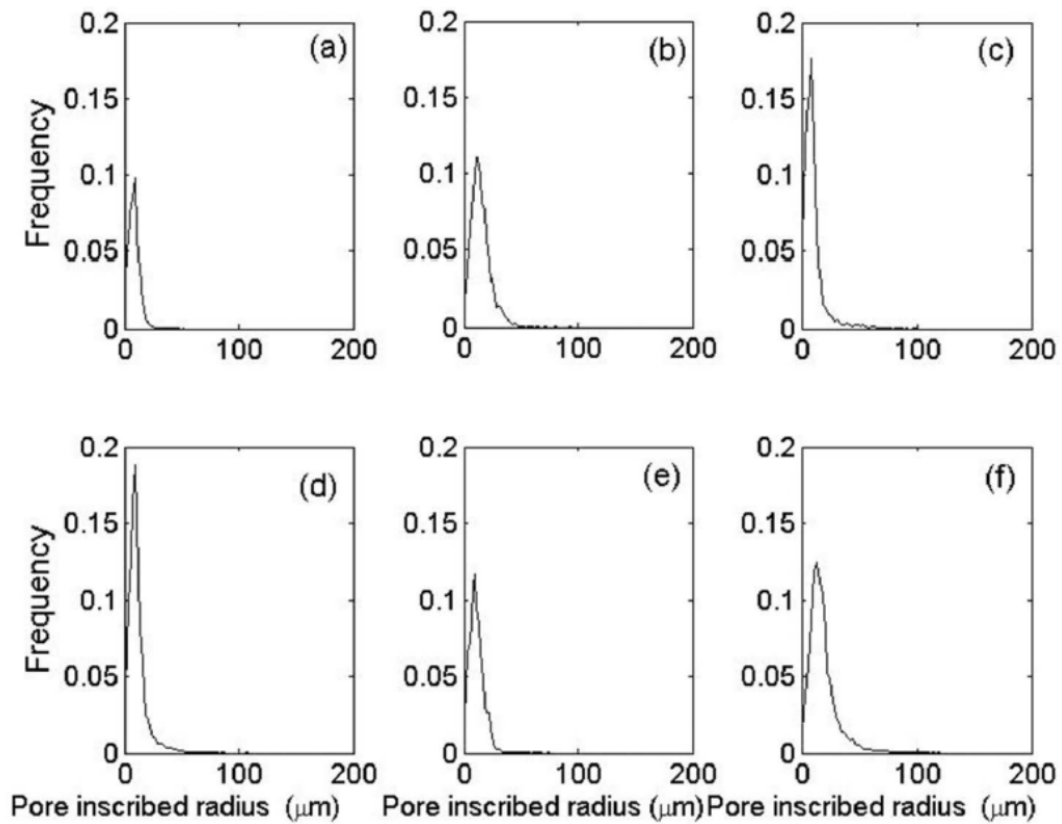
**Pore networks extracted from the images shown in the previous figure. The pore space is represented by a lattice of pores (represented by spheres) and throats (represented by cylinders): in cross-section each pore and throat is a scalene triangle.**

A detailed description of the extracted networks is provided in the table below. The samples cover a wide range of average coordination numbers: ME1 and Portland are poorly connected with coordination numbers of approximately 2.5 whereas Guiting and Mount Gambier are highly connected with average coordination numbers of 5.1 and 7.4 respectively. As we show later, the average coordination number (average number of throats connected to a single pore) is a key determinant of relative permeability and residual saturation. It is derived from the network extraction analysis and is an indicator of the connectivity of the void space.

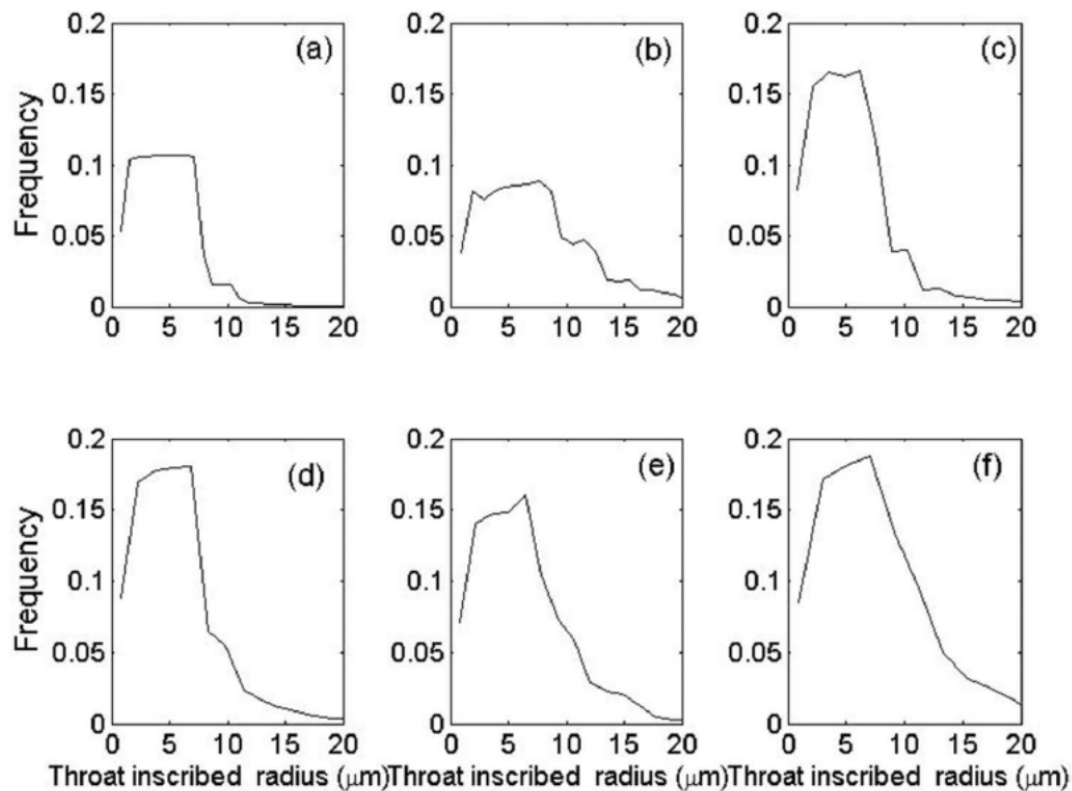
	ME1	Portland	Indiana	ME2	Guiting	Mount Gambier
Voxel resolution ( $\mu\text{m}$ )	7.7	9	7.7	7.7	7.7	9
Number of voxels	$380^3$	$320^3$	$330^3$	$320^3$	$350^3$	$350^3$
Physical volume ( $\text{mm}^3$ )	25.05	23.89	16.41	14.96	19.57	31.26
Number of pores	55828	6129	5653	10855	25707	22665
Number of throats	70612	7939	8539	20071	66279	84593
Total number of elements	126440	14068	14192	30926	91986	107258
Average coordination number	2.50	2.53	2.97	3.64	5.11	7.41
Min pore radius ( $\mu\text{m}$ )	7.7	9	7.7	7.7	7.7	9
Max pore radius ( $\mu\text{m}$ )	51.52	93.51	99.48	107.82	74.09	119.88
Average pore radius ( $\mu\text{m}$ )	8.44	14.89	10.17	10.90	11.16	18.17
Average aspect ratio	1.87	2.28	1.88	2.08	2.00	2.59
Porosity (%)	14.37	9.32	13.05	18.60	29.79	56.27
Permeability ( $\text{m}^2$ )	$3.23 \times 10^{-14}$	$1.37 \times 10^{-13}$	$5.69 \times 10^{-13}$	$9.40 \times 10^{-13}$	$3.72 \times 10^{-13}$	$2.20 \times 10^{-11}$

**Description of the extracted networks.** Average coordination number is the average number of throats connected to each pore. The average aspect ratio is the average of the ratio of the pore radius to the mean radius of the throats connected to it. The permeability is computed from a flow simulation through the network.

The pore and throat distributions of the networks are presented below.



Pore inscribed radius distributions for (a) Middle Eastern sample 1 (b) Portland limestone (c) Indiana limestone (d) Middle Eastern sample 2 (e) Guiting carbonate and (f) Mount Gambier limestone. In this and subsequent figures, samples are presented in order of increasing coordination number: from a low connectivity sample (a) to a very high connectivity sample (f).



**Throat inscribed radius distributions for (a) Middle Eastern sample 1. (b) Portland limestone. (c) Indiana limestone. (d) Middle Eastern sample 2. (d) Guiting carbonate. (f) Mount Gambier limestone. Samples are presented in order of increasing coordination number.**

Capillary controlled displacement is simulated using the pore network model developed by Valvatne and Blunt (2004). Initially the medium is assumed to be filled with the wetting phase (brine) and oil is then injected. After oil invasion, we alter the wettability of the pore spaces in direct contact with oil to represent mixed-wet conditions. Waterflooding is then simulated and relative permeability curves are generated.

We study the impact of wettability in mixed-wet media where some fraction,  $f$ , of the pore space occupied by oil is made oil-wet and a fraction  $1-f$  remains water-wet. We vary the oil-wet fraction from zero (a strongly water-wet case) to 1 (strongly oil-wet rock). In addition to modelling mixed-wet media, this methodology reproduces wettability alteration which is due to asphaltene deposition/ precipitation in carbonates. This alteration, governed by oil composition, brine salinity and rock mineralogy is difficult to predict *a priori*.



Where oil has been in contact with the carbonate surface (pores and throats), random contact angles with no spatial correlation are assigned with different distributions – given in the table on the next page – for the water-wet and oil-wet pores and throats.

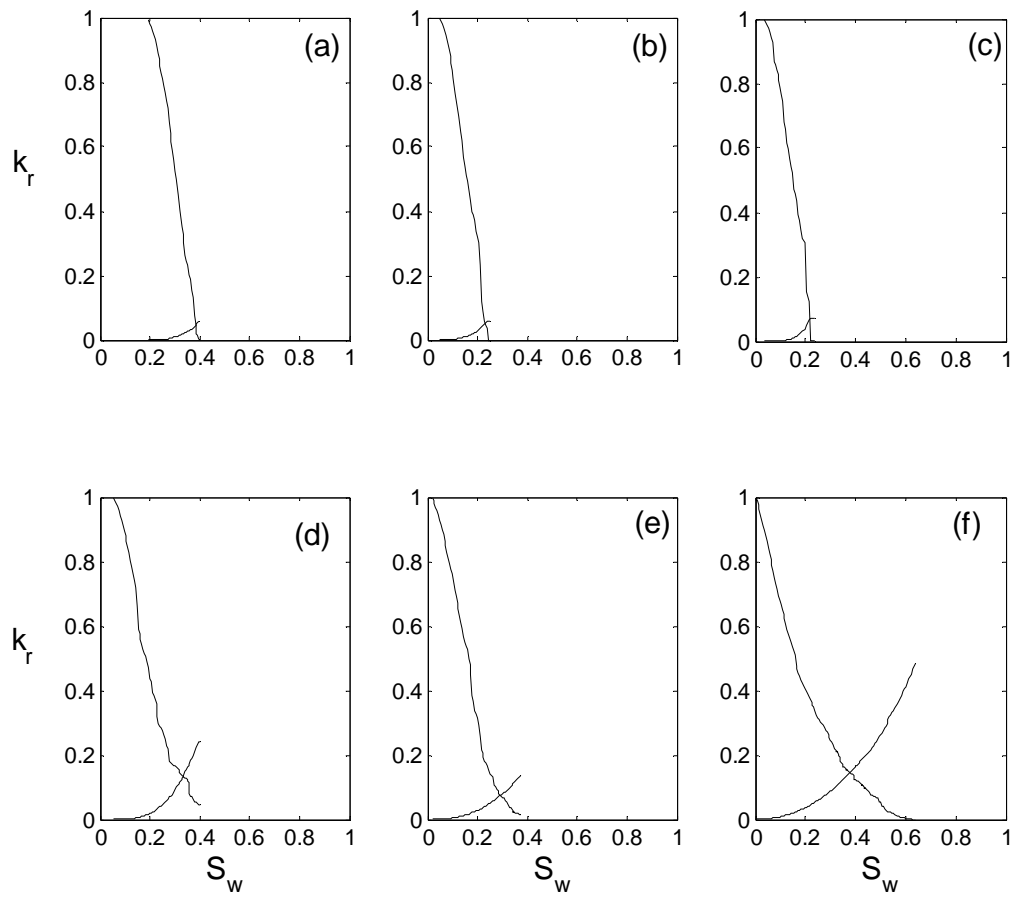
The three-dimensional networks are composed of individual elements (pores and throats) with circular, triangular or square cross-sectional shapes. Using square or triangular-shaped networks elements allows for the explicit modelling of wetting layers where non-wetting phase occupies the centre of the element and wetting phase remains in the corners. The pore space in carbonates is highly irregular with water remaining in the grooves and crevices after primary oil flooding due to capillary forces. The wetting layers might not be more than a few microns in thickness, with little effect on the overall saturation or flow. Their contribution to wetting phase connectivity is, however, of vital importance, ensuring low residual wetting phase saturation by preventing trapping. Wetting layers of water are always present in the corners, while layers of oil-sandwiched between water in the corners and water in the centre can be observed in oil-wet regions. Layer drainage is when oil flows in these layers, allowing, slowly, very low saturations to be reached.

<b>Input parameters</b>	
Initial contact angle (degrees)	0
Interfacial tension (mN/m)	48.3
Water-wet contact angles (degrees)	0-60
Oil-wet contact angles (degrees)	100-160
Oil viscosity (mPa.s)	0.547
Water viscosity (mPa.s)	0.4554

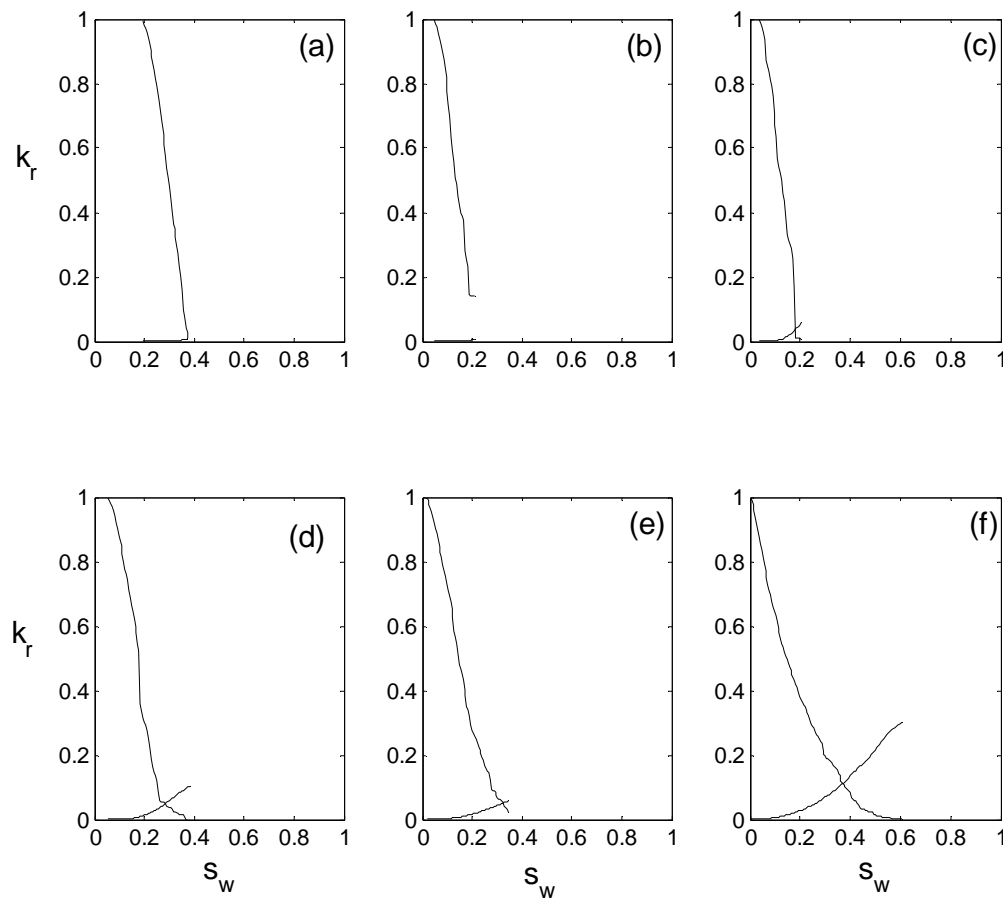
#### **Input parameters for relative permeability computations.**

Five wettability distributions are studied:  $f=0$ ,  $f=0.25$ ,  $f=0.5$ ,  $f=0.75$  and  $f=1$ . For the water-wet case, as expected, water remains in the smallest portions of the pore space, giving very low water relative permeability and significant trapping of oil in the larger pores at the end of waterflooding, mainly caused by snap-off. In the case of poorly connected carbonates (ME1, Portland and Indiana limestones), up to 75% of the pore space can be trapped. However, for the better connected networks, namely ME2, Guiting and Mount Gambier, the water relative permeability is higher and there is less trapping (there are more pathways for the oil to escape), although the residual saturation is around 40% or higher in all cases.

For a mixed-wet case with  $f=0.25$ , the small fraction of oil-wet pores tends to increase the amount of oil trapping, particularly in the less connected networks where now there is little or no range of saturation when two phases flow simultaneously, except very slow flow in wetting layers. The water phase connectivity is reduced and the water relative permeability is in general lower than the strongly water-wet case. The water-wet regions fill first in a capillary-controlled displacement at the pore scale: these are the small pores and poorly connected; however, they surround most of the oil-wet pores that are then trapped. These pores cannot then be displaced during forced water injection, which explains the increase in residual oil saturation. Here again, for the highly connected networks, the water relative permeability is higher since the water has more possible pathways through the system and there is both spontaneous and forced displacement by water.



**Waterflood relative permeability for the strongly water-wet case ( $f=0$ ). Curves are presented in order of increasing connectivity. (a) Middle Eastern sample 1. (b) Portland limestone. (c) Indiana limestone. (d) Middle Eastern sample 2. (e) Guiting carbonate. (f) Mount Gambier limestone.**

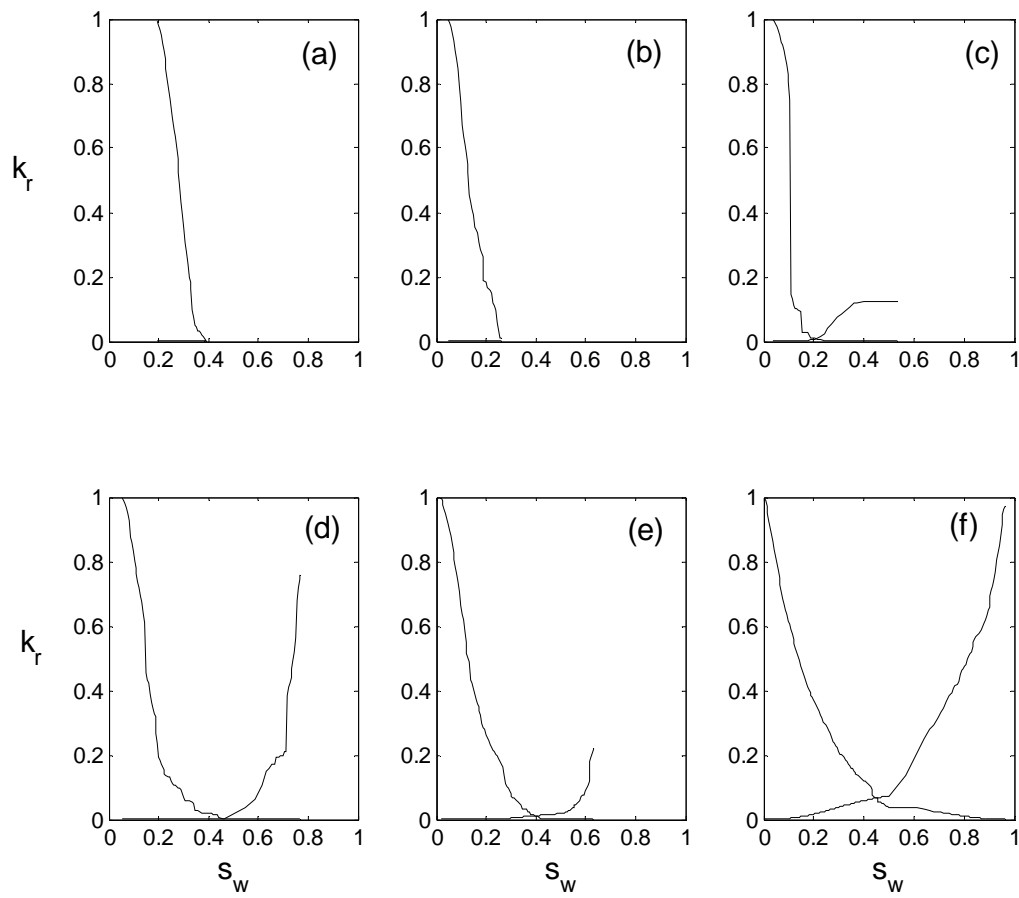


**Waterflood relative permeability for the mixed-wet case ( $f=0.25$ ). Curves are presented in order of increasing connectivity. (a) Middle Eastern sample 1. (b) Portland limestone. (c) Indiana limestone. (d) Middle Eastern sample 2. (e) Guiting carbonate. (f) Mount Gambier limestone.**

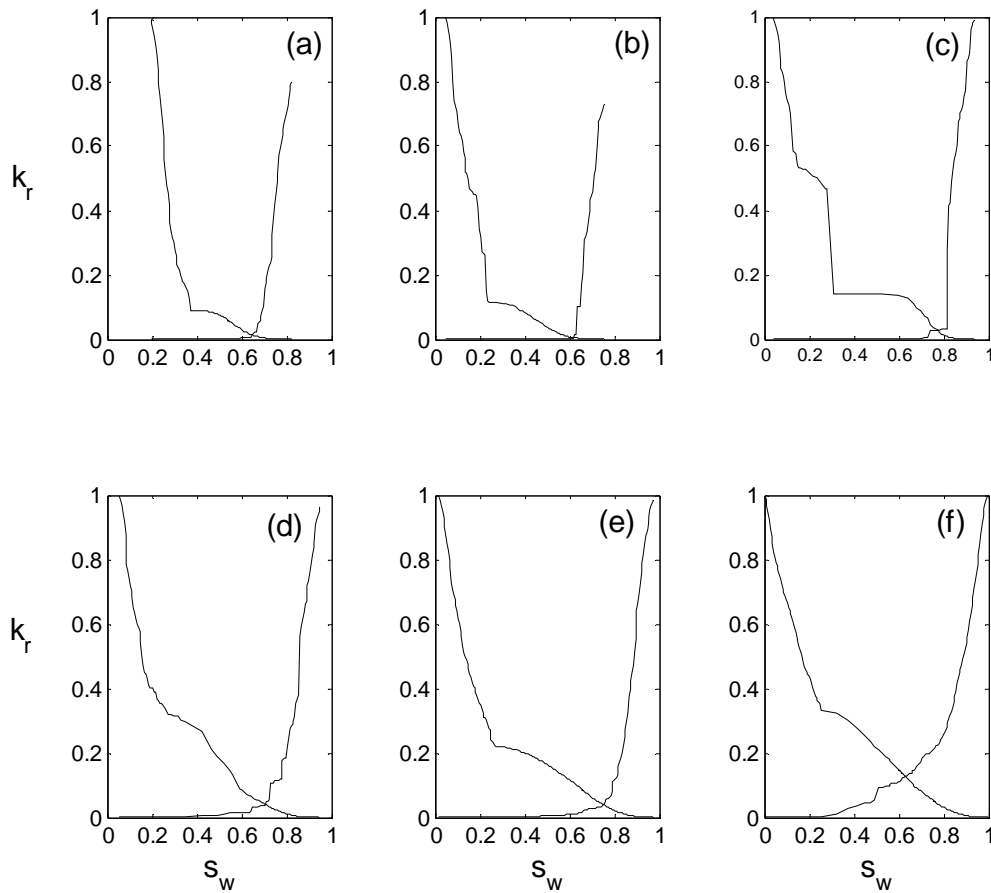
When the fractional wettability is 0.5, an equal mix of water-wet and oil-wet pores, at low water saturations, a similar behaviour is observed regardless of the connectivity of the pore space. At the beginning of the water flooding, the water is still poorly connected and flows only through the smallest water-filled pores and thin wetting layers of the pore space; therefore the water relative permeability is low. However, in an equal mix of water-wet and oil-wet fractions of the pore space, depending on the connectivity, an important increase in the water relative permeability is noticeable. After spontaneous imbibition, a significant forced displacement of oil occurs as the oil-wet pores and throats connect through the network. The residual oil saturation is generally lower since oil remains connected in the oil-wet region in layers. This

effect is noticeable in the shape of the oil relative permeability, for the well-connected samples, that show a long region where the oil relative permeability is very low, but there is still displacement – this behaviour is controlled by slow flow in oil layers, Salathiel (1973). The poorly connected samples still show a water-wet controlled behaviour, where there is a sharp decrease in the oil relative permeability and significant trapping. Here there is little connectivity of the oil-wet regions and as a consequence layer drainage is unable to achieve low residual saturations. In addition, the maximum water relative permeability varies from very low to very high values dependent on the degree of trapping and the connectivity of the water phase. Where the residual saturation is low, water can fill most of the pore space – and the larger pores in the oil-wet regions – and has a high end-point value. A wide range of behaviour is seen in this case dependent on the pore structure of the medium.

When the oil-wet fraction is higher,  $f=0.75$ , the residual saturation is now very low as the oil remains connected in layers throughout the displacement. The water relative permeability can rise to high values in all cases as the water fills the centres of the larger regions of the pore space. This is a sign of a more typical oil-wet behaviour with displacement over a wide saturation range and low relative permeabilities of both oil and water at low saturations of their respective phases, controlled by wetting layer flow (Valvatne and Blunt, 2004). This behaviour is generically similar to network modelling calculations for sandstones (Valvatne and Blunt, 2004; Zhao *et al.*, 2010). The jumps in some of the curves reflect the relatively small size of the networks studied: improvements in imaging should soon allow larger networks to be constructed.

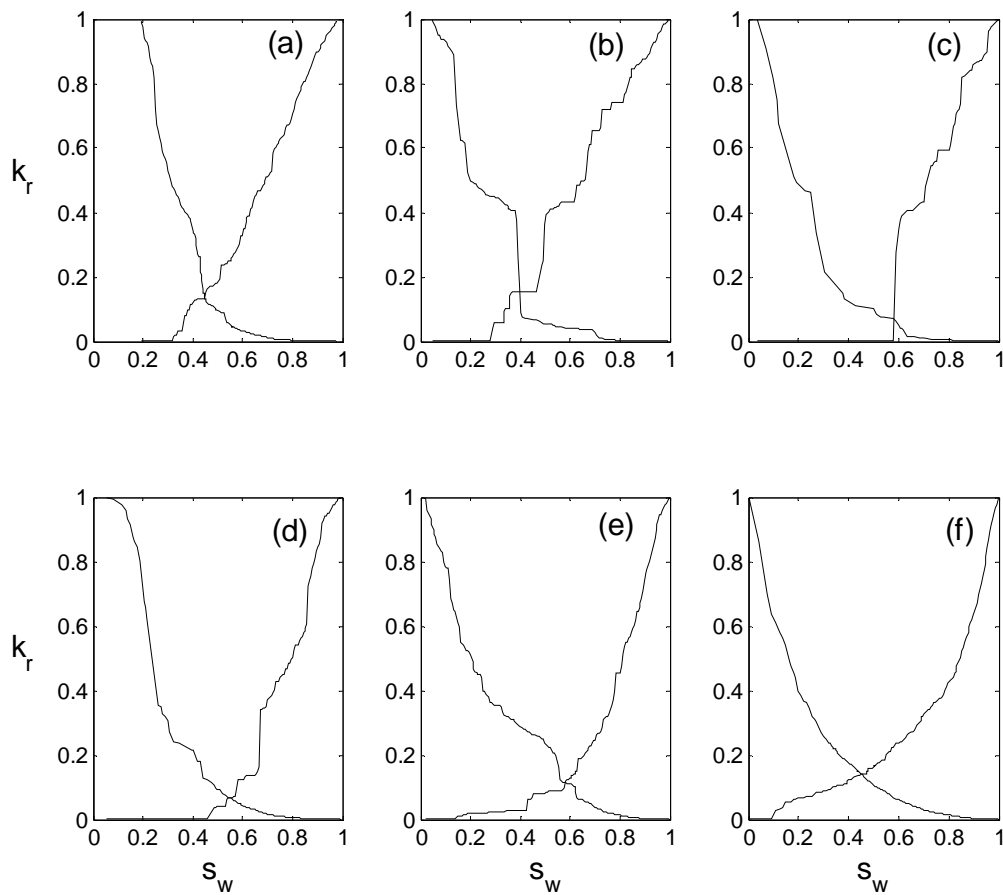


**Waterflood relative permeability for the mixed-wet case ( $f=0.5$ ). Curves are presented in order of increasing connectivity. (a) Middle Eastern sample 1. (b) Portland limestone. (c) Indiana limestone. (d) Middle Eastern sample 2. (e) Guiting carbonate. (f) Mount Gambier limestone.**



**Waterflood relative permeability for A mixed-wet case ( $f=0.75$ ). Curves are presented in order of increasing connectivity. (a) Middle Eastern sample 1. (b) Portland limestone. (c) Indiana limestone. (d) Middle Eastern sample 2. (e) Guiting carbonate. (f) Mount Gambier limestone.**

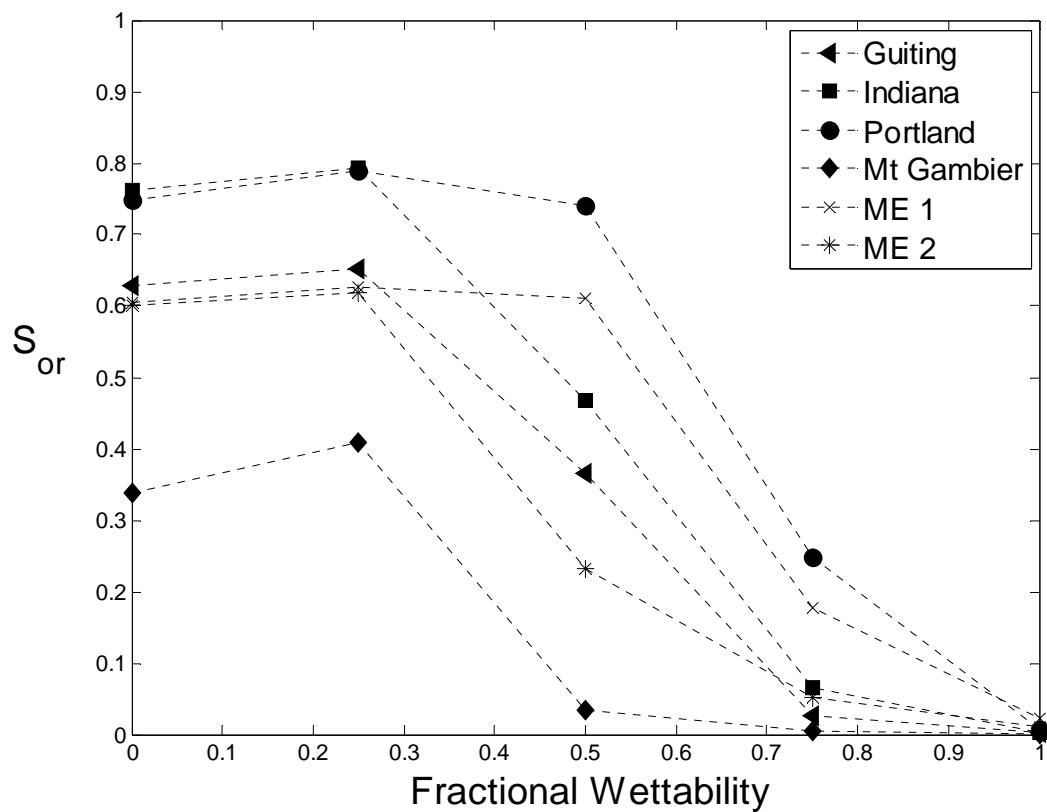
For the fully oil-wet case ( $f=1$ ) the behaviour is generally quite similar to that observed for the mixed-wet case ( $f=0.75$ ): very low residual oil saturation, a prolonged layer drainage regime (low oil relative permeability at low oil saturation) and high end-point water relative permeability.



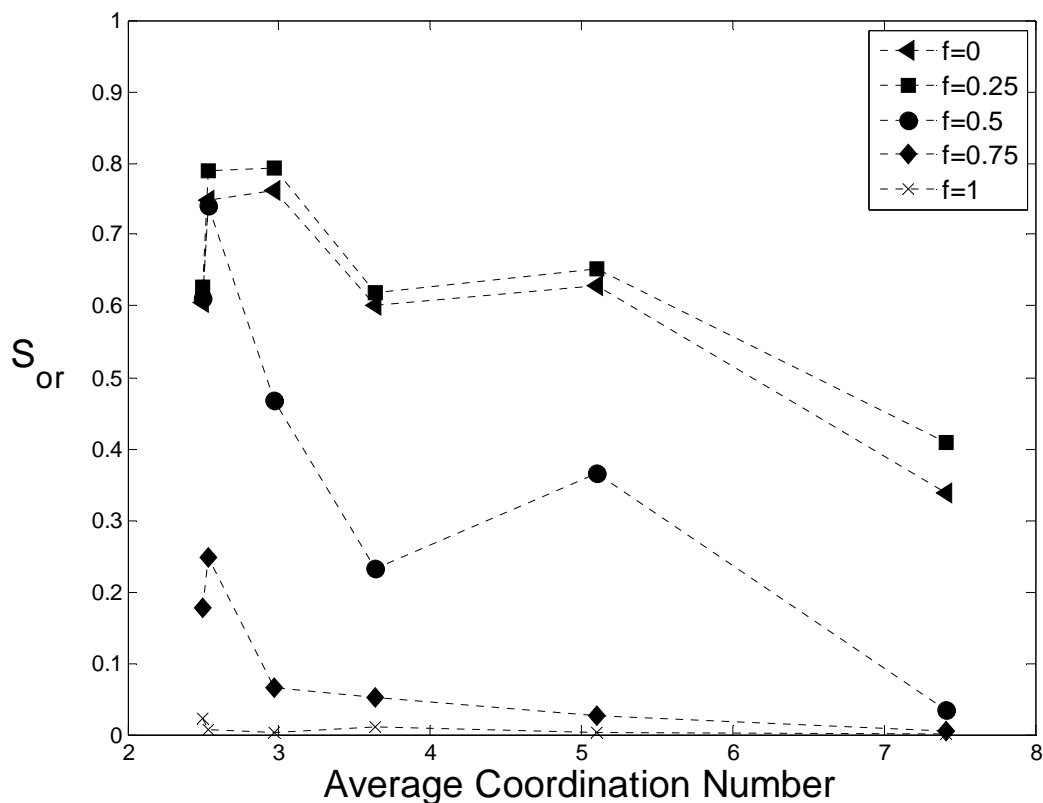
**Waterflood relative permeability for the strongly oil-wet case ( $f=1$ ). Curves are presented in order of increasing connectivity. (a) Middle Eastern sample 1. (b) Portland limestone. (c) Indiana limestone. (d) Middle Eastern sample 2. (e) Guiting carbonate. (f) Mount Gambier limestone.**

To summarize the previous description, we analyze the impact of wettability and average coordination number on the relative permeability behaviour. The evolution of residual oil saturation with the fractional wettability shows that the residual oil saturation reaches a maximum for the fractionally-wet case with  $f=0.25$ , and then decreases sharply to very low saturations as the medium becomes more oil-wet. Waterflooding gives a high local displacement efficiency for the cases  $f=0.75$  and  $f=1$ , where the behaviour is controlled by oil layers.





**Residual oil saturation as a function of fractional wettability for: Guiting (triangles), Indiana (rectangles), Portland (circles), Mount Gambier (diamonds), Middle Eastern sample 1 (crosses), and Middle Eastern sample 2 (stars).**

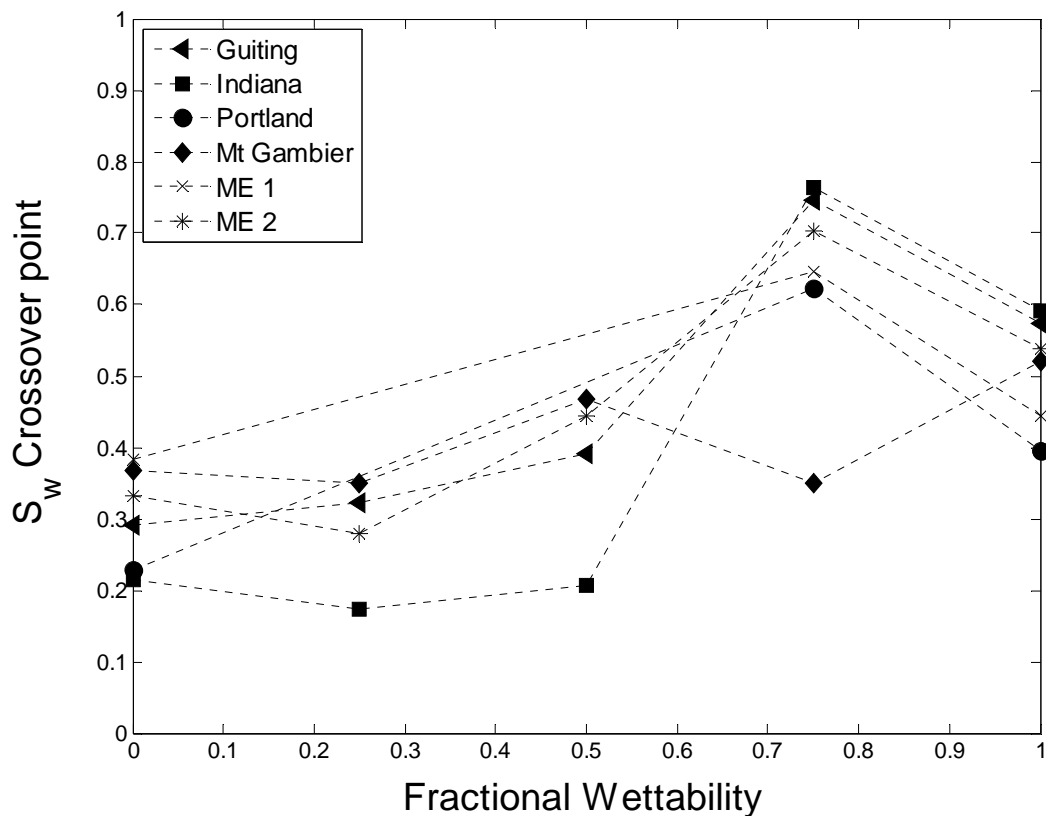


**Residual oil saturation as a function of the average coordination number for: Guiting (triangles), Indiana (rectangles), Portland (circles), Mount Gambier (diamonds), Middle Eastern sample 1 (crosses), and Middle Eastern sample 2 (stars).**

The impact of connectivity on the residual oil saturation is shown above. The residual oil saturation tends to decrease with increasing connectivity, regardless of wettability.

One indication of waterflood displacement efficiency that is used to characterize the wettability is the water saturation value at which the oil and water relative permeabilities are equal ( $S_w$  where  $k_{rw}=k_{ro}$ ) (Craig, 1971). For water saturations higher than the crossover saturation, waterflooding becomes less efficient, since (for equal viscosities) more water flows than oil. The water saturation at the cross-over as a function of wettability for the different carbonate samples is shown below. In most cases, the water saturation is highest for the mixed-wet case  $f=0.75$ . This confirms that waterflooding is most effective for mixed-wet carbonates that have preference to an oil-wet behaviour. The smallest water saturation at the crossover point is

reached for the water-wet and weakly mixed-wet cases ( $f=0.25$ ): these are least efficient for waterflooding. This contrasts with traditional analyses of relative permeability which suggests that the cross-over point is at more than 50% water saturation for water-wet cases and less than 50% water saturation for mixed-wet or oil-wet samples (Craig, 1971). We only see this trend in the near oil-wet region; this rule does not apply in general because of the low estimated water relative permeability.



The water saturation at the relative permeability cross-over point ( $S_w$  where  $k_{rw}=k_{ro}$ ) with fractional wettability for Guiting (triangles), Indiana (rectangles), Portland (circles), Mount Gambier (diamond), Middle Eastern sample 1 (crosses), and Middle Eastern sample 2 (stars).

### 13.4 COMPARISON OF NETWORK MODEL RESULTS WITH EXPERIMENTAL DATA

---

We will compare our computations to measurements found in the literature on reservoir carbonate samples. The approach is not necessarily genuinely predictive as scans of the reservoir samples and an independent measurement of wettability are not available: we simply make an assessment if the estimated connectivity and wettability are plausible for the experimental sample studied. Also, the objective of this comparison is not to have a perfect match between the laboratory measurements and the results of the network modelling by fine-tuning the oil-wet fraction or the contact angles; rather, the goal is to determine if our calculated behaviour is supported by the available experimental evidence and discuss the impact of wettability and pore structure on field-scale recovery.

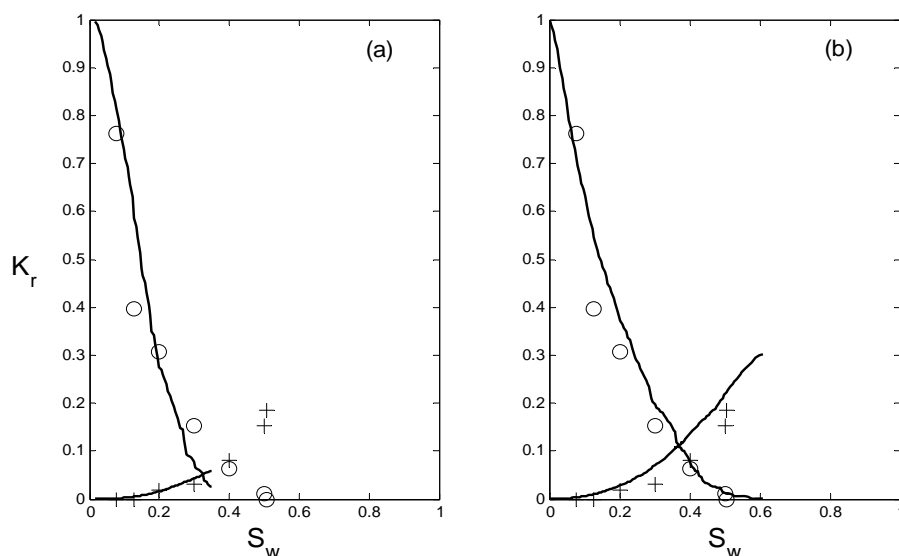
We study three sets of waterflood relative permeabilities measured on Middle Eastern carbonate reservoir samples. A summary of the petrophysical and geological description of the samples is provided in the table overleaf.

**Case 1.** Al-Sayari (2009) measured steady-state waterflood relative permeability on an aged (restored state) reservoir carbonate sample from the Middle East. Through analysis of thin sections, mercury injection capillary pressure and NMR response, the reservoir sample was described as having a well-connected pore structure with a relatively low fraction of microporosity.

A similar relative permeability to that measured can be observed for the case of  $f=0.25$  for the well-connected Guiting and Mount Gambier networks. The relatively low residual oil saturation and the shape of the oil relative permeability curve indicate a mixed-wet behaviour. For Guiting, the discrepancies in the water relative permeability can be explained by the un-resolved microporosity.

	Wettability	Wettability measurement	Geology	Lithology	NMR Description
Al-Sayari, 2009	Mixed-wet	N/A	Kharaib formation	Dual pore system	Multi-modal, microporosity
Meissner <i>et al.</i> , 2009	Mixed-wet preference to oil	USBM	Arab-D reservoir	Lime grainstone	Complex multi-modal pore structures, Microporosity
Meissner <i>et al.</i> , 2009	Mixed-wet preference to oil	USBM	Arab-D reservoir	Lime mudstone	
Meissner <i>et al.</i> , 2009	Mixed-wet preference to oil	USBM	Arab-D reservoir	Lime grainstone	
Meissner <i>et al.</i> , 2009	Mixed-wet preference to oil	USBM	Arab-D reservoir	Lime grainstone	
Okasha <i>et al.</i> , 2007	Neutral to slightly water-wet	Amott	Arab-D reservoir Haradh area	N/A	N/A
Okasha <i>et al.</i> , 2007	Generally oil-wet to intermediate-wet	Static imbibition Amott USBM	Arab-D reservoir Utmaniyah area	N/A	N/A

A summary of the petro-physical and geological descriptions of the reservoir samples found in the literature. USBM stands for US Bureau of Mines and is a somewhat cumbersome method to measure wettability: it measures the ratio of the area under the capillary pressure curves for spontaneous and forced displacement.



Comparison between relative permeability measurements from a Middle Eastern reservoir (oil relative permeability, circles, water relative permeability, crosses; Al-Sayari, 2009) with (a) Guiting limestone and (b) Mount Gambier limestone for a fractional wettability of  $f=0.25$ .

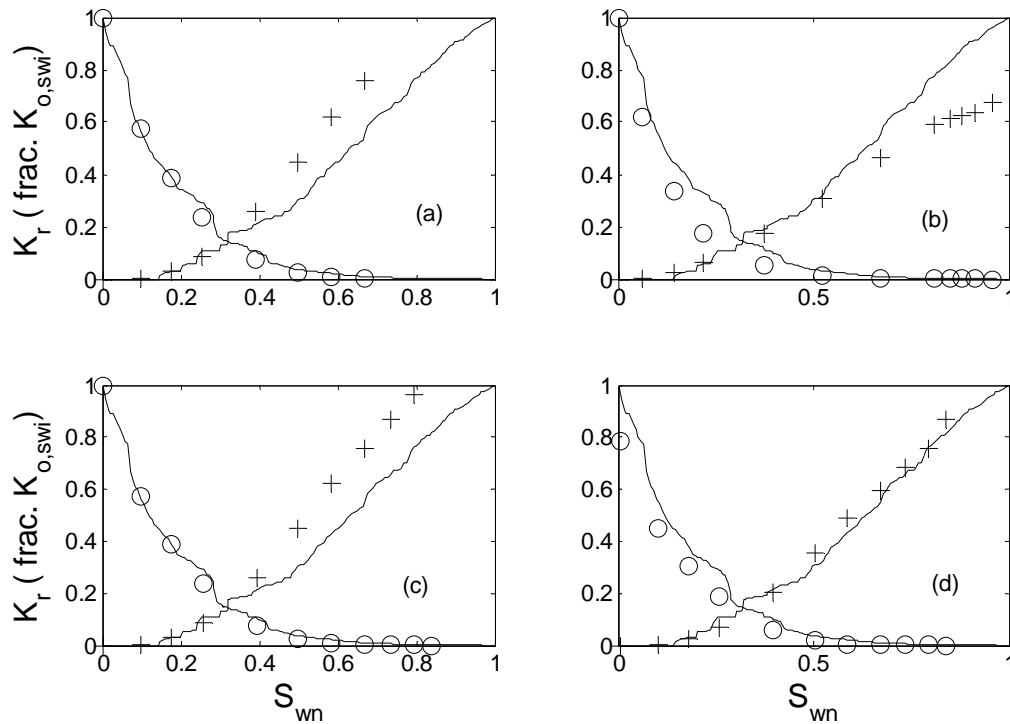
**Case 2.** Meissner *et al.* (2009) performed detailed measurements on several samples from the Arab-D reservoir of the Dukhan field, onshore Qatar. They reported the results of several of steady-state relative permeability tests for oil/brine and gas/oil systems. Results were reported for both native and the restored state cores. The results were reported in terms of normalized saturations and relative permeabilities:

$$S_{wn} = \frac{S_w - S_{wi}}{1 - S_{wi} - S_{or}} \quad (13.8)$$

where  $S_{wi}$ , the initial water saturation, is determined after primary drainage and  $S_{or}$  is the residual oil saturation determined by extrapolation of the oil relative permeability as it asymptotically approaches zero.

In this case, to introduce an initial water saturation, we set the maximum primary drainage capillary to be equal to 690 kPa (approximately 100 psi). This value is chosen based on the different capillary pressure measurements that showed a sharp increase in the pressure for an average pressure of around 100 psi.

The figure overleaf shows a comparison between the four measurements reported of water/oil relative permeability on the native state subsurface cores with the relative permeability generated for the strongly oil-wet case  $f=1$  for ME1. The suggestion here is that the reservoir is strongly oil-wet with a structure similar to that observed in the subsurface sample from which we extracted a network.



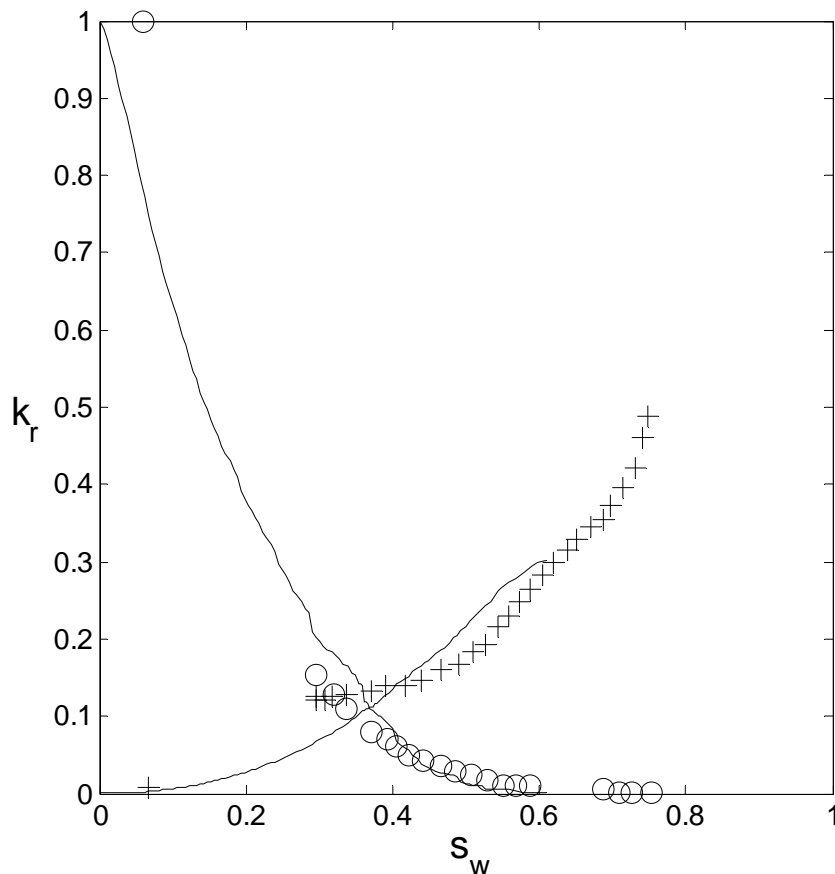
**A comparison between the water flood relative permeability for the Middle Eastern sample 1, for a strongly oil-wet case  $f=1$  with measurements on native state subsurface reservoir cores (oil relative permeability, circles, and water relative permeability, crosses) obtained from Meissner et al. (2009).**

**Case 3.** Okasha *et al.*, (2007) reported unsteady-state relative permeability measurements on carbonate reservoir samples from the Arab-D reservoir of the Ghawar field in Saudi Arabia. This is the world's largest conventional oilfield. Three data sets were presented for three samples obtained from different areas of the Ghawar field: Utmaniyah, Hawiyah and Haradh. Here, since the measured values are presented in a non-normalized form; we simply compare with the data, without changing the initial water saturation.

The figure overleaf shows a good agreement between the measurements and the relative permeability generated by network modelling for the mixed-wet Mount Gambier network ( $f=0.25$ ) for one of the three samples. Note that we suggest that in this field the wettability and pore structure are different from the subsurface Middle Eastern sample in the previous section. The figure below shows good agreement for the second measured sample with low connectivity

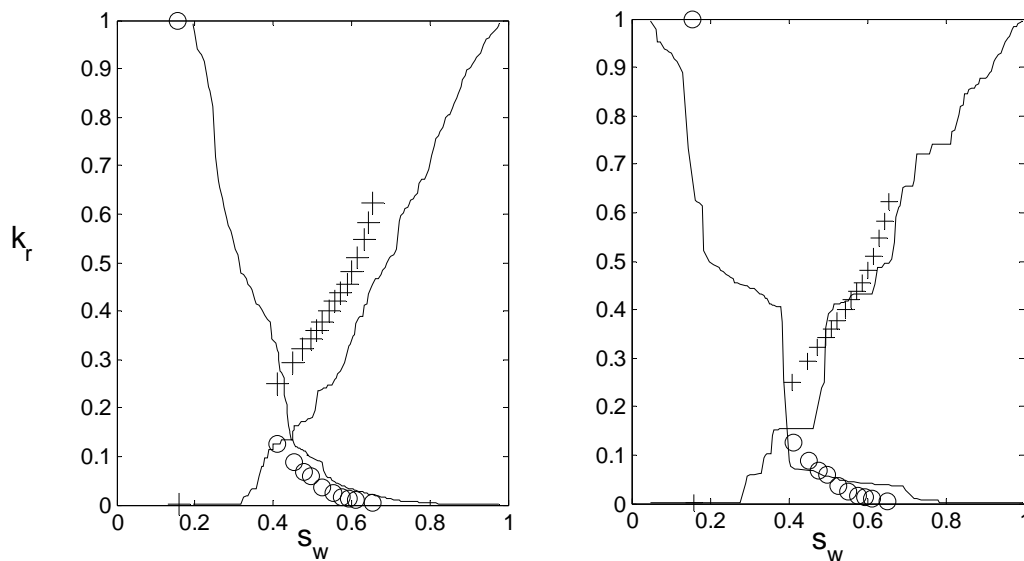
carbonates i.e. Portland and ME1 for a strongly oil-wet case. The difference of the wettabilities is evidence of local variations of wettability within the reservoir.

Good agreement was not obtained for the third sample which had high connate water saturation.



**Mount Gambier water flood relative permeability for the mixed-wet case with an oil-wet fraction of  $f=0.25$  (solid) compared to measurements on a reservoir sample obtained from Okasha et al. (2007) (oil relative permeability, circles, and water relative permeability, crosses).**





**Middle Eastern sample 1 (right) and Portland limestone (left) waterflood relative permeability for the strongly oil-wet case with an oil-wet fraction of  $f=1$  (solid) compared to measurements on reservoir samples obtained from Okasha et al. (2007) (oil relative permeability, circles, and water relative permeability, crosses).**

### 13.5 IMPACT OF RELATIVE PERMEABILITY ON FIELD-SCALE RECOVERY

In waterflooding, for oil and water of similar viscosity, the saturation at which the relative permeabilities cross – as discussed below – gives a useful and simple indicator of the recovery. For water saturations beyond the crossover point, more water will be produced than oil – beyond this point, oil production becomes increasingly uneconomic. Hence, a rough guide to recovery can be derived from the change in saturation from its initial value to when the relative permeabilities cross.<sup>4</sup> Later, we show how to perform this analysis rigorously and predict – for given relative permeabilities and fluid viscosities – the amount of oil recovered as a function of the amount of water injected.

<sup>4</sup> Please note, that this change in saturation is not a recovery factor. For this, we need to compute the volume of oil produced, convert it to surface conditions and then divide by the total volume of oil initially in the reservoir (also measured at surface conditions). Last this is an approximate physically-motivated assessment of recovery and no excuse for not doing a proper analysis, as described later.

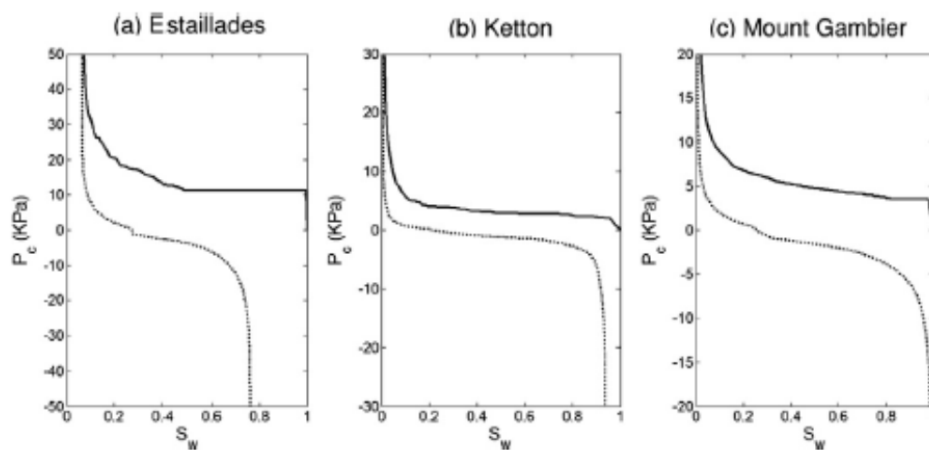
Our simulations indicate that the optimal water flood efficiency is observed for a mixed-wet system with a large fraction of oil-wet pores, around 0.75. The highest waterflood efficiency is implied for the less well-connected samples, since in these cases the waterflood relative permeability is very low and this holds back the movement of water, allowing oil to be displaced. For better connected samples, there is less sensitivity to wettability and overall a lower crossover saturation, indicating less favourable recoveries.

This is a somewhat surprising conclusion and implies that waterflooding in mixed to oil-wet carbonates of poor pore-space connectivity may be an effective process. This behaviour stands in contrast to sandstones, where network modelling studies indicate that more neutrally-wet conditions provide optimal recovery (Øren *et al.*, 1998; Valvatne and Blunt, 2004). Moreover, experimental measurements presented by Jadhunandan and Morrow (1995) have shown that oil recovery by waterflooding in sandstones reach a maximum at close to neutral wettability.

As mentioned at the beginning of this section there are two distinct recovery processes in carbonates, depending on whether or not fractures dominate the flow. If they do not, then viscous forces are significant for displacement through the porous matrix and local recovery is determined by the relative permeabilities. It is possible to perform a Buckley-Leverett analysis to compute, analytically, recovery for a homogeneous one-dimensional displacement from the relative permeabilities: the method to do this is presented later in these notes. However, as mentioned previously, the likely local waterflood displacement efficiency can be estimated rapidly from direct inspection of the relative permeability curves. Imagine that the reservoir-condition oil and water viscosities are the same. Then, if the saturation near the production well is where the relative permeabilities cross, the subsurface ratio of oil to water production will be 1:1. Wells are abandoned when the cost of recycling and processing the produced water exceeds the economic benefit of the oil produced: this is normally when the oil:water ratio is between 1:2 and 1:10. On the other hand, the oil viscosity is typically greater than that of water, and the flow rate is determined by the ratio of relative permeability to viscosity. Hence, in most cases, production ceases close to where the relative permeabilities cross – between the producer, where water has displaced oil, the saturations will be higher, but this very simple trick allows a quick comparative study of recovery trends. Hence, waterflooding is quite favourable in the less well connected carbonate samples. Most of the moveable pore volume is displaced, and the residual saturation is low. The reason for this is that the poorly connected water phase

holds back water advance, allowing the efficient displacement of oil. For better connected samples, the water is better connected and rapidly finds a pathway of large pores through the system. This allows water to bypass oil at the pore scale, leading to less favourable waterflood recovery.

Now consider a reservoir where flow is dominated by fractures. In this case the fractures effectively short-circuit the flow field and it is not possible to impose a substantial viscous pressure drop across the matrix. Recovery is mediated by capillary and gravitational forces. Imagine that water quickly invades the fractures surrounding a region of matrix (a so-called matrix block, although it does not have to be exactly, or even remotely, cuboidal in shape). Then recovery will occur by spontaneous imbibition – that is recovery will occur until the capillary pressure is zero. Shown below are the capillary pressures for three carbonate samples. These are not the same samples as already discussed, with the exception of Mount Gambier, with a well-connected pore space. Ketton and Estailades are both more poorly connected and are – for the sake of this discussion – similar in behaviour to the other low coordination number samples, Portland, Indiana and ME1.



**Primary drainage (solid line) and waterflood (dotted line) capillary pressures predicted using pore-scale network modelling. Here the oil-wet fraction  $f$  is 0.75. If recovery occurs by imbibition – in a fractured reservoir – the final recovery is controlled by the saturation when the capillary pressure is zero, not the residual saturation.**

In our examples in the figures above this means that only around 25% of the moveable pore volume is recovered. Furthermore, the rate of recovery is limited by the rate at which water can advance into the pore space – that is the relative permeability in the low water saturation range where the capillary pressure is positive. In this case now the more favourable system is the Mount Gambier – the water relative permeability is higher, indicating a more rapid displacement, while the degree of spontaneous imbibition is larger, since the well-connected pore space allows all the water-wet regions of the rock to be accessed easily; in contrast the poorly connected Ketton and Estailades has a lower water relative permeability and not all the water-wet regions of the pore space are interconnected, leading to less displacement at a positive capillary pressure.

Gravitational forces can also play an important role in the displacement. If water floods a vertical fracture then oil, being less dense, is preferentially produced from the top of the matrix, then the weight of water in the fracture acts as a driving force. If we assume that the capillary pressure in the fractures is very small and is equal to zero at the top of a matrix block, then the capillary pressure at the base is  $\Delta\rho gh$ , where  $\Delta\rho$  is the density difference between water and oil and  $h$  is the effective height of the matrix block. The capillary pressure is negative: the water has a higher pressure than oil. This allows forced displacement to a lower oil saturation. Taking typical values:  $g = 9.81 \text{ ms}^{-2}$ ;  $\Delta\rho = 300 \text{ kg.m}^{-3}$  and, say,  $h = 2 \text{ m}$ , then the negative capillary pressure that can be reached is around -6 kPa. Reading off the graph above, we can see that this driving force displaces a further 15% of the oil for the lowest permeability sample, Estiallades. Even if we consider lower permeability rocks (the capillary pressure approximately increases as  $1/K^{1/2}$ , where  $K$  is the permeability – this is a consequence of Leverett J-function scaling, section 10), there is likely to be significant displacement with this driving force and demonstrates how both capillary and gravitational forces mediate recovery in field settings.

Gravity also determines the initial water saturation before waterflooding. As is apparent from the capillary pressures, for the lowest permeability sample, Estailades (which is still high permeability compared to most reservoir rocks) an effective matrix block height of around 10 m would be required to displace all the oil to close to residual saturation. There is a corollary to this: it also indicates that the initial saturation determined by capillary-gravity equilibrium (based, typically on the primary drainage capillary pressure) has a transition zone – with varying saturation above the irreducible value – of height around 10 -100m for rocks with permeabilities

between 1mD and 100mD (using the  $1/k^{1/2}$  scaling mentioned above). The initial water saturation affects both the wettability (at high saturation less of the rock is contacted directly by oil and, as the imposed capillary pressure is lower, the wettability alteration is likely to be less strong) and the starting point for waterflooding. There is often a wettability trend from water-wet near the oil-water contact, through mixed-wet in most of the reservoir with more oil-wet conditions at the crest, as discussed previously. Usually, coreflood measurements are made from samples near the top of the reservoir: this could suggest oil-wet conditions and unfavourable waterflood recovery, when the reality is a much more efficient displacement in most of the reservoir column. Pore-scale modelling, allowing the prediction of relative permeabilities as a consistent function of initial water saturation, has enormous potential to improve the characterization of such reservoirs.

This rather simple analysis already leads to some interesting and surprising conclusions. For the same wettability, in a reservoir where flow is not fracture dominated, local waterflood recovery is higher in the lower-permeability less well-connected sample, since the low water relative permeability holds back the water advance. On the other hand, if the reservoir is extensively fractured, the better-connected sample gives faster and better recovery, since there is a greater degree of spontaneous imbibition allowed. This is a clear indication that both the nature of the reservoir – fractured or unfractured – and the multiphase flow properties are both crucial for any reasonable assessment of recovery.

I call this conundrum over recovery – mixed-wet systems are good for displacement, but bad for imbibition – the ‘trillion barrel question’ since it will determine the recovery of most of our remaining conventional reserves of oil, mainly in the Middle East. While I do not have a simple answer – and it is unlikely that there is a simple answer – it does underscore the importance of this topic and how important it is to have good measurements (and predictions) of relative permeability.

## 14. THREE-PHASE FLOW

---

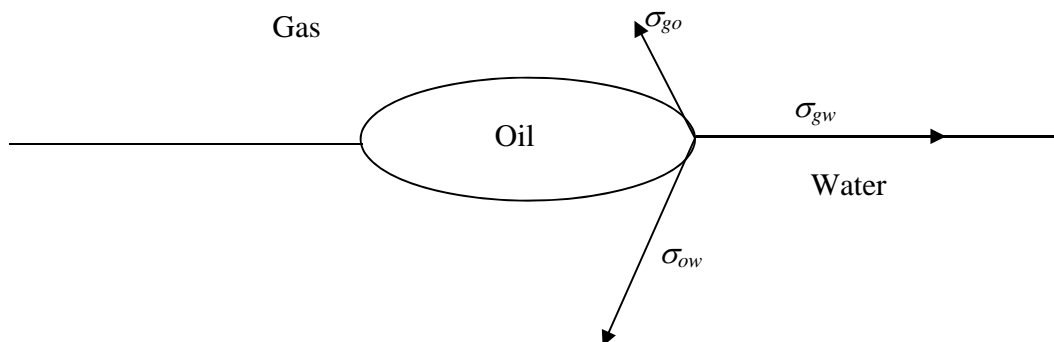
Oil, water and gas may all flow together in reservoirs. Examples include gas injection, including carbon dioxide injection, solution gas drive (when the reservoir pressure is dropped below the bubble point), gas cap expansion and steam injection. In environmental settings, when a non-aqueous phase pollutant migrates downwards towards the water table in a moist soil, there are three mobile fluid phases.

First we will consider oil, water and gas at the pore scale, and how they are arranged. We use this insight to discuss wettability and relative permeability, as well as oil recovery.

### 14.1 SPREADING, WETTING AND OIL LAYERS

---

What happens when I place a drop of oil on water?



**The arrangement of a small droplet of oil floating on water in the presence of a gas.**

Consider the spreading coefficient, which is defined by:

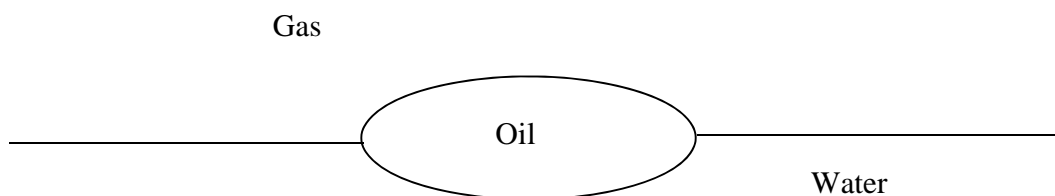
$$C_s = \sigma_{gw} - \sigma_{go} - \sigma_{ow} \quad (14.1)$$

If  $C_s > 0$ , the oil spreads on water. Light alkanes and many alkane mixtures – and indeed most crude oils – spread: the arrangement shown in the figure above is not stable and it will be energetically favourable for the oil to cover the interface between gas and water.

If  $C_s < 0$ , the oil does not spread on water. Dense (denser than water) non-aqueous phase liquids (such as chlorinated solvents) and long chain alkanes (such as decane, dodecane etc) do not spread.

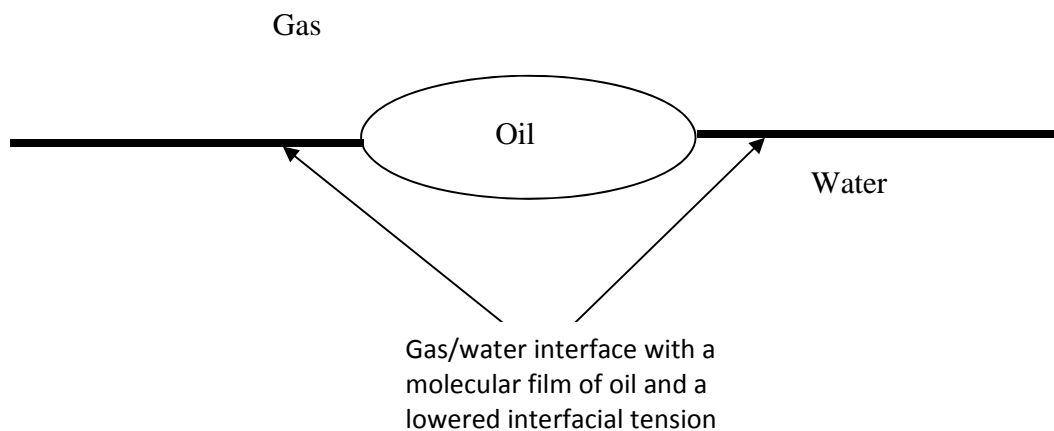
In thermodynamic equilibrium, there are then three things that can happen to the drop of oil.

1.  $C_s < 0$  and the drop is stable.



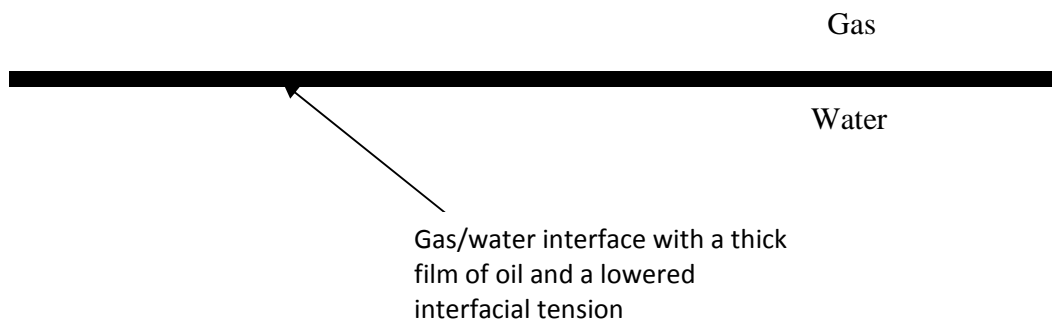
**The equilibrium arrangement of a small droplet of oil floating on water in the presence of a gas. Here the spreading coefficient is negative and no oil film forms between the gas and water.**

2.  $C_s > 0$  but if we define an equilibrium spreading coefficient when the gas/water interface is covered by a molecular film of oil. We can define a spreading coefficient using Eq. (14.1) when the phases are in equilibrium,  $C_s^e$ , coated by films. In this case, the oil film reduces the effective gas/water tension,  $C_s^e < 0$  and the drop is stable.



**The equilibrium arrangement of a small droplet of oil floating on water in the presence of a gas. Here the initial spreading coefficient is positive; an oil film forms, generating a new effective gas/water interface with a negative equilibrium spreading coefficient.**

3.  $C_s > 0$  and  $C_s^e = 0$ . The oil film swells without limit as more oil is added to the system.

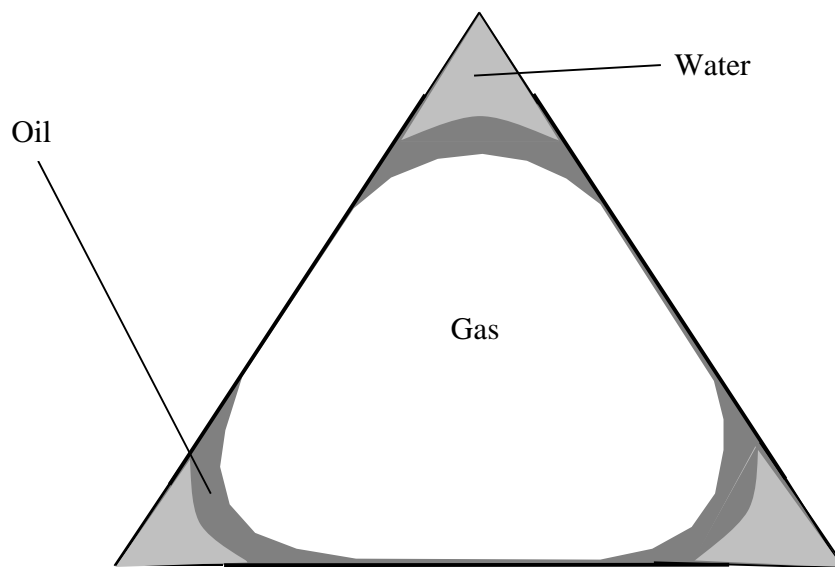


**The equilibrium arrangement of a small droplet of oil floating on water in the presence of a gas. Here the initial spreading coefficient is positive; an oil film forms, generating a new effective gas/water interface with a negative equilibrium spreading coefficient.**

In thermodynamic equilibrium  $C_s^e \leq 0$ .

Now we will discuss what this implies about the arrangement and flow of three phases in the pore space. The typical arrangement of the phases is shown in the figure overleaf.





**The arrangement of oil, water and gas in a water-wet pore of triangular cross-section. Note that the oil resides as a layer sandwiched between the water in the corners and gas occupying the centre of the pore.**

The oil can form layers in a (water-wet) pore space, sandwiched between water in the corners and gas in the centre. This formation of the oil layer is favoured by having a low (or zero) equilibrium spreading coefficient, as this controls the contact angle between the gas and oil.

However, for an oil layer to form – that is to be able to draw a layer in an angular pore space:<sup>5</sup>

$$\alpha + \theta_{go} < \pi/2 \quad (14.2)$$

Spreading oils (with an equilibrium spreading coefficient of zero) have  $\theta_{go} = 0$  since, at the microscopic level, there is no angle of contact between the gas and oil.  $\theta_{go}$  increases as the spreading coefficient becomes more negative, as we will show below.

---

<sup>5</sup> This is a necessary, but not sufficient condition for the formation of a layer. Strictly, we need to consider an energy balance for the displacement. Conceptually this is straightforward, as we consider the change in interfacial energy associated with different possible fluid configurations, but can be complex when dealing with three-phase flow.

Consider the Young equation on a flat surface, with different combinations of fluids, shown in the diagrams overleaf. Re-arranging the equations leads to an important equality in three-phase flow, known as the Bartell-Osterhoff (1927) equation:

$$\sigma_{gw}\cos\theta_{gw} = \sigma_{go}\cos\theta_{go} + \sigma_{ow}\cos\theta_{ow} \quad (14.3)$$

Here we assume that the contact angles and interfacial tensions are measured in thermodynamic equilibrium. This relationship provides a constraint between the contact angles and the interfacial tensions: there are only two independent contact angles. Conventionally we consider that the wettability controls  $\theta_{ow}$ , while spreading controls  $\theta_{go}$ .

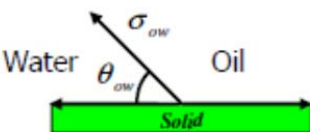
If the system is strongly water-wet with  $\theta_{gw} = \theta_{ow} = 0$ , then the gas/oil contact angle  $\theta_{ow}$  is simply:

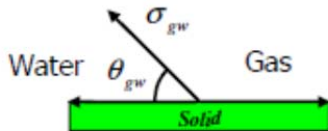
$$\cos\theta_{go} = 1 + \frac{C_s^e}{\sigma_{go}} \quad (14.4)$$

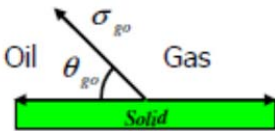
using our definition of spreading coefficient, which has a negative (or zero) value.

Now consider that we have residual oil surrounded by water. The gas enters the system. Examples of this include lowering the water table in a soil with non-aqueous phase pollutants present, gas injection in oil reservoirs, solution gas drive (the primary production mechanism that occurs when the pressure in an oilfield drops below the bubble point) and gravity drainage through gas cap expansion. In a water-wet system, this oil will occupy the centres of the larger pore spaces.

When the gas phase is introduced, oil spreads in the porous medium between water (coating the solid surfaces) and gas (which as the most non-wetting phase preferentially fills the centres of the largest pores). Oil layers for that occupy the crevices and corners of the pore space between water and gas – it is now connected wherever there is gas, and the oil can flow. We can drain to essentially zero saturation. Remaining oil saturations as low as 0.1% have been observed after gravity drainage in sand packs (Sahni *et al.*, 1998).



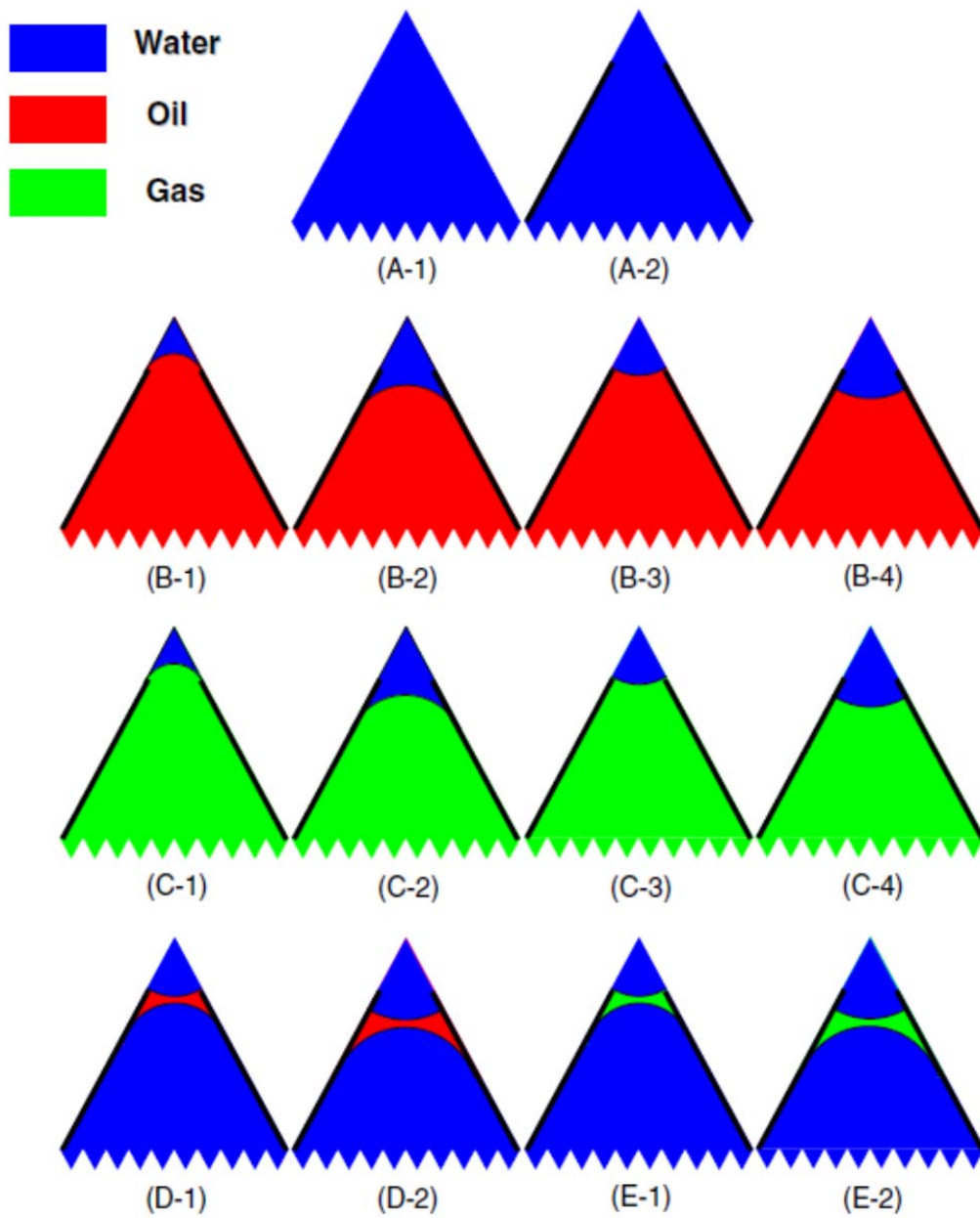
$$\sigma_{os} = \sigma_{ws} + \sigma_{ow} \cos \theta_{ow}$$


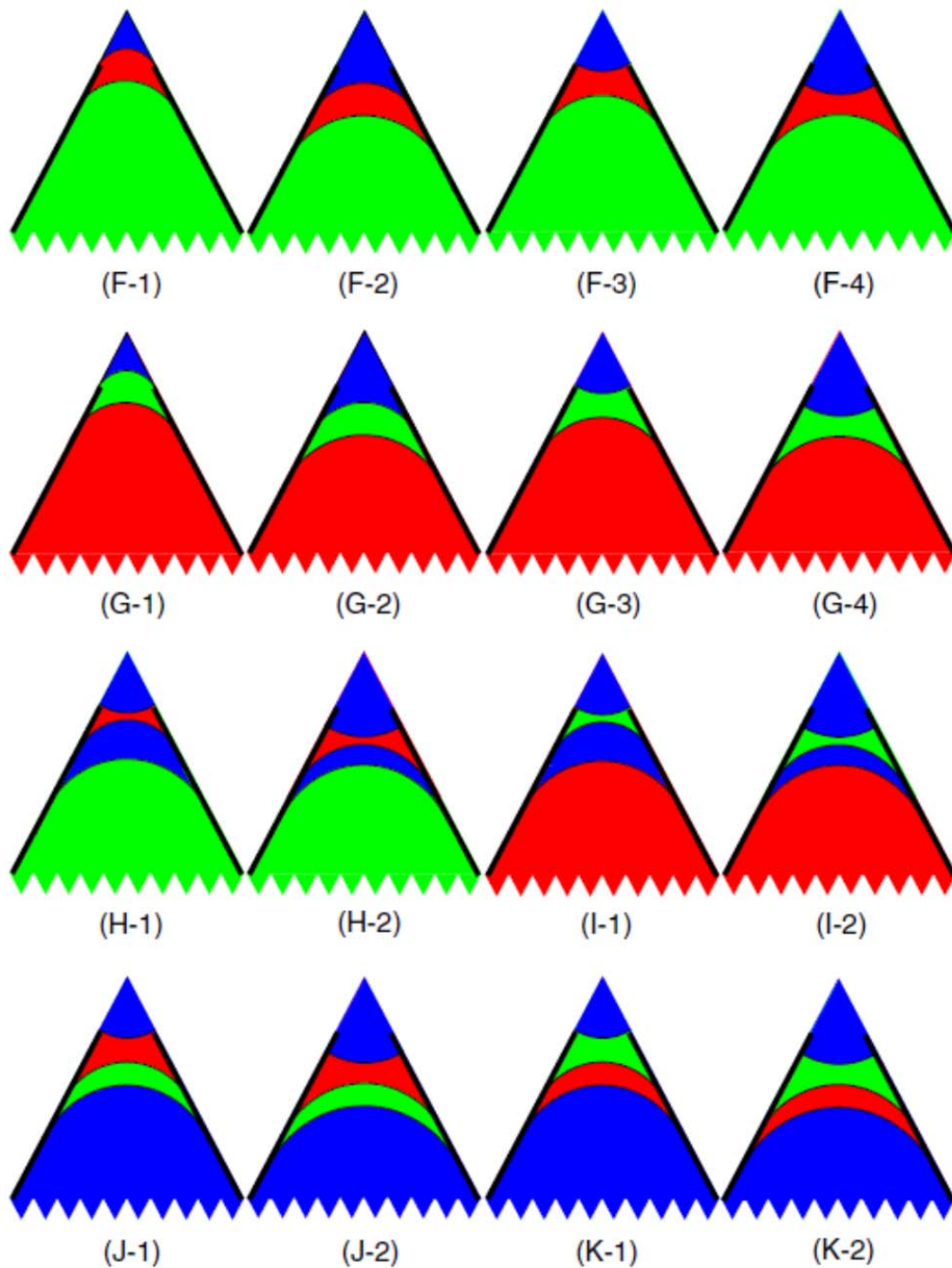
$$\sigma_{gs} = \sigma_{ws} + \sigma_{gw} \cos \theta_{gw}$$


$$\sigma_{gs} = \sigma_{os} + \sigma_{go} \cos \theta_{go}$$

**The Young equations for different combinations of fluids on a solid surface. From this an important constraint between contact angles and interfacial tensions can be derived, Eq. (14.3).**

A full discussion of three-phase flow rapidly becomes rather complicated, beyond the key concept of oil layers: as an example the figure on the next two pages shows (just some of) the configurations of two and three phases in a pore space, dependent on saturation path and wettability. All of these fluid configurations simply use the concepts of wetting, spreading, contact angle and the Young-Laplace equation. Rather than go through all the details, we will present, briefly a discussion on wettability, pore-scale configurations (specifically layers) and recovery later in this section.





**(This and the previous page) Some of the possible configurations of three phases – oil, water and gas – in a corner of the pore space, taken from Piri and Blunt (2005).**

## 14.2 THREE-PHASE RELATIVE PERMEABILITY AND TRAPPED SATURATIONS

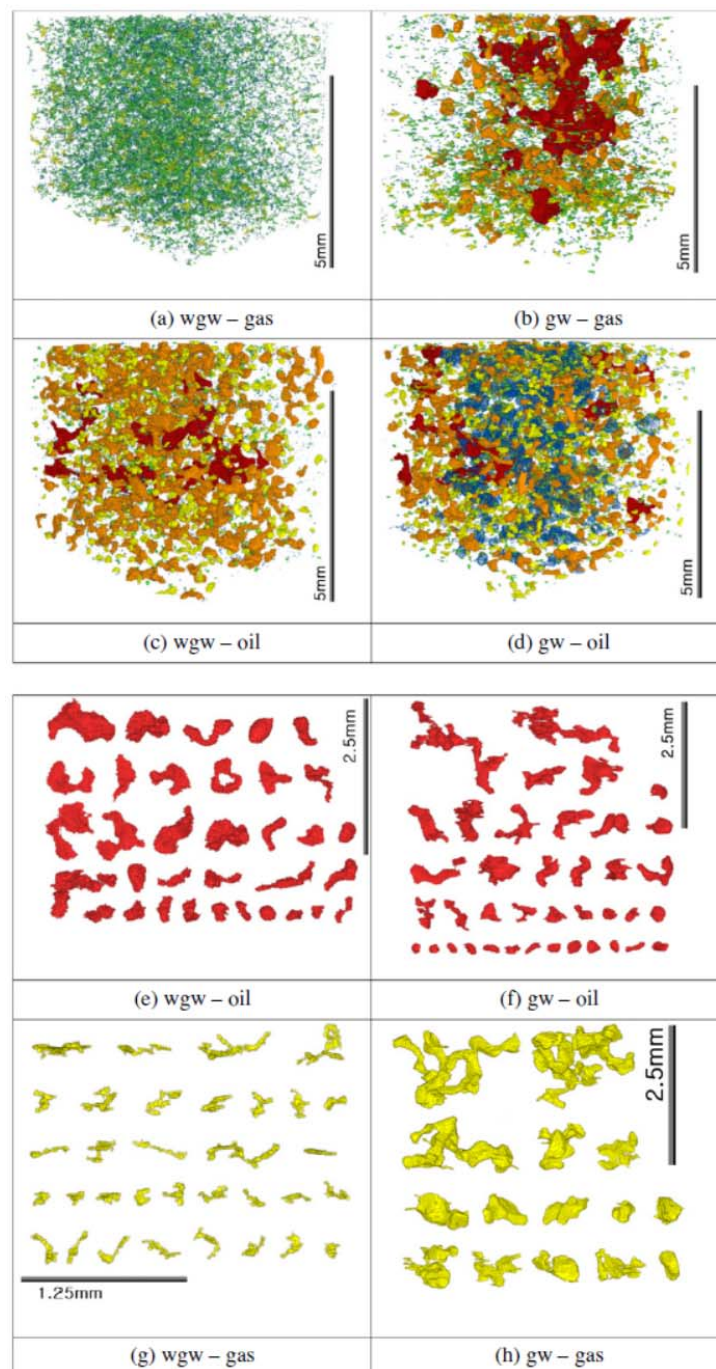
---

We expect to find very low values of the residual oil saturation in the presence of water and gas, because of oil layers, as discussed above, but the relative permeability will be low as well.

Three-phase relative permeability is extremely difficult to measure. There are also a huge range of different saturation paths that may be taken during a displacement that all may have different relative permeabilities.

Normally three phase relative permeabilities are predicted using empirical models with a dubious physical basis. A full discussion of the various models is outside the scope of this class. In a water-wet system, the water tends to reside in the small pores, the oil in the intermediate pores and the gas in the large pores, consistent with our pore-scale picture. This means that the exact pore sizes seen by the oil depends on the amount of water and gas present in the porous medium, leading to relative permeabilities that depend on two independent saturations. If the system is mixed-wet this picture is further complicated. In general, in three-phase flow - in the presence of gas - the oil relative permeability is lower, making recovery low, but the residual oil can also be very low, leading to high ultimate recoveries, because of the drainage of oil layers. The gas relative permeability - in a water-wet system - is high, since gas resides in the larger pores, leading to early breakthrough and poor overall recovery when gas is injected. On the field scale, the main design criterion is how to keep the injected gas in the reservoir, allowing the oil to flow to low saturation. It is less easy to make general statements about recovery, as the system is now much more complex, and we have to rely on field-scale simulation models to assess recovery efficiency.

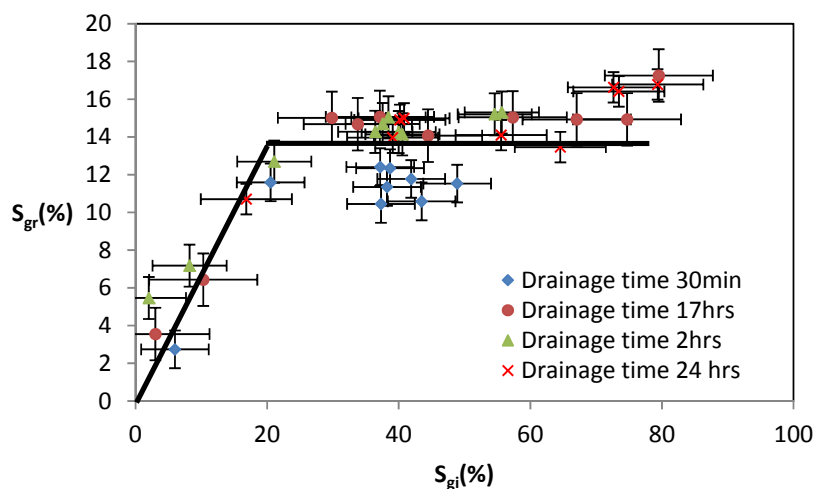
To help advance a more physically-based picture of three-phase flow, micro-CT images of trapped phases in three-phase flow, over the page. When water is injected into a porous medium containing gas and oil, both gas and oil can be trapped. If the system is water-wet, then snap-off can strand ganglia of both hydrocarbon phases, as shown.



**Trapped oil and gas imaged in a water-wet sandstone (Iglauer et al., 2012).** Initially the core is full of water. Then oil is injected – this is primary drainage. Then two displacement sequences are considered. The first is gas injection, followed by water injection (gw), while the second is waterflooding, followed by gas injection followed by a further waterflood (wgo). The gw sequence leads to considerably more trapping of gas in the pore space.

The amount of trapping – of both gas and oil – is dependent on the displacement sequence, with less trapped if we waterflood the reservoir before gas injection (this is called tertiary injection, as opposed to gas injection straight away, which is secondary gas injection). The morphology of the trapped clusters is also different, with smaller clusters of gas seen for the wgw sequence. This is an active topic of research and we do not have, as yet, a full understanding of recovery and displacement processes in three-phase flow.

One important observation is that – in water-wet systems – more gas can be trapped in a three-phase displacement than if displaced only by water. This could be used to design gas injection to retain the gas in the reservoir, while mobile oil is produced. Experimental evidence for this is shown below for experiments on sand packs: more gas can be trapped in a three-phase displacement involving oil and water than when gas is displaced by water alone. In general, there is more trapping of oil and gas combined than in two-phase flow, more trapping of gas, but less trapping of oil alone.

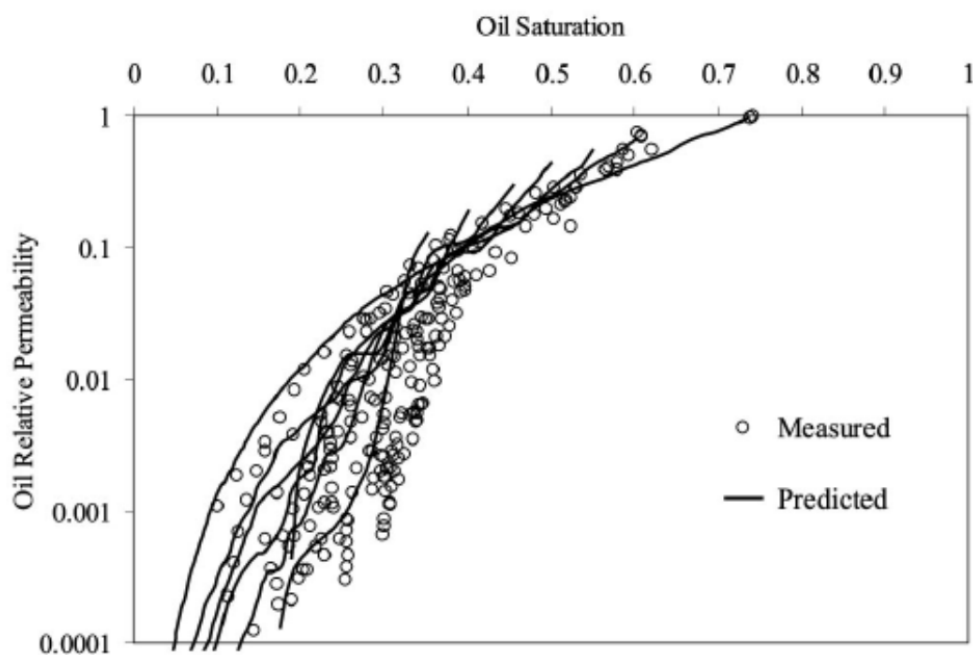


**Trapped gas saturation as a function of initial gas saturation for three-phase displacements in a water-wet sand-pack. More gas can be trapped in the presence of oil than when gas is displaced by water alone (the solid black lines). From Amaechi *et al.* (2014).**

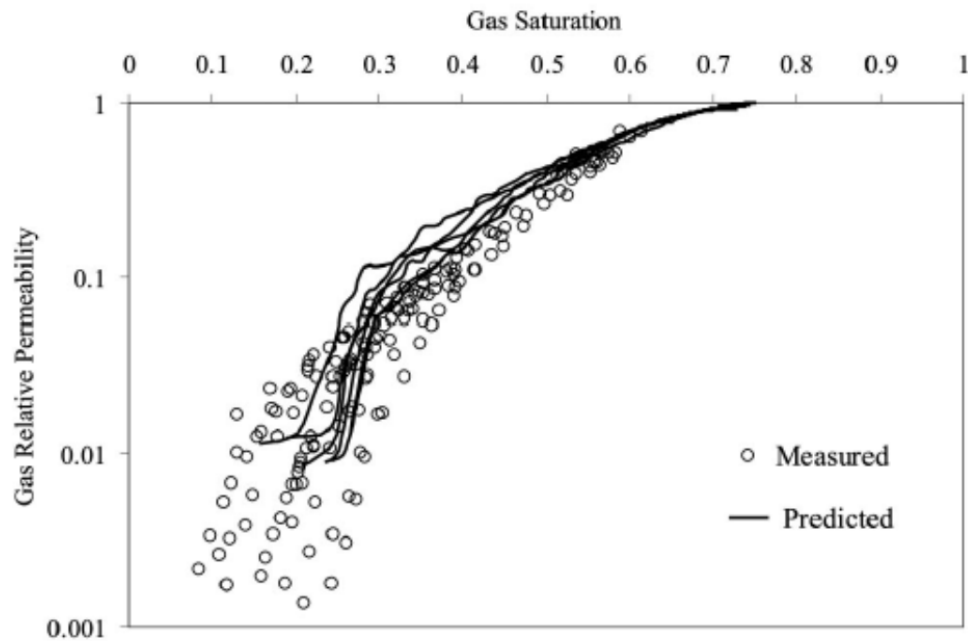


### 14.3 RELATIVE PERMEABILITY PREDICTIONS USING PORE-SCALE MODELLING

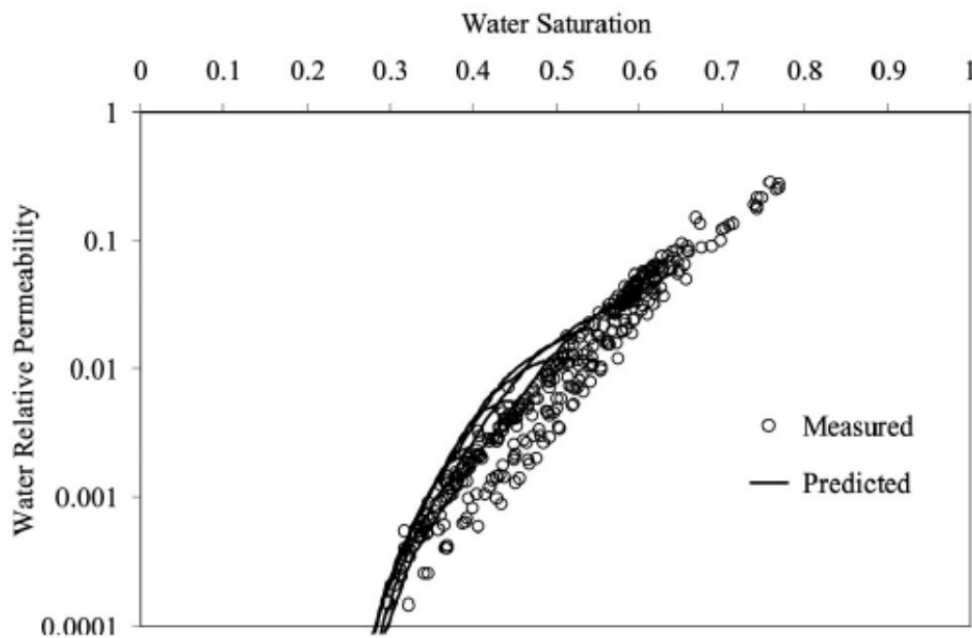
If we consider all the various possible configurations of phases in the pore space, and have a good network representation of the rock, it is possible to make predictions of three-phase relative permeabilities. The dataset is the classic Berea measurements of Oak (1990) compared to network model predictions of Piri and Blunt (2005). Overall, bearing in mind the complexity of the problem, the predictions shown are a good test of the ability of pore-network modelling to predict the behaviour of complex systems.



**Measured and predicted oil relative permeabilities for water-wet Berea sandstone. The different points refer to different displacement sequences in the experiments. In this and the subsequent two figures, the data comes from Oak (1990), while the predictions are based on the work of Piri and Blunt (2005).**



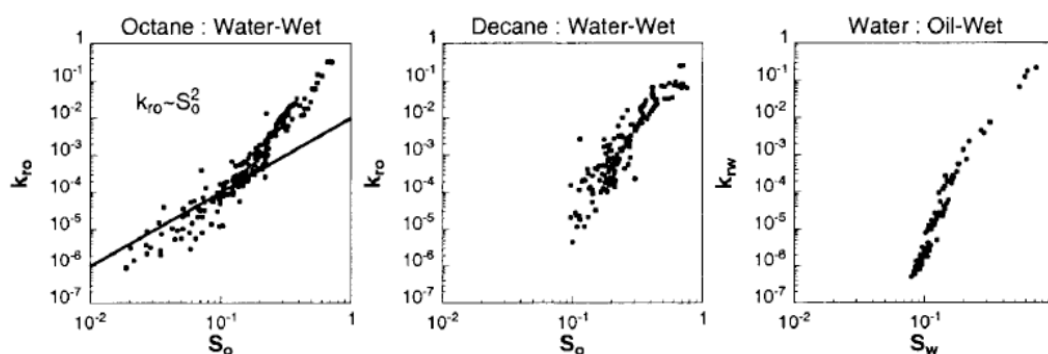
**Measured and predicted gas relative permeabilities. The different points refer to different displacement sequences in the experiments. From Piri and Blunt (2005).**



**Measured and predicted water relative permeabilities. The different sets of points refer to different displacement sequences in the experiments. From Piri and Blunt (2005).**

#### 14.4 LAYER DRAINAGE AND WETTABILITY

We will now make some statements concerning wettability, layers and recovery. The figure below shows the results of gravity drainage experiments (gas enters a long sand column, while oil and water drain out of the bottom of the column under gravity the same process occurs in an oil reservoir, if gas is introduced to the crest of the field, or a natural gas cap expands). The relative permeability is shown for three cases: octane as the oil in a water-wet system; decane as the oil in a water-wet system; and the water relative permeability for an oil-wet case.



**Measured relative permeabilities for gas gravity drainage in a sand pack. From left to right: the oil relative permeability in a water-wet medium, when octane is the oil phase; the same experiment but with decane as the oil; the water relative permeability in an oil-wet system. From DiCarlo et al. (2000).**

The behaviour is different in each case and we can understand this and discuss the implications for recovery using our discussion of spreading coefficient and the Bartell-Osterhoff relation, Eq. (14.3).

Octane spreads – or almost spreads – on water, with an effective gas/oil contact angle in a water-wet system close to zero. Hence, oil layers readily form. If gas is injected, oil layers form and allow drainage down to very low saturation – below 1% in the sand pack studied. At low oil saturation, the flow is dominated by this layer drainage. The oil saturation is simply proportional to the area of oil open to flow. The conductance scales as the square of the area – this is important – the square of the area, rather than proportional to it. This is a direct consequence of the Navier-Stokes equation: consider Poiseuille flow where the flow rate is proportional to the fourth power of radius (second power of area). Physically, this is because there is no flow at a solid boundary. If we increase the area to flow, then the flow speed in the

centre of the channel can increase, as it is further away from the walls. This, combined with the fact that the area is greater, is what leads to the quadratic dependence on area. This result contrasts with electrical conductance, which scales linearly with area.

The oil relative permeability is just the fractional flow conductance of the oil and so this discussion leads to the prediction:

$$k_{ro} \sim S_o^2 \quad (14.5)$$

This is seen in the experimental results shown, and in other measurements.

Decane has a higher interfacial tension with water than octane and does not spread on water. Its contact angle in the presence of gas is non-zero and this non-spreading oil does not form oil layers in the pore space. Hence there is no oil layer drainage regime, the oil relative permeability drops rapidly at low saturation and we see significant trapping. This is observed in the middle figure above.

It is considered likely that in reservoir settings, most oils are spreading, and so high recoveries are potentially possible. However, in environmental applications many non-aqueous phase liquids, particularly chlorinated solvents, do not spread on water and therefore can remain trapped even in the presence of gas (air).

## 14.5 WHY DUCKS DON'T GET WET

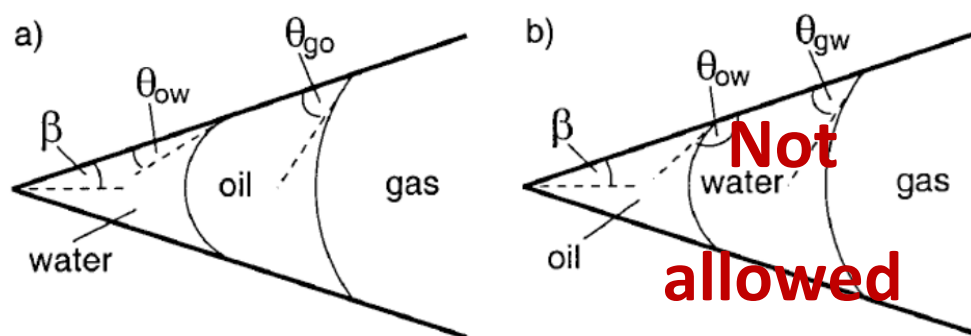
---

If instead the porous medium is oil-wet, then perhaps we can simply swap phases. That is, the water relative permeability in an oil-wet system is the same as the oil relative permeability in a water-wet system. The right-hand figure for the gravity drainage experiments shows that this is not the case if the oil is spreading. The water relative permeability drops sharply and has an irreducible saturation. Why is this, and what has it got to do with ducks?

The figure below explains this. If we re-arrange the Bartell-Osterhoff equation to find the gas/water contact angle for a spreading oil ( $\theta_{go} = 0$ ) in a strongly oil-wet system ( $\theta_{ow} = 180^\circ$ ), we find:

$$\cos\theta_{gw} = \frac{\sigma_{go} - \sigma_{ow}}{\sigma_{gw}} \quad (14.6)$$

The interfacial tension between oil and water is always larger than between gas and oil. Hence the gas/water contact angle has a negative cosine and is greater than  $90^\circ$ . Water cannot spread on oil in the presence of gas. Indeed, in a strongly oil-wet system water is the most non-wetting phase and can be trapped by gas and water.



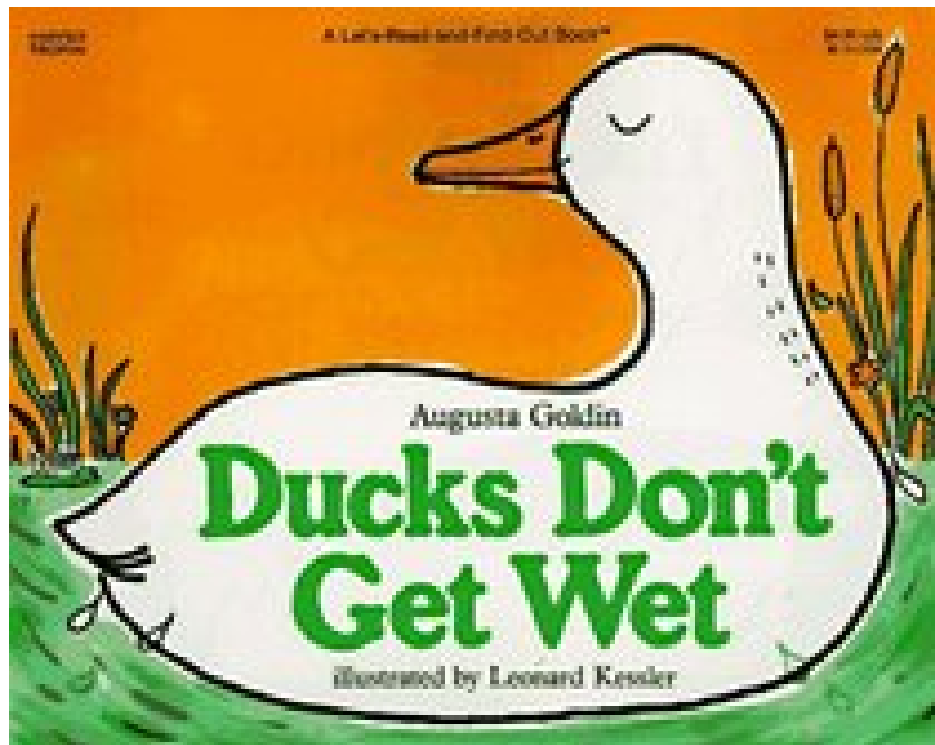
**Diagram showing oil layers in the pore space of a water-wet medium (left). In contrast, water layers cannot form in an oil-wet system, as the gas/water contact angle will be greater than  $90^\circ$ .**

This is why ducks don't get wet. Their feathers are covered in oil and form an oil-wet porous medium. This makes water the most non-wetting phase: you have to force water into the feathers – they prefer to be surrounded by air keeping the duck dry and insulated. This is also why water beads and runs off an oily surface. It also why sea-bird often die if crude oil (from a spill) is washed off their feathers using soap: now their feathers are water-wet, they imbibe water and the birds soon die of hypothermia.

While this observation is the topic of a children's book (see the next page), the concept still struggles to be accepted by petroleum engineers, where it is still widely assumed that gas 'must' be the most non-wetting phase.

The consequences of wettability for recovery in three-phase flow are still not fully understood. We do expect good ultimate recoveries if oil layers form – as they do in a spreading system,

regardless of wettability (oil is always more wetting than gas). We can also trap and suppress the movement of gas in mixed-wet media, which is favourable for recovery.

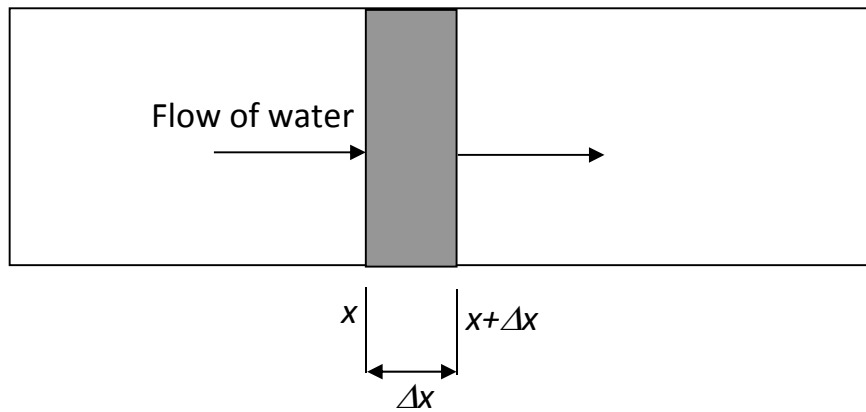


**You have got near the end of a demanding and difficult course and now you know as much as ....., a young child who has read this book!**

## 15. CONSERVATION EQUATION FOR MULTIPHASE FLOW

The approach so far in the course has been somewhat physically motivated with a minimum of equations. However, to provide some rigour and background to our comments on recovery, we will now derive flow equations for multiple phases in a porous medium.

We will consider a conservation equation for a case where we have multiple phases. This is an extension of the derivations for single-phase flow in section 14. The approach will be very slightly different, but is straightforward. Here we consider the transport of saturation, rather than concentration. Consider conservation of mass of one phase (water) in the diagram below.



**Figure illustrating conservation of water for one-dimensional flow. Here we will allow other phases – oil and/or gas – to be flowing as well.**

The mass of water that enters the box – the shaded region shown in the figure above – in a time  $\Delta t = A \Delta t \rho_w q_w(x)$ , where  $q_w$  is given by the multiphase Darcy law, Eq. (13.1).  $A$  is the cross-sectional area to flow. Similarly, the mass that leaves is given by  $A \Delta t \rho_w q_w(x + \Delta x)$ . The mass of water in the box is given by  $A \Delta x \phi S_w$ . The mass in minus the mass out is the change in mass:

$$A \Delta t \rho_w (q_w(x) - q_w(x + \Delta x)) = A \Delta x \rho_w \phi (S_w(t + \Delta t) - S_w(t)) \quad (15.1)$$

$$\phi \frac{S_w(t + \Delta t) - S_w(t)}{\Delta t} + \frac{q_w(x + \Delta x) - q_w(x)}{\Delta x} = 0 \quad (15.2)$$

Where we have assumed that the density and porosity are constant (assuming, as in section 11, that the flow is incompressible). Then we take the limit of small  $\Delta x$  and  $\Delta t$  to obtain a differential equation:

$$\phi \frac{\partial S_w}{\partial t} + \frac{\partial q_w}{\partial x} = 0 \quad (15.3)$$

This simple form of the conservation equation can be rearranged by substituting in Darcy's law, Eq. (13.1). This takes some algebra and ends with an equation that can be solved analytically for saturation. We start with Eq. (13.1) for one-dimensional flow of the water phase:

$$q_w = -\frac{Kk_{rw}}{\mu_w} \left( \frac{\partial P_w}{\partial x} - \rho_w g_x \right) \quad (15.4)$$

Similarly for oil:

$$q_o = -\frac{Kk_{ro}}{\mu_o} \left( \frac{\partial P_o}{\partial x} - \rho_o g_x \right) \quad (15.5)$$

and  $P_c = P_o - P_w$  is the capillary pressure.  $k_{ro}$ ,  $k_{rw}$  and  $P_c$  are known as functions of  $S_w$ .

We can write a similar conservation equation to Eq. (15.3) for oil:

$$\phi \frac{\partial S_o}{\partial t} + \frac{\partial q_o}{\partial x} = 0 \quad (15.6)$$

Add the two conservation equations (15.3) and (15.6):

$$\phi \frac{\partial (S_w + S_o)}{\partial t} + \frac{\partial (q_w + q_o)}{\partial x} = 0 \quad (15.7)$$

We define  $q_t = q_w + q_o$  as the total velocity. Then Eq. (15.7) is (the saturation term is zero as for two-phase flow, the sum of the oil and water saturation is one, a constant):



$$\frac{\partial q_t}{\partial x} = 0 \quad (15.8)$$

The total velocity is constant in space (it can vary over time) for one-dimensional flow.

From the multiphase Darcy equations for oil and water, Eqs. (15.4) and (15.5) and writing the expression in terms of the water pressure only:

$$q_t = q_w + q_o = -\frac{Kk_{rw}}{\mu_w} \left( \frac{\partial P_w}{\partial x} - \rho_w g_x \right) - \frac{Kk_{ro}}{\mu_o} \left( \frac{\partial P_w}{\partial x} + \frac{\partial P_c}{\partial x} - \rho_o g_x \right) \quad (15.9)$$

Then defining mobilities by  $\lambda_w = k_{rw}/\mu_w$  and  $\lambda_o = k_{ro}/\mu_o$ , with the total mobility given by  $\lambda_t = \lambda_w + \lambda_o$ , Eq. (15.9) becomes:

$$q_t = -K\lambda_t \frac{\partial P_w}{\partial x} + Kg_x(\rho_w \lambda_w + \rho_o \lambda_o) - K\lambda_o \frac{\partial P_c}{\partial x} \quad (15.10)$$

Then we substitute  $\frac{\partial P_w}{\partial x}$  from Eq. (15.10) in  $q_w$  in the Darcy equation (15.4):

$$q_w = \frac{\lambda_w}{\lambda_o} q_t - K \frac{\lambda_o \lambda_w}{\lambda_t} \rho_o g_x - K \frac{\lambda_w^2}{\lambda_t} \rho_w g_x + K \lambda_w \rho_w g_x - K \frac{\lambda_o \lambda_w}{\lambda_t} \frac{\partial P_c}{\partial x} \quad (15.11)$$

Rearrange terms to find:

$$q_w = \frac{\lambda_w}{\lambda_o} q_t + K \frac{\lambda_o \lambda_w}{\lambda_t} (\rho_w - \rho_o) g_x + K \frac{\lambda_o \lambda_w}{\lambda_t} \frac{\partial P_c}{\partial x} \quad (15.12)$$

In words the water Darcy velocity = pressure gradient + capillary pressure + gravity

The conservation equation (15.3) becomes:

$$\phi \frac{\partial S_w}{\partial t} + q_t \frac{\partial f_w}{\partial x} = 0 \quad (15.13)$$

$f_w$  is the water fractional flow defined by:  $q_w = f_w q_t$ :

$$f_w = \frac{\lambda_w}{\lambda_t} \left[ 1 + K \frac{\lambda_o}{q_t} \left( \frac{\partial P_c}{\partial x} + (\rho_w - \rho_o) g_x \right) \right] \quad (15.14)$$

The fractional flow has three terms representing the three physical forces that impact the fluid movement: advection (governed by the pressure gradient); capillary pressure and gravity (buoyancy).

### 15.1 NOTE ABOUT NOMENCLATURE

---

Many authors define mobility as  $\lambda_w = K k_{rw} / \mu_w$ , with an extra factor of  $K$ . Also we use  $Q$  (volume per unit time) and  $q$  (Darcy velocity) rather than  $q$  and  $v$  respectively, as in some books. Often you see conservation equations with an explicit area  $A$ . Our equations are per unit area:  $Q = qA$ .

### 15.2 RICHARDS EQUATION

---

The conservation equations we have developed are for an oil/water displacement, where water displaces oil, as occurs in a hydrocarbon reservoir.

We will now address some special cases, where simplifications to the equations can be made. While we cannot solve the full equation directly, we can explore solutions in a variety of different limits. One case will be considered in this section.

If we have gas/water flow, then the mobility of the gas phase can be considered to be much larger than for the water. The Richard's equation describes transport of water in this case.

In Eqs. (15.13) and (15.14)  $\lambda_o$  is replaced by  $\lambda_g$  (for gas) and  $\lambda_g \gg \lambda_w$  and so  $\lambda_t = \lambda_g$ . Then the fractional flow can be written as:

$$q_t f_w = K \lambda_w \left( \frac{\partial P_c}{\partial x} + (\rho_w - \rho_g) g_x \right) \quad (15.15)$$

where the first – advection – term in Eq. (15.14) is now considered to be negligible. Then the conservation Eq. (15.13) is:

$$\phi \frac{\partial S_w}{\partial t} + K \frac{\partial}{\partial x} \left[ \lambda_w \left( \frac{\partial P_c}{\partial x} + (\rho_w - \rho_g) g_x \right) \right] = 0 \quad (15.16)$$

More usually this equation is written in terms of the pressure head  $p = P_w / \rho_w g + z$ . Write  $\psi = P_w / \rho_w g$ . If the gas (air) density is considered to be negligible and the air pressure constant at atmospheric ( $P_c = P_{atm} - P_w$ ) then Eq. (15.16) becomes for vertical flow ( $g_x = g$ ):

$$\phi \frac{\partial S_w}{\partial t} = K_H \frac{\partial}{\partial x} \left[ k_{rw} \left( \frac{\partial \psi}{\partial x} - 1 \right) \right] \quad (15.17)$$

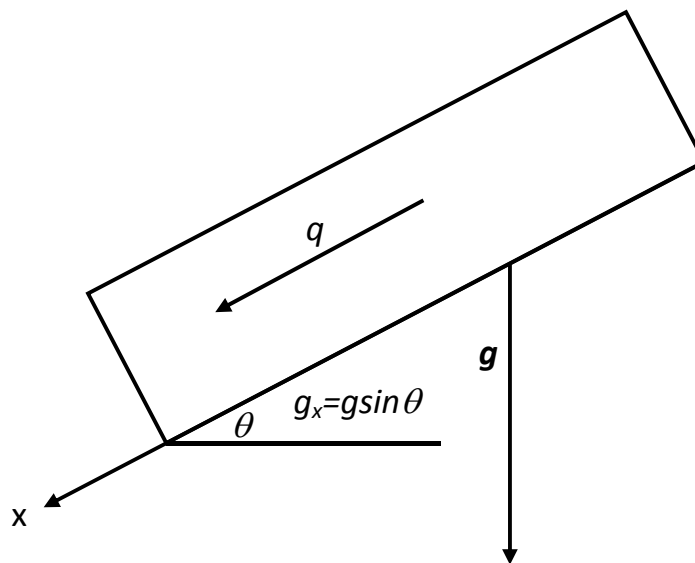
using the standard definition for hydraulic conductivity,  $K_H$  (see section 9). Often rather than seeing the relative permeability and capillary pressure written as a function of pressure, the saturation and relative permeability are written as a function of scaled capillary pressure ( $\psi$ ).

Eq. (15.17) is the standard transport equation in hydrology to describe the movement of water under gravity and capillary pressure.

## 16. FRACTIONAL FLOW AND ANALYTIC SOLUTIONS

---

We will now begin to construct an analytical solution for flow in one dimension. The derivation can be somewhat cumbersome and is helped if we first develop the concept of the fractional flow: the fraction of the total flow of oil and water that is taken by water alone.



**A schematic showing one-dimensional flow in a tilted reservoir.**

Consider a reservoir with constant dip and linear flow, as shown in the figure above. Using the conservation equation (15.13), we can write the fractional flow Eq. (15.4) as:

$$f_w = \frac{\lambda_w}{\lambda_t} \left[ 1 + K \frac{\lambda_o}{q_t} \left( \frac{\partial P_c}{\partial x} + \Delta \rho g \sin \theta \right) \right] \quad (16.1)$$

where  $\theta$  is the angle to the horizontal and the density difference is written as  $\Delta \rho$ .

$\theta > 0$  represents downwards flow, while  $\theta < 0$  is flow uphill.

How important is the capillary pressure term at the field scale? While it dominates at the pore scale, as discussed previously in this course, it is small over 100s m to km: the effect of capillary pressure is encapsulated in the relative permeabilities. This was discussed in section 15 in the context of capillary and Bond numbers.

We will estimate the relative contribution of viscous forces (advection), capillary pressure and buoyancy to the fractional flow by considering the magnitude of each of the three terms in the brackets of Eq. (16.1). By definition the viscous term is 1. For  $q_t$  of the order of  $10^{-5} \text{ ms}^{-1}$  (around 1 m/day),  $K$  of  $10^{-13} \text{ m}^2$  (100 mD), a viscosity of  $10^{-3} \text{ Pa.s}$  and a relative permeability of order 1, then the  $K \frac{\lambda_o}{q_t}$  term in Eq. (16.1) is around  $10^{-5} \text{ m.Pa}^{-1}$ . Then for a typical capillary pressure of  $10^4 \text{ Pa}$  varying over a typical distance between wells (say 100 m), the capillary pressure term in Eq. (16.1) is of order  $10^{-3}$ . The gravitational term, for, say, a density difference of  $300 \text{ kg.m}^{-3}$ , is around 0.03. This indicates that buoyancy forces are generally small (but not negligible) in comparison to advection, while the effect of capillary pressure – at the field scale – is tiny. Another way of seeing this is to consider the pressure drop between injection and production wells – generally a few MPa – compared to capillary pressures of 0.01 to 0.1 MPa.

So, to construct an analytical solution applicable at large scales we ignore the capillary pressure (later we solve for the opposite limit – no Darcy flow and only capillary pressure) and write Eq. (16.1) as:

$$f_w = \frac{\lambda_w}{\lambda_t} \left[ 1 + K \frac{\lambda_o}{q_t} \Delta \rho g \sin \theta \right] \quad (16.2)$$

Define a gravity number (this is different from the Bond number introduced in section 12):

$$N_G = \frac{K \Delta \rho g}{\mu_o q_t} \quad (16.3)$$

Also, traditionally we write:

$$\frac{\lambda_w}{\lambda_t} = \frac{1}{1 + \frac{\lambda_o}{\lambda_w}} = \frac{1}{1 + \frac{k_{ro}\mu_w}{k_{rw}\mu_o}} \quad (16.4)$$

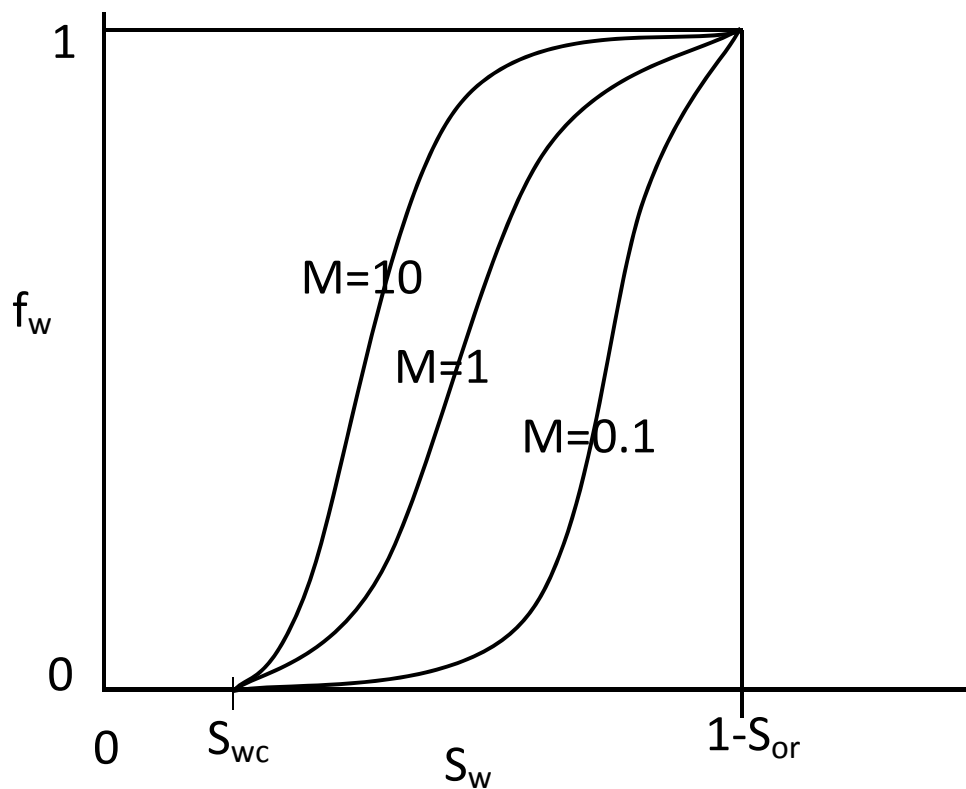
Then the fractional flow Eq. (16.2) becomes:

$$f_w = \frac{1 + N_G k_{ro} \sin \theta}{1 + \frac{k_{ro}\mu_w}{k_{rw}\mu_o}} \quad (16.5)$$

Let's look at typical fractional flow curves, shown overleaf, for  $\theta = 0$  as a function of the endpoint water/oil mobility ratio,

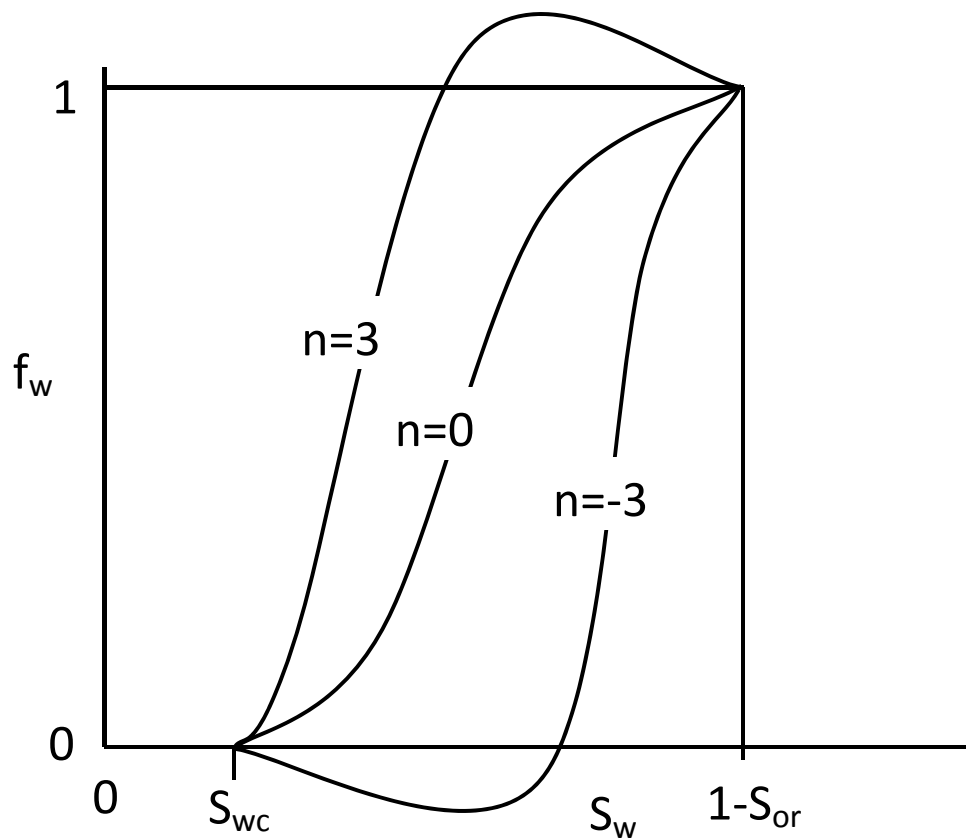
$$M = \frac{k_{rw}^{max} \mu_o}{k_{ro}^{max} \mu_w} \quad (16.6)$$

The curves have a characteristic S shape, with a point of inflection when we consider horizontal flow (without gravity).



**Example fractional flow curves for a horizontal system with different end-point mobility ratios,  $M$ , Eq. (16.6).**

If we include gravity, we can study the behaviour schematically for  $M=1$ , where  $n = N_G k_{ro}^{max} \sin \theta$ . Here the fractional flow curves can be greater than one, or less than zero. This represents, physically, counter-current flow, where water moves downwards while oil moves up: if the overall flow direction is downwards and the oil flows up, then the water flow is greater than  $q_t$  and the fractional flow is greater than one. Conversely, if the flow is uphill and water is flowing downhill, then the water fractional flow is negative. Mathematically,  $f_o + f_w = 1$ . Thus when  $f_w > 1$ ,  $f_o < 0$  and *vice versa*: the phases are flowing in opposite directions. Hence, if gravity is sufficiently strong, it can generate counter-current flow of oil and water. To repeat: this means that the water moves downhill, while oil moves uphill.



**Example fractional flow curves including the effect of gravity. If gravitational effects are sufficiently strong, we can have – for some range of saturation – counter-current flow where the oil and water flow in opposing directions. In this case, the water fractional flow is either greater than 1 or negative.**

We have now derived the conservation equation and plotted different typical fractional flow curves. For reference, we will continue with a specific example, shown in the figure below. The water and oil relative permeabilities are written as follows (this is a common parameterization of these curves and normally fit to somewhat scattered experimental data):<sup>6</sup>

---

<sup>6</sup> These are sometimes called Corey curves and the power-laws Corey exponents. In reality, the original paper was a little more confused and did not directly present these simple forms, but in



$$k_{rw} = k_{rw}^{max} \frac{(S_w - S_{wc})^a}{(1 - S_{or} - S_{wc})^a} \quad (16.7)$$

$$k_{ro} = k_{ro}^{max} \frac{(S_o - S_{or})^b}{(1 - S_{or} - S_{wc})^b} \quad (16.8)$$

In this specific case we take a maximum water relative permeability of 0.5, a maximum oil relative permeability of 0.8,  $a=4$  and  $b=1.5$  with  $S_{wc}=0.2$  and  $S_{or}=0.3$ . For the fractional flow the water and oil viscosities are 0.001 and 0.03 Pa.s respectively: the relative permeabilities and fractional flow are shown below. From Eq. (16.6) the mobility ratio  $M=18.75$  and  $n=0$  (horizontal flow).

### 19.1 BUCKLEY-LEVERETT SOLUTION

---

We will now show how to solve the conservation equation (15.13) with the fractional flow given by Eq. (16.5).

We can write the saturation conservation equation (15.13) as:

$$\frac{\partial S_w}{\partial t} + v \frac{\partial f_w}{\partial x} = 0 \quad (16.9)$$

where  $v = q_t/\phi$  is an interstitial velocity. This can be written as:

$$\frac{\partial S_w}{\partial t} + v \frac{\partial f_w}{\partial S_w} \frac{\partial S_w}{\partial x} = 0 \quad (16.10)$$

We are interested in water injection from a well into a reservoir containing some initial (usually irreducible) water saturation. We consider one-dimensional flow with an injection well placed

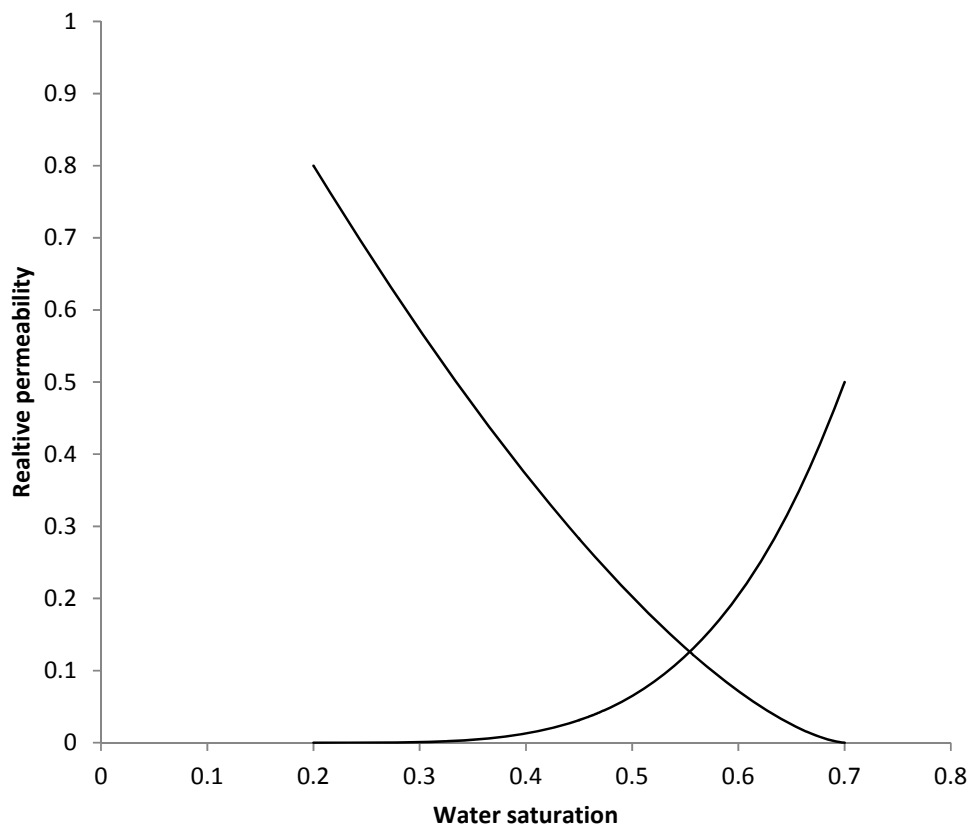
---

any event Corey (or Brooks and Corey) were the first authors to suggest fitting relative permeability data to a power-law form.

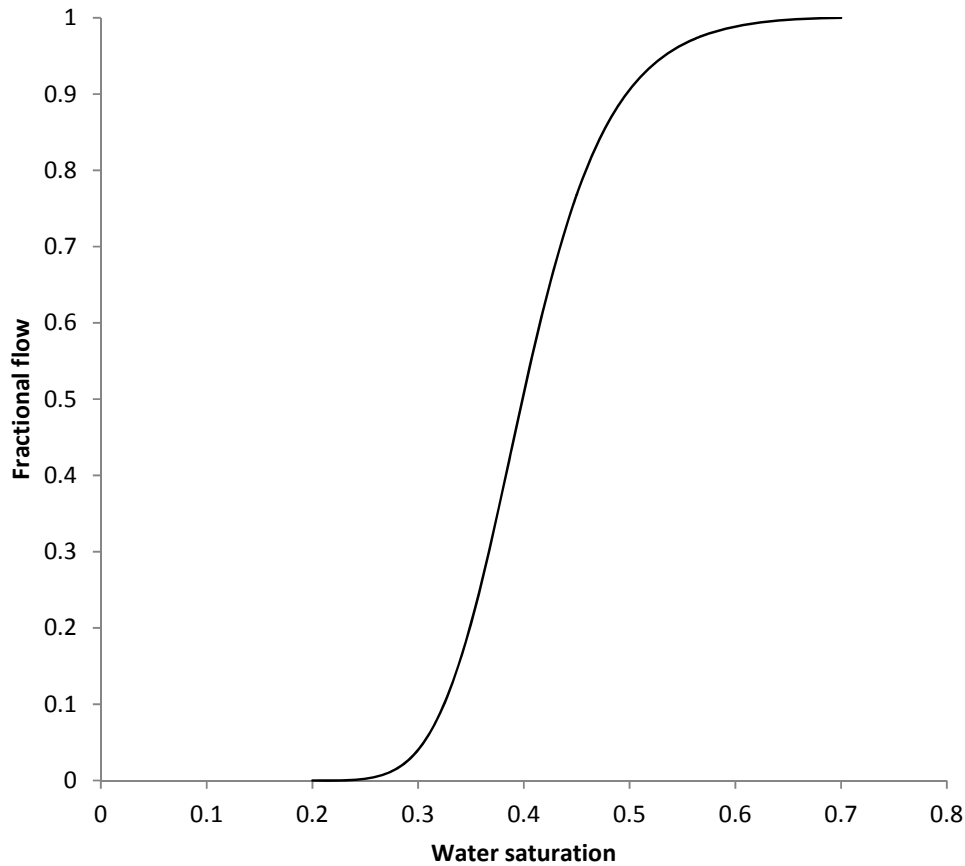
at  $x=0$  and a producer at  $x=L$ . Then the initial condition is:  $t=0$ ,  $S_w(x,0) = S_{wi}$ , while the boundary condition at the well is  $x=0$ , (well)  $S_w(0,t) = S_{w0}$ .

We control rates ( $f_w$ ) at wells, not saturation. Thus we find  $S_{w0}$  that has given  $f_w(0,t)$ . Normally we have  $S_{wi} = S_{wc}$  and inject 100% water: hence  $f_w(0,t) = 1$ , and  $S_{w0} = 1 - S_{or}$ .

## Relative permeabilities



**Relative permeabilities used for our example test case. This represents a weakly water-wet system.**



**The water fractional flow corresponding to the relative permeabilities shown previously.**

We now define dimensionless variables:

$$x_D = \frac{x}{L} \quad (16.11)$$

This is the fractional distance between wells.

We also define a dimensionless time. This requires some more thought –  $t_D$  is the pore volumes of water injected. This gives an indication of how much water has entered the system, in comparison with the total capacity of the reservoir. It is defined as follows:

$$t_D = \int_0^t \frac{v}{L} dt = \int_0^t \frac{q_t}{\phi L} dt = \int_0^t \frac{Q}{\phi A L} dt = \frac{1}{V_p} \int_0^t Q dt \quad (16.12)$$

where  $Q$  is the total flow rate and  $V_p = \phi AL$  is the pore volume. If the flow rate is constant, then the integral simply becomes  $Qt$ : however, this definition does allow varying flow rates to be accommodated in the analysis. A useful relationship, which we will use later is to convert dimensional speeds to a dimensionless quantity. If we have a speed  $v=x/t$ , then using Eqs.(16.11) and (16.12),  $v=q/\phi v_D$ , where  $v_D=x_D/t_D$ .

Then transformation of variables means that the conservation equation (16.10) becomes:

$$\frac{\partial S_w}{\partial t_D} + \frac{\partial f_w}{\partial S_w} \frac{\partial S_w}{\partial x_D} = 0 \quad (16.13)$$

We will now solve this equation by the method of characteristics (MOC). What this means is that we will find the dimensionless velocity with which a given saturation moves. This means that we find the solution as a function of dimensionless velocity. At first, this can be a confusing concept. However, for a given time, the profile of saturation as a function of velocity is the same shape as saturation as a function of distance: the profile elongates linearly with time. It is also straightforward to convert between dimensionless and real variables, with care.

Write Eq. (16.13) as a function of  $v_D=x_D/t_D$ :<sup>7</sup>

$$\frac{\partial S_w}{\partial t_D} = \frac{dS_w}{dv_D} \frac{dv_D}{dt} \Big|_x = - \frac{v_D}{t_D} \frac{dS_w}{dv_D} \quad (16.14)$$

$$\frac{\partial S_w}{\partial x_D} = \frac{dS_w}{dv_D} \frac{dv_D}{dx} \Big|_t = \frac{1}{t_D} \frac{dS_w}{dv_D} \quad (16.15)$$

Thus Eq. (16.13) becomes:

---

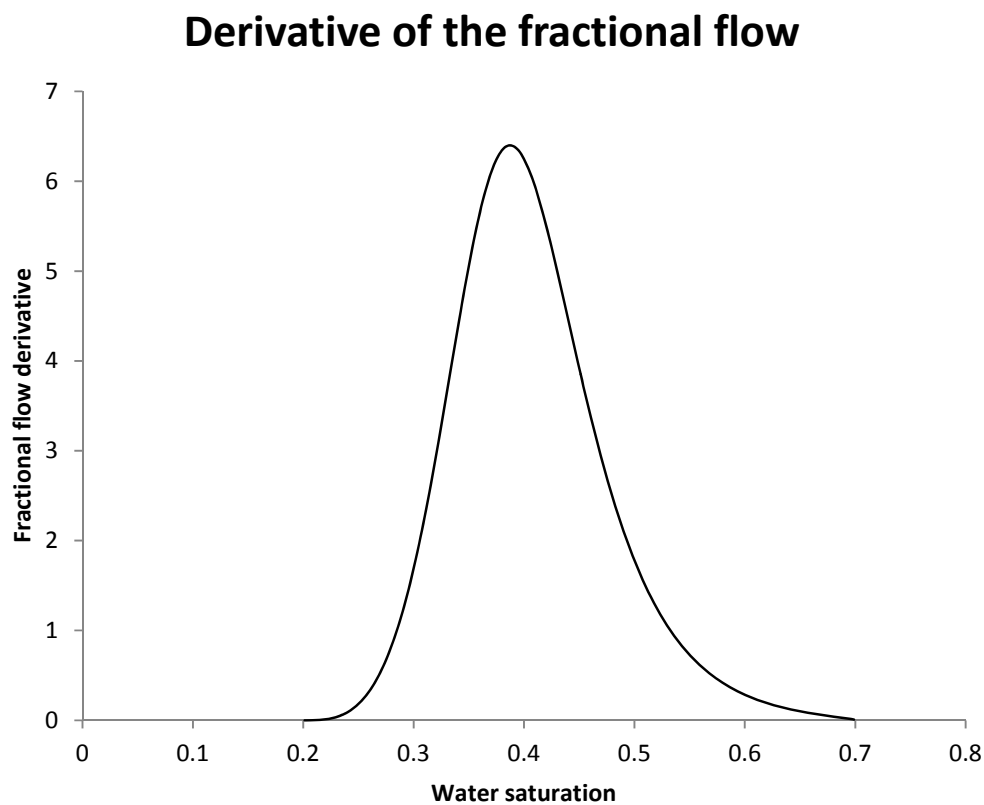
<sup>7</sup> An entirely equivalent approach is to assume that the solution for water saturation is a function of  $z=x-vt$  only and find  $v$ . This makes it even more explicit that the solutions are profiles which move with some characteristic speed.

$$\frac{dS_w}{dv_D} \left( v_D - \frac{\partial f_w}{\partial S_w} \right) = 0 \quad (16.16)$$

One solution is a so-called constant state – that is a saturation that does not change with dimensionless wavespeed. The non-trivial solution is:

$$v_D = \frac{\partial f_w}{\partial S_w} \quad (16.17)$$

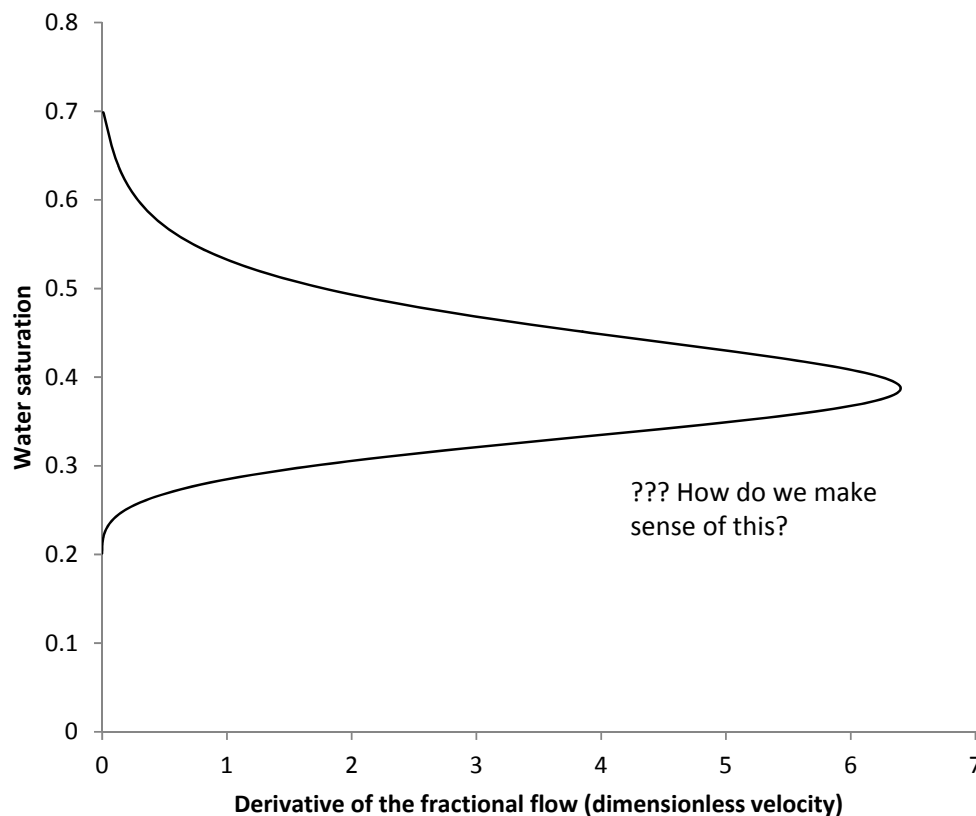
Let's look at the example fractional flow shown previously: since  $v_D = df_w/dS_w$  we find the derivative which resembles the curve shown below.



**A schematic of the derivative of the fractional flow. Note that the derivative – indicating dimensionless wavespeed – has a maximum at intermediate water saturation.**

Re-arranging the plot, to find water saturation as a function of speed (which – at a fixed time – would represent water saturation as a function of distance) we arrive at something that does not make sense – we have multiple solutions, as shown in the plot below.

The solution to this conundrum is to introduce the concept of a shock, or a discontinuity in saturation that moves with a distinct speed: it is not possible to construct a solution where the saturation varies smoothly with dimensionless speed (or distance).

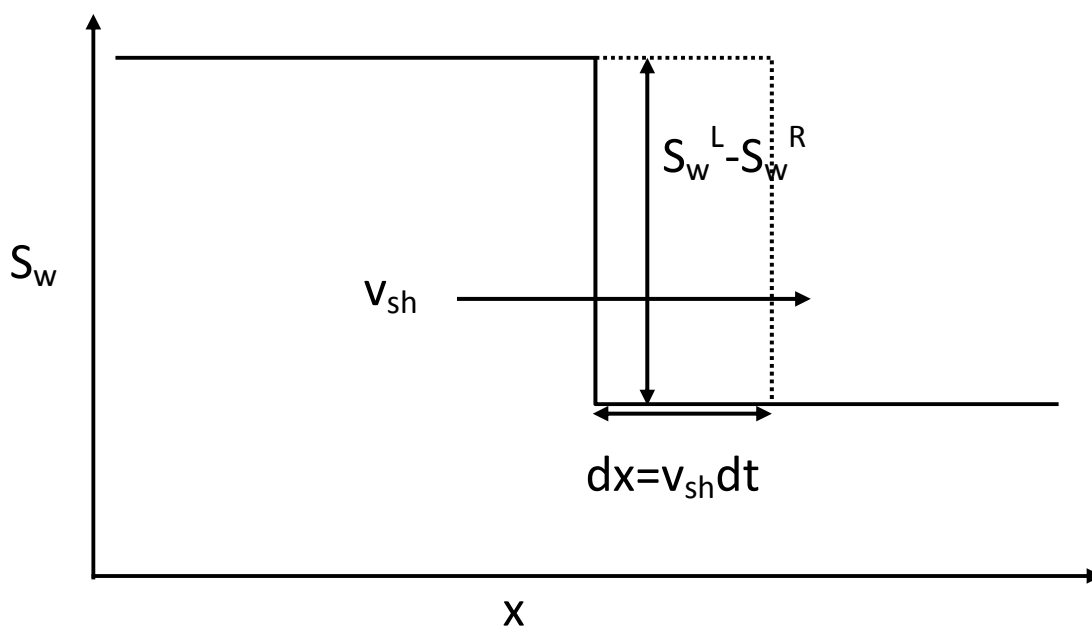


**A schematic of the saturation as a function of dimensionless wavespeed ( $v_D$ ). This appears to give two values of saturation for a given speed (or, if we consider some fixed time, for a given distance between the wells). This does not make physical sense. What happens in reality is that a shock, or discontinuity in saturation, builds up, as described next.**

## 16.2 SHOCKS

Shocks are discontinuities in saturation, which means that we can't use a differential equation to describe them. Shocks are encountered in other physical situations, such as a bomb blast, the flash of light after a nuclear explosion, or traffic jams.

Consider the situation overleaf with a shock between two saturations – a left state and a right state.



**A diagram illustrating conservation of volume across a shock front. A left state of saturation is displacing a right state at a characteristic speed  $v_{sh}$ .**

Imagine a shock moving at speed  $v_{sh}$ , as shown above. Similar to our derivation of the conservation equation consider the change in mass as the shock moves in a time  $dt$ . Just as before, when deriving a differential equation, the flux in – flux out = rate of change of mass:

$$\rho_w q_t (f_w^L - f_w^R) = \rho_w v_{sh} \phi (S_w^L - S_w^R) \quad (16.18)$$

$$v_{sh} = \frac{q_t (f_w^L - f_w^R)}{\phi (S_w^L - S_w^R)} = \frac{q_t \Delta f_w}{\phi \Delta S_w} \quad (16.19)$$

again assuming incompressible flow (constant density and porosity). In dimensionless form:

$$v_{shD} = \frac{\Delta f_w}{\Delta S_w} \quad (16.20)$$

This is the difference form of the governing equation for speed. Notice that if there is no shock, but a smooth change in wavespeed, the speed reduces to Eq. (16.17). Indeed, this is a more elegant and rapid derivation to find the wavespeed than the cumbersome derivation of a partial differential equation for volume conservation. In the next section I show how to find the correct shock and its speed using a graphical construction.

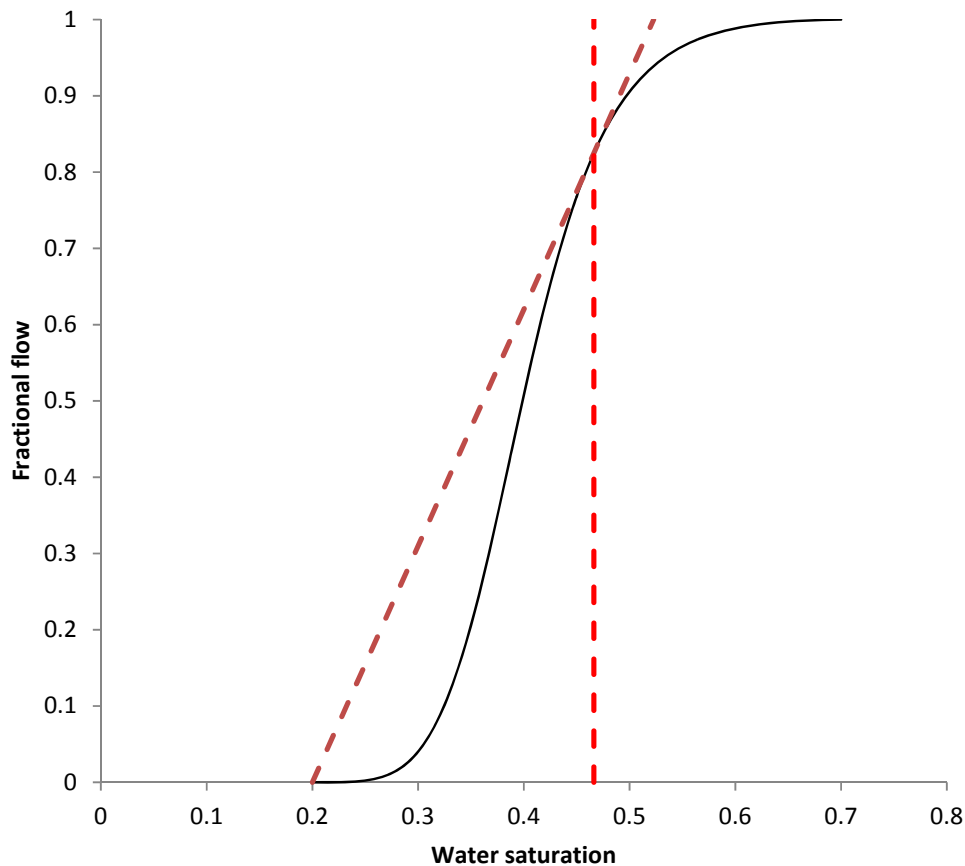
### 16.3 WELGE CONSTRUCTION

---

The solution for saturation must represent a monotonic decrease in water saturation from 1-Sor ( $f_w=1$ ) for  $v_D=0$  to  $S_{wc}$  ( $f_w=0$ ) for large  $v_D$  (large distance for a given time). The solution can be a constant saturation, a smooth variation (called a rarefaction) obeying Eq. (16.13) or a shock which obeys Eq. (16.20). Mathematically there are many ways to do this, but only one that makes physical sense – that is, a solution which is the correct physical limit when capillary pressure (which smooths out the shock) becomes small. It is possible to find this physically correct solution graphically, as shown in the figure overleaf. This is the Welge construction: a line is drawn from the initial condition ( $S_w=S_{wc}$ ;  $f_w=0$ ) which is tangent to the fractional flow curve. The shock is from the initial condition (this is the right state of the shock) to the saturation (and fractional flow) where the line hits the fractional flow curve (the left state). The slope of the line is the change in fractional flow divided by the change in saturation, and so represents the dimensionless shock speed. Mathematically this can be written as:

$$v_{shD} = \left. \frac{\partial f_w}{\partial S_w} \right|_{S_w^L} = \frac{\Delta f_w}{\Delta S_w} \quad (16.21)$$

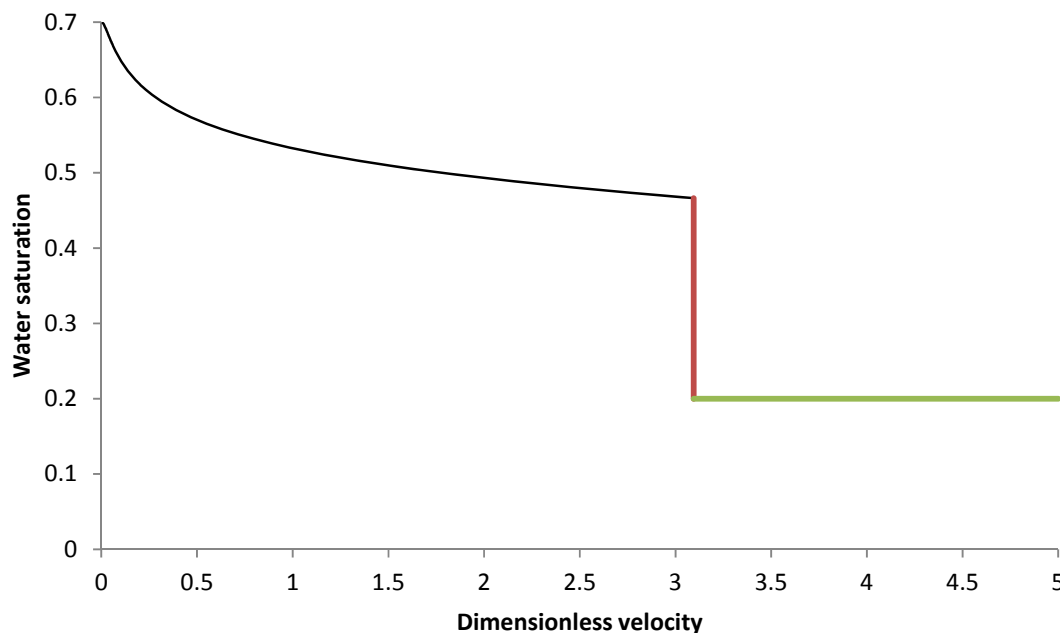




**A diagram illustrating the Welge construction to find the correct shock for the Buckley-Leverett solution. The dotted purple line is tangent from the initial conditions to the fractional flow curve. Where the dotted line hits the fractional flow curve represents the left state of the shock (the saturation indicated by the red dotted vertical line). The slope of the tangent is the dimensionless shock speed.**

The solution for water saturation as a function of dimensionless speed is then as shown schematically above for our example case. The smooth part of the profile – the rarefaction – is found by computing the slope of the fractional flow curves for saturations higher than the shock front, as a function of saturation. This can be done analytically (from a closed-form expression of the fractional flow) or – with care – graphically.

## Buckley-Leverett solution



The Buckley-Leverett solution, featuring constant states (saturation constant – the green line), a rarefaction (black curve) where the saturation varies smoothly with velocity and a shock (red vertical line), constructed as explained in the previous figure.

The solution shown in the figure above, obeys conservation of volume and the boundary conditions. Other possible shocks either give unphysical solutions (multiple values of saturation for a given speed) or are unstable physically. The correct shock is self-sharpening. To explain this, consider the real situation where there is some capillary pressure. The capillary pressure has a diffusive effect and tends to smear out the shock. At the leading edge – small saturations – the wavespeed is slower than the shock speed, so this saturation is caught up by the saturation behind it. To the left side of the shock, any smearing appears to slow down the saturation. But here, the natural wavespeed will be higher than the shock speed and so this water will speed up. The net result is a shock which is stable against perturbations due to capillary pressure. Any other possible shock (and to avoid confusion I will not present them here) lead to a shock that will decompose and rearrange as the stable shock we have just described.

This solution is called the Buckley-Leverett solutions after the authors who first presented it; the conservation equation (15.13) and its variants are often called the Buckley-Leverett equation.

## 16.4 WAVE, PARTICLE SPEEDS AND DEFINITIONS

---

Remember that the wave speed IS NOT the same as the particle (tracer) velocity:

$$v_{pD} = \frac{f_w}{S_w} \quad (16.21)$$

The particle speed is the speed with which a single molecule of water moves through the pore space. This can be explained simply by considering conservation of volume in a system where the saturation is constant (or over a length where the change in saturation is small). Imagine that, say, blue water is injected to displace red water. Then if we inject a volume  $q_w = f_w q_t$  per unit area per unit time, this blue water will fill a volume  $f_w q_t / (\phi S_w)$  of the porous medium – in dimensionless form this is the speed given by Eq. (16.21).

This is distinct from the wavespeed. This is the speed with which a given saturation moves, not a single particle. Why is this different? One way to consider this is through analogy with traffic flow. Travelling in a car on a motorway, you are always moving forwards, or stationary. But now imagine yourself in a helicopter flying above the motorway (and, for a more graphic illustration this is the M25 during the rush hour, so there are many traffic jams). You can see waves of traffic density – this is analogous to saturation. If there is an accident, for instance, the cars at the crash site are stationary – the particle speed is zero. However, a wave of stationary cars moves *backwards* up the motorway: the wavespeed associated with a dense packing of (unmoving) cars is negative.<sup>8</sup> So, here, the wavespeed for saturation is a speed that a particular value of saturation moves, but this is not the same as the speed of a particular water molecule (the particle speed).

---

<sup>8</sup> This is why driving when there is an accident (particularly in poor visibility) is so dangerous. You might think that you have sufficient time (and space) to stop before the car in front comes to a halt, but in reality a wave of stationary traffic is moving *towards* you – this is less safe than there being a brick wall just out of sight.

Now we briefly present some definitions useful for understanding the terminology used to describe these solutions. A **spreading wave or rarefaction** is when the wave becomes more diffuse with time – smooth changes in saturation.

A **sharpening wave** is when the wave becomes less diffuse and sharpens to form a shock.

**Indifferent** is the case when the wave neither spreads nor sharpens.

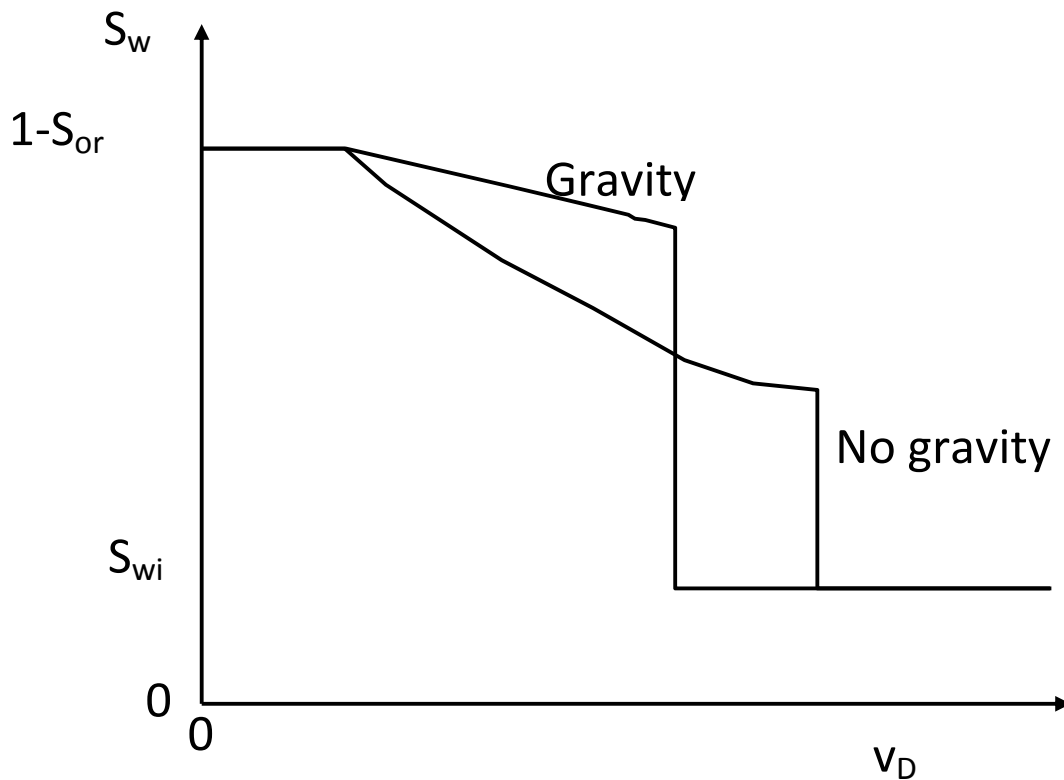
A **constant state** is a fixed saturation with distance (or velocity). This is also an acceptable solution to the equations.

## 16.5 EFFECT OF GRAVITY

---

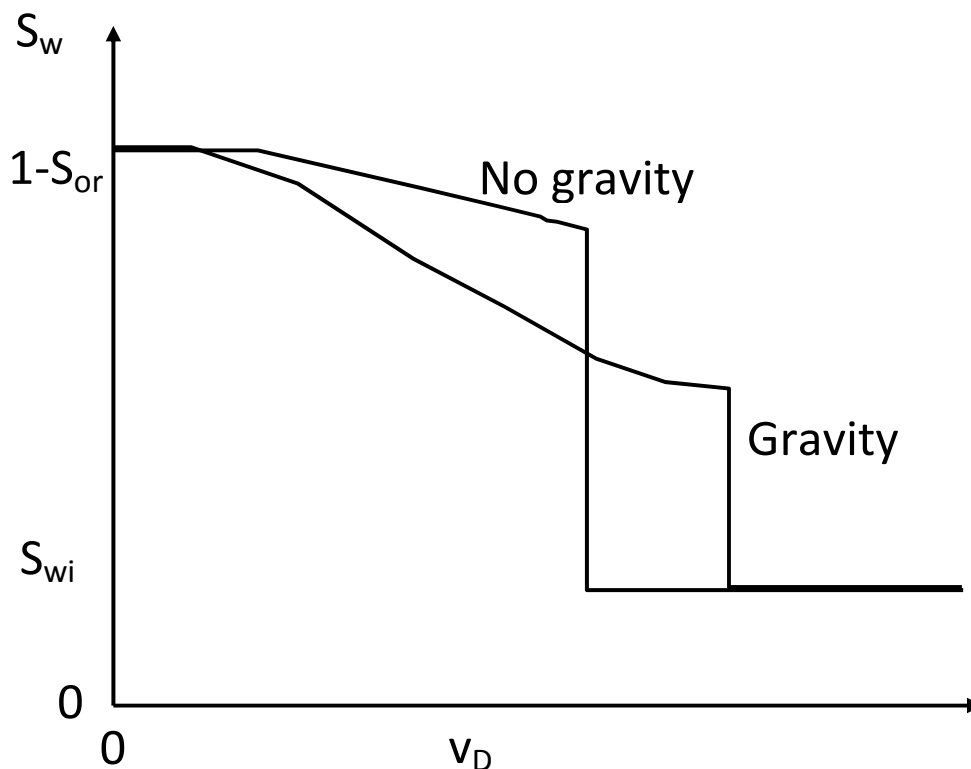
We can also consider the impact of gravity on our analytical solutions, as shown below with some schematic curves. If the water flow is uphill, then the water flow is held back, resulting in a higher shock saturation moving more slowly than a corresponding case with no gravity. Even if the fractional flow becomes negative, the shock jumps across this region and so we do not see explicit counter-current flow for water injected at the bottom of the formation.

Note that it is possible that the wavespeed at  $1-S_{or}$  is not zero (as in the previous examples) but finite – this is the derivative of the fractional flow at  $S_w=1-S_{or}$ . In this case we have a constant state from  $v_D=0$ , to the computed value. As mentioned previously, this is a perfectly acceptable solution of the conservation equation.



**The Buckley-Leverett solution showing the effect of gravity for water flowing uphill: buoyancy here leads to a higher slower-moving water shock.**

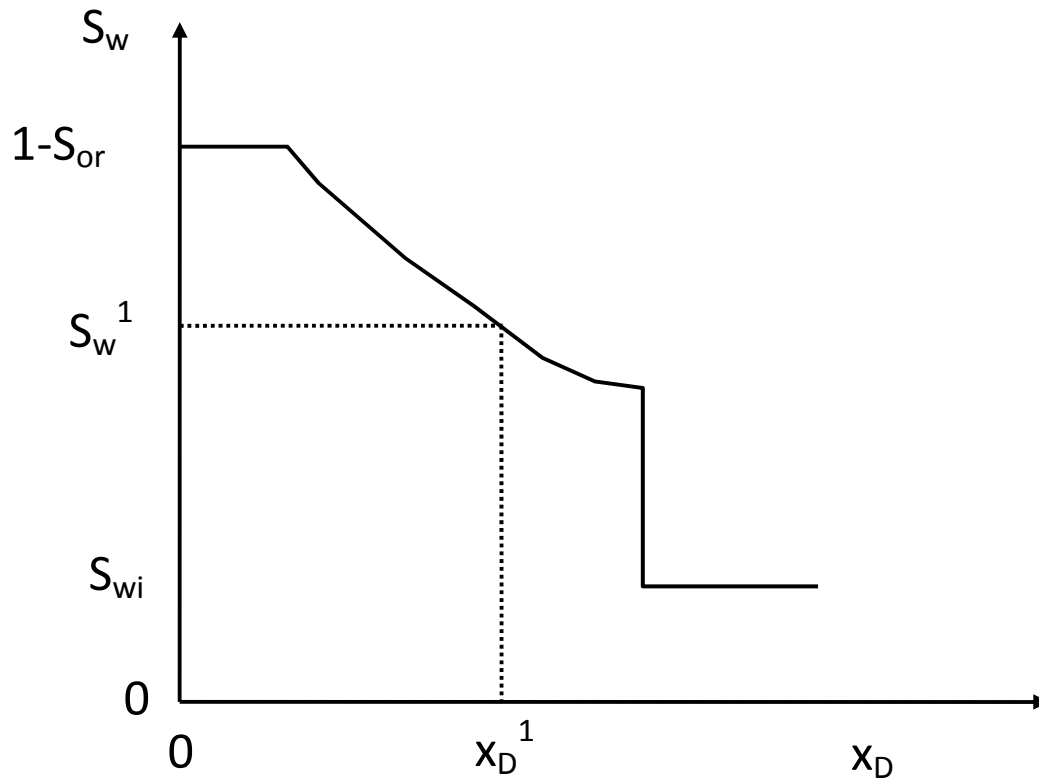
If we flow downhill, then water moves faster and we see a faster-moving, shallower water shock. If the water fractional flow at  $v_D=0$  is 1, then again we cannot observe strictly counter-current flow. However, it is possible to construct solutions where we have a backwards moving shown or rarefaction, representing the portion of the fractional flow curve which is greater than 1.



**The Buckley-Leverett solution showing the effect of gravity for water flowing downhill: buoyancy in this case leads to a lower faster-moving water shock.**

## 16.6 AVERAGE SATURATION AND RECOVERY

The final stage in the analysis is to use the analytical solution for saturation as a function of speed (and hence, for a given time, as a function of distance) to compute recovery. In our previous discussions we have always discussed how recovery is a function of how much water is injected (the pore volumes of water injected). The way to derive a recovery calculation is first to consider the average saturation. The recovery is proportional to the change from the initial (usually connate) water saturation to this average value. Specifically, the average saturation in a domain after breakthrough – that is where the shock front has already reached the production well. Consider the schematic saturation profile shown on the next page.



The Buckley-Leverett solution as a function of dimensionless distance employed to compute the average saturation and hence recovery.  $x_D^1$  represents the production well ( $x_D=1$ ) and we compute the average saturation between this and the injector at  $x_D=0$ .

The average saturation behind  $x_D^1$  is easy to define, but the mathematics is somewhat tedious to produce a tractable solution:

$$\bar{S}_w(t_D) = \frac{1}{x_D^1} \int_0^{x_D^1} S_w dx_D \quad (16.22)$$

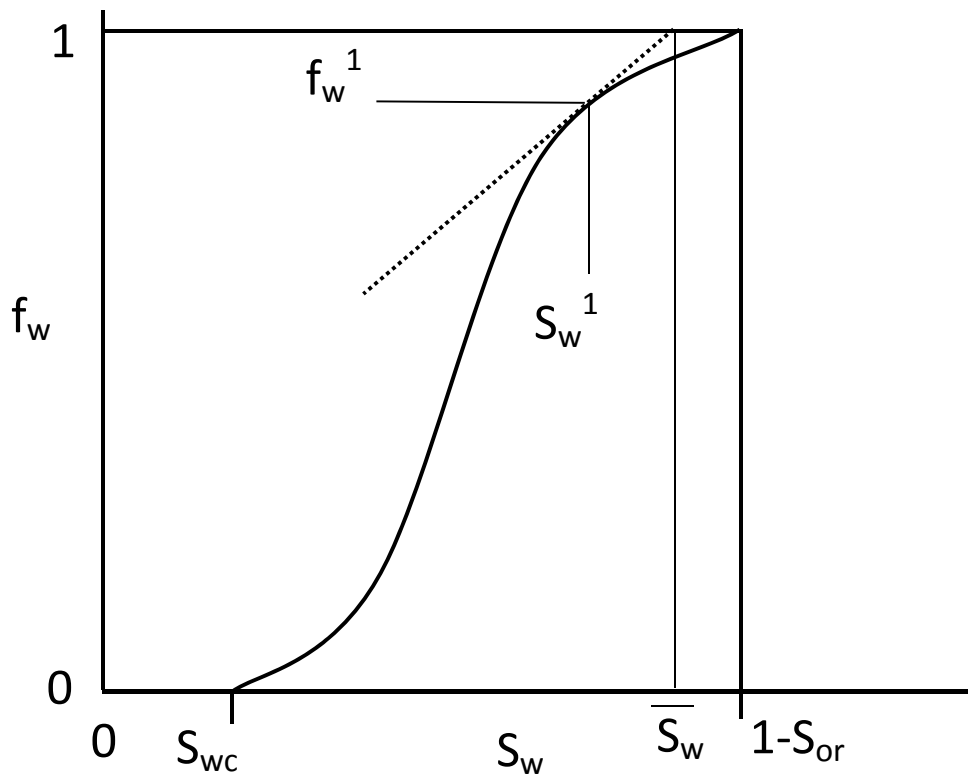
Integrate by parts:

$$\bar{S}_w(t_D) = \frac{1}{x_D^1} \left( [x_D S_w]_0^{x_D^1} - \int_{1-S_{or}}^{S_w^1} x_D dS_w \right) \quad (16.23)$$

We can write  $x_D^1 = \frac{df_w}{dS_w} \Big|_{S_w=S_w^1} t_D$ , and thus Eq. (16.23) becomes:

$$\bar{S}_w(t_D) = S_w^1 - \frac{t_D}{x_D^1} \int_{1-S_{or}}^{S_w^1} \frac{df_w}{dS_w} dS_w = S_w^1 - \frac{t_D}{x_D^1} \int_1^{f_w^1} df_w = S_w^1 + \frac{t_D}{x_D^1} (1 - f_w^1) = S_w^1 + \frac{1 - f_w^1}{f_w^{1'}} \quad (16.24)$$

Notice the prime on the final equation, denoting the derivative. Graphically this can be represented as the extension of the tangent of the curve at some location on the rarefaction to  $f_w=1$  gives the average saturation behind the front. This construction is shown schematically below. From a practical perspective, choose any saturation above the shock-front value, draw a tangent and find the saturation value when this tangent reaches  $f_w=1$ .



**A schematic of the construction used to find the average saturation when the saturation at the well ( $x_D=1$ ) is some arbitrary value  $S_w^1$ .**

We now use this construction to compute the recovery – pore volumes of oil produced – as a function of time, or pore volumes of water injected:  $N_{pD}$  vs.  $t_D$ . We know that by definition, the average saturation =  $S_{wi} + N_{pD}$ , where  $N_{pD}$  are the pore volumes of oil produced.



Before breakthrough, the reservoir volume of oil produced is equal to the reservoir volume of water injected and so  $N_{pD}=t_D$ . Breakthrough occurs when the shock moving at dimensionless speed  $v_{shD}$  reaches  $x_D=1$ : this is a dimensionless time  $t_D=1/v_{shD}$ . So, the first step in constructing a recovery curve is to draw a straight line of unit slope from  $N_{pD}=t_D=0$  to  $N_{pD}=t_D=1/v_{shD}$ .

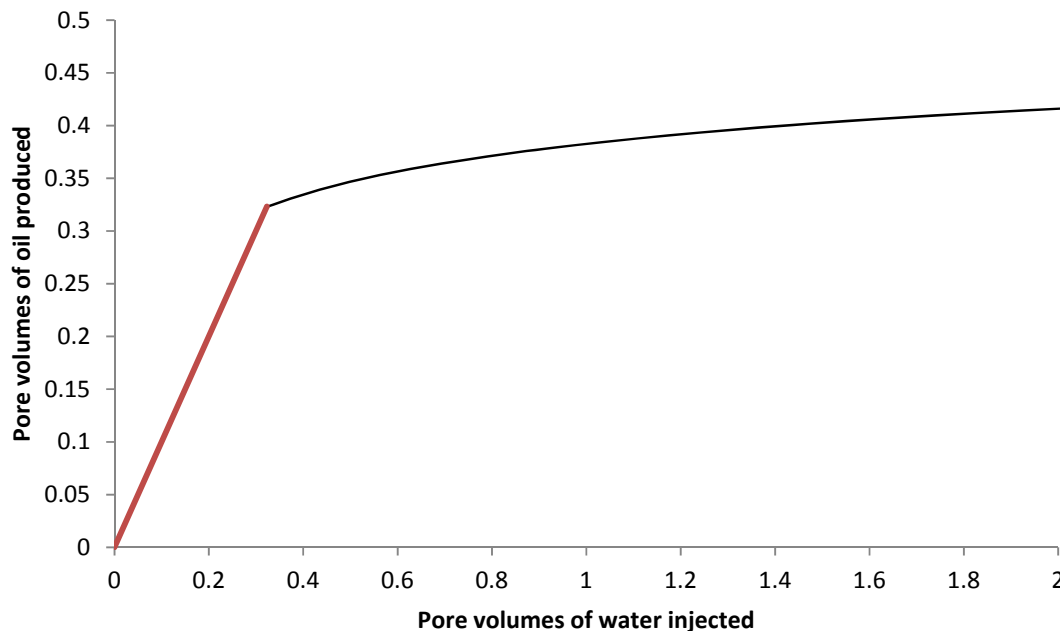
After breakthrough, the recovery curve has a slope less than one, indicating the production of both oil and water. What is the maximum recovery? This is  $1-S_{or}-S_{wc}$ : you cannot produce more oil than this. When will this occur? If the wavespeed for  $S_w=1-S_{or}$  is zero, this happens at infinite time, so the maximum recovery is met asymptotically at infinite time. If the wavespeed has a finite minimum values, say  $v_{Dmin}$ , then maximum recovery is met at a time  $1/v_{Dmin}$ . Now construct one or two points in between. Choose a value of saturation in the rarefaction. Find the tangent through this saturation value on the fractional flow curve. The slope of the tangent is the wavespeed,  $v_D$ , while the intersect when  $f_w=1$  is the average saturation. The recovery is the average saturation minus the initial value, while the dimensionless time  $t_D=1/v_D$ .

The resultant plot for our example case is shown in the figure below. In words, the procedure does seem a little bewildering – the only way to learn this is through performing the exercise yourself.

To recap, the steps to do a complete Buckley-Leverett analysis are as follows.

1. Given relative permeability curves, you first compute the fractional flow and plot this as a function of saturation.
2. Perform the Welge construction to find the shock front saturation and shock speed.
4. Plot the saturation as a function of dimensionless velocity: in the rarefaction the speed is the slope of the fractional flow curve.
5. Compute the dimensionless recovery (pore volumes produced) as a function of dimensionless time (pore volumes injected). Before breakthrough, since we have assumed that the oil and water are incompressible, these two quantities are the same. After breakthrough of water (when the shock front reaches the production well), the pore volumes of oil produced are less than the pore volumes of water injected, since some water is produced as well. You find the recovery from choosing points in the rarefaction and extrapolating a tangent on the fractional flow curve to  $f_w=1$ , as described above.

## Dimensionless recovery



Pore volumes produced as a function of pore volumes of water injected for our example case. The red line has unit slope and occurs before breakthrough. After breakthrough the black line was constructed using the methodology described in the text. The ultimate recovery is 0.5, but this is only reached asymptotically once an infinite number of pore volumes are produced. Rarely is more than pore volume injected in a reservoir waterflood and so there is no point showing recovery beyond, say, 2 pore volumes, as here.

This is an important exercise, and is performed by any reservoir engineer to assess waterflood recovery. In the end the behaviour at the field scale is determined by both this analysis and the geology of the field, which defines the preferential flow paths for the injected water, and the placement of the wells – an assessment of this usually requires reservoir simulation methods and lies outside the scope of the course.

We will now discuss different types of behaviour physically and the implications for recovery. Note though, that this rigorous analysis can substitute for the rather empirical approach used previously and should be used to assess recovery when both the relative permeabilities and viscosities are known. There are generically three types of solution.

1. **Classic Buckley-Leverett.** This is the case we have shown with a rarefaction and a shock. This is observed for most power-law relative permeabilities and reproduces the behaviour of most weakly water-wet or mixed-wet systems. Note though that the minimum wavespeed is not necessarily zero (as in our example) and so the rarefaction may be preceded by a constant state.
2. **All shock.** For strongly water-wet media, or if the water mobility is extremely low (say polymer flooding) the shock may extend all the way to  $1-S_{or}$ : indeed it is not possible to construct a tangent and the fractional flow curve is entirely concave. This is the simplest solution with a shock moving with speed  $1/(1-S_{or}-S_{wc})$  and a recovery that reaches its maximum at breakthrough. Physically this is why waterflooding a water-wet system is favourable (apart from the high residual saturation) since the water is held back in the pore space, and the oil moves ahead, leading to a sharp front.
3. **No shock.** It is possible, for oil-wet systems and/or with a very unfavourable viscosity ratio (the oil is much more viscous than the water), for there to be no shock, in that the maximum wavespeed  $v_{Dmax}$  occurs for  $S_w=S_{wc}$ . In this case the fractional flow is convex and the solution only a rarefaction. Breakthrough occurs at a dimensionless time  $1/v_{Dmax}$ .

The last point to note that a Buckley-Leverett style analysis is not confined to a one-dimensional analytical analysis: it is also useful to compare field-scale recovery (either real data or simulation predictions) to Buckley-Leverett predictions. It is straightforward (with a very careful scrutiny of the definitions) to convert data for oil produced at surface conditions into pore volumes produced, and real time into pore volumes of water injected. Since the real reservoir is heterogeneous, the recovery will always lie below that from an idealized Buckley-Leverett analysis, but does serve as a very useful basis of comparison. This is also helpful in field management: the closer the predicted (or real) recovery to Buckley-Leverett, the better the injection wells are contacting and sweeping the reservoir. It also serves as a guide to how much water needs to be injected to achieve optimal recovery.

## 16.7 OIL RECOVERY AND THE IMPACT OF WETTABILITY

---

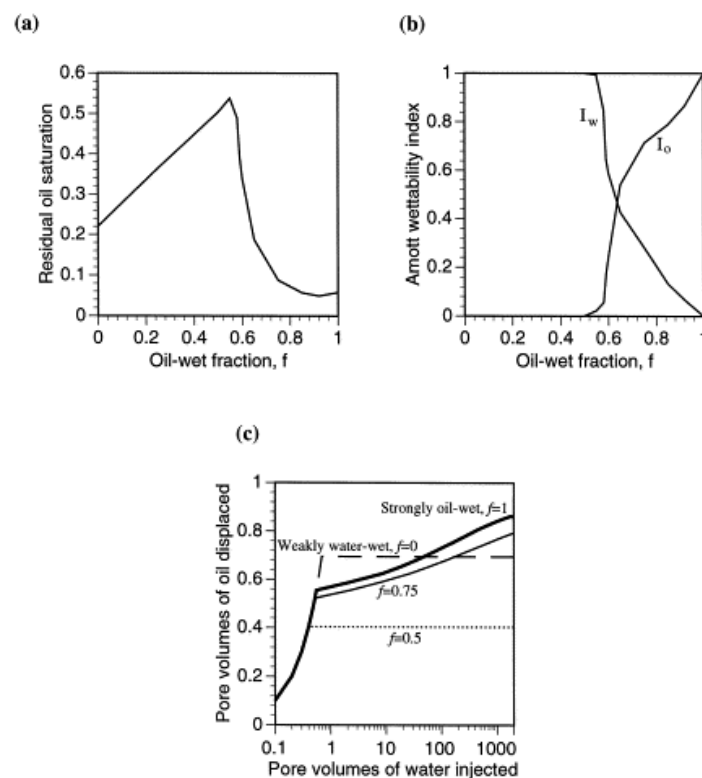
We can now return to our previous analysis of relative permeability and use these curves to compute recovery for a linear displacement. It is important to emphasize that in most field cases we rarely inject more than one pore volume of water. Hence, the fact that very low oil saturations can be achieved by oil layer drainage when hundreds or thousands of pore volumes are injected is not economically relevant, even if it can be seen in laboratory experiments. Of much greater import is the shock front saturation: this generally determines the local efficiency of waterflooding, which a high shock front being most favourable.

In general, strongly water-wet samples give a Buckley-Leverett displacement that is all shock, with the maximum recovery reached at breakthrough. This is efficient, but the high residual saturation makes the process less than ideal. Strongly oil-wet systems also give poor recovery – often even poorer recovery – since the oil breaks through very early and there is only substantial production after breakthrough, where water is also produced. This is economically unfavourable. The best recovery is for wettability states in between: mixed-wet or weakly water-wet rocks. One of the new research areas at the moment is in how to control wettability through adjusting the chemistry of the injected brine. This is the idea behind low salinity waterflooding that aims to adjust the rock wettability to a favourable near water-wet state.

The reality is that for any given system, a careful assessment of relative permeability is warranted. First I show below some results from Blunt (1998) from pore-scale network modelling. Here the relative permeabilities are computed for different fractions of oil-wet pores, the fractional flow curves determined and from this recovery as a function of pore volumes injected is found. This is exactly the exercise – bar finding the relative permeabilities in the first place – that I will expect you to be able to do by hand, and which has been described above.

Note in this case the trend of residual oil saturation with wettability, showing the lowest residual – thanks to layer drainage – for the most oil-wet case. The wettability indices for oil and water are shown, indicating mixed-wet behaviour. For around 1 pore volume of water injected, it is not the oil-wet case, but the weakly water-wet system (with no oil-wet pores), that gives the best recovery. Adding some oil-wet pores reduces recovery, since these pores are

trapped during waterflooding and do not themselves connect through the system, meaning that layer drainage cannot allow low residual saturations to be reached. It is only for higher oil-wet fractions, when these pores connect across the system, that low residual saturations are seen. The completely oil-wet case only gives the highest recovery after the injection of around 100 pore volumes of water – something that never practically occurs in a field setting.



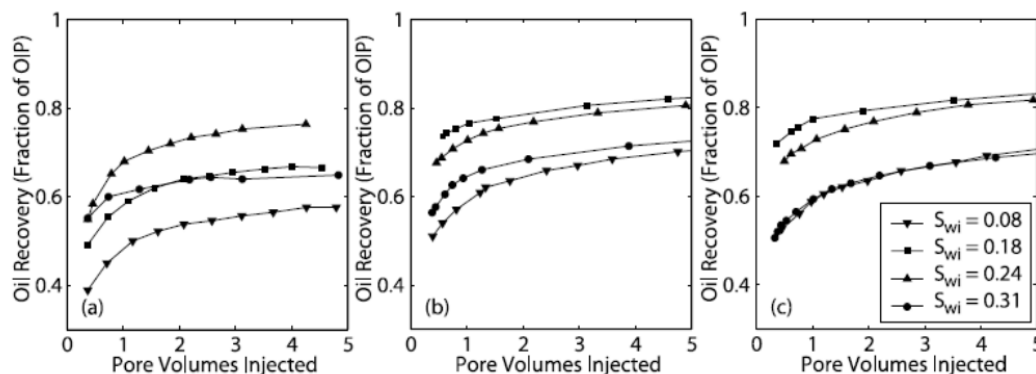
**Residual oil saturation, wettability indices and oil recovery from network modelling of a mixed-wet system, with a fraction  $f$  of oil-wet pores indicated. Taken from Blunt (1998).**

I will now illustrate the remarks above with some experimental data on sandstones. Note, however, that for the carbonates discussed earlier, the most favourable conditions for waterflooding were more mixed-to-oil-wet than shown here.

The example I choose uses the computations of relative permeability for mixed-wet Berea sandstone made by Valvatne and Blunt (2004). In this work, a fixed fraction of the pores contacted by oil after primary drainage became oil-wet. Different initial saturations of water (that is saturations after primary drainage) were considered: if the initial water saturation is

high, the system appears to be more water-wet, as the pores that remain full of water remain water-wet. As the initial saturation decreases, the system becomes more oil-wet. This is the trend with height that is observed in the transition zone of an oil reservoir.

The graphs below show measured recovery profiles for waterflooding from Jadhunandan and Morrow (1995) – with different initial water saturations – compared to different predictions using pore-scale modelling. For this sandstone sample, we see unfavourable recovery for the most water-wet case (because of the high residual saturation) and for the most oil-wet case (because of the slow drainage of oil layers). The ideal cases have an intermediate initial water saturation and are overall weakly water-wet to mixed-wet in character, meaning that the Amott-Harvey wettability index is close to zero.



**Measured (left) and predicted (middle and right) oil recoveries as a function of pore volumes injected in a mixed-wet Berea sandstone. The different initial water saturations are indicated. Note that the most favourable recoveries occur for intermediate saturations. The two modelling predictions use slightly different assignments of wettability.**

This behaviour, as alluded to previously, is different from the trend we expect in carbonates, where the most favourable recoveries are seen when most of the pores are oil-wet: the difference is a result of the connectivity of the pore space, the nature of the pore and throat size distributions and the local variations in wettability (contact angle). Carbonates display a very wide range of connectivity and pore sizes, and can have very low recoveries in the water-wet limit; however, a definitive characterization requires detailed analysis of the sample of interest coupled with an accurate assessment of wettability. At present, we do not have a way to assign contact angle on a pore-by-pore basis unambiguously, and so, at present, we have to rely on

macroscopic measurements of wettability (such as Amott index) to tune the contact angle distribution in our pore-scale models.

One last comment: the pore volumes produced is NOT the recovery factor shown in the graphs above. The recovery factor,  $R_F$ , is a ratio of the volume of oil produced to the total of oil initially in place. It is easy to relate these two quantities as follows:

$$R_F = N_{PD} \frac{B_{oi}}{B_o(1 - S_{wc})} \quad (16.25)$$

## 17. ANALYTIC SOLUTIONS FOR SPONTANEOUS IMBIBITION

---

### 17.1 COUNTER-CURRENT IMBIBITION

---

We will now present a solution for spontaneous imbibition, where displacement is controlled entirely by capillary forces. This is a useful complement to the Buckley-Leverett solution. It is valuable experimentally as a way to determine, or at least constrain, capillary pressure and relative permeability. It is also useful for the analysis of recovery in fractured reservoirs, discussed previously.

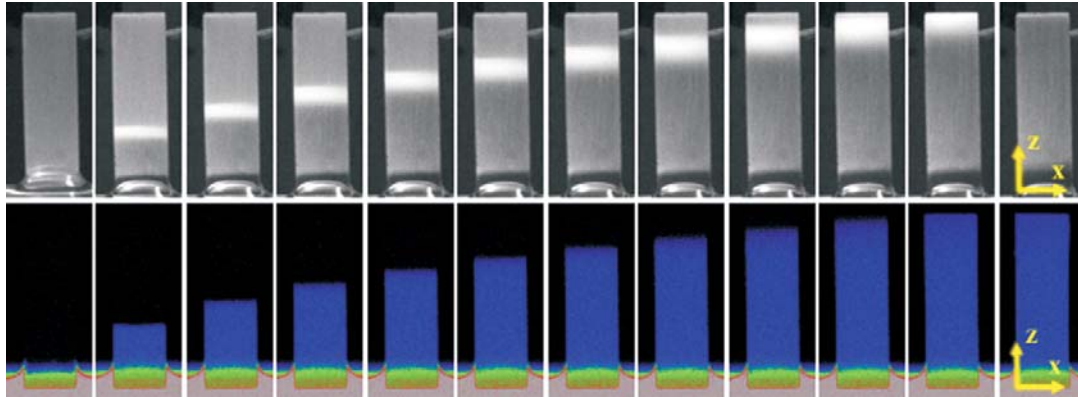
The formulation here is quite new in the literature. While the solutions were first proposed by McWhorter and Sunada (1990), it was not until the work of Schmid and Geiger (2012) that it was appreciated that this was indeed a closed-form solution.

Before wading into the mathematical details, let us review the physical situation. It is illustrated below, where bubbles of non-wetting phase escape from a core when the wetting phase imbibes from all sides.



**Photograph illustrating imbibition in a rock core – the bubbles are the displaced non-wetting phase.**





**Experimental measurements of imbibition.** Here the set-up is similar to that proposed mathematically – except that we ignore gravity: there is a reservoir of fluid at one end of the core and water imbibes. This is co-current imbibition. In the text we consider a slightly simpler case where the total velocity is zero, which means that the non-wetting phase must escape through the inlet. This is counter-current imbibition. Both co- and counter-current imbibition can be analysed analytically in one dimension.

For clarity, we start with the conservation Eqs. (15.3) and (15.2) which are written here in terms of the water Darcy velocity (rather than the total velocity, since this will be zero):

$$\phi \frac{\partial S_w}{\partial t} + \frac{\partial q_w}{\partial x} = 0 \quad (17.1)$$

$$q_w = \frac{\lambda_w}{\lambda_t} \left\{ q_t + K \lambda_o \left( \frac{\partial P_c}{\partial x} + (\rho_w - \rho_o) g_x \right) \right\} \quad (17.2)$$

For spontaneous imbibition, we ignore gravitational forces (assume that they are either small compared to capillary forces at the core – cm – scale, or that the displacement is horizontal) and the total velocity. Setting the total velocity  $q_t$  to zero means that no fluid is injected and the flow is counter-current: the movement of water into the porous medium is matched exactly by the volume of oil (or gas) that leaves. Then we write:

$$q_w = \frac{K \lambda_w \lambda_o}{\lambda_t} \frac{\partial P_c}{\partial x} \quad (17.3)$$

The conservation equation (17.1) becomes:

$$\phi \frac{\partial S_w}{\partial t} + \frac{\partial}{\partial x} \left( \frac{K \lambda_w \lambda_o}{\lambda_t} \frac{\partial P_c}{\partial S_w} \frac{\partial S_w}{\partial x} \right) = 0 \quad (17.4)$$

Assuming a constant porosity we can write Eq. (17.4) as a non-linear diffusion equation:

$$\frac{\partial S_w}{\partial t} = \frac{\partial}{\partial x} \left( D(S_w) \frac{\partial S_w}{\partial x} \right) \quad (17.5)$$

where the non-linear capillary diffusion coefficient is:

$$D(S_w) = - \frac{K \lambda_w \lambda_o}{\phi \lambda_t} \frac{\partial P_c}{\partial S_w} \quad (17.6)$$

Note the negative sign.  $D$  is positive, so we assert that the gradient of the capillary pressure as a function of water saturation is always negative. You should now appreciate that this is indeed correct.

The boundary conditions are a porous medium containing initially irreducible water ( $S=S_{wc}$ ) and a non-wetting phase (which we call oil for convenience here). At the inlet –  $x=0$ , we maintain a capillary pressure of zero. In a strongly water-wet system, the saturation will be  $1-S_{ori}$ ; in any other case this will simply be the saturation at which the capillary pressure is zero, which we define as  $S^*$ .

We will now try to find a solution as follows. We write

$$\omega = \frac{x}{\sqrt{t}} \quad (17.7)$$

where we assume that the solution can be stated as  $S_w(\omega)$  only. I also will state that we can write:

$$\omega = \frac{dF}{dS_w} \quad (17.8)$$

for some capillary fractional flow  $F(S_w)$ . We assume that  $F$  has a maximum value  $F^*=F(S^*)$  and is zero for the irreducible water saturation:  $F(S_{wc})=0$ .

Note the approach here. I have assumed a certain functional form of the solutions, based – please note – on both the previous solution for diffusion and the Buckley-Leverett analysis. However, this is an educated guess and we have to test if we can solve the governing partial differential equations and the boundary conditions. There is no *a priori* manner to know – before we start – if this approach is correct. Despite what you may be told in mathematics classes, solving partial differential equations is more inspiration (guessing the correct approach) than application (of all the methods you are given in class).

Then we define the following derivatives:

$$\frac{\partial S_w}{\partial t} = -\frac{\omega}{2t} \frac{dS_w}{d\omega} \quad (17.9)$$

$$\frac{\partial S_w}{\partial x} = \frac{1}{\sqrt{t}} \frac{dS_w}{d\omega} \quad (17.10)$$

Then Eq. (17.5) becomes an ordinary differential equation:

$$\omega \frac{dS_w}{d\omega} + 2 \frac{d}{d\omega} \left( D \frac{dS_w}{d\omega} \right) = 0 \quad (17.11)$$

We integrate once:

$$\int \omega dS_w = -2D \frac{dS_w}{d\omega} \quad (17.12)$$

where the integration constant is zero since we define  $F(S_{wc})=0$  and also  $D(S_{wc})=0$ . Then substitute in  $F$  from Eq. (17.8) to find:

$$F \frac{d^2 F}{dS_w^2} = -2D \quad (17.13)$$

Eq. (17.13) is the key equation to define  $F$  and hence construct a solution.

In a formal mathematical sense, the solution can be expressed in closed form simply by integrating Eq. (17.13) twice – this is the solution presented in Schmid and Geiger. The problem – that appears – at first sight – somewhat off-putting is that the solution is expressed in terms of implicit integrals: that is the integral to find  $F$  involves  $F$  itself. Indeed it is presented in terms of two implicit integrals, since we have to define  $F(1-S_{or})$ , noting that  $F$  is a dimensional quantity and so we cannot set it to 1.

Instead here I choose a simpler approach, related simply to the physics of the solution. We have already defined one boundary condition on  $F$ :  $F(S_{wc})=0$ . Since we have a second-order equation for  $F$ , we require two conditions. The second, applicable in most cases, is that for  $S_w=1-S_{or}$ ,  $dF/dS_w=0$  (the saturation front does not move at the inlet, which again makes physical sense).

However, before proceeding, let us first study the implications for the amount of water that enters the porous medium. The water Darcy velocity can be found from Eqs. (17.3) and (17.6):

$$q_w = -\phi D \frac{\partial S_w}{\partial x} \quad (17.14)$$

which from Eq. (17.10) is:

$$q_w = -\frac{\phi D}{\sqrt{t}} \frac{dS_w}{d\omega} \quad (17.15)$$

and substituting in Eq. (17.13):

$$q_w = \frac{\phi F F''}{2\sqrt{t}} \frac{dS_w}{d\omega} = \frac{\phi F}{2\sqrt{t}} \quad (17.16)$$

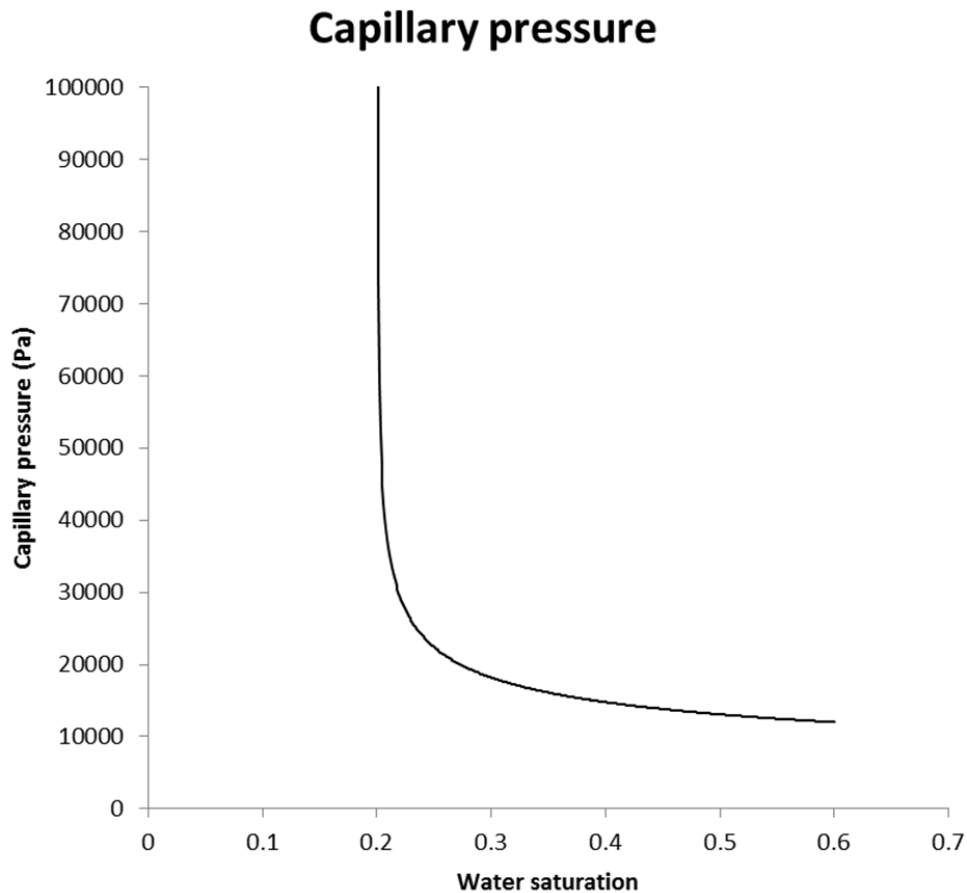
and noting the identity  $F'' = d\omega/dS_w$ .

The inlet flux is then related to the value of  $F^*$ . The total amount of water that enters the system,  $Q_w$  is:

$$Q_w = \int_0^t \frac{\phi F^*}{2\sqrt{t}} dt = \phi F^* \sqrt{t} \quad (17.17)$$

The amount imbibes scales as the square-root of time. Note that this expression differs from the solutions presented previously, where we allowed the flux injected to reach a maximum in a block of finite size: here we consider only the early-time behaviour before the imbibing front has reached a boundary.

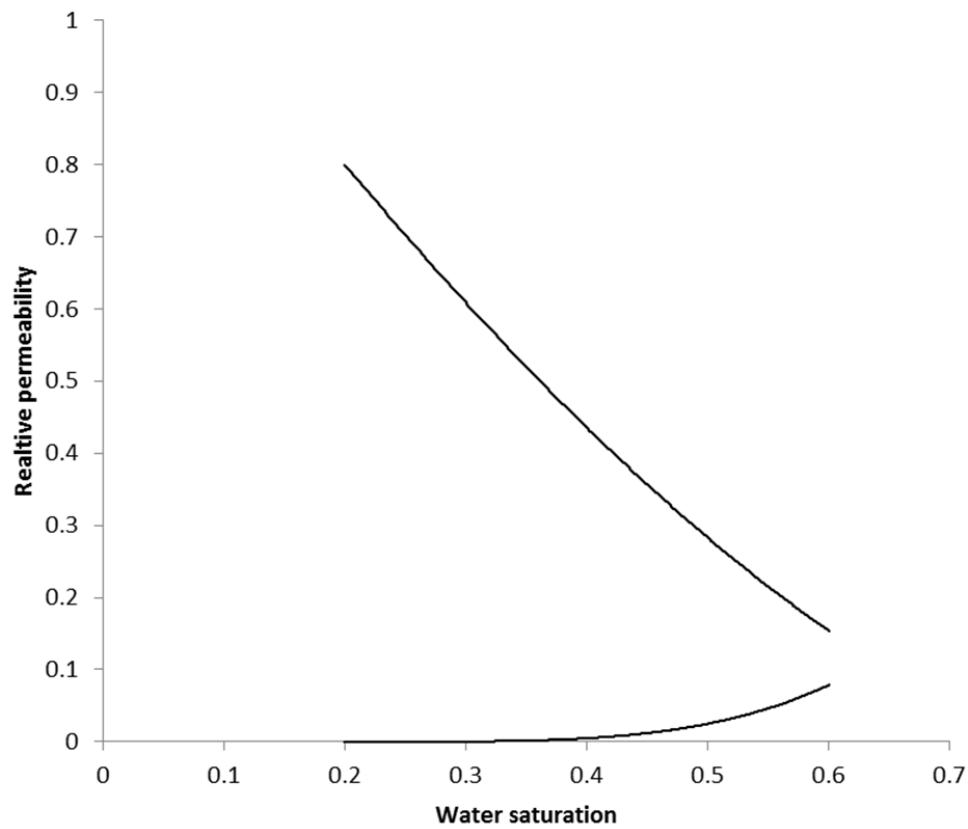
We will find a solution using a simple numerical approach. For given relative permeabilities and capillary pressures, we compute  $D$ . We then solve Eq. (17.13) numerically in a spreadsheet starting from  $S^*$  and then decreasing saturation in small increments. We guess  $F^*$  and impose  $F'(S^*)=0$ . We then iterate to find the value of  $F^*$  such that when  $S_w=S_{wc}$ ,  $F=0$ . I will not go through the details, but it is readily computed using a backwards difference scheme. I will show some example results below. Notice that using a Buckley-Leverett analogy, this is a simple case, since there are no shocks: the saturation profile is smeared out and we have, technically, an all rarefaction solution.



The capillary pressure used in my example calculation for imbibition. This resembles a primary drainage curve, but in fact – as we see below – this is a mixed-wet case. I assume that for saturations beyond  $S^*=0.6$  the capillary pressure is negative.

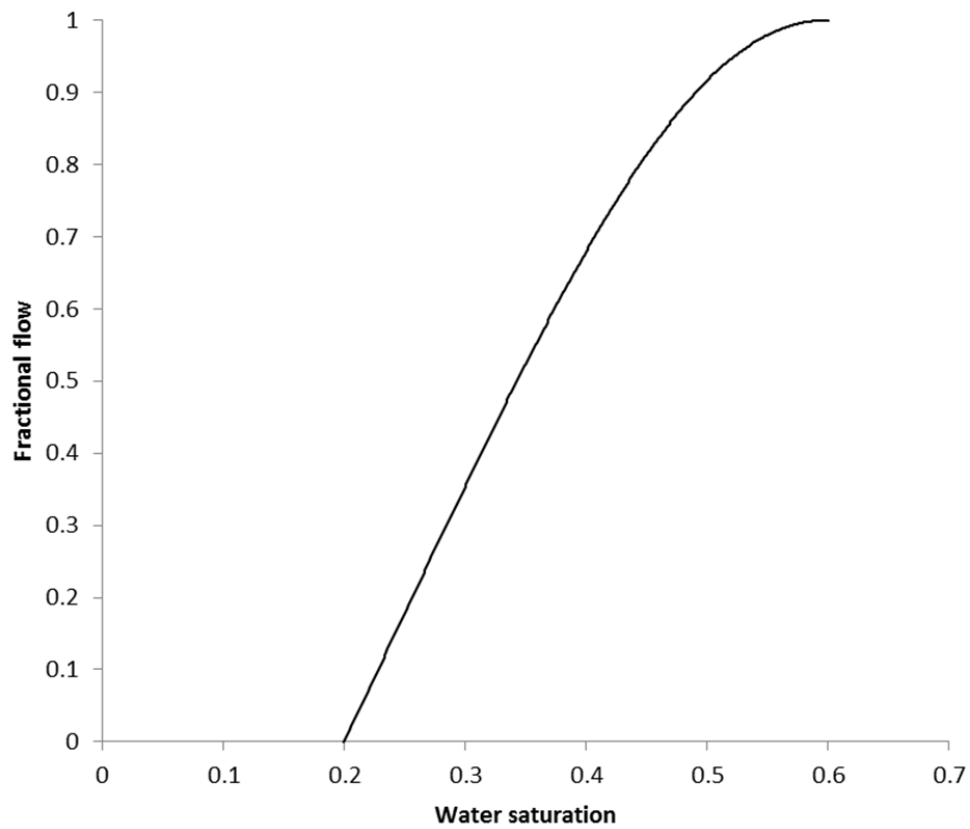
I show the capillary pressure and relative permeabilities in the saturation range for which there is spontaneous imbibition. I then show the dimensionless fractional flow that varies between 0 and 1: this is defined as  $f=F/F^*$ . Similarly I can define dimensionless wavespeeds  $\omega_D=\omega/F^*$ . In the example I show  $F^*=2.284\times 10^{-4}$  m/Vs. I then show the saturation as a function of  $\omega$ : this is the full solution, with the distance moved by the saturation scaling not linearly with time (as for water injection in the Buckley-Leverett analysis) but as the square root of time.

## Relative permeabilities



The relative permeabilities used in my example calculation for imbibition. The values are truncated when the capillary pressure is zero.

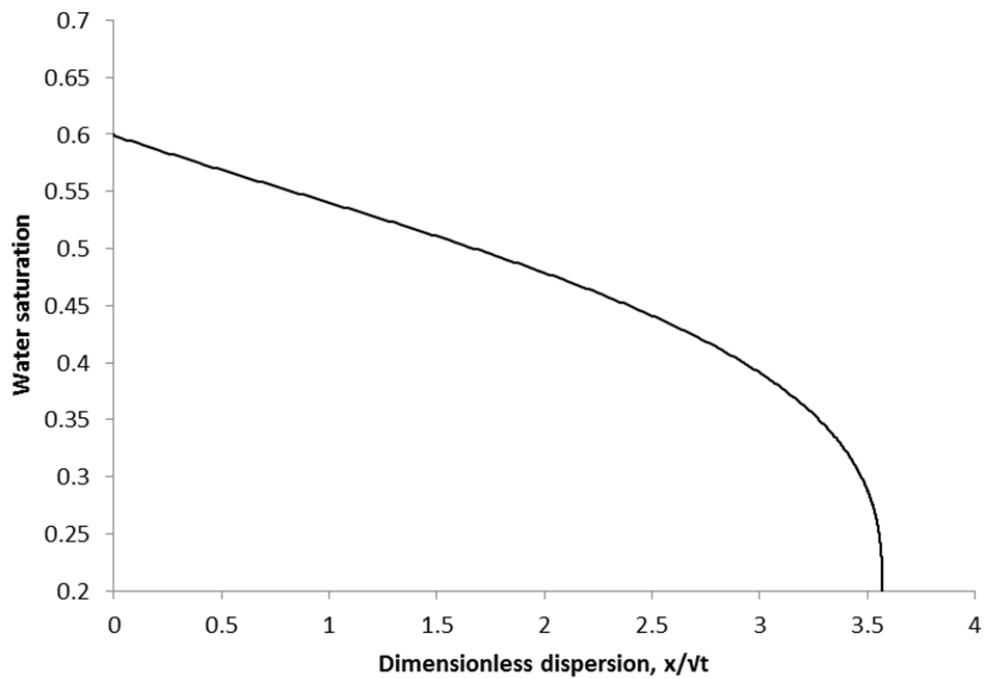
### Dimensionless imbibition fractional flow



The dimensionless capillary fractional flow  $f$ . From the Buckley-Leverett analogy, we can see that the solution is a dispersed profile with no shock front.

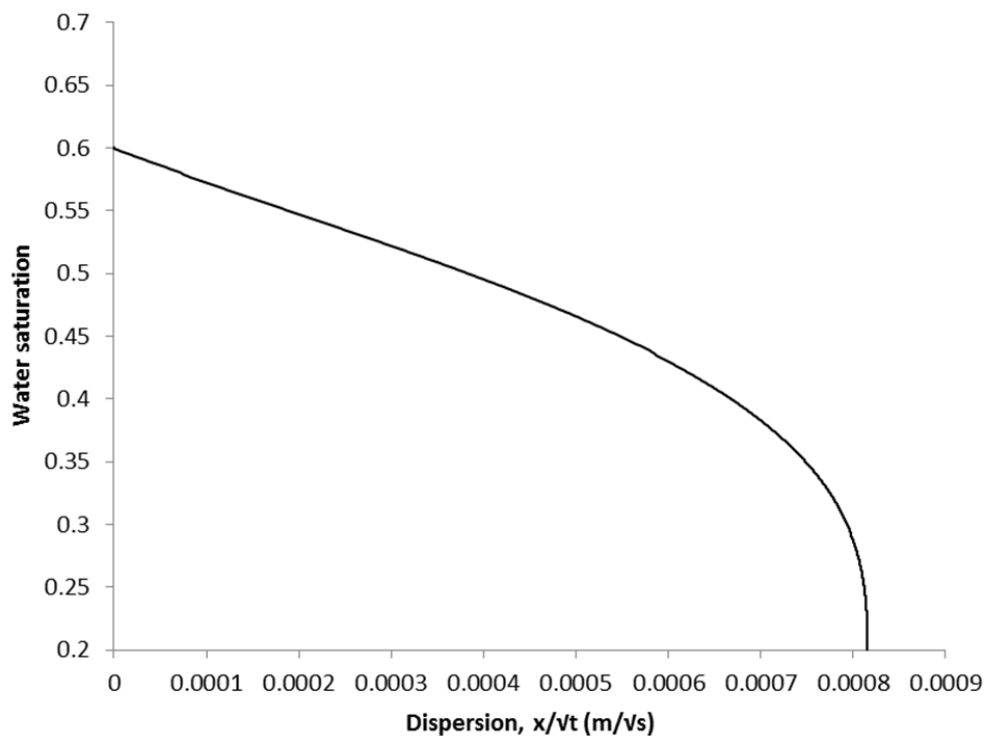


## Saturation as a function of dimensionless dispersion



The dimensionless wavespeed found from the derivative of the fractional flow shown above.

### Saturation as a function of dispersion



The same curve as before, but now multiled by  $F^*$  to give the dimensional wavespeed.

If, instead, we had experimental measurements, then we can use the measured saturation profiles, obtained from in situ scanning (which give us  $F'$ ) to find  $D$  using Eq. (17.13). This is now the topic of on-going research. My hope is that combining pore-scale modelling from images, macroscopic corefloods using Buckley-Leverett theory, this imbibition solution and steady-state measurements of relative permeability, we can readily and very reliably determine capillary pressure and relative permeability. At present, the subject woefully lacks good experimental data; the methods described in this class offer a new opportunity to produce results that are reliable and accurate.

## 17.2 EXTENSIONS TO ANALYTIC THEORY AND RESERVOIR SIMULATION

---

The method of characteristics can be extended to study a whole range of one-dimensional displacements, including tracer flooding (combined with water injection), floods involving the injection of both a miscible solvent (miscible gas) and water, polymer flooding, and well as three-phase flow.

A complete discussion of this is beyond the scope of the class, but uses the same ideas – derive an appropriate conservation equation and identify wave and shock speeds.

Needless to say, however, this is a powerful and relatively simple way to assess recovery and displacement in porous media and serves as a useful complement to more sophisticated numerical approaches. In any event, numerical models require relative permeability curves as input and it is important to be able to understand their impact on the flow behaviour.

In the end, to describe flow in heterogeneous reservoirs with many wells and complex constraints on pressure and rates, it is necessary to perform a numerical analysis, solving the flow and transport equations presented in these notes in three dimensions. This is a rich and fascinating topic in its own right and lies outside the scope of this course. However, it is important to retain a physical insight into the displacement and recovery processes and how core-scale analysis and measurements relate to field-scale recovery.

## 18. BIBLIOGRAPHY AND FURTHER READING

---

Here are the references of the papers mentioned in the notes as well as other papers that are useful for reference and further reading.

Many of these papers can be accessed through the Society of Petroleum Engineers database, if they are not available through Web of Science or Google Scholar – [www.onepetro.org](http://www.onepetro.org). If you use an Imperial College computer to access this site, you can download papers for free.

### 18.1 RELEVANT RESEARCH PAPERS

---

M Akbarabadi and M Piri “Relative permeability hysteresis and capillary trapping characteristics of supercritical CO<sub>2</sub>/brine systems: an experimental study at reservoir conditions,” *Advances in Water Resources*, doi: <http://dx.doi.org/10.1016/j.advwatres.2012.06.014> (2013).

W G Anderson, “Wettability literature survey part 1: Rock/oil/brine interactions and the effects of core handling on wettability,” *J. Petrol. Technol.*, **38**(10), 1125–1144, doi: 10.2118/13932-PA. (1986).

W G Anderson, “Wettability literature survey-part 6: the effects of wettability on waterflooding,” *J. Petrol. Technol.*, **39**(12), 1605–1622, doi:10.2118/16471-PA. (1987).

C H Arns, F Bauget, A Limaye, A Sakellariou, T J Senden, A P Sheppard, R M Sok, V W Pinczewski, S Bakke, L I Berge and P-E Øren, “Pore-scale characterization of carbonates using X-ray microtomography,” *SPE Journal* **10**(4) 475-484 (2005).

J Y Arns, A P Sheppard, C H Arns, M A Knackstedt, A Yelkhovsky and W V Pinczewski, “Pore-level validation of representative pore networks obtained from micro-CT images,” *Proceedings of the Annual Symposium of the society of Core Analysis, SCA2007-A26*, Calgary, Canada (2007).

J S Aronofsky, L Masse, and S G Natanson, “A model for the mechanism of oil recovery from the porous matrix due to water invasion in fractured reservoirs,” *Petrol. Trans. AIME*, **213**, 17–19 (1958).

S Bakke and P-E Øren, “3-D pore-scale modelling of sandstones and flow simulations in the pore networks,” *SPE Journal* **2** 136-149 (1997).

S E Buckley and M C Leverett, “Mechanisms of fluid displacement in sands,” *Trans. AIME*, **146**, 107116 (1942).

H S Carslaw and J C Jaeger, *Conduction of Heat in Solids*, 2<sup>nd</sup> Edition, Oxford Science Publications, Clarendon Press, Oxford (1946).

I Chatzis and N Morrow, “Correlation of Capillary number relationships for sandstone,” *SPE Journal*, **24**(5), 555–562, doi:10.2118/10114-PA (1984).

J H Dunsmuir, S R Ferguson, K L D'Amico and J P Stokes, “X-ray microtomography. A new tool for the characterization of porous media,” SPE 22860, *Proceedings of the 1991 SPE Annual Technical Conference and Exhibition*, October 1991, Dallas (1991).

- I Fatt, "The network model of porous media I. Capillary pressure characteristics," *Trans AIME* **207** 144-159 (1956).
- B P Flannery, H W Deckman, W G Roberge and K L D'Amico, "Three-dimensional X-ray microtomography," *Science* **237** 1439-1444 (1987).
- P P Jadhunandan and N R Morrow, "Effect of wettability on waterflood recovery for crude oil/brine/rock systems," *SPE Reservoir Eng.*, **10**(1), 40-46, doi:10.2118/22597-PA (1995).
- P P Jadhunandan and N R Morrow, "Spontaneous imbibition of water by crude oil/brine/rock systems," *In Situ*, **15**(4), 319-345 (1991).
- G R Jerauld and S J Salter, "Effect of pore-structure on hysteresis in relative permeability and capillary pressure: Pore-level modeling," *Transport in Porous Media*, **5**, 103-151 (1990).
- S Krevor, R Pini, L Zuo and S Benson "Relative permeability and trapping of CO<sub>2</sub> and water in sandstone rocks at reservoir conditions" *Water Resources Research*, **48**(2), W02532, (2012).
- S C M Krevor, R Pini, B Li and S M Benson "Capillary heterogeneity trapping of CO<sub>2</sub> in a sandstone rock at reservoir conditions", *Geophysical Research Letters*, **38**, L15401. doi:10.1029/2011GL048239 (2011).
- C R Killins, R F Nielsen and J C Calhoun "Capillary Desaturation and Imbibition in Porous Rocks," *Producers Monthly*, **18**(2), 30-39, (1953).
- C Land, "Calculation of imbibition relative permeability for two- and three-phase flow from rock properties," *SPE Journal*, **24**, 149 – 156, doi:10.2118/1942-PA (1968).
- R Lenormand, C Zarcone and A Sarr "Mechanisms of the displacement of one fluid by another in a network of capillary ducts" *Journal of Fluid Mechanics*, **135**, 337-353, (1983).
- R Lenormand and C Zarcone "Role of roughness and edges during imbibition in square capillaries" SPE 13264, in Proceedings of the 59th Annual Technical Conference and Exhibition of the Society of Petroleum Engineers of AIME, Houston, Texas, September 16-19, (1984).
- R Lenormand "Invasion Percolation in an etched network: measurement of a fractal dimension," *Physical Review Letters*, **54**(20), 2226-2231, (1985).
- D B McWhorter and D K Sunada, "Exact Integral Solutions for Two-Phase Flow," *Water Resources Research* **26**(3) 399-413 (1990).
- N R Morrow and G Mason, "Recovery of oil by spontaneous imbibition," *Curr. Opin. Colloid Interface Sci.*, **6**(4), 321-337, doi:10.1016/S1359-0294(01)00100-5 (2001).
- M Muskat, "Physical Principles of Oil Production," McGraw Hill, New York (1949).
- M J Oak, L E Baker and D C Thomas, "Three-phase relative permeability of Berea sandstone, *J. Petrol. Technol.*, **42**(8), 1054-1061, doi:10.2118/17370-PA (1990).
- P-E Øren, S Bakke and O J Arntzen, "Extending predictive capabilities to network models," *SPE Journal*, **3** 324-336 (1998).
- P-E Øren and S Bakke, "Process based reconstruction of sandstones and prediction of transport properties," *Transport in Porous Media*, **46**(2-3) 311-343 (2002)
- P-E Øren and S Bakke, "Reconstruction of Berea sandstone and pore-scale modelling of wettability effects," *Journal of Petroleum Science and Engineering*, **39** 177-199 (2003).
- T W Patzek, "Verification of a complete pore network simulator of drainage and imbibition," *SPE Journal*, **6** 144-156 (2001).
- M Sahimi, "Flow and transport in porous media and fractured rock," Wiley-VCH Verlag GmbH. (1995).

R A Salathiel, "Oil recovery by surface film drainage in mixed-wettability rocks," *SPE Journal*, **25**(10), 1216–1224, doi:10.2118/4104-PA (1973).

K S Schmid and S Geiger, "Universal scaling of spontaneous imbibition for water-wet systems," *Water Resources Research*, **48**, W03507, doi:10.1029/2011WR011566, (2012).

N C Wardlaw and R P Taylor, "Mercury capillary pressure curves and the interpretation of pore structure and capillary behaviour in reservoir rocks," *Bulletin of Canadian Petroleum Geology*, **24**(2), 225–262 (1976).

X Zhou, N R Morrow and S Ma, "Interrelationship of wettability, initial water saturation, aging time, and oil recovery by spontaneous imbibition and waterflooding," *SPE Journal*, **5**(2), 199–207, doi:10.2118/62507-PA (2000).

## 18.2 PAPERS FROM IMPERIAL COLLEGE

---

These are presented in date order. Most of these papers can be downloaded from our website:

<http://www3.imperial.ac.uk/earthscienceandengineering/research/perm/porescalemodelling>

M J Blunt, "Physically Based Network Modeling of Multiphase Flow in Intermediate-Wet Media" *Journal of Petroleum Science and Engineering*, **20** 117-125 June (1998).

P H Valvatne and M J Blunt, "Predictive pore-scale modeling of two-phase flow in mixed wet media," *Water Resources Research*, **40**, W07406, doi:10.1029/2003WR002627 (2004).

H Okabe and M J Blunt, "Prediction of permeability for porous media reconstructed using multiple-point statistics," *Physical Review E* **70**, 066135 (2004).

M S Al-Gharbi and M J Blunt, "Dynamic network modeling of two-phase drainage in porous media," *Physical Review E* **71**, 016308 (2005).

M Piri and M J Blunt, "Three-dimensional mixed-wet random pore-scale network modeling of two- and three-phase flow in porous media. I. Model description," *Physical Review E* **71**, 026301 (2005).

M Piri and M J Blunt, "Three-dimensional mixed-wet random pore-scale network modeling of two- and three-phase flow in porous media. II. Results," *Physical Review E* **71**, 026302 (2005).

P H Valvatne, M Piri, X Lopez and M J Blunt, "Predictive Pore-Scale Modeling of Single and Multiphase Flow," *Transport in Porous Media* **58**, 23–41, doi:10.1007/s11242-004-5468-2 (2005).

Z Tavassoli, R W Zimmerman and M J Blunt, "Analytic Analysis for Oil Recovery During Counter-Current Imbibition in Strongly Water-Wet Systems," *Transport in Porous Media* **58**, 173–189, doi:10.1007/s11242-004-5474-4 (2005).

M D Jackson, P H Valvatne and M J Blunt, "Prediction of Wettability Variation Within an Oil/Water Transition Zone and Its Impact on Production," *SPE Journal* **10**(2), 184-195, June (2005).

Z Tavassoli, R W Zimmerman and M J Blunt, "Analysis of counter-current imbibition with gravity in weakly water-wet Systems," *Journal of Petroleum Science and Engineering* **48**, 94– 104 (2005).

H Behbahani and M J Blunt, "Analysis of Imbibition in Mixed-Wet Rocks Using Pore-Scale Modeling," *SPE Journal*, **10**(4) 466-474, December (2005).

H Behbahani, G Di Donato and M J Blunt, "Simulation of counter-current imbibition in water-wet fractured reservoirs," *Journal of Petroleum Science and Engineering* **50**, 21– 39 (2006).

- B Bijeljic and M J Blunt, "Pore-scale modeling and continuous time random walk analysis of dispersion in porous media," *Water Resources Research* **42**, W01202, doi:10.1029/2005WR004578 (2006).
- R Juanes, E J Spiteri, F M Orr, Jr. and M J Blunt, "Impact of relative permeability hysteresis on geological CO<sub>2</sub> storage," *Water Resources Research*, **42**, W12418, doi:10.1029/2005WR004806 (2006).
- V S Suicmez, M Piri and M J Blunt, "Pore-scale Simulation of Water Alternate Gas Injection," *Transport in Porous Media*, **66**, 259–286 doi:10.1007/s11242-006-0017-9 (2007).
- A S Al-Kharusi and M J Blunt, "Network extraction from sandstone and carbonate pore space images," *Journal of Petroleum Science and Engineering* **56**, 219–231 (2007).
- B Bijeljic and M J Blunt, "Pore-scale modeling of transverse dispersion in porous media," *Water Resources Research*, **43**, W12S11, doi:10.1029/2006WR005700 (2007).
- H Okabe and M J Blunt "Pore space reconstruction of vuggy carbonates using microtomography and multiple-point statistics," *Water Resources Research*, **43**, W12S02, doi:10.1029/2006WR005680 (2007).
- M I J van Dijke, M Piri, J O Helland, K S Sorbie, M J Blunt, and S M Skjæveland, "Criteria for three-fluid configurations including layers in a pore with nonuniform wettability," *Water Resources Research*, **43**, W12S05, doi:10.1029/2006WR005761 (2007).
- V S Suicmez, M Piri and M J Blunt, "Effects of wettability and pore-level displacement on hydrocarbon trapping," *Advances in Water Resources* **31**, 503–512 (2008).
- E J Spiteri, R Juanes, M J Blunt and F M Orr, Jr., "A New Model of Trapping and Relative Permeability Hysteresis for All Wettability Characteristics," *SPE Journal* **13**(3), 277-288 (2008).
- A S Al-Kharusi and M J Blunt, "Multiphase flow predictions from carbonate pore space images using extracted network models," *Water Resources Research* **44**, W06S01, doi:10.1029/2006WR005695 (2008).
- O Talabi, S AlSayari, S Iglauer and M J Blunt, Pore-scale simulation of NMR response , *Journal of Petroleum Science and Engineering* **67**(3-4), 168-178 (2009).
- H Dong and M J Blunt, "Pore-network extraction from micro-computerized-tomography images," *Physical Review E* **80**, 036307, doi: 10.1103/PhysRevE.80.036307 (2009).
- S K Al Mansoori, S Iglauer, C H Pentland and M J Blunt, "Three-phase measurements of oil and gas trapping in sand packs," *Advances in Water Resources* **32**, 1535-1542 (2009).
- S K Al Mansoori, E Itsekiri, S Iglauer, C H Pentland, B Bijeljic and M J Blunt, "Measurements of non-wetting phase trapping applied to carbon dioxide storage," *International Journal of Greenhouse Gas Control* **4** 283–288 (2010).
- N A Idowu and M J Blunt, "Pore-Scale Modelling of Rate Effects in Waterflooding," *Transport in Porous Media* **83** 151–169 (2010).
- X Zhao, M J Blunt and J Yao, "Pore-scale modeling: Effects of wettability on waterflood oil recovery," *Journal of Petroleum Science and Engineering* **71** 169–178 (2010).
- C H Pentland, E Itsekiri, S Al-Mansoori, S Iglauer, B Bijeljic and M J Blunt, "Measurement of Non-Wetting Phase Trapping in Sandpacks," *SPE Journal* **15** 274-281 (2010).
- S Iglauer, S Favretto, G Spinelli, G Schena and M J Blunt, "X-ray tomography measurements of power-law cluster size distributions for the nonwetting phase in sandstones," *Physical Review E* **82** 056315 (2010).
- C H Pentland, R El-Maghraby, S Iglauer and M J Blunt, "Measurements of the capillary trapping of super-critical carbon dioxide in Berea sandstone," *Geophysics Research Letters* **38**, L06401, doi:10.1029/2011GL046683 (2011).
- B Bijeljic, P Mostaghimi and M J Blunt, "The signature of Non-Fickian Solute Transport in Complex Heterogeneous Porous Media," *Physical Review Letters* **107** 204502 (2011).

S Iglauer, A Paluszny C H Pentland and M J Blunt, "Residual CO<sub>2</sub> imaged with X-ray micro-tomography," *Geophysical Research Letters* **38** L21403 (2011).

S Iglauer, W Wüling, C H Pentland, S K Al Mansoori and M J Blunt, "Capillary Trapping Capacity of Rocks and Sandpacks," *SPE Journal* **16**(4) 778-783 (2011).

S Iglauer, M A Fernø, P Shearing and M J Blunt, "Comparison of residual oil cluster size distribution, morphology and saturation in oil-wet and water-wet sandstone," *Journal of Colloid and Interface Science* **375** 187–192 (2012).

A Q Raeini, M J Blunt and B Bijeljic, "Modelling two-phase flow in porous media at the pore scale using the volume-of-fluid method." *Journal of Computational Physics* **231**(17) 5653-5668 (2012).

P Mostaghimi, B Bijeljic and M J Blunt, "Simulation of Flow and Dispersion on Pore-Space Images," *SPE Journal* **17** 1131-1141 (2012).

O Gharbi and M J Blunt, "The impact of wettability and connectivity on relative permeability in carbonates: A pore network modeling analysis," *Water Resources Research* **48** W12513, doi:10.1029/2012WR011877 (2012).

R M El-Maghraby and M J Blunt, "Residual CO<sub>2</sub> Trapping in Indiana Limestone," *Environmental Science and Technology* **47** 227–233, doi:10.1021/es304166u (2013).

S Iglauer, A Paluszny and M J Blunt, "Simultaneous oil recovery and residual gas storage: A pore-level analysis using in situ X-ray micro-tomography," *Fuel* **103** 905–914 (2013).

B Bijeljic, A Raeini, P Mostaghimi and M J Blunt, "Predictions of non-Fickian solute transport in different classes of porous media using direct simulation on pore-scale images," *Physical Review E* **87**, 013011 (2013).

M J Blunt, B Bijeljic, H Dong, O Gharbi, S Iglauer, P Mostaghimi, A Paluszny and C Pentland, "Pore-scale imaging and Modelling." *Advances in Water Resources*, **51** 197–216 (2013).

B Bijeljic, P Mostaghimi and M J Blunt, "Insights into non-Fickian solute transport in carbonates," *Water Resources Research* **49**, 2714–2728, doi:10.1002/wrcr.20238 (2013).

M Andrew, B Bijeljic and M J Blunt, "Pore-scale imaging of geological carbon dioxide storage under in situ conditions," *Geophysical Research Letters*, **40** 3915–3918 (2013).

Y Tanino and M J Blunt, "Laboratory investigation of capillary trapping under mixed-wet conditions," *Water Resources Research* **49**(7) 4311-4319 (2013).

A Q Raeini, B Bijeljic and M J Blunt, "Numerical Modelling of Sub-pore Scale Events in Two-Phase Flow Through Porous Media," *Transport in Porous Media*, **101** 191–213 (2014).

M Andrew, B Bijeljic and M J Blunt, "Pore-scale imaging of trapped supercritical carbon dioxide in sandstones and carbonates," *International Journal of Greenhouse Gas Control*, **22** 1-14 (2014).



## 19. HOMEWORK PROBLEMS

---

These problems are of the sort of style and difficulty that you can expect in the exam.

1. Define in a single sentence the following terms: (i) capillary pressure; (ii) drainage; (iii) imbibition; (iv) forced water injection.
2. Draw a typical oil/water capillary pressure curves for a water-wet sandstone with a porosity of 0.2 and a permeability of 100mD. Draw primary drainage, imbibition and secondary drainage curves. Also indicate on the graph typical values for the residual oil saturation and connate water saturation and typical values for the capillary pressure. These need only be estimates, but please explain clearly why you chose these values. Also explain why the primary and secondary drainage curves are different and why the imbibition curve is lower than the secondary drainage curve.
3. You are planning a surfactant flood. You perform some core flood experiments to find the effect of capillary number on the residual oil saturation. You find a correlation of the form:

$$S_{or} = \text{Max} \left[ 0, 0.4 - \frac{\sqrt{N_{cap}}}{0.08} \right]$$

You now perform a reservoir-scale flood. The injection and production wells are 100 m apart and have a pressure drop of 10 atm between them. The rock permeability is 200 mD. With surfactant the oil/water interfacial tension is 0.01 mN/m. What is the predicted residual oil saturation? What pressure difference between the wells is necessary to remove all the oil?

4. In this question we consider the relative permeability of a bundle of capillary tubes of different radii. A fraction  $f(r)dr$  tubes have a radius between  $r$  and  $r+dr$ . By definition:

$$\int_0^{\infty} f(r)dr = 1$$

All the tubes are aligned horizontally and have the same pressure drop across them. They are all of the same length. The flow (volume per unit time) in each tube is given by:

$$Q = \frac{\pi r^4}{8\mu l} \Delta P$$

The total volume of each tube =  $\pi r^2 L$ . The tubes are water-wet and are initially filled with water. Oil is now injected into the tubes. What size tubes does the oil preferentially occupy? The last tube to be filled with oil has a radius  $R$ . Derive an expression for the oil saturation and the oil relative permeability.

5. You are planning a tracer test in a portion of a reservoir that is entirely full of water. The tracer dissolves in water and flows with the water. You also know that the tracer absorbs to the reservoir rock. The mass of tracer that absorbs per unit volume of the reservoir,  $\rho^a$  is given by the following equation:

$$\rho^a = ac$$

$a$  is a dimensionless constant and  $c$  is the concentration of tracer in the water, measured in units of mass of tracer per unit volume of water.

Starting with the expression:

$$\frac{\partial}{\partial t} \left( \begin{array}{l} \text{mass per unit volume} \\ \text{of the reservoir} \end{array} \right) + \frac{\partial}{\partial x} \left( \begin{array}{l} \text{mass flux per} \\ \text{unit area} \end{array} \right) = 0$$

derive a conservation equation for tracer in one dimension, where  $q$  is the water volumetric flux per unit area and  $\phi$  is the rock porosity. You may assume that  $q$  and  $\phi$  are both constant.

With what speed does the tracer flow through the rock? Find this speed when  $q = 10^{-6} \text{ ms}^{-1}$ ,  $\phi = 0.2$  and  $a = 3$ .

6. Derive a conservation equation in one direction (the  $x$  direction) for a radioactive tracer moving through a fully water-saturated porous medium. Write the equation in terms of

the tracer concentration (mass per unit volume of fluid)  $c$ . As well as moving with the fluid, the tracer also diffuses. Fick's law of diffusion states that the diffusive flux is

$$F_D = -D \frac{\partial c}{\partial x}, \text{ where } D \text{ is the diffusion coefficient. Since the tracer is radioactive its}$$

concentration in a static fluid with no concentration gradient will decrease with time as

$$c(t) = c(t=0)e^{-\alpha t}, \text{ which is the same as saying that with no flow } \frac{\partial c}{\partial t} = -\alpha c.$$

## 7. Unit conversions

A committee is set up to increase North Sea oil production by 1,000,000 barrels per day. The committee members disagree on what units to use. For all the sections below express 1,000,000 barrels per day in the unit systems described.

- (a) Milton Keynes, an economist, wants to use millions of \$ per year. The oil price is \$105 per barrel.
- (b) Napoleon Laval, a Frenchman, wants to use SI units.
- (c) Abdus Goldstein, a theoretical physicist, wants to use units in which  $\hbar/2\pi = 1$ ,  $c = 1$  and  $G = 1$ .  $\hbar/2\pi = 1.055 \times 10^{-36}$  Js,  $c = 3.0 \times 10^8$  ms<sup>-1</sup>,  $G = 6.7 \times 10^{-11}$  m<sup>3</sup>kg<sup>-1</sup>s<sup>-2</sup>.
- (d) Jerry R. Beltbuckle III, an oil industry representative, prefers to use acre-feet per month. What is the target in (i) February 1999, (ii) December?

- 8. Oil formation volume factor.** A production well in an undersaturated reservoir has a bottom-hole water-cut ( $f_w$ ) of 0.2. If  $B_w = 1.01$  and  $B_o = 1.3$ , what is the water-oil ratio into the stock tank?

- 9.** Derive a conservation equation for radial two-phase flow in a cylindrical geometry appropriate for near wellbore flow of a water injector. Show in that the Buckley-Leverett rarefaction, the flow speed is given by:

$$v = \frac{\partial f}{\partial S}$$

where  $f$  is the fractional flow,  $S$  is the water saturation and:

$$v = \frac{\pi r^2 h \phi}{Qt}$$

where  $r$  is the radial distance from the well,  $h$  is the perforated interval,  $t$  is the time,  $\phi$  is the porosity and  $Q$  is the flow rate at the well.

10. For each of the examples below provide a graph of: (i)  $S_w$  as a function of  $v_D = x_D/t_D$ ; and (ii) pore volumes of oil produced  $N_{pD}$  as a function of  $t_D$ .

In all cases  $S_{wi} = S_{wc} = 0.2$ .

There is no gravity and the relative permeabilities are given by:

$$k_{rw} = k_{rw}^{\max} \frac{(S_w - S_{wc})^a}{(1 - S_{or} - S_{wc})^a}$$

$$k_{ro} = k_{ro}^{\max} \frac{(1 - S_{or} - S_w)^b}{(1 - S_{or} - S_{wc})^b}$$

$$M = \frac{\mu_o}{\mu_w} \frac{k_{rw}^{\max}}{k_{ro}^{\max}}$$

- (a) A strongly water-wet rock with  $a = 3$ ,  $b = 1$ ,  $k_{rw}^{\max} = 0.18$ ,  $k_{ro}^{\max} = 0.9$ ,  $S_{wc} = 0.2$ ,  $S_{or} = 0.4$  and  $\mu_w = \mu_o$  ( $M = 0.2$ ).
- (b) An oil-wet rock with  $a = 1$ ,  $b = 3$ ,  $k_{rw}^{\max} = 0.9$ ,  $k_{ro}^{\max} = 0.18$ ,  $S_{wc} = 0.2$ ,  $S_{or} = 0.1$  and  $\mu_w = \mu_o$  ( $M = 5$ ).
- (c) Repeat part (a) for  $M = 5$  and  $M = 50$ .
- (d) Repeat part (b) for  $M = 0.2$  and  $M = 50$ .

Comment on your results. Is it better to waterflood a water-wet or an oil-wet reservoir?  
What is the effect of mobility ratio on recovery?

Hints: Yes, this is a tedious exercise, but after it you will really know how to perform a Buckley-Leverett analysis. Either plot out the fractional flow and find the shock height graphically by hand, or do everything analytically/numerically. It is not possible to find a closed form expression for the shock saturation for this type of relative permeability, but you could write a small computer program to find everything you need automatically. Once you have worked it out for one case, the others should be easy.

## 20. PREVIOUS EXAM PAPERS

---

### MEng. EXAMINATION 2000

For internal students of the Imperial College of Science, Technology and Medicine

Taken by students of the T.H. Huxley School (Engineering)

This paper is also taken for the relevant examination for the Associateship of the Royal School of Mines

### ERE 202. ENVIRONMENTAL AND RESERVOIR PHYSICS

Friday 7 May 2000: 10.00 to 13.00

Answer TWO questions from the section below.

1. Capillary pressure and the oil/water contact. (20 marks total)

- (i) Explain what is meant by the oil/water contact in a reservoir. (2 marks)
- (ii) Draw a sketch of the water saturation versus depth in an oil reservoir. Mark the location of the oil/water contact. (3 marks)
- (iii) In the appraisal stage of a reservoir, an estimate is made of the initial oil in place. Sometimes it is assumed that  $S_o = 0$  below the oil/water contact and  $S_o = 1 - S_{wc}$  above it. Is this likely to give a good estimate of the oil in place, or over-estimate the value or under-estimate the value? Explain your answer with reference to your answer to part (ii). (2 marks)
- (iv) In order to determine the water saturation versus depth (part (ii)) a laboratory measurement of capillary pressure is performed on a rock sample. Should this be a primary drainage, imbibition or secondary drainage experiment? Explain your answer. (2 marks)
- (v) Using the same fluids as in the reservoir the following measurement of capillary pressure is performed.

Water saturation	Capillary pressure (Pa)
1.0	0
1.0	15,000
0.5	18,000
0.3	24,000
0.3	50,000

Use this information to plot a graph of water saturation versus height above the oil/water contact in the reservoir (as in Part (ii), but with real numbers!). The water (brine density) =  $1050 \text{ kg m}^{-3}$ , the oil density =  $750 \text{ kg m}^{-3}$ , the acceleration due to gravity =  $9.81 \text{ ms}^{-2}$ . The porosity of the rock sample = 0.25 and the permeability is 500 mD. The average porosity of the reservoir is 0.2 and the average permeability is 200 mD. (11 marks)

2. Planning water injection. (20 marks total)

- (i) Vertical injection and production wells are 200m apart in a reservoir with an average permeability of 200 mD. The oil column is 50 m deep, and the width of the reservoir is 200 m. The average porosity is 0.15. The oil and water viscosities =  $10^{-3} \text{ Pa.s}$ . The pressure difference between the wells = 5 atm. Assuming simple linear flow, estimate the production rate of oil (in  $\text{m}^3 \text{s}^{-1}$ ). (6 marks)
- (ii) In part (i) is this a surface or reservoir rate? If  $B_o = 1.5$ , find the surface production rate of oil. (2 marks)
- (iii) Water is injected to maintain the reservoir pressure. If  $B_w = 0.98$ , what is the surface injection rate of water? (2 marks)
- (iv) Estimate *approximately* how long (in days) it will take for water to break through at the production well. (4 marks)
- (v) To perform a full analysis of this problem would require the measurement of the oil/water relative permeabilities. List and briefly explain three differences between the relative permeabilities for an oil-wet rock and a water-wet rock. (6 marks)

**MEng. EXAMINATION 2001**

For internal students of the Imperial College of Science, Technology and Medicine

Taken by students of the T.H. Huxley School (Engineering)

This paper is also taken for the relevant examination for the Associateship of the Royal School of Mines

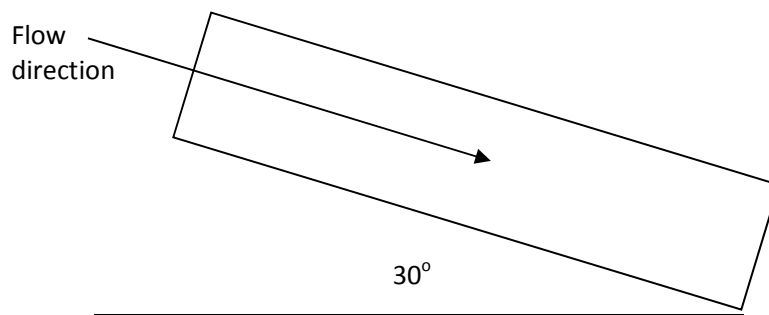
**ERE 202. ENVIRONMENTAL AND RESERVOIR PHYSICS**

Friday 7 May 2001: 10.00 to 13.00

Answer any TWO questions from the section below

**1. Calculating permeability. (20 marks total)**

- (i) You perform an experiment on a core aligned as shown below. The cross-sectional area is  $10 \text{ cm}^2$ , the flow rate of water is  $20 \text{ cm}^3$  per minute, the inlet pressure is 1.1 atmospheres and the outlet pressure is 1 atmosphere. The rock porosity is 0.25. The core has a length of 20 cm. The water density is  $1,000 \text{ kgm}^{-3}$  and the acceleration due to gravity is  $9.8 \text{ ms}^{-2}$ . The water viscosity is  $10^{-3} \text{ Pa.s}$ . You may assume that atmospheric pressure is 101 kPa. What is the permeability of the rock? (15 marks)
- (ii) At what speed is water moving through the rock? How long would it take for the injected water to be produced? (5 marks)

**2. Wettability and capillary pressure. (20 marks total)**

- (i) Describe the Amott wettability test and define the water and oil Amott wettability indices -  $A_w$  and  $A_o$ . (4 marks)
- (ii) Draw schematic water injection and oil re-injection capillary pressure curves for the following situations. You need not indicate the magnitude of the capillary pressure, but clearly indicate the positive and negative portions of the capillary pressure curve, and representative values for the connate water and residual oil saturations. For each case indicate if the system would be described as 'water-wet,' 'oil-wet,' 'mixed-wet,' or 'neutrally-wet.' Explain your answers briefly. (16 marks)
- $A_w=1$  and  $A_o=0$ .
  - $A_w=0.1$  and  $A_o=0$ .
  - $A_w=0.3$  and  $A_o=0.2$ .
  - $A_w=0$  and  $A_o=0.6$ .

3. Three-phase flow. (20 marks total)

- (i) Consider the flow of oil, water and gas in a water-wet system. Two measurements of relative permeability are made. The first is a normal waterflood relative permeability with no gas present. The second is a measurement of gas and oil relative permeabilities for gas injection into oil and connate water. By considering the size of pores that the different phases might occupy, comment on whether you expect the residual oil saturation after waterflooding to be larger, smaller or the same size as the residual oil saturation after gas flooding. (6 marks)
- (ii) What other arguments, apart from that used in part (i) above, could you use to explain low residual oil saturations in the presence of gas? (4 marks)
- (iii) Derive a conservation equation for the one-dimensional flow of water and gas for three-phase flow – find expressions relating the change in water and gas saturations and the water and gas Darcy velocities. You may assume that both the water and gas are incompressible. You may start with the equation below, if it helps: (10 marks)

$$\frac{\partial \text{Mass per unit volume}}{\partial t} + \frac{\partial \text{Mass flux}}{\partial x} = 0$$



**BSc. and MSci EXAMINATION 2004**

For internal students of the Imperial College of Science, Technology and Medicine

Taken by students of the Department of Earth Science and Engineering

This paper is also taken for the relevant examination for the Associateship of the Royal School of Mines

**HYDROGEOLOGY EXAM**

Answer any FIVE questions

**1. Hydrological Cycle. (20 marks total)**

- (i) Explain the Hydrological Cycle and illustrate its various components with an appropriate diagram. (10 marks)
- (ii) A river catchment of  $100\text{km}^2$  receives 800mm of rainfall a year. Evaporation is 100mm a year and the river run-off is estimated to be  $4 \times 10^7 \text{m}^3$  per year. Calculate how much water is expected to enter the ground per year. (5 marks)
- (iii) What assumptions have you made and what observations would you make to reduce these? (5 marks)

**2. Measuring permeability (20 marks total)**

- (i) Give the definition and units of hydraulic conductivity and intrinsic permeability. (5 marks)
- (ii) Describe how permeability can be measured for a sand. (5 marks)
- (iii) Use the data below from a permeameter to compute the hydraulic conductivity of the sample of sand. The sample is cylindrical with a diameter of 20 mm. (10 marks)

Flow ( $\text{mm}^3$ )	Time (s)	Hydraulic gradient (mm/mm)
180	20	0.09
400	25	0.16
360	15	0.24
4200	60	0.7
800	10	0.8

**3. Porosity and specific yield (20 marks total)**

- (i) Define total and effective porosity. Explain the units used to measure them. (5 marks)
- (ii) How may these quantities be measured on a sample of material taken to the surface? (5 marks)
- (iii) A saturated unconfined aquifer yields  $0.02\text{m}^3$  of water per square metre of aquifer for a reduction in water table level of 0.1m. What is the specific yield of the aquifer? (5 marks)
- (iv) What is the difference between the specific yield and effective porosity? (5 marks)

**4. Coefficient of storage (20 marks total)**

- (i) Define coefficient of storage. Explain the units used to measure it. (5 marks)
- (ii) What happens physically when the pressure is dropped in a confined aquifer for which the coefficient of storage is defined? Why is the coefficient of storage much lower than the specific yield in an unconfined aquifer? (10 marks)
- (iii) A confined and fully saturated aquifer has a coefficient of storage of 0.002. How much water is released from an aquifer of area  $1000\text{m}^2$  for a drop in head of 1m? (5 marks)

**5. Darcy's law (20 marks total)**

- (i) Define and explain Darcy's law. (6 marks)
- (ii) What is transmissivity and what are its units? (4 marks)
- (iii) A confined aquifer has a measured head gradient of 0.001 m/m, a depth of 15m, a width of 150m and an average intrinsic permeability of  $10^{-12} \text{m}^2$ . What is the flow rate of water – quote in units of  $\text{m}^3$  water per day? You may assume that the water density times the acceleration due to gravity divided by the water viscosity is  $9.81 \times 10^6 \text{m}^{-1}\text{s}^{-1}$ . (10 marks)

6. Capillary fringe (20 marks total)
- (i) Draw a diagram showing the zones of subsurface water. Define the water table and the capillary fringe. (8 marks)
  - (ii) A well is being drilled. At a depth of 6m below the ground surface moist sandy silt is encountered. At 10m there is standing water in the hole. What do these results mean in terms of the zones defined in part (i) above? (4 marks)
  - (iii) A pressure measurement is made at a depth of 12m. The measured pressure is 30 kPa above atmospheric pressure. What can be said about the direction of groundwater flow? (8 marks)
7. Discharge and recharge of an aquifer (20 marks total)
- (i) You have an unconfined aquifer. Define the irreducible water saturation. Explain how, by taking a sample of the aquifer sediment, the irreducible water saturation can be measured. (6 marks)
  - (ii) The aquifer has an effective porosity of 0.25 and an irreducible water saturation of 0.2. The aquifer depth is 40m and its area is  $1.4\text{km}^2$ . What is the water volume contained in the aquifer if it is completely saturated? What is the specific yield of the aquifer? How much water can be extracted from the aquifer if it were completely drained? (10 marks)
  - (iii) The annual rainfall is 600mm. Neglecting evaporation or run-off, how long would it take to recharge the aquifer completely? (4 marks)
8. Water quality (20 marks total)
- (i) Discuss the issues to be addressed when assessing water quality in an unconfined aquifer. (10 marks)
  - (ii) What samples should be taken, how can you ensure that they are representative and what significance would you attach to different measurements? (10 marks)

END OF EXAM

## BSc and MSci PRACTICE EXAMINATION 2005

For internal students of Imperial College London

Taken by students of Geoscience

This paper is also taken for the relevant examination for the Associateship of the Royal School of Mines

**HYDROGEOLOGY AND FLUID FLOW**

Answer any FIVE questions

1. **Darcy's law.** (20 marks total)

An experiment is performed on a 30 cm long cylindrical sand pack with a cross-sectional area of  $3 \text{ cm}^2$ . The pressure drop across the pack is 6,000 Pa and the flow rate is  $0.1 \text{ cm}^3/\text{s}$ . You may assume that the viscosity of water is  $10^{-3} \text{ Pa.s}$ . The pack is held at an angle  $30^\circ$  from horizontal so that the water is flowing uphill. The water density is  $1,000 \text{ kg m}^{-3}$  and the acceleration due to gravity  $g = 9.81 \text{ ms}^{-2}$ .

  - (i) Write down Darcy's law. Explain all the terms in the equation and give their units. (4 marks)
  - (ii) What is the permeability of the sand pack? (6 marks)
  - (iii) The porosity is 0.35. What are the Darcy velocity and interstitial velocities of the water? (4 marks)
  - (iv) A sorbing tracer is injected that has a retardation coefficient of 5. How long will it take for the tracer to reach the end of the pack? (6 marks)
2. **Three-phase relative permeability.** (20 marks total)
  - (i) Give two physical situations where the simultaneous flow of three fluid phases occurs. (4 marks)
  - (ii) Define the spreading coefficient of oil. What does it mean physically? (4 marks)
  - (iii) Explain why at low oil saturation the oil relative permeability in the presence of gas is proportional to the oil saturation squared. (6 marks)
  - (iv) Why don't ducks get wet? (6 marks)
3. **Dissolution.** (20 marks total)

There has been a spill of a DNAPL. Below the water table, the spill is contained in a cross-sectional area of  $20 \text{ m}^2$ , a length (in the direction of the groundwater flow) of 5 m and with an average saturation of 0.01. The soil porosity is 0.4. The solubility of the DNAPL is  $0.2 \text{ kg m}^{-3}$  and the groundwater flow speed is  $10^{-7} \text{ ms}^{-1}$ . The DNAPL density is  $1,200 \text{ kg m}^{-3}$ .

  - (i) What does DNAPL stand for? (2 marks)
  - (ii) What is the initial mass of DNAPL? (4 marks)
  - (iii) At what rate is DNAPL being dissolved? (7 marks)
  - (iv) Estimate how long it will take for all the DNAPL to dissolve. What approximations have you made? (7 marks)
4. **Partitioning.** (20 marks total)

There has been a spill of a hydrocarbon. The hydrocarbon density is  $700 \text{ kg m}^{-3}$ , the solubility is  $0.12 \text{ kg m}^{-3}$  and the saturated vapour density is  $0.06 \text{ kg m}^{-3}$ . The hydrocarbon is spilled over a volume of soil 5 m by 40 m to a depth of 3 m in the unsaturated zone. The average water saturation in this region is 0.3 and the average oil saturation is 0.02. The retardation factor is 20. The porosity is 0.3.

  - (i) Estimate the maximum amount of hydrocarbon that is dissolved in water, in air, sorbed and in its own phase. What is the total mass of oil that has been spilled? (14 marks)
  - (ii) How might the spill be cleaned up? Mention the different options and discuss which ones are most likely to work. (6 marks)

**5. Conservation equation – three-phase flow.***(20 marks total)*

- (i) Starting from the equation:

$$\frac{\partial}{\partial t} \left( \frac{\text{mass per unit}}{\text{volume of reservoir}} \right) + \frac{\partial}{\partial x} \left( \frac{\text{mass flux}}{\text{per unit area}} \right) = 0$$

derive a conservation equation for three-phase flow where oil, water and gas phases are all flowing. You can assume that the flow is incompressible. Hint – you need only consider a conservation equation for the water and gas phases.

*(8 marks)*

- (ii) Assume that the solution is a function of speed
- $v = x/t$
- only. Find an expression for the possible wavespeed.

*(8 marks)*

- (iii) For given saturations, how many wavespeeds are possible? What might these correspond to physically? Will you always get a sensible solution?

*(4 marks)***6. Capillary pressure and the Leverett J function.***(20 marks total)*

- (i) Write down the relation between capillary pressure and the Leverett J function.

*(4 marks)*

- (ii) A primary drainage mercury injection experiment is performed on a rock sample. A pressure of 10,000 Pa is measured. The rock permeability is 500 mD and the porosity is 0.35. The mercury/air interfacial tension is 140 mN/m. What is the estimated capillary pressure at the same saturation for an oil/water system with an interfacial tension of 30 mN/m, a permeability of 80 mD and a porosity of 0.18?

*(8 marks)*

- (iii) Draw representative capillary pressure curves for a water-wet medium for primary drainage, imbibition (water displacement) and secondary drainage. Explain carefully the different features of the curves.

*(8 marks)***7. Aquifers.***(20 marks total)*

- (i) Define the following terms and give appropriate units: specific yield, coefficient of storage and transmissivity.

*(6 marks)*

- (ii) An unconfined aquifer has an area of 10,000 m
- <sup>2</sup>
- and a depth of 15 m. How much water can be released from the aquifer if the specific yield is 0.15.

*(10 marks)*

- (iii) The porosity is 0.4. What is the connate or irreducible water saturation?

*(4 marks)***8. Relative permeability and the effect of flow rate.***(20 marks total)*

- (i) Write down the multiphase Darcy law and define relative permeability.

*(5 marks)*

- (ii) Define the capillary number. What does it represent physically?

*(5 marks)*

- (iii) Draw schematic figures that show the effect of capillary number on relative permeability and residual oil saturation. Explain the figures.

*(10 marks)*

END OF EXAM

**BSc and MSci EXAMINATION 2005**

For internal students of Imperial College London

Taken by students of Geoscience

This paper is also taken for the relevant examination for the Associateship of the Royal School of Mines

**HYDROGEOLOGY AND FLUID FLOW**

Answer any FIVE questions

1. **Darcy's law.** (20 marks total)  
 You perform an experiment on a 1 m long cylindrical sand pack with a cross-sectional area of  $2 \text{ cm}^2$ . The pressure drop across the pack is 10,000 Pa and the flow rate is  $0.072 \text{ cm}^3/\text{s}$ . You may assume that the viscosity of water is  $10^{-3} \text{ Pa.s}$ . The pack is held horizontal.
  - (i) Write down Darcy's law. Explain all the terms in the equation and give their units. (5 marks)
  - (ii) What is the permeability of the sand pack? (5 marks)
  - (iii) The porosity is 0.4. What are the Darcy velocity and interstitial velocities of the water? (5 marks)
  - (iv) A conservative (non-sorbing) tracer is injected. How long will it take for the tracer to reach the end of the pack? (5 marks)
  
2. **Sorption.** (20 marks total)  
 You perform test in a long column of soil containing some organic material where you measure the speed at which toluene travels. The retardation factor of toluene is 25.
  - (i) Explain physically why sorption causes a contaminant to move slower through a porous medium than a species that does not sorb. (5 marks)
  - (ii) If the interstitial velocity is  $v$  and the retardation factor is  $R$ , at what speed does the contaminant travel? (2 marks)
  - (iii) The Darcy velocity of the water in the column is  $1 \text{ mm/s}$  and the porosity is 0.3. What is the speed of the toluene? (5 marks)
  - (iv) You perform two other experiments. In the first you use the same column but measure the speed of octane that is much less soluble than toluene. In the second you measure the speed of toluene but for a clean soil containing no organic material. For these two cases would you expect the retardation factor to be higher, lower or the same? Explain your answer. (8 marks)
  
3. **Diffusion and dispersion.** (20 marks total)
  - (i) Explain physically what is meant by molecular diffusion and by dispersion. (5 marks)
  - (ii) If the diffusion coefficient is  $D$  approximately how far will a contaminant diffuse in a time  $t$ ? How far will the contaminant move by advection in a time  $t$  if the flow speed is  $v$ ? (5 marks)
  - (iii)  $D = 10^{-9} \text{ m}^2\text{s}^{-1}$  and  $v = 10^{-5} \text{ ms}^{-1}$ . What is the ratio of advective movement to diffusive movement for  $t = 1\text{s}$  and for  $t = 10^5 \text{ s}$ ? Comment on your answers. (10 marks)

**4. Partitioning. (20 marks total)**

There has been a spill of a volatile hydrocarbon. Laboratory measurements indicate that the hydrocarbon density is  $700 \text{ kg m}^{-3}$ , the solubility is  $0.45 \text{ kg m}^{-3}$  and the saturated vapour density is  $0.25 \text{ kg m}^{-3}$ . The hydrocarbon is spilled over a volume of soil 10 m by 10 m to a depth of 5 m in the unsaturated zone. The average water saturation in this region is 0.2 and the average oil saturation is 0.01. The retardation factor is 11. The porosity is 0.4.

- (i) Estimate the maximum amount of hydrocarbon that is dissolved in water, in air, sorbed and in its own phase. What is the total mass of oil that has been spilled? (14 marks)
- (ii) How might the spill be cleaned up? Discuss briefly the different options and mention which ones are most likely to work. (6 marks)

**5. Conservation equation – partitioning tracers. (20 marks total)**

Tracers that dissolve in both oil and water are often used to determine how much oil is left behind (the residual oil saturation) after water is used to push out oil in a hydrocarbon reservoir. In this question you are asked to derive a conservation equation for such a tracer (a partitioning tracer) and then use it to determine the residual oil saturation for an example problem.

The tracer has a concentration  $c$  in water. The units of  $c$  are mass of tracer per unit volume of water. The tracer does not absorb to the rock, but it does dissolve in oil. There is a saturation  $S_w$  of water and an oil saturation  $1 - S_w = S_o$ . The oil is not flowing. Both the oil and water saturations are constant throughout the tracer test.

If the concentration of tracer in the water is  $c$ , the concentration in oil is  $ac$ .

- (i) Starting from the equation:

$$\frac{\partial}{\partial t} \left( \frac{\text{mass per unit}}{\text{volume of reservoir}} \right) + \frac{\partial}{\partial x} \left( \frac{\text{mass flux}}{\text{per unit area}} \right) = 0$$

derive a conservation equation for the tracer. (10 marks)

- (ii) Find the speed with which the tracer travels through the porous medium. (5 marks)
- (iii) Two tracers are injected. One does not dissolve in oil ( $a = 0$ ) and another where  $a = 5$ . The speed of the non-dissolving tracer (measured by how long it takes the tracer to go from an injection well to a producing well) is 4 times greater than for the dissolving tracer. What is the oil saturation? (5 marks)

**6. Relative permeability. (20 marks total)**

- (i) Write down the multiphase Darcy law. Explain what relative permeability means and the assumptions that are made in its definition. (5 marks)
- (ii) Explain physically how the wettability of soil and rock changes from water-wet to oil-wet, or mixed-wet, on contact with oil. (5 marks)
- (iii) Draw representative relative permeability curves for a water-wet system and a mixed-wet system. Explain carefully the differences between the two curves. (10 marks)

**7. Aquifer storage. (20 marks total)**

- (i) Define coefficient of storage. Explain the units used to measure it. (5 marks)
- (ii) What happens physically when the pressure is dropped in a confined aquifer for which the coefficient of storage is defined? Why is the coefficient of storage much lower than the specific yield in an unconfined aquifer? (10 marks)
- (iii) A confined and fully saturated aquifer has a coefficient of storage of 0.001. How much water is released from an aquifer of area  $2000 \text{ m}^2$  for a drop in head of 2 m? (5 marks)

8. **Capillary fringe and pollution.** *(20 marks total)*
- (i) Draw a diagram that carefully shows all the zones of subsurface water and marks clearly the capillary fringe. *(5 marks)*
  - (ii) What do the terms LNAPL and DNAPL stand for? *(4 marks)*
  - (iii) Explain what happens when an LNAPL and a DNAPL reach the capillary fringe. *(5 marks)*
  - (iv) How does the behaviour of the two types of pollutant affect clean-up options? *(6 marks)*

END OF EXAM

**BSc and MSci EXAMINATION 2007**

For internal students of Imperial College London

Taken by students of Geoscience

This paper is also taken for the relevant examination for the Associateship of the Royal School of Mines

**HYDROGEOLOGY AND FLUID FLOW 2**

Answer any FOUR questions.

**1. Capillary pressure and Leverett J function. (25 marks total)**

You measure the following primary drainage capillary pressure in the laboratory. The core has a permeability of 500 mD, a porosity of 0.25 and the interfacial tension is 50 mN/m.

Pressure (Pa)	Saturation
0	1
8,000	1
12,000	0.5
15,000	0.35
20,000	0.25
30,000	0.25

- (i) Write an equation that relates the capillary pressure to the Leverett J function. Define all the terms and give appropriate units. (5 marks)
- (ii) In the field the average permeability is 100 mD, the porosity is 0.2 and the interfacial tension is 30 mN/m. Plot a graph of water saturation against height above the free water level in the reservoir. The oil density is  $800 \text{ kgm}^{-3}$  and the brine density is  $1100 \text{ kgm}^{-3}$ .  $g=9.81 \text{ ms}^{-2}$ . (15 marks)
- (iii) What approximations have you made in this analysis? (5 marks)

**2. Relative permeability. (25 marks total)**

- (i) Write down the multiphase Darcy equation, define all terms and give them suitable units. (5 marks)
- (ii) Draw a schematic of the waterflood relative permeabilities for oil and water for a water-wet sandstone. Label the graph and comment on the values given. (7 marks)
- (iii) Draw a schematic of the waterflood relative permeabilities for oil and water for a structurally similar sandstone to part (ii) but where the system is mixed-wet. Comment on the differences with a water-wet system. (7 marks)
- (iv) If oil has a density of  $700 \text{ kgm}^{-3}$  and brine a density of  $1050 \text{ kgm}^{-3}$ , what is the Darcy velocity of oil flowing vertically under gravity if the permeability is 100 mD, the oil viscosity is 2.5 mPa.s and the relative permeability is 0.05?  $g=9.81 \text{ ms}^{-2}$ . (6 marks)



**3. Young Laplace equation and contact angles. (25 marks total)**

- (i) Write down the Young-Laplace equation, define all the terms and give units. (3 marks)
- (ii) Derive the capillary pressure between two phases between parallel plates a distance  $d$  apart. The contact angle is  $\theta$ . (4 marks)
- (iii) Find the capillary pressure between two fluids residing between two parallel glass plates a distance of  $1\text{ }\mu\text{m}$  apart with a contact angle of  $40^\circ$  and an interfacial tension of  $40\text{ mN/m}$ . (3 marks)
- (iv) Derive the Young equation that relates interfacial tensions to contact angles on a flat surface for two fluid phases labelled 1 and 2 with a contact angle  $\theta_{12}$  between them. The contact angle is measured through phase 2. (3 marks)
- (v) Write down the Young equations for each possible pair of fluids if there are three fluids 1, 2 and 3 in equilibrium. (3 marks)
- (vi) Use the answer to part (v) to derive an equation that relates the contact angles and interfacial tensions of the three phases. This is the Bartlell-Osterhof equation. (6 marks)
- (vii) If the interfacial tension between phase 1 and 2 is  $30\text{ mN/m}$  and the contact angle is  $50^\circ$  the interfacial tension between phase 2 and 3 is  $20\text{ mN/m}$  and the contact angle is  $150^\circ$ . If the interfacial tension between phases 1 and 3 is  $45\text{ mN/m}$ , what is the contact angle? (3 marks)

**4. How do trees transpire? (25 marks total)**

Trees transpire – that is take up water – thanks to capillary action. There is an unresolved mystery concerning how tall trees can do this. A tree can be considered a porous medium – the water moves upwards through the tree in narrow vessels and then evaporates in the leaves.

- (i) Assume that the air pressure and the water pressure are the same at the water table. Neglecting the density of the air, write an equation for the water pressure as a function of height  $h$  above the water table. (5 marks)
- (ii) Is the answer to part (i) the correct equation for the water pressure inside the tree? Explain your answer. (4 marks)
- (iii) What is the capillary pressure between two phases in a cylindrical tube of radius  $r$ ? (3 marks)
- (iv) Assuming that the contact angle between water and air in the tree is zero, find the radius of a vessel (assuming it is cylindrical) necessary to support water to a height of  $50\text{ m}$ . The water density is  $1000\text{ kgm}^{-3}$  and the interfacial tension between water and air is  $70\text{ mN/m}$ .  $g=9.81\text{ ms}^{-2}$ . (7 marks)
- (v) What is the water pressure at this height? Atmospheric pressure =  $10^5\text{ Pa}$ . Comment on your answer. (6 marks)

**5. Conservation equations for miscible WAG. (25 marks total)**

Water alternate gas (WAG) injection is often performed as an enhanced oil recovery technique in oil reservoirs. Here we assume that the gas injected is completely miscible with the oil. There are two phases: hydrocarbon and water. In the hydrocarbon phase gas (solvent) has a concentration  $c$ , measured in mass of solvent per unit volume of hydrocarbon phase.

- (i) Derive conservation equations for one-dimensional incompressible flow for the water saturation and for the solvent concentration. (11 marks)
- (ii) Simplify the solvent concentration equation by writing out all the terms. (5 marks)
- (iii) What is the speed of the solvent? (4 marks)
- (iv) Find the speed of the solvent if only solvent is injected into the reservoir, the connate water saturation is  $0.3$ , the total velocity is  $1\text{ m/day}$  and the porosity is  $0.2$ . (5 marks)

END OF EXAM

**IMPERIAL COLLEGE LONDON****BSc and MSci EXAMINATION 2009**

For internal students of Imperial College London

Taken by students of Geoscience

This paper is also taken for the relevant examination for the Associateship of the Royal School of Mines

**HYDROGEOLOGY AND FLUID FLOW 2**

Answer any FOUR questions.

Wednesday 29<sup>th</sup> April 2009, 10:00 to 12:00**1. Capillary pressure and Leverett J function.****(25 marks total)**

You measure the following primary drainage capillary pressure in the laboratory using mercury. The core has a permeability of 600 mD, a porosity of 0.20, the interfacial tension is 487 mN/m and the contact angle is  $140^\circ$ .

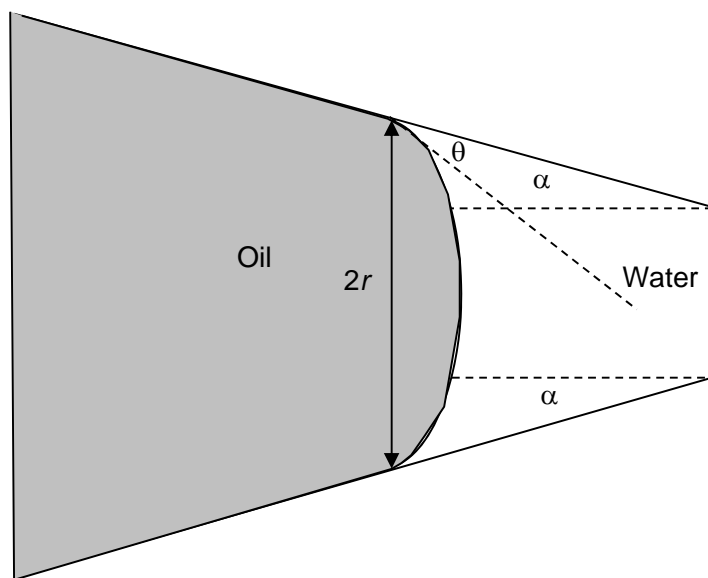
Pressure (Pa)	Saturation
0	1
50,000	1
74,000	0.6
150,000	0.4
350,000	0.3
300,000	0.3

- (i) Write an equation that relates the capillary pressure to the Leverett J function. Define all the terms and give appropriate units. (5 marks)
- (ii) In the field the average permeability is 200 mD, the porosity is 0.15 and the interfacial tension is 25 mN/m. Plot a graph of water saturation against height above the free water level in the reservoir. The oil density is  $700 \text{ kgm}^{-3}$  and the brine density is  $1050 \text{ kgm}^{-3}$ .  $g=9.81 \text{ ms}^{-2}$ . (15 marks)
- (iii) What approximations have you made in this analysis and what did you have to assume? (5 marks)

**2. Relative permeability.****(25 marks total)**

- (i) Write down the multiphase Darcy equation, define all terms and give them suitable units. (5 marks)
- (ii) Draw a schematic of the water flood (water displacing oil) and gas flood (gas displacing oil and connate water) relative permeabilities for a water-wet sandstone. Label the graph and comment on the values given and any differences between the relative permeability functions. (6 marks)
- (iii) Discuss briefly how the three-phase oil relative permeability can be estimated when all three phases – oil, water and gas – are flowing. (6 marks)
- (iv) Estimate the oil production rate from a reservoir of cross-sectional area 1 km by 5km. The oil drains under gas gravity drainage: oil has a density of  $700 \text{ kgm}^{-3}$  and gas a density of  $300 \text{ kgm}^{-3}$ . The permeability is 50 mD and the oil viscosity is 1.5 mPa.s and the relative permeability is 0.001.  $g=9.81 \text{ ms}^{-2}$ . Comment on your result. Why is the oil relative permeability so low? (8 marks)

3. **Wettability and contact angle.** (25 marks total)
- (i) Define intrinsic, advancing and receding contact angles. (3 marks)
  - (ii) Give all the reasons why the advancing contact angle in a porous medium is typically significantly higher than the receding contact angle. (3 marks)
  - (iii) Draw a graph of primary drainage capillary pressure for a fine sand pack. Also show the waterflood capillary pressure if the sand pack becomes oil-wet after drainage. Explain why the waterflood capillary pressure is lower than the drainage capillary pressure. (4 marks)
  - (iv) What is the capillary pressure for invasion through a tube of circular cross-section, but which has sides sloping at an angle  $\alpha$  and a contact angle  $\theta$  – see the figure below? The interfacial tension is  $\sigma$ . (10 marks)
  - (v) Comment on your answer to part (iv) – how can it be used to explain capillary pressure hysteresis (consider a porous medium with diverging and converging pores)? (5 marks)



4. **Gas storage** (25 marks total)
- You are asked to consider using a depleted gas field to store  $\text{CO}_2$  as part of a carbon-capture-and-storage project.
- (i) The natural gas originally in the reservoir had a density of  $300 \text{ kg.m}^{-3}$ . The brine in the formation has a density of  $1,100 \text{ kg.m}^{-3}$ . The cap-rock has a porosity of 0.1 and a permeability of 0.01 mD. The gas/brine interfacial tension is 50 mN/m. Make an *approximate estimate* of the capillary pressure necessary for the gas to enter the cap-rock. Explain your calculation carefully. (10 marks)
  - (ii) Use the answer to part (i) to estimate the maximum height of a gas column that could be sustained under the cap rock. (7 marks)
  - (iii) If  $\text{CO}_2$  were stored in the same formation, what would the maximum height of the  $\text{CO}_2$  be? The  $\text{CO}_2$  density – at reservoir conditions – is  $600 \text{ kg.m}^{-3}$  and the interfacial tension is 20 mN/m. Comment on the result. Can  $\text{CO}_2$  be safely stored in this field if it were to replace the gas? (8 marks)

**5. Conservation equations for a partitioning tracer. (25 marks total)**

After waterflooding, there is a non-flowing residual oil saturation  $S_{or}$ . A tracer is injected in the water that partitions (dissolves) in the oil. If the concentration in the water is  $C$ , then the concentration in oil is  $\alpha C$ .

- (i) Derive a conservation equation for the tracer concentration for one-dimensional incompressible flow. Explain all the terms carefully. (10 marks)
- (ii) With what speed does the tracer move? What is the speed of a conservative tracer that does not dissolve in oil? (5 marks)
- (iii) A conservative tracer and a partitioning tracer ( $\alpha=2$ ) are injected into a waterflooded oilfield. The conservative tracer breaks through at a production well after 100 days, while the partitioning tracer breaks through at 150 days. Estimate the residual oil saturation. (10 marks)

END OF EXAM

**IMPERIAL COLLEGE LONDON****BSc and MSci EXAMINATION 2011**

For internal students of Imperial College London

Taken by students of Geoscience

This paper is also taken for the relevant examination for the Associateship of the Royal School of Mines

**HYDROGEOLOGY AND FLUID FLOW 2**

Answer any FOUR questions.

**1. Capillary pressure and Leverett J function.****(25 marks total)**

You measure the following waterflood capillary pressure in the laboratory. The core has a permeability of 10 mD, a porosity of 0.20, the interfacial tension is 50 mN/m. The core is carbonate taken from a fractured oil field.

Pressure (Pa)	Saturation
300,000	0.35
200,000	0.40
15,000	0.50
0	0.60
-15,000	0.65
-100,000	0.75
-300,000	0.80

- (i) Write an equation that relates the capillary pressure to the Leverett J function. Define all the terms and give appropriate units. (5 marks)
- (ii) In the field the average permeability is 1 mD, the porosity is 0.15 and the interfacial tension is 25 mN/m. Plot a graph of capillary pressure as a function of water saturation for the field. (10 marks)
- (iii) The reservoir is waterflooded. The matrix is surrounded by fractures, forming blocks approximately 6 m tall. The brine density is  $1,150 \text{ kgm}^{-3}$  and the oil density is  $800 \text{ kgm}^{-3}$ . Estimate the final water (brine) saturation in the matrix. (10 marks)

**2. Relative permeability.****(25 marks total)**

- (i) Write down the multiphase Darcy equation, define all terms and give them suitable units. (5 marks)
- (ii) Draw a schematic of the water flood (water displacing oil) relative permeabilities for water-wet, oil-wet and mixed-wet rock, noting differences between them. (7 marks)
- (iii) Comment on the implications for waterflood recovery in an oil field. For a light oil with a viscosity similar to water, which wettability type gives the most favourable recovery? (6 marks)
- (iv) Polymer flooding is being proposed for an oil field. Polymer is injected with the water to increase the water viscosity. This method only works if it improves recovery beyond normal waterflooding. Why does polymer flooding work? For what wettability type(s) is this likely to most favourable? Explain your answer carefully. (7 marks)

3. **Pore-scale displacement.** (25 marks total)
- (i) Define snap-off and piston-like advance. What is meant by pore-filling? Explain the processes that control the degree of non-wetting phase trapping. (7 marks)
  - (ii) Derive an equation for the entry pressure for piston-like advance through a cylindrical throat of inscribed radius  $r$  with contact angle  $\theta$ . (4 marks)
  - (iii) Derive an equation for the threshold capillary pressure for filling by snap-off for a throat with an equilateral triangular cross-section of inscribed radius  $r$  and contact angle  $\theta$ . What is the ratio of the threshold pressures for snap-off divided by piston-like advance? (8 marks)
  - (iv) Comment on your answer to part (iii). Use this result to explain how the residual non-wetting phase saturation varies with contact angle, for contact angles less than  $90^\circ$ . (6 marks)
4. **Gravity drainage and three-phase flow** (25 marks total)
- (i) Explain the concept of layer drainage in three-phase flow and explain carefully why the oil relative permeability is proportional to the square of the oil saturation in the layer drainage regime. (7 marks)
  - (ii) In an oilfield that is being produced by gravity drainage, the oil relative permeability is  $k_{ro} = 0.1 \times S_o^2$ . Write down the conservation equation for oil saturation, putting in the expression for the oil Darcy velocity for vertical flow under gravity. Use this to find the speed with which a saturation  $S_o$  travels. (9 marks)
  - (iii) Estimate the time needed to drain the oil saturation to 20%. The reservoir has an oil column of height 50 m, the oil density is  $850 \text{ kg.m}^{-3}$ , the gas density is  $350 \text{ kg.m}^{-3}$ , the oil viscosity is  $0.3 \text{ mPa.s}$  and the vertical permeability is 50 mD. The porosity is 0.2. Comment on your answer. (9 marks)
5. **Conservation equations for CO<sub>2</sub> storage in a fractured medium.** (25 marks total)
- Huge fractured aquifers are possible storage locations for CO<sub>2</sub> collected from power stations and other industrial plants. The CO<sub>2</sub> flows through the fractures. CO<sub>2</sub> also dissolves in brine – this CO<sub>2</sub> saturated brine can enter the matrix.
- (i) The CO<sub>2</sub> in its own phase remains in the fractures. Explain physically what prevents the CO<sub>2</sub> in its own phase entering the matrix. (5 marks)
  - (ii) By what physical mechanism does the CO<sub>2</sub> dissolved in brine move through the matrix? (4 marks)
  - (iii) If the fractures are closely spaced, then all the water in the matrix in contact with a fracture containing CO<sub>2</sub> will have the same dissolved CO<sub>2</sub> concentration, equal to the solubility. If this solubility is  $C_s$ , write down a conservation equation for the flow of CO<sub>2</sub>. You may assume that the only Darcy flow is in the fractures and can ignore water in the fractures themselves. To simplify the analysis, you can assume the Darcy flow of CO<sub>2</sub> is  $S_c q_t$ , where  $S_c$  is the saturation and  $q_t$  is the total (Darcy) velocity.  $\phi_f$  is the porosity of the fractures and  $\phi_m$  is the porosity of the matrix. Derive an expression for the speed of the CO<sub>2</sub> if the fracture saturation is 1. Draw a sketch to illustrate how the CO<sub>2</sub> moves that explains your answer. (13 marks)
  - (iv) Find the speed of the CO<sub>2</sub> in the fractures with dissolution if the total, Darcy velocity is  $10^{-7} \text{ ms}^{-1}$ ,  $\phi_f = 0.05\%$ ,  $\phi_m = 30\%$ .  $C_s = 40 \text{ kgm}^{-3}$  and the density of CO<sub>2</sub> in its own phase is  $600 \text{ kg.m}^{-3}$ . (3 marks)

END OF EXAM

**IMPERIAL COLLEGE LONDON****BSc and MSci EXAMINATION 2013**

For internal students of Imperial College London

Taken by students of Geoscience

This paper is also taken for the relevant examination for the Associateship of the Royal School of Mines

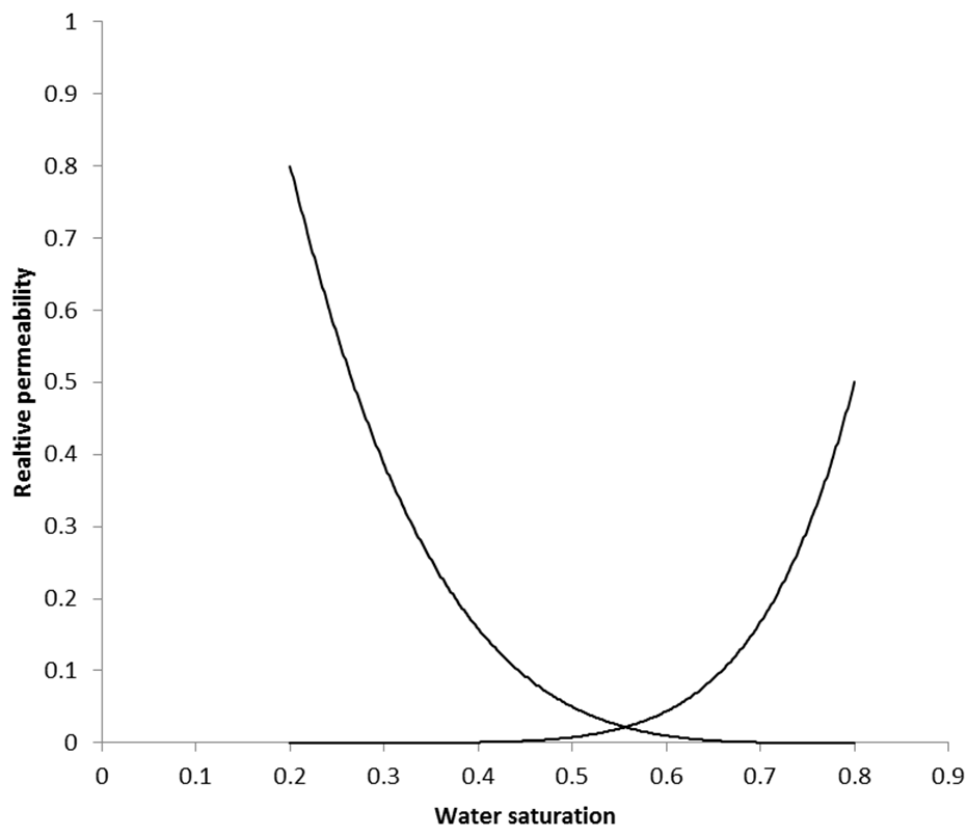
**HYDROLOGEOLOGY AND FLUID FLOW 2**

Answer ANY FOUR questions.

- 1. Pore-scale displacement. (25 marks total)**
- (i) Define and explain the pore-scale filling processes that govern trapping in porous media when water displaces oil in a water-wet porous medium. Under what circumstances do you expect to see a significant amount of capillary trapping (a high residual non-wetting phase saturation). Draw pictures to help illustrate your explanation. (7 marks)
  - (ii) Explain clearly what is meant by an oil layer in two-phase flow. Under what circumstances are oil layers observed? How do they affect the degree of trapping of oil? (4 marks)
  - (iii) Derive an equation for the threshold capillary pressure for filling by snap-off for a throat with a square cross-section of inscribed radius  $r$  and contact angle  $\theta$ . What is the largest contact angle possible for snap-off to occur (for the threshold capillary pressure to be positive)? (10 marks)
  - (iv) Comment on your answer to part (iii). What happens to the amount of trapping for larger contact angles than the value found in part (iii)? (4 marks)
- 2. Carbon dioxide storage. (25 marks total)**
- (i) Write down the multiphase Darcy equation. Define all the terms and provide units. (5 marks)
  - (ii) Write down the equation that describes the Darcy flow – under gravity only – of one fluid in the presence of another fluid. Write down the equation when the fluid that is moving is much more mobile than the fluid it displaces. (7 marks)
  - (iii) In carbon dioxide storage, find the Darcy flow rate under gravity of  $\text{CO}_2$  if the density of  $\text{CO}_2$  is  $600 \text{ kg.m}^{-3}$ , the density of brine is  $1,050 \text{ kg.m}^{-3}$ , and the viscosity of  $\text{CO}_2$  is  $2 \times 10^{-5} \text{ Pa.s}$ . The permeability is  $2 \times 10^{-13} \text{ m}^2$  and the relative permeability of  $\text{CO}_2$  is 0.8. Assume negligible water mobility. In what direction does the  $\text{CO}_2$  move? (8 marks)
  - (iv)  $\text{CO}_2$  is injected at the bottom of a storage aquifer that is 200 m tall. Use the answer to part (iii) to estimate how long it takes for the  $\text{CO}_2$  to rise to the top of the formation. You may assume that the  $\text{CO}_2$  saturation is 1 and the porosity is 0.25. What prevents  $\text{CO}_2$  from escaping to the surface? (5 marks)

**3. Relative permeability.****(25 marks total)**

- (i) In words explain what is meant by the concept of relative permeability. (4 marks)
- (ii) Explain what is meant by 'wettability'. Why do we often encounter oil-wet surfaces in oil fields? (5 marks)
- (iii) Define the terms water-wet, oil-wet and mixed-wet. (4 marks)
- (iv) The relative permeability curve below is measured on a core sample from a giant oil-field in the Middle East. What is the likely wettability of the sample? Explain your answer carefully. (5 marks)



- (v) In this field, water is injected to displace oil. If the oil and water viscosities are similar, estimate – approximately – the water saturation at which more water than oil will be produced from the field. What fraction of the oil that was originally in the reservoir will be produced? (7 marks)

**4. Capillary-controlled displacement.****(25 marks total)**

- (i) Write down the Young-Laplace equation. Define all the terms with units. (4 marks)
- (ii) On a rock sample, a typical pore radius is  $1\ \mu\text{m}$  and the interfacial tension is  $25\ \text{mN/m}$ . What – approximately – is a typical capillary pressure? (4 marks)
- (iii) If I have another rock sample, where all the pores are twice the size as before, by what amount does the typical capillary pressure change? By what factor does the permeability change? (5 marks)
- (iv) It takes  $1,000\ \text{s}$  for water to imbibe into a core of radius  $1\ \text{cm}$ , how long – all else being equal – does it take for water to imbibe into a matrix block in a reservoir that is around  $1\ \text{m}$  in radius? Explain your answer. (6 marks)
- (v) For the reservoir-scale matrix block, how long will it take for imbibition if all the pore sizes are now half the size than in the core-scale experiment? (6 marks)



**5. Capillary pressure and Leverett J function.****(25 marks total)**

You measure the following waterflood capillary pressure in the laboratory. The core has a permeability of 50 mD, a porosity of 0.25, the interfacial tension is 50 mN/m.

Pressure (Pa)	Saturation
200,000	0.30
100,000	0.35
10,000	0.45
0	0.50
-10,000	0.55
-100,000	0.75
-200,000	0.85

- (i) Write an equation that relates the capillary pressure to the Leverett J function. Define all the terms and give appropriate units. (5 marks)
- (ii) In the field the average permeability is 20 mD, the porosity is 0.15 and the interfacial tension is 20 mN/m. Plot a graph of capillary pressure as a function of water saturation for the field. (10 marks)
- (iii) Is the core sample water-wet, oil-wet or mixed-wet? Explain your answer. What is the Amott wettability index for water? (10 marks)

END OF EXAM